

THESE DE DOCTORAT DE

L'UNIVERSITE DE RENNES 1

ECOLE DOCTORALE N° 601

*Mathématiques et Sciences et Technologies
de l'Information et de la Communication*

Spécialité : *Signal, Image, Vision*

L'UNIVERSITE LIBANAISE

Ecole Doctorale des Sciences et Technologie

Spécialité : *Génie Biomédical*

Par

Sahar ALLOUCH

La variabilité analytique dans l'estimation des réseaux cérébraux fonctionnels à partir de l'électroencéphalographie

Thèse présentée et soutenue à Rennes, le « date »

Unité de recherche : Laboratoire Traitement du Signal et de l'Image (LTSI – UMR 1099)

Rapporteurs avant soutenance :

Tomas Ros	Chercheur, Université de Genève
Imad ElHajj	Professor, American University of Beirut

Composition du Jury :

Président :	Prénom Nom	Fonction et établissement d'exercice (<i>à préciser après la soutenance</i>)
Examinateurs :	Claudio Babiloni	Professeur, Université de Rome
	Camille Maumet	Chargé de Recherche, INRIA, IRISA
Dir. de thèse :	Julien Modolo	Chargé de Recherche, Université de Rennes 1
	Mohamad Khalil	Professeur, Université Libanaise
Co-dir. de thèse :	Mahmoud Hassan	Chercheur et CEO de l'entreprise MINDig
	Aya Kabbara	Chercheure, Lebanese Association for Scientific Research

ANALYTICAL VARIABILITY IN ELECTROENCEPHALOGRAPHY-BASED FUNCTIONAL BRAIN NETWORKS ESTIMATION

Sahar Allouch

Under the supervision of Prof. Julien Modolo, Prof. Mahmoud Hassan, Dr. Aya Kabbara, &
Prof. Mohamad Khalil

October 25, 2022

إلى التي أرادت، سنتين خلت، ترك هذا الطريق...

To the one who wanted to quit this journey two years ago...

RESUME EN FRANÇAIS

La reproductibilité constitue depuis toujours un critère essentiel dans la méthode scientifique (Braude, 1979; Fidler & Wilcox, 2021; Munafò et al., 2017; B. A. Nosek et al., 2015; Open Science Collaboration, 2015; Schmidt, 2009; Shapin & Schaffer, 1985). Pourtant, durant la dernière décennie, de graves préoccupations concernant la reproductibilité des recherches publiées ont été soulevées (Baker, 2016; Bishop et al., 2015; Errington et al., 2021; Goodman et al., 2016; Munafò et al., 2020, 2017; Brian A. Nosek et al., 2022; Open Science Collaboration, 2015), suite à l'échec à reproduire des résultats publiés dans de nombreux domaines : l'économie, les neurosciences, la biologie évolutive, la biologie marine, la chimie organique et la psychologie (Ritchie, 2020). Ce débat sur la reproductibilité scientifique s'est accompagné par des préoccupations concernant la grande variabilité et flexibilité des approches d'analyse. En fait, en menant une étude, le(la) chercheur(e) est confronté(e) à un grand nombre de choix, souvent faits de manière arbitraire. Selon (Ioannidis, 2005), plus la flexibilité des approches analytiques est élevée, moins les résultats de recherche sont susceptibles d'être vrais. Plus précisément, la flexibilité analytique augmente la probabilité d'obtenir des faux positifs (Wicherts et al., 2016), affectant ainsi les conclusions qui pourraient être tirées d'une étude (Botvinik-Nezer et al., 2020), et entravant en fin de compte la reproductibilité des recherches scientifiques (Wicherts et al., 2016). Les risques de la haute variabilité dans les approches analytiques se traduit d'une part, par l'exploitation des degrés de liberté du chercheur (p-hacking), c'est-à-dire effectuer plusieurs analyses et modifier l'étude tout en progressant jusqu'à trouver un résultat positif significatif, puis ne rapporter que le résultat positif et l'analyse correspondante (Bishop et al., 2015; Carp, 2012; Simmons et al., 2011). D'autre part, le chercheur pourrait effectuer une seule analyse, et obtenir des résultats positifs significatifs, mais uniquement en raison de certains choix analytiques le long de la chaîne d'analyse. Cette conduite est distincte du p-hacking puisqu'aucune tentative d'atteindre une signification statistique n'est faite. Néanmoins, les résultats peuvent être entravés par des faux positifs. Par conséquent, les décisions analytiques prises sans tentative directe d'atteindre une signification statistique peuvent quand même produire une grande variabilité dans les résultats (Botvinik-Nezer et al., 2020; Carp, 2012; Silberzahn et al., 2018; Simmons et al., 2011). En raison de la haute dimensionnalité des données et de la complexité des chaînes d'analyse, le problème de la variabilité analytique est considéré prépondérant dans la recherche en neuroimagerie

(Botvinik-Nezer et al., 2020). Dans cette thèse, on est particulièrement intéressé à la question de la variabilité analytique dans le contexte de l'approche « connectivité de sources EEG ».

Les trois dernières décennies ont été marquées par une croissance explosive des études de neuroimagerie conceptualisant le cerveau humain comme étant un réseau (Bassett & Sporns, 2017; Fornito et al., 2016; Sporns, 2014). Les avancées technologiques des techniques de neuroimagerie (imagerie par résonance magnétique fonctionnelle (IRMF), électroencéphalographie (EEG), magnétoencéphalographie (MEG)), ainsi que les nouveaux outils d'analyse, ont permis une caractérisation sans précédent de la structure et de la fonction du cerveau humain. Dans ce contexte, l'EEG présente une technique de neuroimagerie directe non invasive qui mesure les potentiels électriques provenant principalement des courants intracellulaires dans les neurones pyramidaux (Grech et al., 2008; He et al., 2018) et se propageant à travers les couches du cortex, du crâne et de la peau pour être finalement enregistrés par les électrodes du cuir chevelu. L'EEG offre une technique non invasive, peu coûteuse et facile à utiliser pour capturer l'activité neuronale à l'échelle de la milliseconde (Baillet et al., 2001). A partir des signaux EEG enregistrés, on peut reconstruire les réseaux cérébraux fonctionnels au niveau cortical. Nous désignons cette approche par le terme « connectivité des sources EEG » (Hassan et al., 2015, 2014; Hassan & Wendling, 2018; Kabbara et al., 2017; Mehrkanoon et al., 2014). En bref, l'analyse « connectivité des sources EEG » se compose de deux étapes principales : (i) la reconstruction de la dynamique des sources corticales (c'est-à-dire les signaux électrophysiologiques au niveau cortical) en résolvant le problème inverse de l'EEG, et (ii) le calcul de la connectivité fonctionnelle entre les sources reconstruites. Bien que les deux étapes mentionnées ci-dessus soient relativement standard dans le domaine de la connectivité cérébrale à base EEG, des dizaines de sous-étapes y sont impliquées, et chacune d'entre elles nécessite de nombreux choix analytique souvent arbitraires. Citons à titre d'exemple, la densité spatiale (c'est-à-dire le nombre d'électrodes) du système EEG qui doit être déterminée. Puis, lors de la résolution du problème inverse, de nombreuses méthodes sont disponibles pour reconstruire la dynamique de sources corticales, chacune imposant des hypothèses et des contraintes concernant les propriétés spatiales et temporelles des sources reconstruites, sans parler des différents paramètres qui doivent être réglés pour chacun de ces algorithmes. Ceci est également valable pour les mesures de connectivité, avec des métriques évaluant diverses caractéristiques du signal (synchronisation de phase, synchronisation d'amplitude), omettant ou pas les connexions zero-lag, etc... Ces nombreux choix qui doivent être faits dans la chaîne d'analyse « connectivité des sources

EEG » sont potentiellement problématiques. Le degré de liberté élevé du chercheur pourrait entraîner une variabilité substantielle dans les résultats rapportés, ce qui, en fin de compte, entraverait la reproductibilité de la recherche sur la connectivité des sources EEG.

Ainsi, l'objectif de cette thèse est de remettre en question la variabilité analytique dans la chaîne d'analyse « connectivité des sources EEG » et ses effets sur la cohérence des résultats. Nous nous sommes principalement concentrés sur trois facteurs clés de l'analyse :

1. Le nombre d'électrodes EEG,
2. Les algorithmes de résolution du problème inverse,
3. Les mesures de connectivité fonctionnelle.

Plus précisément, nous avons abordé cette question dans cette thèse à travers trois études :

1. Dans une première étude, nous avons démontré l'intérêt de l'utilisation d'un modèle computationnel pour caractériser quantitativement la variabilité dans l'analyse « connectivité des sources EEG ». On a simulé de l'activité corticale épileptique à l'aide d'un modèle computationnel. Les signaux EEG scalp ont été générés en résolvant le problème direct (forward problem). Ensuite, on a évalué l'effet du nombre d'électrodes (19, 32, 64, 128, 256 électrodes), de deux solutions inverses (weighted minimum norm estimate (wMNE) (Fuchs et al., 1999; Lin et al., 2006), exact low-resolution brain electromagnetic tomography (eLORETA) (Pascual-Marqui, 2007)), et de deux mesures de connectivité fonctionnelle (phase-locking value (PLV) (Lachaux et al., 2000), weighted phase-lag index (wPLI) (Vinck et al., 2011)) sur la précision des réseaux corticaux reconstruits.
2. Dans une deuxième étude, on a simulé de l'activité corticale à l'état de repos (plus précisément, les réseaux « default mode network » et « dorsal attention network ») à l'aide du modèle computationnel. La correspondance entre les réseaux de référence et les réseaux estimés a été évaluée pour différents montages d'électrodes (19, 32, 64, 128, 256 électrodes), trois algorithmes de reconstruction de source (eLORETA, linearly constrained minimum variance beamforming (LCMV) (Van Veen et al., 1997), wMNE) et quatre mesures de connectivité (PLV), phase-lag index (PLI) (Stam et al., 2007), amplitude envelope correlation (AEC) avec et sans source leakage correction (Matthew J. Brookes et al., 2011; Colclough et al., 2015; Hipp et al., 2012)).
3. Dans une troisième étude, on a étudié la cohérence au niveau du groupe et la variabilité inter- et intra-sujet en utilisant des signaux EEG des sujets sains au repos. Les facteurs

étudiés comprenaient : le montage d'électrodes (19, 32, 64), l'algorithme de reconstruction de sources (eLORETA, LCMV, wMNE), et les mesures de connectivité fonctionnelles (PLV et AEC avec et sans source leakage correction, PLI, et wPLI).

Les principaux résultats de cette thèse peuvent être résumés comme suit :

1. L'analyse « connectivité des sources EEG » est largement affectée par le problème de variabilité analytique. En pratique, les choix analytiques à faire sont innombrables : par exemple, en restreignant nos choix possibles à 5 montages d'électrodes, 3 solutions inverses, et 4 mesures de connectivité, on obtient déjà 60 combinaisons à tester. Et ce, sans parler de tous les paramètres qui doivent être réglés dans chaque méthode. Une variabilité aussi importante dans la chaîne d'analyse entraîne évidemment une variabilité substantielle dans les résultats de la recherche.
2. Les modèles computationnels électrophysiologiques sont assez importants dans le contexte de l'étude de la variabilité des approches d'analyse et/ou de l'optimisation des pipelines analytiques, car ils constituent la seule solution raisonnable possible pour fournir une vérité de terrain. Il est en effet très difficile, avec la technologie actuelle, d'obtenir des acquisitions simultanées de milliers d'enregistrements au niveau du scalp et du cortex chez l'homme. Ainsi, la présence d'un véritable terrain offre la possibilité d'effectuer une évaluation précise des méthodes et des paramètres testés, ce qui est généralement impossible à réaliser avec des données EEG expérimentales.
3. Les simulations EEG de l'activité épileptique et des réseaux à l'état de repos montrent une variabilité significative des réseaux corticaux reconstruits en raison du nombre d'électrodes EEG, de la solution inverse, de la mesure de connectivité, ainsi que de la combinaison solution inverse/mesure de connectivité. Ceci a un impact direct en termes de discussion de la reproductibilité des résultats associés.
4. Nos résultats basés sur les simulations démontrent que la résolution spatiale des systèmes EEG affecte considérablement la précision des réseaux cérébraux estimés : une résolution spatiale plus élevé améliore significativement la précision des réseaux reconstruits. Nous recommandons d'utiliser au moins 64 électrodes pour estimer avec précision les réseaux corticaux basés sur l'EEG.
5. L'effet de la variabilité analytique dans l'analyse « connectivité des sources EEG » est également démontré en utilisant de l'EEG au repos chez des sujets sains. La cohérence au niveau du groupe, ainsi que la similarité inter et intra-sujets sont considérablement

affectées par le choix du nombre d'électrodes, de l'algorithme de reconstruction des sources et de la mesure de connectivité fonctionnelle.

ABSTRACT

In the debate over scientific reproducibility in the last decade, concerns have been raised regarding the significant degree of variability and flexibility in analysis approaches. This issue has gained much attention within the neuroimaging community, due to the extremely high dimensionality of data and complex analysis workflows promoting increased variability. This dissertation addresses specifically the analytical variability within a neuroimaging pipeline that is increasingly used by the research community, namely the electroencephalography (EEG) source connectivity pipeline.

Over the past two decades, there has been an increased interest in studying functional brain networks. In this context, the “EEG source connectivity” approach has emerged, offering the possibility to infer functional brain networks at the cortical level using scalp EEG data. From a methodological point of view, the EEG source connectivity, like most neuroimaging analyses, involves the processing of high dimensional data and is characterized by a complex workflow: in the course of running a study, the researcher is indeed faced with a large number of choices often made arbitrarily. Those numerous choices to be made have the potential to be problematic and produce substantial variability in results, ultimately hindering replicability in EEG source connectivity research.

Therefore, this dissertation calls into question the analytical variability in the EEG source connectivity pipeline and its effects on the consistency/discrepancy of the outcomes. We conducted two simulation-based studies and one study using experimental EEG data. Mainly, we focused on the results’ variability induced by three factors along the analysis pipeline: 1) number of EEG electrodes, 2) inverse solution algorithms, and 3) functional connectivity metrics. Our findings confirm that the EEG source connectivity analysis is largely affected by the analytical variability. EEG simulations of epileptiform and resting-state activity show significant variability in reconstructed cortical networks due to the number of EEG electrodes, inverse solution, connectivity measure, as well as inverse solution/connectivity measure combination. Our simulation results demonstrate that the spatial resolution of the sensor array dramatically affects the accuracy of network estimation: increasing spatial resolution significantly improves the accuracy of reconstructed networks. Resting-state EEG in healthy controls shows an effect of the aforementioned factors on the group-level consistency, inter-, and intra-subjects variability. We believe that this dissertation could be useful for the field of

electrophysiology connectomics, by increasing awareness regarding the challenge of variability in methodological approaches and its implications on reported results.

ACKNOWLEDGMENTS

First and foremost, all praises to Allah, the most Gracious and the Most Merciful, for His blessing and guidance which enabled me to complete this research.

I am extremely grateful for all the things I learned during this journey, not only the scientific stuff, but most importantly the things I learned about myself, my strengths, and my weaknesses.

I would like to express my deepest gratitude to my supervisors who endured this long journey, Prof. Julien Modolo, Prof. Mahmoud Hassan, and Dr. Aya Kabbara. The completion of this thesis would not have been possible without their guidance and support. I have benefited greatly from their knowledge and invaluable feedback. I highly appreciate Julien's efforts throughout this journey. Many thanks to Mahmoud for always motivating me even when I am at my lowest points. His passion for what he is doing is always inspiring. I cannot stress how much I learned from him. Aya was the first to teach me how to do science. It has been a long journey since she supervised my master's thesis. I am extremely grateful for working with her and I will always be inspired by her work. During this thesis, I also had the pleasure of working with Prof. Joan Duprez. I gratefully recognize his help throughout this thesis. I am also thankful to Prof. Mohamad Khalil who gave me the opportunity to pursue this thesis.

My deepest gratitude goes to my family: Mom, Dad, Omar, Anas, and Rida, to whom I am forever indebted. A lot of thanks to my friends, Sana, Maria, Israa, and Sahar. I couldn't imagine my journey in France without you. I also highly appreciate Hadi Abdine's unceasing help. Special thanks to Abdel Rahman Allouche for all the things I learn from him.

Lastly, I would like to acknowledge the Lebanese National Council for Scientific Research (CNRS-L), the Agence Universitaire de la Francophonie (AUF) and the Lebanese University for providing me with the financial means (doctoral scholarship) to complete this thesis.

CONTENTS

1 INTRODUCTION 1

- 1.1 TERMINOLOGY 1
- 1.2 A REPLICATION CRISIS 2
- 1.3 REPLICATION IN NEUROIMAGING RESEARCH 3
- 1.4 ANALYTICAL FLEXIBILITY AS A POTENTIAL CAUSE OF POOR REPRODUCIBILITY 4
- 1.5 ANALYTICAL FLEXIBILITY IN NEUROIMAGING RESEARCH 5
- 1.6 ANALYTICAL FLEXIBILITY IN EEG SOURCE CONNECTIVITY 6
 - 1.6.1 EEG source connectivity 6*
 - 1.6.2 Problem statement 7*
 - 1.6.3 Thesis objective 8*

2 MATERIALS AND METHODS 10

- 2.1 THE HUMAN BRAIN: A COMPLEX SYSTEM 10
- 2.2 NEUROIMAGING TECHNIQUES 12
 - 2.2.1 Functional magnetic resonance imaging (fMRI) 12*
 - 2.2.2 Magnetoencephalography (MEG) 13*
 - 2.2.3 Electroencephalography (EEG) 13*
- 2.3 EEG-BASED FUNCTIONAL NETWORKS 14
 - 2.3.1 EEG scalp connectivity and volume conduction 14*
 - 2.3.2 From scalp to source-space connectivity 15*
- 2.4 VARIABILITY IN EEG SOURCE CONNECTIVITY ANALYSIS 19
 - 2.4.1 EEG sensor density 19*
 - 2.4.2 Inverse solution 20*
 - 2.4.3 Functional connectivity 21*

3 RESULTS 24

- 3.1 STUDY I: MEAN-FIELD MODELING OF BRAIN-SCALE DYNAMICS FOR THE EVALUATION OF EEG SOURCE-SPACE NETWORKS 24
- 3.2 STUDY II: EFFECT OF CHANNEL DENSITY, INVERSE SOLUTIONS AND CONNECTIVITY MEASURES ON EEG RESTING-STATE NETWORKS: A SIMULATION STUDY 45
- 3.3 STUDY III: EFFECT OF ANALYTICAL VARIABILITY IN ESTIMATING EEG-BASED FUNCTIONAL CONNECTIVITY 82

4 DISCUSSION 123

4.1 SIMULATIONS VS EMPIRICAL DATA	124
4.2 FURTHER ASPECTS OF ANALYTICAL VARIABILITY	125
4.3 SO, WHAT NOW?... POSSIBLE SOLUTIONS	126
5 CONCLUSION	128
5.1 SUMMARY	128
5.2 FUTURE WORK	128
6 DATA AND CODE AVAILABILITY	130
7 REFERENCES	131

LIST OF FIGURES

FIGURE 1. EEG SOURCE CONNECTIVITY PIPELINE. THIS METHOD CONSISTS OF TWO MAIN STEPS: (I) RECONSTRUCTING THE DYNAMICS OF CORTICAL SOURCES (I.E., ELECTROPHYSIOLOGICAL SIGNALS AT THE CORTICAL LEVEL) BY SOLVING THE SO-CALLED EEG INVERSE PROBLEM, AND (II) COMPUTING FUNCTIONAL CONNECTIVITY BY MEASURING THE STATISTICAL COUPLING BETWEEN RECONSTRUCTED SOURCES.....	7
FIGURE 2. A) SCHEMATIC OF A GRAPH WITHIN THE GRAPH THEORY FRAMEWORK. B-F) EXAMPLES OF REAL-WORLD COMPLEX SYSTEMS REPRESENTED AS NETWORKS WHERE THE NODES REPRESENT THE SYSTEM COMPONENTS AND THE EDGES REPRESENT THE INTERACTIONS BETWEEN THOSE COMPONENTS. (B-F ADAPTED FROM (CHESWICK ET AL., 2000; GANAPATHIRAJU ET AL., 2016; MATAMALAS ET AL., 2018; McNERNEY ET AL., 2013; PARK & FRISTON, 2013), RESPECTIVELY).....	11
FIGURE 3. FUNCTIONAL NEUROIMAGING DEVICES. (IMAGE ADAPTED FROM: HTTPS://WWW.RED-DOT.ORG/KO/PROJECT/TOSHIBA-MRI-VANTAGE-TITAN-MRI-2004-30859 ; HTTPS://MEGIN.FI/TRIUX-NEO ; HTTPS://COMPUMEDICSNEUROSCAN.COM/PRODUCT/32-CHANNELS-QUIK-CAP-NEO-NET-GRAEL)	12
FIGURE 4. SPATIO-TEMPORAL RESOLUTION OF THE MOST COMMONLY EMPLOYED FUNCTIONAL NEUROIMAGING TECHNIQUES BASED ON MEASUREMENTS OF HEMODYNAMIC (fMRI, PET, SPECT) AND ELECTRICAL (EEG, MEG) BRAIN ACTIVITY (ADAPTED FROM (LAUREYS ET AL., 2002)).....	13
FIGURE 5. A) EXAMPLE OF SCALP-LEVEL FUNCTIONAL NETWORK: FUNCTIONAL CONNECTIVITY IS COMPUTED BETWEEN RECORDED EEG SIGNALS. B) SIGNAL SPREAD (VOLUME CONDUCTION) PROBLEM: DUE TO THE (ELECTROMAGNETIC) VOLUME CONDUCTION PROPERTIES OF THE HEAD, THE ACTIVITY OF A BRAIN SOURCE IS PICKED UP BY MORE THAN ONE SENSOR, RESULTING IN A WIDE REPRESENTATION OF ANY SOURCE AT THE SENSOR LEVEL.	15
FIGURE 6. EEG SOURCE CONNECTIVITY PIPELINE PROVIDING AN OVERVIEW OF THE NUMEROUS CHOICES OFFERED BY THE ANALYSIS PIPELINE. ANALYSIS STEPS INCLUDE: 1) EEG RECORDINGS. 2) EEG SIGNALS PRE-PROCESSING. 3) GAIN (LEAD FIELD) MATRIX COMPUTATION. 4) SOLVING THE INVERSE PROBLEM TO RECONSTRUCT CORTICAL ACTIVITY. 5) REGIONAL TIME SERIES EXTRACTION. 6) FUNCTIONAL CONNECTIVITY ESTIMATION.....	18

LIST OF ABBREVIATIONS AND ACRONYMS

AEC:	Amplitude envelope correlation
BOLD:	Blood-oxygen-level-dependent
DISC:	Dynamic imaging of coherent sources
EEG:	Electroencephalography
ERP:	Event-related potential
fMRI:	Functional magnetic resonance imaging
eLORETA:	Exact low-resolution brain electromagnetic tomography
LCMV:	Linearly constrained minimum variance beamforming
LORETA:	Low-resolution brain electromagnetic tomography
MEG:	Magnetoencephalography
MNE:	Minimum norm estimate
MRI:	Magnetic resonance imaging
PET:	Positron Emission Tomography
PLI:	Phase-lag index
PLV:	Phase-locked value
ROI:	Region of interest
sLORETA:	Standardized low-resolution brain electromagnetic tomography
wMNE:	Weighted minimum norm estimate
wPLI:	Weighted phase-lag index

1 INTRODUCTION

“We want to be discovering new things but not generating too many false leads.”

Marcus Munafò

Replication has long been a core feature of the scientific method (Braude, 1979; Fidler & Wilcox, 2021; Munafò et al., 2017; B. A. Nosek et al., 2015; Open Science Collaboration, 2015; Schmidt, 2009; Shapin & Schaffer, 1985). The first attempt to document replicability could be traced back to the seventeenth century when chemist Robert Boyle repeatedly demonstrated his experiments to a group of observers and then had them sign sworn testimony that they had witnessed the phenomena in question (Ritchie, 2020). Interestingly, serious concerns have been raised, in the last decade, regarding the reproducibility of published research (Baker, 2016; Bishop et al., 2015; Errington et al., 2021; Goodman et al., 2016; Munafò et al., 2020, 2017; Brian A. Nosek et al., 2022; Open Science Collaboration, 2015). Glimmers of the issue were detected across many fields, to name a few, economics, neuroscience, evolutionary biology, marine biology, organic chemistry, and psychology where the most systematic investigation of replicability rates was achieved (Ritchie, 2020).

1.1 Terminology

To begin with, a distinction is sometimes made in the literature between the terms “reproducible”, “replicable”, and “robust”. A research study is described as “reproducible” if running the same analysis over the same data results in the same outcomes (Natl. Acad. Sci. Eng. Med, 2019; Brian A. Nosek et al., 2022). Therefore, one might theoretically expect all reported -excluding fraudulent- findings to be reproducible (Brian A. Nosek et al.,

2022). “Replicability” stands for using the same analysis approach, but with different data and obtaining the same results (Natl. Acad. Sci. Eng. Med, 2019; Brian A. Nosek et al., 2022). “Robustness”, on the other hand, is achieved when the same outcomes are obtained using the same data with different analysis approaches (Brian A. Nosek et al., 2022). However, this terminological distinction does not always stand across disciplines. Definitions differ indeed from field to field, and/or terms may be used interchangeably (Baker, 2016; Bishop et al., 2015; Errington et al., 2021; Goodman et al., 2016; Munafò et al., 2020, 2017; Brian A. Nosek et al., 2022; Open Science Collaboration, 2015). In the remainder of this thesis, we chose to use those terms interchangeably.

1.2 A replication crisis

Replication has long been fundamental for establishing stability in our knowledge of nature (Radder, 1996) since it enables checking the accuracy and truth of published results (Gould & Kolb, 1964), thereby ensuring the validity of scientific findings, and that they are not the result of a mere chance (Schmidt, 2009). Accordingly, replication can be seen as a defining feature of science (Braude, 1979; Fidler & Wilcox, 2021; Munafò et al., 2017; B. A. Nosek et al., 2015; Open Science Collaboration, 2015; Schmidt, 2009; Shapin & Schaffer, 1985), its basic spirit (Ritchie, 2020).

Interestingly, serious concerns have been raised recently regarding the reproducibility and credibility of published research (Baker, 2016; Bishop et al., 2015; Errington et al., 2021; Goodman et al., 2016; Munafò et al., 2020, 2017; Brian A. Nosek et al., 2022; Open Science Collaboration, 2015). In an online survey led by the journal *Nature*, more than half of the researchers who responded stated failing to reproduce their own research findings, and more than 70% declared failing to reproduce another scientist's experiments (Baker, 2016). Replication failures were spotted by large-scale collaborative projects, such as the *Reproducibility project: Psychology* and the *Reproducibility project: cancer biology*. For instance, in an attempt to replicate 100 experimental and correlational studies in psychology, the percentage of studies showing significant results dropped from 97% in original studies to 36% in replication studies (Open Science Collaboration, 2015), and in cancer biology, when replicating 50 experiments from 23 preclinical research, the median effect size dropped by 85% as compared to the original studies (Errington et al., 2021). Further replication failures were spotted in psychology (Soto, 2019), preclinical cancer research (Begley & Ellis, 2012; Prinz et al., 2011), Amyotrophic Lateral Sclerosis (Perrin, 2014), spinal cord injury

research (Steward et al., 2012), marine biology (Clark et al., 2020), social sciences (Camerer et al., 2018), economics (Camerer et al., 2016), among others (see (Ritchie, 2020)).

1.3 Replication in neuroimaging research

Similarly to other scientific fields, the neuroimaging community was concerned with the reproducibility topic (Button et al., 2013; Niso, Botvinik-Nezer, et al., 2022; Pavlov et al., 2021; Pernet et al., 2020; Pernet & Poline, 2015; Poldrack et al., 2017, 2020). For instance, the replicability of structural brain-behavior associations was questioned in (Boekel et al., 2015; Genon et al., 2017; Kharabian Masouleh et al., 2019). (Dinga et al., 2019) failed to replicate a previous study identifying subtypes of depression based on resting-state connectivity in functional magnetic resonance imaging (fMRI). Similarly, (Geller et al., 2019) failed to replicate a previously found difference between binary and continuous measures of structural white matter associated with language function in post-stroke aphasia. Interestingly, a meta-analysis, by (Müller et al., 2017), of 99 neuroimaging studies did not reveal consistency in altered brain activity in unipolar depression. Multi-site replications in electroencephalography (EEG) studies related to linguistic prediction, musical training and neural processing of sounds, amplitude of brain activity and music beat frequencies can be found in (Bishop et al., 2015). Importantly, the #EEGManyLabs initiative (Bishop et al., 2015; Ioannidis, 2005; Munafò et al., 2017; Nuzzo, 2014; Simonsohn et al., 2014) is currently conducting a large-scale international collaboration to test the replicability of 20 of the most influential psychological EEG studies, in at least three independent laboratories. Besides individual and collaborative replication attempts, increased awareness regarding the reproducibility issue can be recognized by the many efforts suggesting guidelines and “best” practices for conducting neuroimaging studies. For instance, in (Bishop et al., 2015; Button et al., 2013; Ioannidis, 2005; Munafò et al., 2017), the authors discussed the practices that underlie poor reproducibility in fMRI studies and possible solutions to promote reliability in neuroimaging studies. Moreover, the Organization for Human Brain Mapping (OHB) developed the COBIDAS MEEG reports presenting guidelines (covering data acquisition, analysis, reporting, and data and code sharing) that enhance the reproducibility of magnetoencephalography (MEG) and EEG research (Bishop et al., 2015; Munafò et al., 2017; Wicherts et al., 2006). More recently, a review of resources supporting open and reproducible neuroimaging research (particularly MEG, EEG, magnetic resonance imaging (MRI), and positron emission tomography (PET)) from inception to publication was provided in (Niso, Botvinik-Nezer, et al., 2022).

1.4 Analytical flexibility as a potential cause of poor reproducibility

Given the high rate of replication failures, concerns have been raised regarding the credibility of published research, and an explanation for such poor reproducibility was needed. Going back to 2005, Ioannidis published a theoretical analysis examining the factors that lead to a low replication rate and claimed that “most research findings are false for most research designs and most fields” (Bishop et al., 2015; Munafò et al., 2017). Since then, there has been growing evidence that the high rates of replication failures are rooted in the scientific practice itself as well as the culture driving the scientific community. For example, scientists can be promoting low replicability in their field by, consciously or unconsciously, adopting poor scientific practices (Bishop et al., 2015). These practices include, and are not limited to, *p*-hacking (data-dredging, running multiple analyses until finding the desired significant result (Bishop et al., 2015; Ioannidis, 2005; Munafò et al., 2017; Nuzzo, 2014; Simonsohn et al., 2014)), HARKing (formulating the hypothesis after running the data analysis and reporting it as has been thought of from the beginning (Bishop et al., 2015; Kerr, 1998; Wicherts et al., 2016)), underpowered studies (small sample and effect sizes unable to reliably indicate whether an effect exists or not (Bishop et al., 2015; Button et al., 2013; Ioannidis, 2005; Munafò et al., 2017)) underspecified methods and poor data sharing (Bishop et al., 2015; Munafò et al., 2017; Wicherts et al., 2006), publication bias and omission of null results (Bishop et al., 2015; Rosenthal, 1979; Sterling, 1959), weak experimental design and/or technical errors (Bishop et al., 2015; Munafò et al., 2017), and importantly, analytical flexibility which refers the numerous analytical approaches which could be used to study the same dataset and test the same hypothesis.

In the course of running a study, the researcher is faced with a large number of choices often made arbitrarily. Those choices are known as the researcher’s “degree of freedom” (Simmons et al., 2011), and are spread out across all research phases. For instance, in (Wicherts et al., 2016), the authors presented a list of 34 degrees of freedom that psychologists have in designing, collecting, analyzing, and reporting results. Recently, the question of analytical flexibility has received much attention in many scientific fields as a potential source of poor reproducibility (Botvinik-Nezer et al., 2020; Carp, 2012; Silberzahn et al., 2018; Simmons et al., 2011; Wicherts et al., 2016). According to (Ioannidis, 2005), the higher the flexibility in analytical approaches, the less likely research findings are to be true. More specifically, analytical flexibility is thought to increase the likelihood of obtaining false positives and inflating effect sizes (Wicherts et al., 2016), hence affecting conclusions that could be drawn

from a study (Botvinik-Nezer et al., 2020), and ultimately hindering the reproducibility of scientific research (Wicherts et al., 2016).

The risks of high variability in analytical approaches are twofold. Firstly, one may chase statistical significance by taking advantage of the researcher's degrees of freedom, i.e., run several analyses and modify the study while progressing until finding a significant positive result, and then only reporting the positive result and the corresponding analysis (Bishop et al., 2015; Carp, 2012; Simmons et al., 2011). This misconduct is usually referred to as "p-hacking" (Simonsohn et al., 2014). Obviously, when running multiple analyses, the probability of rejecting the null hypothesis at a level of 5% is necessarily greater than 5% (Simmons et al., 2011). Secondly, the researcher may run only one analysis, and that analysis yields significant positive results, but only due to certain choices along the analysis pipeline. This conduct is distinct from p-hacking since no attempts to achieve statistical significance are made. Still, the results could be impeded by false positives. (Simmons et al., 2011) demonstrated how choosing dependent variables, sample size, using covariates, and reporting subsets of experimental conditions can substantially inflate the rate of false positives. Hence, analytic decisions made without direct attempts to achieve statistical significance can still produce high variability in results (Botvinik-Nezer et al., 2020; Carp, 2012; Silberzahn et al., 2018; Simmons et al., 2011).

1.5 Analytical flexibility in neuroimaging research

Due to the high dimensionality of the data and complexity of analysis workflows, analytical variability issues are thought to be prominent in neuroimaging research (Botvinik-Nezer et al., 2020). A decade ago, (Carp, 2012) estimated the flexibility of neuroimaging analysis by running 6912 analysis pipelines (10 analysis steps with 2 to 4 methods per step) on the same data. While activation significance was relatively consistent for some regions across pipelines, activations strength, location and extent were substantially variable. More recently, the sensitivity of EEG results to the variability in preprocessing strategies was investigated in (Clayson et al., 2021; Robbins et al., 2020; Šoškić et al., 2022). In (Šoškić et al., 2022), preprocessing and data cleaning steps such as high-pass filter cut-off, artifact removal method, baseline duration, reference, measurement latency, locations, and amplitude measure (peak vs. mean) were all shown to affect the outcomes in event-related potential (ERP) analysis. Similar conclusions were found in (Clayson et al., 2021) following a multiverse analysis (i.e., running the whole (or a large) set of possible analytical combinations of choices and reporting the corresponding results) assessing the impact of key preprocessing steps. Analogous efforts were

done in the fields of PET (Nørgaard et al., 2020) and diffusion MRI (Schilling et al., 2021) studies. In addition to the specific method chosen to process the data, the software package can be a substantial source of variability. This topic was more extensively tackled in fMRI studies where different analysis softwares (Bowring et al., 2019; Glatard et al., 2015), software versions (Gronenschild et al., 2012), and operating systems (Glatard et al., 2015; Gronenschild et al., 2012) were compared. Recently, (Aya Kabbara, Forde, et al., 2022) examined the degree of consistency between EEG software toolboxes used to preprocess evoked-related potentials. Inspired by the “Many analysts, one data set” project (Silberzahn et al., 2018) and following a similar approach, (Botvinik-Nezer et al., 2020) conducted a large collaborative study, named Neuroimaging Analysis Replication and Prediction Study (NARPS), in which they addressed the issue of analytical flexibility in fMRI research and its effects on the associated conclusions. Seventy independent teams were asked to analyze the same data set and test nine hypotheses. In five hypotheses, the rate of teams reporting significant results varied between 21.4% and 37.1%. A high rate of significant findings was obtained for only one hypothesis, while consistent non-significance was reported in three hypotheses. Along similar lines, the still ongoing EEGManyPipelines project focused on testing the effect of diversity of analysis pipelines in the context of EEG data (<https://www.eegmanypipelines.org>) and was launched in August 2021: different teams have been requested to analyze the same EEG data and to test a set of predefined hypotheses.

1.6 Analytical flexibility in EEG source connectivity

Along with the efforts of the neuroimaging community to investigate and quantify the effect of analytical variability in different analysis workflows, we are particularly interested, in this thesis, in the question of analytical variability in the specific context of functional brain connectivity inferred from EEG data.

1.6.1 EEG source connectivity

The past three decades have witnessed an explosive growth in neuroimaging studies conceptualizing the human brain as a network; and more specifically a highly complex, yet highly organized network (Bassett & Sporns, 2017; Fornito et al., 2016; Sporns, 2014). Technological advances in neuroimaging techniques (fMRI, EEG, MEG), along with new analytical tools, paved the way towards an unprecedented characterization of human brain structure and function. In this context, EEG presents a non-invasive direct neuroimaging technique that measures scalp electric potentials primarily originating from intracellular

currents in pyramidal neurons (Grech et al., 2008; He et al., 2018) and propagating through the cortex, skull, and skin layers to be finally recorded by scalp electrodes. Overall, EEG offers a valuable easy-to-use, low-cost, and non-invasive technique to capture neural activity at the millisecond timescale (Baillet et al., 2001). Here, we denote by “EEG source connectivity” the approach consisting in using scalp EEG to infer functional brain networks at the cortical level (Hassan et al., 2015, 2014; Hassan & Wendling, 2018; A. Kabbara et al., 2017; Mehrkanoon et al., 2014). In brief, the EEG source connectivity analysis consists of two main steps (Figure 1): (i) reconstructing the dynamics of cortical sources (i.e., electrophysiological signals at the cortical level) by solving the so-called EEG inverse problem, and (ii) computing functional connectivity between reconstructed sources (detailed description of the analysis is provided in Chapter 2).

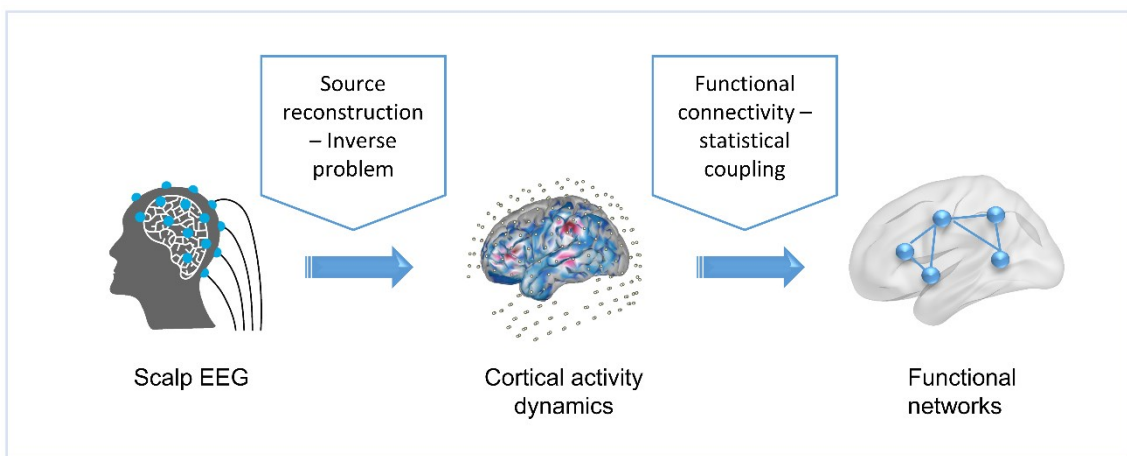


Figure 1. EEG source connectivity pipeline. This method consists of two main steps: (i) reconstructing the dynamics of cortical sources (i.e., electrophysiological signals at the cortical level) by solving the so-called EEG inverse problem, and (ii) computing functional connectivity by measuring the statistical coupling between reconstructed sources.

1.6.2 Problem statement

Although the two steps mentioned above are relatively standard in the field of EEG-based brain connectivity, combining them can be much more cumbersome than it seems in terms of choices and flexibility. Dozens of sub-steps are involved, and each entails numerous choices that are often arbitrary. For instance, during the first steps of the analysis pipeline, the spatial density (i.e., number of electrodes) of the EEG system must be determined. When solving the inverse problem, a large set of mathematical methods is available, each imposing assumptions and constraints regarding the spatial and temporal properties of the reconstructed sources, without mentioning the various parameters that require tuning for each of those algorithms. This is also

valid for connectivity measures, with metrics assessing various signal features such as phase synchronization, amplitude synchronization, omitting or keeping zero-lag connections, and a set of parameters that require tuning in each method. Therefore, the numerous choices that have to be made in the EEG source connectivity analysis pipeline are potentially problematic. The researcher's high degree of freedom could produce a substantial variability in reported results, ultimately hindering replicability in EEG source connectivity research.

1.6.3 Thesis objective

Considering the aforementioned issues, the overall goal of this thesis is to call into question the analytical variability in the EEG source connectivity pipeline and its effects on the consistency/discrepancy of the outcomes. Mainly, we focused on three key factors in the analysis:

1. Number of EEG electrodes (i.e., electrode density),
2. Inverse solution algorithms,
3. Functional connectivity metrics.

More specifically, we addressed those issues in this thesis in three studies:

1. In the first study, we aimed to provide a proof-of-concept of the interest of using a computational model to quantitatively characterize the variability in the EEG source-connectivity pipeline. Epileptiform cortical activity was simulated using a brain-scale computational model of electrophysiological source-level signals. Scalp EEGs were generated by solving the forward problem. Then, the effect of the number of electrodes (19, 32, 64, 128, 256), two inverse solutions (weighted minimum norm estimate (wMNE), exact low-resolution brain electromagnetic tomography (eLORETA)), two functional connectivity metrics (phase-locking value (PLV), weighted phase-lag index (wPLI)) on the accuracy of reconstructed cortical networks was assessed.
2. In the second study, resting-state cortical activity (more specifically, default mode and dorsal attention resting-state networks) was simulated using the aforementioned model of brain-scale electrophysiological activity. The correspondence between the reference and estimated networks was assessed for different electrode montages (19, 32, 64, 128, 256 channels), three inverse solution algorithms (eLORETA), linearly constrained minimum variance beamforming (LCMV), (wMNE)) and four connectivity measures (PLV), phase-lag index (PLI), amplitude envelope correlation (AEC) with and without source leakage correlation).

3. In a third study, with the absence of ‘ground truth’, group-level consistency, inter-, and intra-subject variability in resting-state healthy controls real EEG were assessed. The investigated factors included: electrode configurations (19, 32, 64), inverse solution (eLORETA, LCMV, wMNE), and connectivity measures (PLV and AEC with and without source leakage correction, PLI, and wPLI).

2 MATERIALS AND METHODS

2.1 The Human brain: a complex system

With more than 100 billion (10^{11}) neurons and 100 trillion (10^{14}) synapses, the human brain is considered the most complex system in the known universe (Fornito et al., 2016). Mathematically, complex systems can be studied through network science and graph theory concepts (Avena-Koenigsberger et al., 2018; Bullmore & Sporns, 2009). Thus, the human brain can be modeled as a graph or network composed of: 1) a set of nodes (vertices) representing neural elements ranging from a single synapse, a neuron, a neuronal population, or an entire brain region, and 2) a set of edges representing the structural, functional, or effective connectivity between those nodes (Avena-Koenigsberger et al., 2018; Bassett & Sporns, 2017; Fornito et al., 2016; Sporns, 2014). In brief, structural connectivity represents anatomical links (Park & Friston, 2013), that is, the set of physical or structural (synaptic) connections linking neuronal units at a given time (Sporns et al., 2004), and can be assessed using diffusion MRI. In contrast, functional connectivity does not necessarily coincide with direct neuronal communication, rather it expresses the statistical dependencies between neuronal units, without explicit reference to causal effects (Sporns et al., 2004). Functional connectivity can be inferred from blood-oxygen-level-dependent (BOLD) signals, or MEG/EEG data. Conversely, effective connectivity describes the causal effects between neuronal assemblies (Sporns et al., 2004) and refers to the influence that one neural system exerts over another, either at a synaptic or population level (Friston, 2011). Such effective connectivity is inferred by using a model of

neuronal integration and estimating the model parameters (effective connectivity) that best explain observed BOLD or EEG/MEG signals (Park & Friston, 2013). (See (Friston, 2011) for a review of functional and effective connectivity).

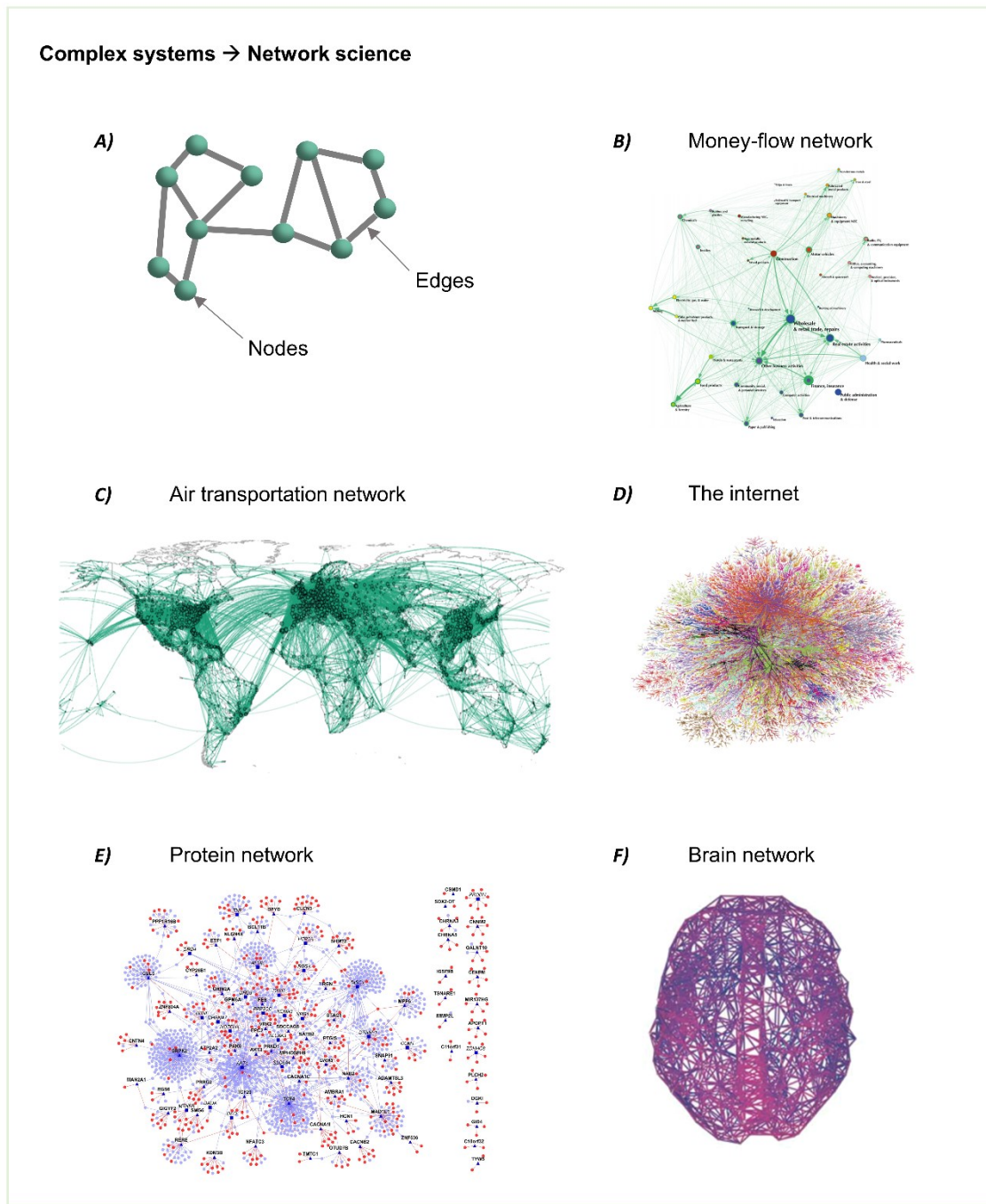


Figure 2. A) Schematic of a graph within the graph theory framework. B-F) Examples of real-world complex systems represented as networks where the nodes represent the system components and the edges represent the interactions between those components. (B-F adapted from (Cheswick et al., 2000; Ganapathiraju et al., 2016; Matamalas et al., 2018; McNerney et al., 2013; Park & Friston, 2013), respectively).

2.2 Neuroimaging techniques

Over the past two decades, there has been an increased interest in studying functional brain networks at rest (Elena A. Allen et al., 2014; Baker et al., 2014; Damoiseaux et al., 2006; de Pasquale et al., 2018; De Pasquale et al., 2016; Hipp et al., 2012; Jiao et al., 2020; A. Kabbara et al., 2017, 2021) as well as during goal-directed tasks (Bassett et al., 2011; Bola & Sabel, 2015; M. J. Brookes, Liddle, et al., 2012; Hassan et al., 2015; Kitzbichler et al., 2011; Luckhoo et al., 2012; O'Neill et al., 2017), in healthy (Elena A. Allen et al., 2014; Bassett et al., 2011; M. J. Brookes, Liddle, et al., 2012; Damoiseaux et al., 2006; Hipp et al., 2012; O'Neill et al., 2017) and pathological conditions (Damaraju et al., 2014; Gratton et al., 2018; Hassan, Chaton, et al., 2017; A. Kabbara et al., 2018; Aya Kabbara, Robert, et al., 2022; Vecchio et al., 2014; Yassine et al., 2022). This has been possible due to technological advances *in vivo* neuroimaging (fMRI, MEG, EEG) tracking mental processes as they occur.



Figure 3. Functional neuroimaging devices. (Image adapted from: <https://www.red-dot.org/ko/project/toshiba-mri-vantage-titan-mri-2004-30859>; <https://megin.fi/triux-neo>; <https://compumedicsneuroscan.com/product/32-channels-quik-cap-neo-net-grael>)

2.2.1 Functional magnetic resonance imaging (fMRI)

fMRI is a non-invasive neuroimaging technique that measures the blood oxygenation level-dependent (BOLD) signal. The amount of oxygen carried by hemoglobin affects its magnetic properties, resulting in small fluctuations that can be detected by magnetic resonance imaging (MRI) (Laureys et al., 2002). Changes in blood flow and oxygenation level occur when neurons become active. Hence, the BOLD signal can be considered a correlate of the underlying neural activity (Baillet et al., 2001). However, the exact relation through which BOLD signal models the neural activity remains unknown (Singh, 2012). Furthermore, the main limitation of fMRI resides in its inability to match the fast dynamics of the electrical neural activity. As an illustration, while an electrical signal propagates in the brain on average in 10 ms or less, the

change rate of the blood oxygenation level ranges from hundreds of milliseconds to several seconds (Laureys et al., 2002).

2.2.2 Magnetoencephalography (MEG)

In contrast to fMRI, MEG is a direct measure of brain activity that measures the extra-cranial magnetic field generated by neuronal electric currents. A major advantage of MEG is its excellent temporal resolution enabling the tracking of brain dynamics at a millisecond timescale. However, MEG suffers from a reduced spatial resolution as compared to fMRI: the number of spatial measurements is about a few hundred, versus tens of thousands in fMRI (Baillet et al., 2001). Another difficulty is that noise is a major concern in MEG due to the small magnitude of the magnetic fields generated by neuronal activity (femto-Tesla order of magnitude at the scalp level), requiring using superconducting materials for instrumental noises, gradiometers as sensing units for low-frequency artifacts, and shielded rooms made of successive layers of mu-metal, copper, and aluminum for high-frequency perturbations, all leading to a high-cost technology (Baillet et al., 2001).

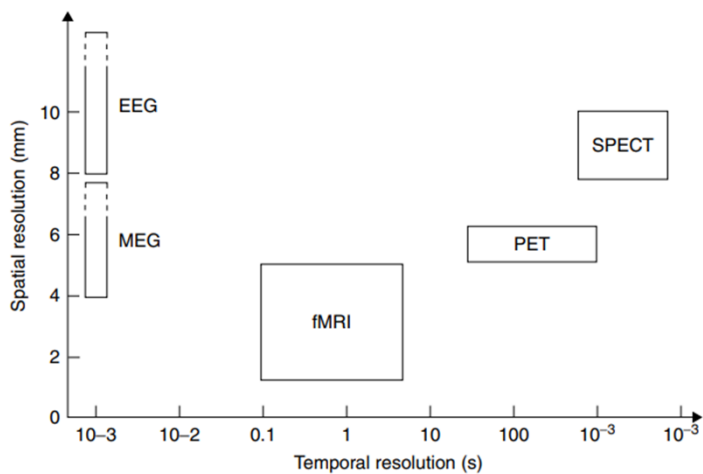


Figure 4. Spatio-temporal resolution of the most commonly employed functional neuroimaging techniques based on measurements of hemodynamic (fMRI, PET, SPECT) and electrical (EEG, MEG) brain activity (adapted from (Laureys et al., 2002)).

2.2.3 Electroencephalography (EEG)

Similar to MEG, EEG is a non-invasive direct neuroimaging technique that measures scalp-level electric potentials generated by currents of neuronal origin. Electrical currents generated by active neuronal assemblies -mainly in cortical regions- propagate through different layers (cortex, skull, and skin), and are then detected by scalp electrodes and massively amplified

(Laureys et al., 2002). Like MEG, the main advantage of EEG is its high temporal resolution, measuring neural activity at a millisecond timescale (Baillet et al., 2001), whereas spatial resolution is lower in EEG as compared to MEG (Laureys et al., 2002). The benefits of EEG, in several applications, as compared to MEG are notably the relatively low operating cost, ease of use, and portability as compared to MEG devices.

2.3 EEG-based functional networks

2.3.1 EEG scalp connectivity and volume conduction

Using EEG to analyze brain networks was originally limited to the so-called scalp connectivity (Figure 5. A)), which refers to the assessment of statistical dependencies between recorded scalp potentials (i.e., at the sensor level) (Fraschini et al., 2015; González et al., 2016; Ponten et al., 2009; Uhlhaas & Singer, 2006; Vourkas et al., 2014).. However, due to the volume conduction properties of the head, the activity of a brain source is picked up by more than one sensor, resulting in a wide representation of any source at the sensor level (Schoffelen & Gross, 2009). In other words, each channel is reflecting a superposition of activities arising from multiple, distinct cortical sources (Figure 5 B)), and hence statistical coupling computed at the sensor level may not reflect actual connectivity between distributed brain regions (Hassan & Wendling, 2018; Schoffelen & Gross, 2009). In order to mitigate signal spread (volume conduction) effects, metrics and methods that neglect or suppress zero-lag synchrony such as the imaginary coherence, imaginary part of the phase locking value, phase-slope index, the phase-lag index, the so-called signals orthogonalization method has been proposed (Brookes et al., 2012; Colclough et al., 2015; S. Palva & Palva, 2012). However, these approaches usually come at the cost of removing actual, physiologically-relevant zero-lag connections. In addition to volume conduction effects, the interpretation of sensor-level connectivity is also limited by the low spatial resolution of EEG systems and the difficulty to relate sensor connectivity to known anatomical regions (J. M. Palva et al., 2018).

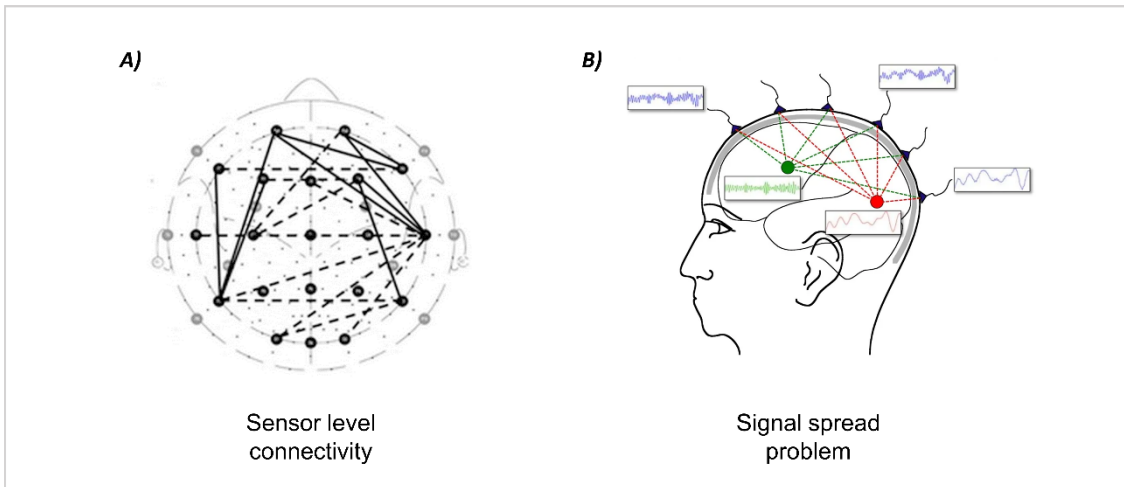


Figure 5. A) Example of scalp-level functional network: functional connectivity is computed between recorded EEG signals. B) Signal spread (volume conduction) problem: due to the (electromagnetic) volume conduction properties of the head, the activity of a brain source is picked up by more than one sensor, resulting in a wide representation of any source at the sensor level.

2.3.2 From scalp to source-space connectivity

To reduce volume conduction effects and improve spatial resolution, the “EEG source connectivity” method has been proposed (Hassan et al., 2015, 2014; Hassan & Wendling, 2018; A. Kabbara et al., 2017; Mehrkanoon et al., 2014; Schoffelen & Gross, 2009). This method consists of assessing connectivity between cortical sources, rather than between recorded EEG signals, thereby increasing spatial resolution and attenuating source-leakage (volume conduction) effects. The EEG source connectivity method involves two main steps: 1) reconstructing the temporal dynamics of cortical sources by solving the EEG inverse problem, and 2) assessing the functional connectivity between reconstructed sources (Hassan & Wendling, 2018; A. Kabbara et al., 2017). The full analysis pipeline is illustrated in Figure 6.

Solving the EEG inverse problem refers to estimating the intracranial neural activity that gives rise to recorded scalp potentials (Grech et al., 2008; He et al., 2018; Michel & Brunet, 2019). Methods developed to estimate the brain activity that best fits the recordings can be classified into *over-determined* (dipolar) models and *under-determined* (distributed) models, based on whether or not they assume a fixed number of sources (Michel et al., 2004). While the dipolar model assumes that a small number of current sources can explain EEG measurements, distributed source models do not impose an *a priori* fixed number of source points (Michel et al., 2004). Instead, current sources are distributed on the 2D cortical sheet or 3D brain volume. The source model, which provides information about the location and orientation of the dipole

sources to be estimated, can be computed from anatomical MRI segmentation (template or subject-specific MRI). Since the location of the sources is known and does not need to be estimated, the inverse problem is linear. EEG signals $X(t)$ recorded from Q channels can therefore be expressed as a linear combination of P time-varying current dipole sources $S(t)$:

$$X(t) = G \cdot S(t) + N(t) \quad (2.1)$$

where G ($Q \times P$) is the lead field (gain) matrix and $N(t)$ is the additive noise. G reflects the contribution of each cortical source to the scalp sensors and is computed from a multiple layer head model (volume conduction) and the position of the Q electrodes. For realistic head models, numeric solutions are available such as the boundary element method (Gramfort et al., 2010). Since EEG recordings primarily originate from intracellular currents in pyramidal neurons (Grech et al., 2008; He et al., 2018), the source model can be constrained to a field of current dipoles homogeneously dispersed over the cortex and normal to the cortical surface (since pyramidal cells, the largest contributor to the generation of EEG signals, are organized “en palissade” normally to the cortical surface). In this case, the inverse problem is reduced to computing the magnitude of dipolar sources $S(t)$ as follows:

$$S(t) = W \cdot X(t) \quad (2.2)$$

Due to the number of current sources that is considerably exceeding the number of electrodes ($P \times Q$), there exists mathematically an infinity of source configurations that could generate the recorded scalp EEGs, i.e., the problem is ill-posed (undetermined). Thus, mathematical and/or biophysical or electrophysiological assumptions need to be imposed to compute W and find a unique solution that fits the data (see (Awan et al., 2019; Baillet et al., 2001; Grech et al., 2008) for a review). The estimation of the W matrix is usually done on a high-resolution surface mesh (e.g., 8000 or 15000 vertices). Brain sources are then clustered into R regions of interest (ROIs), leading to R regional time series $R(t)$. ROIs are usually determined based on predefined anatomical (e.g. Desikan-Killiany atlas (Desikan et al., 2006), Destrieux atlas (Destrieux et al., 2010)) and functional (e.g., Yeo atlas (Yeo et al., 2011)) atlases, or data-driven parcellations (Calhoun & Adali, 2012). Several approaches can be used to extract a single time series representative of an ROI: signal averaging, power averaging, selecting the maximum value at each time point, keeping the first mode of the principal component analysis...

The next step following the reconstruction of cortical dynamics is to assess functional connectivity, i.e., statistical interdependence between spatially distant brain regions (Friston, 2011). A plethora of methods have been proposed in the literature to assess the statistical coupling between regional time series. Those methods can be either linear or nonlinear, parametric or nonparametric, based on phase and/or amplitude synchronization, computed in time and/or frequency domain, robust or prone to source leakage (see (Cao et al., 2022; Friston, 2011; Pereda et al., 2005) for a review)... At the end of this step, an $R \times R$ matrix is obtained, where each entry a_{ij} of the matrix is equal to the weight of the connection linking node (i.e., ROI) i to node j .

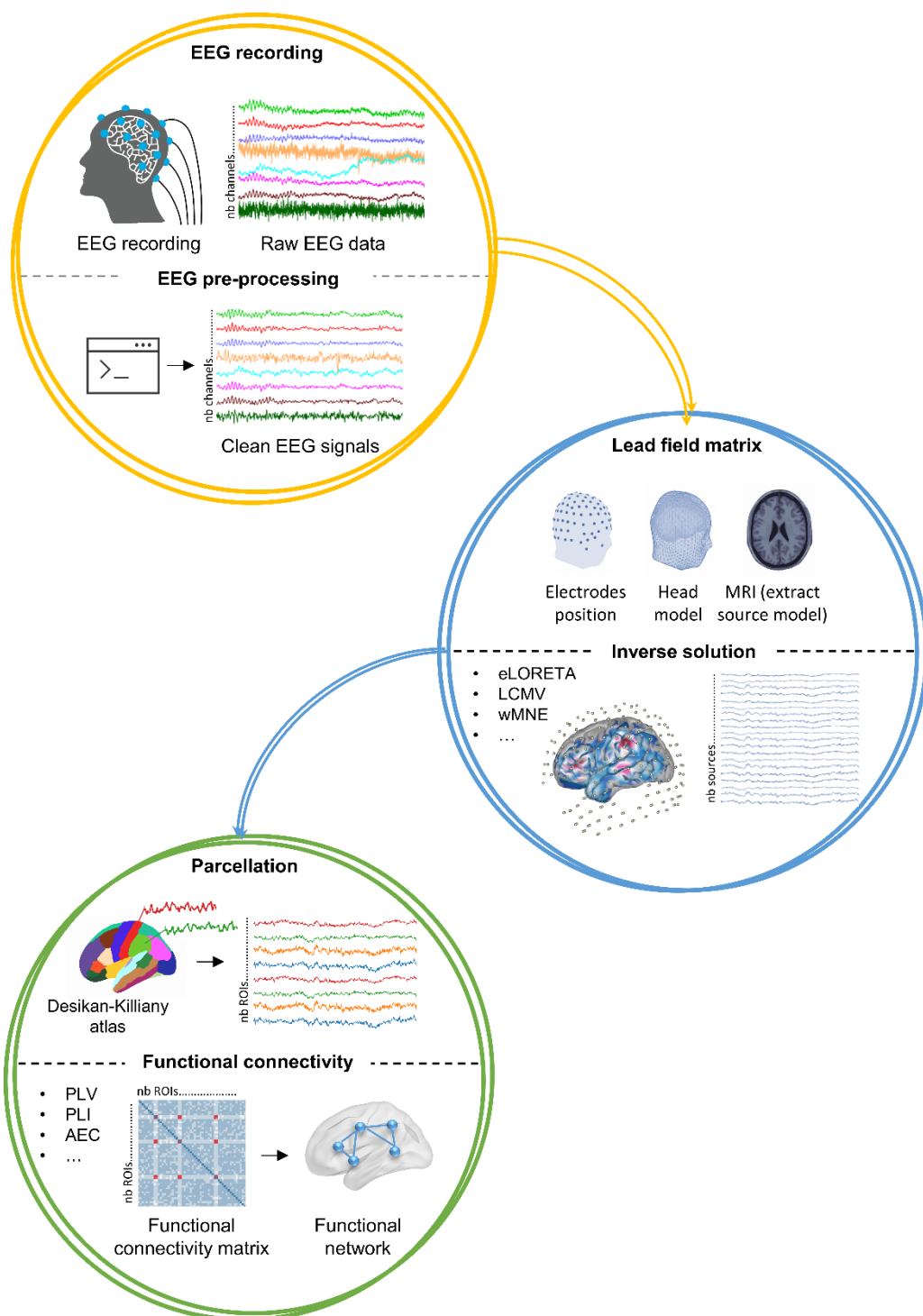


Figure 6. EEG source connectivity pipeline providing an overview of the numerous choices offered by the analysis pipeline. Analysis steps include: 1) EEG recordings. 2) EEG signals pre-processing. 3) Gain (lead field) matrix computation. 4) Solving the inverse problem to reconstruct cortical activity. 5) Regional time series extraction. 6) Functional connectivity estimation.

2.4 Variability in EEG source connectivity analysis

Each of the steps described above entails several flexible choices, leaving the researcher with a relatively high degree of freedom while conducting their analysis. We hypothesize that such analytical flexibility can induce substantial variability in the reported results, ultimately hindering research replicability. Hereafter, we elaborate on the researcher's choices related to 1) EEG sensor density, 2) inverse solution algorithm, and 3) functional connectivity measure. The variability induced in the results by those three key factors was investigated in this thesis.

2.4.1 EEG sensor density

As aforementioned, the spatial density of standard EEG systems ranges from 19 to 256 sensors. Several studies investigated the effect of the number of electrodes on EEG source localization in simulations in the context of epilepsy (Goran Lantz et al., 2003; Sohrabpour et al., 2015; Song et al., 2015). More specifically, it has been shown that the number of EEG electrodes has a direct influence on the localization error: as intuitively expected, a higher number of electrodes is associated with a significant decrease in localization error (Goran Lantz et al., 2003; Sohrabpour et al., 2015; Song et al., 2015). In both studies by (Goran Lantz et al., 2003) and (Sohrabpour et al., 2015), a dramatic decrease in localization error occurred when increasing the number of electrodes from 32 to 64. As established in (Srinivasan et al., 1998), an accurate characterization of the spatial electrophysiological information requires a high number of electrodes: a high inter-electrode distance (i.e., corresponding to a low number of EEG electrodes) can induce aliasing, and therefore high spatial frequency signals are misrepresented as low spatial frequency signals due to the violation of the Nyquist criteria ($F_s > 2 * F_{max}$) (Song et al., 2015; Srinivasan et al., 1998). It is worth mentioning that in (Song et al., 2015) results were found to be independent of the inverse method (minimum norm/standardized low-resolution brain electromagnetic tomography). On the other hand, (Goran Lantz et al., 2003) showed that 63 electrodes were sufficient for decent source localization with EPIFOCUS (a linear inverse solution that optimally localizes single focal sources (Grave de Peralta Menendez et al., 2001; G. Lantz et al., 2001)), however, 100 electrodes were required when using the wMNE. In the three studies that we led and that are at the core of this thesis manuscript, we assessed the effect of the number of electrodes on the EEG network reconstruction.

2.4.2 Inverse solution

Another critical influencing factor in the EEG source connectivity analysis is the algorithm chosen to solve the inverse problem. Several studies quantifying the performance of different inverse methods, in simulated and experimental EEG/MEG data, concluded that the choice of the inverse method significantly influences source estimation results (Anzolin et al., 2019; Bradley et al., 2016; Grova et al., 2006; Halder et al., 2019; Hedrich et al., 2017; Mahjoory et al., 2017; Tait et al., 2021). However, no consistent conclusions have been made regarding one specific method that would stand apart from the others in terms of performance. For example, (Anzolin et al., 2019) showed that LCMV had a better performance globally as compared to eLORETA. Similarly, in (Mahjoory et al., 2017), a relatively strong difference was found between LCMV beamformer on one hand, and eLORETA/wMNE solutions on the other hand. In (Hedrich et al., 2017), the coherent maximum entropy on the mean showed similar localization error to MNE, dynamic statistical parametric mapping, sLORETA, but lower spatial spread. In (Bradley et al., 2016), the use of LORETA for source localization outperformed sLORETA and minimum norm least square. Following an extensive comparison between six inverse methods, (Grova et al., 2006) recommended taking into account results from different methods when localizing actual interictal spikes. Results of source localization in (Halder et al., 2019) did not identify a clear winner between LCMV, eLORETA, MNE, and the dynamic imaging of coherent sources (DISC). (Tait et al., 2021) summarized the conditions where each method can be recommended, following comparison of six inverse methods in resting-state MEG data. In the studies presented in this thesis, we chose to test the variability in the networks obtained using the weighted minimum norm estimate (wMNE) (Fuchs et al., 1999; Lin et al., 2006), exact low-resolution brain electromagnetic tomography (eLORETA) (Pascual-Marqui, 2007), and linearly constrained minimum-variance (LCMV) beamformer (Van Veen et al., 1997).

i. Weighted minimum norm estimate (wMNE)

The minimum norm estimate, initially proposed by (Hämäläinen & Ilmoniemi, 1994) and widely used in EEG source imaging, searches for a solution that fits the data while having the minimum energy (minimum least-square error, L2-norm). An intrinsic consequence of this constraint is a bias toward superficial sources generating strong fields with less energy due to their vicinity to electrodes (He et al., 2018; Michel & Brunet, 2019). To compensate for the tendency of MNE to favor weak and surface sources, the weighted minimum norm estimate (wMNE) (Fuchs et al., 1999; Lin et al., 2006) sets the diagonals of B (eq. 2.4) inversely

proportional to the norm of the lead field vectors, essentially assuming a priori that sources that only weakly influence M/EEG must have a higher variance to be measured by sensors (Tait et al., 2021).

$$W_{MNE} = BG^T(GBG^T + \lambda C)^{-1} \quad (2.3)$$

where λ is the regularization parameter and C is the noise covariance matrix.

$$B_{ij} = \begin{cases} (G_i^T G_i)^{1/2} & \text{if } i = j \\ 0 & \text{if } i \neq j \end{cases} \quad (2.4)$$

ii. Exact low-resolution brain electromagnetic tomography (eLORETA)

eLORETA belongs to the family of weighted minimum norm inverse solutions. In addition to compensating for depth bias, it also has exact zero error localization in the presence of measurement and structured biological noise (determined by the physical properties of the head model and the laws of electrodynamics (dealing with the effects arising from the interactions of electric currents with magnets, with other currents, or with themselves)) (Pascual-Marqui, 2007):

$$B_{ij} = \begin{cases} (G_i^T(G_i B G_i^T + \lambda C)^{-1})^{1/2} & \text{if } i = j \\ 0 & \text{if } i \neq j \end{cases} \quad (2.5)$$

iii. Linearly constrained minimum-variance (LCMV) beamformer

Beamformers (a.k.a. spatial filters or virtual sensors), originally established in radar and sonar signal processing, are now widely used in source imaging, mainly with MEG data (Michel et al., 2004). The basic idea of beamformer approaches is to discriminate between signals arriving from a location of interest, and those originating elsewhere (Baillet et al., 2001). Specifically, the LCMV beamformer (Van Veen et al., 1997) estimates the activity for a source at a given location while simultaneously suppressing (i.e., setting null values) contributions from all other sources and noise captured in the data covariance:

$$W_{LCMV} = ((G^T \cdot (C + \lambda \cdot I)^{-1}) \cdot G)^{-1} \cdot (G^T \cdot (C + \lambda \cdot I)^{-1}) \quad (2.6)$$

2.4.3 Functional connectivity

The choice of the functional connectivity metric is also a critical step when reconstructing brain networks. A wide range of measures are used in the field, and each differs in the aspect of data

that is being investigated (linear/non-linear, amplitude/phase- synchronization, time/spectral domain, prone/robust to source leakage, etc...), (see (Cao et al., 2022; Friston, 2011; Pereda et al., 2005) for a review), resulting in significant variability of performance and interpretations (Colclough et al., 2016; Hassan, Merlet, et al., 2017; H. E. Wang et al., 2014; Wendling et al., 2009). (Colclough et al., 2016) assessed the consistency of different measures in experimental MEG resting-state data and recommended using the correlation between orthogonalized, band-limited, power envelopes (AEC). On the other hand, following extensive simulation studies, (H. E. Wang et al., 2014) and (Wendling et al., 2009) both concluded that there is no ideal “one-fits-all” method for all data types: it was rather suggested to evaluate which conditions are appropriate for each method. In (Hassan et al., 2014) and (Hassan, Merlet, et al., 2017), in the context of epileptic spikes, wMNE combined with PLV had better accuracy as compared to other algorithms. Since our intent in the context of this thesis was not to present an exhaustive comparison between all available metrics, our studies covered, in total, five metrics that are widely used in EEG source connectivity: the phase-locking value (PLV) (Lachaux et al., 2000), phase-lag index (PLI) (Stam et al., 2007), weighted phase-lag index (Vinck et al., 2011) and amplitude envelope correlation (AEC) with and without source leakage correction (Colclough et al., 2015, 2016; Hipp et al., 2012).

i. Phase-locking value (PLV)

For two signals $x(t)$ and $y(t)$, the phase-locking value (Brookes et al., 2012) is defined as:

$$PLV = |E\{e^{i(\phi_x(t)-\phi_y(t))}\}| \quad (2.7)$$

where $E\{\cdot\}$ is the expected value operator, and (t) is the instantaneous phase derived from the Hilbert transform.

ii. Phase-lag index (PLI)

The PLI as originally proposed by (Stam et al., 2007) is a measure of the asymmetry of the distribution of phase differences between two signals. PLI aims at overcoming the issue of source leakage by discarding phase differences centered around 0 and π , i.e., removing zero-lag connections. It is therefore an estimation of the extent on non-equiprobability of phase leads and lags between signals (Vinck et al., 2011). For two signals $x(t)$ and $y(t)$, PLI is defined as follows:

$$PLI = |E\{sign(\phi_x(t) - \phi_y(t))\}| \quad (2.8)$$

where $E\{\cdot\}$ is the expected value operator, and $\phi(t)$ is the instantaneous phase derived from the Hilbert transform.

iii. Weighted phase-lag index (wPLI)

The weighted phase-lag index attempts to further weight the metric away from zero-lag contributions (Vinck et al., 2011). The contribution of observed phase leads and lags is weighted by the magnitude of the imaginary component of the cross-spectrum. This results in reduced sensitivity to additional, uncorrelated noise sources and increased statistical power to detect changes in phase-synchronization. wPLI is mathematically defined as follows:

$$wPLI = \frac{|E\{|imag\{x\}|sign(imag\{x\})\}|}{E\{|imag\{x\}|\}} \quad (2.9)$$

where $imag\{x\}$ denotes the imaginary part of the signal's cross-spectrum.

iv. Amplitude envelope correlation (AEC)

AEC denotes the Pearson correlation between the signals' envelopes derived from the Hilbert transform (Matthew J. Brookes et al., 2011; Hipp et al., 2012).

v. AEC and PLV with source leakage correction

Zero-lag signal overlaps are removed by regressing out (orthogonalizing with respect to) the linear projection of the regional time course (Brookes et al., 2012) or by using a multivariate symmetric orthogonalization approach: the closest orthonormal matrix to the uncorrected regional time courses is first computed; then the magnitudes of the orthogonalized vectors are adjusted iteratively to minimize the least-squares distances between corrected and uncorrected signals (Colclough et al., 2015). Following the orthogonalization procedure, AEC or PLV are computed between corrected time courses.

In this Chapter, we covered the details of the EEG source connectivity analysis and the specific methods we tested. In the following Chapter, we present a summary of each study that we conducted, followed by the corresponding article.

3 RESULTS

3.1 Study I: Mean-Field Modeling of Brain-Scale Dynamics for the Evaluation of EEG Source-Space Networks

Study status: **Published** in *Brain Topography*, 35(1), 54–65. <https://doi.org/10.1007/s10548-021-00859-9>



Mean-Field Modeling of Brain-Scale Dynamics for the Evaluation of EEG Source-Space Networks

Sahar Allouch^{1,2} · Maxime Yochum¹ · Aya Kabbara¹ · Joan Duprez¹ · Mohamad Khalil^{2,4} ·
Fabrice Wendling¹ · Mahmoud Hassan³ · Julien Modolo¹

Received: 15 September 2020 / Accepted: 18 June 2021

© The Author(s), under exclusive licence to Springer Science+Business Media, LLC, part of Springer Nature 2021

Abstract

Understanding the dynamics of brain-scale functional networks at rest and during cognitive tasks is the subject of intense research efforts to unveil fundamental principles of brain functions. To estimate these large-scale brain networks, the emergent method called “electroencephalography (EEG) source connectivity” has generated increasing interest in the network neuroscience community, due to its ability to identify cortical brain networks with satisfactory spatio-temporal resolution, while reducing mixing and volume conduction effects. However, no consensus has been reached yet regarding a unified EEG source connectivity pipeline, and several methodological issues have to be carefully accounted to avoid pitfalls. Thus, a validation toolbox that provides flexible “ground truth” models is needed for an objective methods/parameters evaluation and, thereby an optimization of the EEG source connectivity pipeline. In this paper, we show how a recently developed large-scale model of brain-scale activity, named COALIA, can provide to some extent such ground truth by providing realistic simulations of source-level and scalp-level activity. Using a bottom-up approach, the model bridges cortical micro-circuitry and large-scale network dynamics. Here, we provide an example of the potential use of COALIA to analyze, in the context of epileptiform activity, the effect of three key factors involved in the “EEG source connectivity” pipeline: (i) EEG sensors density, (ii) algorithm used to solve the inverse problem, and (iii) functional connectivity measure. Results showed that a high electrode density (at least 64 channels) is required to accurately estimate cortical networks. Regarding the inverse solution/connectivity measure combination, the best performance at high electrode density was obtained using the weighted minimum norm estimate (wMNE) combined with the weighted phase lag index (wPLI). Although those results are specific to the considered aforementioned context (epileptiform activity), we believe that this model-based approach can be successfully applied to other experimental questions/context. We aim at presenting a proof-of-concept of the interest of COALIA in the network neuroscience field, and its potential use in optimizing the EEG source-space network estimation pipeline.

Keywords Neural mass models · Electroencephalography · EEG sensor density · Inverse problem · Functional connectivity · Network neuroscience

Handling Editor: Katharina Glomb.

Mahmoud Hassan and Julien Modolo have equally contributed.

This is one of several papers published together in Brain Topography on the “Special Issue: Computational Modeling and M/EEG”.

Sahar Allouch
saharallouch@gmail.com

¹ Univ Rennes, LTSI - INSERM U1099, 35000 Rennes, France

² Azm Center for Research in Biotechnology and Its Applications, EDST, Tripoli, Lebanon

Introduction

There is now growing evidence suggesting that large-scale functional brain networks underlie complex brain functions during rest (Allen et al. 2014; Kabbara et al. 2017) and tasks (Hassan et al. 2015; O’Neill et al. 2017). Among the

³ NeuroKyma, 35000 Rennes, France

⁴ CRSI Research Center, Faculty of Engineering, Lebanese University, Beirut, Lebanon

neuroimaging techniques used to derive the functional brain networks, the electroencephalography (EEG) technique provides a direct measure of electrical brain activity at the millisecond time scale. The past years have seen a noticeable increase of interest in “EEG source connectivity” methods to estimate brain networks at the cortical sources level while minimizing the volume conduction and field spread problems. Although consisting only of two main steps: (1) source reconstruction, and (2) connectivity assessment, there is still no consensus on a unified pipeline adapted to this approach, and many methodological questions remain unanswered. A first issue lies at the very first step of data recording with the question of optimal spatial resolution (i.e., density of sensors) needed to avoid misrepresentation of spatial information of brain activity (Song et al. 2015; Srinivasan et al. 1998). Another issue concerns the subsequent analysis: for each of the steps, a large number of methods are available, each having its own properties, advantages and drawbacks, and addressing a different aspect of the data. An additional parameter warranting investigation is the spatial resolution of the reconstructed cortical sources (i.e., number of regions of interest) ranging from dozens to thousands of regions.

To tackle those challenges, several comparative studies have been conducted with the aim of evaluating the performance of the adopted techniques and the influence of different parameters affecting the network estimation procedure (Anzolin et al. 2019; Colclough et al. 2016; Fornito et al. 2010; Halder et al. 2019; Lantz et al. 2003; Sohrabpour et al. 2015; Song et al. 2015; Wang et al. 2009). In the context of EEG, several studies investigated the effect of different electrode montages on the estimation of functional connectivity. Increasing the number of electrodes has been shown to decrease the localization error in different contexts (Lantz et al. 2003; Sohrabpour et al. 2015; Song et al. 2015). Song et al. (2015) recommended using 128 or 256 electrodes, while in (Sohrabpour et al. 2015) the most dramatic decrease in localization error was obtained when going from 32 to 64 electrodes. Other studies have focused on evaluating the performance of different inverse solutions using simulated and real EEG signals (Anzolin et al. 2019; Bradley et al. 2016; Grova et al. 2006; Halder et al. 2019). Compared methods include those based on the minimum norm estimate (MNE, LORETA, sLORETA, eLORETA, etc.) as well as beamformers (DICS, LCMV). However, to the best of our knowledge, there is no consensus yet on which inverse solution provides the most accurate results when estimating EEG source-space networks. In the context of functional connectivity, the performance of various measures covering direct/indirect causal relations, marginal/partial associations, leakage correction, amplitude/phase coupling have been evaluated, and compared using either real data (Colclough et al. 2016), or simulated data in (Wang

et al. 2014; Wendling et al. 2009). Nevertheless, no agreement has been reached on which connectivity measure to adopt.

A challenging issue in such comparative studies resides in the absence of a ‘ground truth’ when dealing with real EEG data. Ideally, simultaneous scalp EEG and depth (intracranial) recordings are needed, which is challenging to perform and is therefore unavailable in most studies. Thus, to overcome this issue, one possible solution is to use simulated data. It is worth mentioning that many studies have attempted to provide a ground truth for the validation of source reconstruction and connectivity estimation algorithms. For example, in (Schelter et al. 2006), a toy model was used in which the signal was considered as an oscillator and was driving the activity of other structures. However, this approach is limited in terms of spectral properties. A frequently adopted method is the use of multivariate autoregressive (MVAR) models as generator filters, in combination along with volume conductor head models to generate pseudo-EEG data (Anzolin et al. 2019; Haufe and Ewald 2016). However, such models are linear and too simple compared to the complexity of actual brain activity. Another solution that overcomes some of the limitations of previous methods is the use of physiologically-inspired models. Here, we use a computational model named “COALIA” (Bensaid et al. 2019), able to generate realistic brain-scale, cortical-level simulations while accounting for macro- (main anatomic connections between distinct cortical regions) as well as the micro-circuitry (between the main cellular types within a single, specific region) of the human cortex, including the specificities of each neuronal type within each region. Scalp EEG signals can be then obtained through solving the EEG forward problem. We highlight the implications of this model in enhancing our interpretation of the reconstructed brain networks and in evaluating the key factors of the EEG source connectivity pipeline, such as (1) EEG sensor density, (2) solution of the EEG inverse problem, and (3) functional connectivity measure.

Here, we generate epileptiform, cortical activity (confined to the left hemisphere) and present a (not exhaustive) comparative study to evaluate, in this specific context, the effect of: (1) five different electrode densities (256, 128, 64, 32, 19); (2) two inverse solution algorithms, the weighted minimum norm estimate (wMNE) and the exact low resolution electromagnetic tomography (eLORETA); and (3) two functional connectivity measures, the phase locking value (PLV) and the weighted phase lag index (wPLI) as they represent one of the most used combination of methods in the context of EEG source-space network estimation. We believe that the present study can be extended to address other methodological/experimental questions related to source connectivity estimation. We aim at presenting a proof-of-concept of

the interest of COALIA in the network neuroscience field, and its potential use in optimizing the EEG source-space network estimation pipeline.

Materials and Methods

The full pipeline of our study is summarized in Fig. 1.

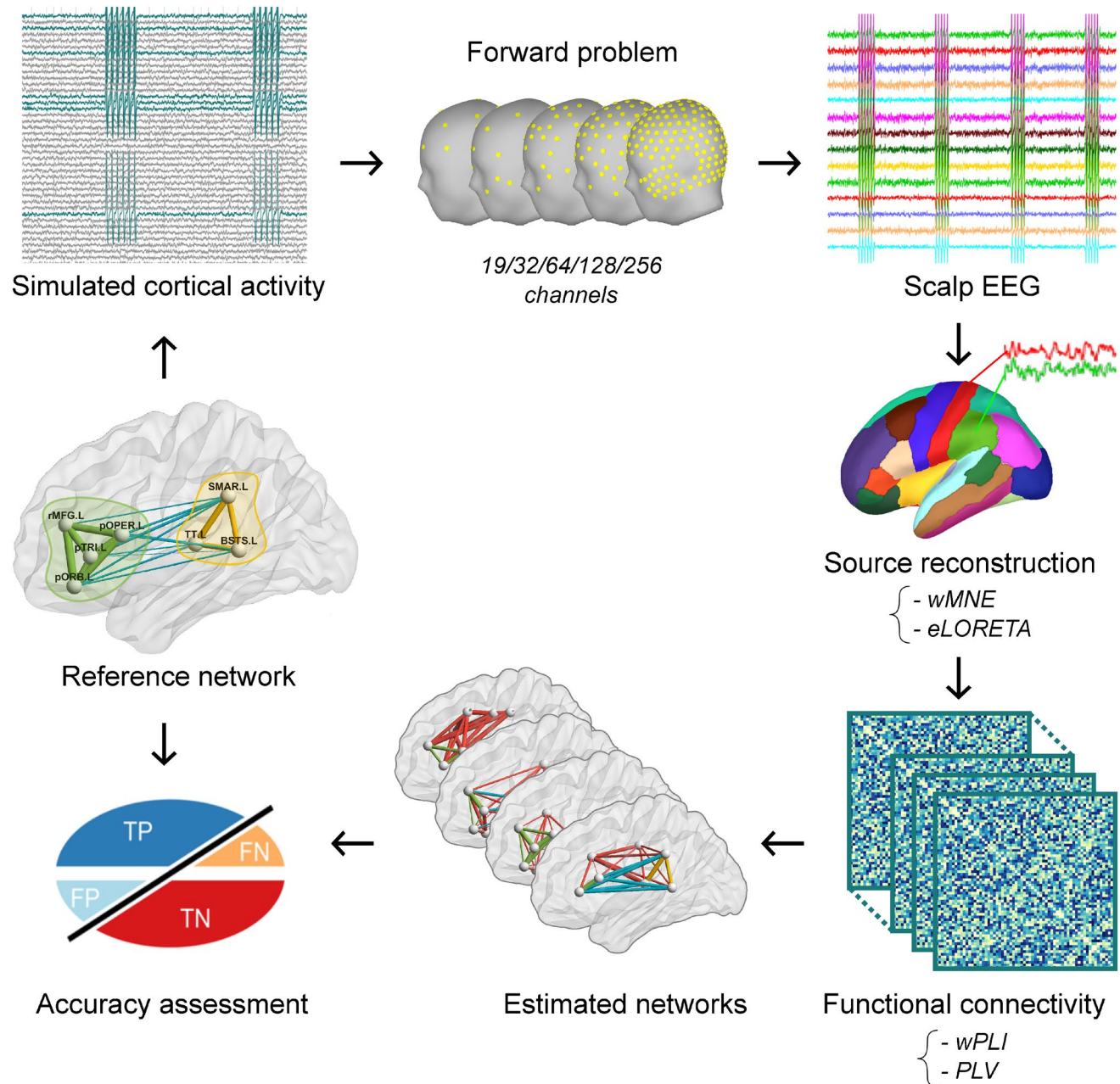


Fig. 1 Pipeline of the study. Cortical sources were simulated using COALIA. The forward model was solved for five electrode montages (19, 32, 64, 128, 256 electrodes). Scalp EEG signals were generated. Cortical sources were reconstructed using wMNE and eLORETA as inverse solutions. Functional connectivity between reconstructed

Simulations

Source-space brain activity was generated using a physiologically-grounded computational model, named COALIA. It generates brain-scale electrophysiology activity while accounting for the macro- (between regions) as well as the micro-circuitry (within a single region) of the brain [for details, see (Bensaïd et al. 2019)]. We considered a scenario inspired from a general scheme of the organization of human

sources was assessed over 30 trials using PLV and wPLI algorithms. Accuracy was computed to assess the performance of the network estimation. *wMNE* weighted minimum norm estimate; *eLORETA* exact low-resolution electromagnetic tomography; *PLV* phase-locking value; *wPLI* weighted phase lag index

partial seizures presented in (Bartolomei et al. 2013), and proposing the existence of an epileptogenic subnetwork as well as a propagation subnetwork. In the present study, the two subnetworks were located in the left hemisphere. The epileptogenic subnetwork included four cortical regions: the rostral middle frontal gyrus, pars opercularis, pars triangularis, and pars orbitalis; the propagation subnetwork included the supramarginal, banks superior temporal sulcus, and transverse temporal cortex. Regions affiliations were based on the Desikan–Killiany atlas (Desikan et al. 2006). Epileptiform activity was generated in the epileptogenic and propagation subnetworks, while background activity was assigned to the remaining cortical regions. A detailed description of the model along with all simulation parameters relative to the data are provided in the Supplementary Materials (See Table S1) and the generated source signals are publicly available. All sources belonging to a single patch were synchronized at a zero lag, while a delay of 30 ms was introduced between the two subnetworks to reflect the propagation of spikes between relatively distant regions in the brain. A timeseries of ~6 min at 2048 Hz was simulated, and was segmented into 10-s epochs. A total of 30 epochs was selected for the subsequent analysis. This value was chosen based on a previous study (Hassan et al. 2017), dealing with similar issues based on computational modeling and epileptic spikes.

EEG Electrodes Density and Direct Problem

Five different electrode montages were used to generate scalp EEG signals. We selected the GSN HydroCel EEG configuration (EGI, Electrical geodesic Inc) for the 256, 128, 64 and 32 channels density, as well as the international 10–20 system (Klem et al. 1999) for the 19 channels array. For each electrode configuration, the lead field matrix describing the electrical and geometrical characteristics of the head was computed for a realistic head model using the Boundary Element Method (BEM) provided by Brainstorm (Tadel et al. 2011) within the OpenMEG package (Gramfort et al. 2010). To generate simulated EEG data, we solved the forward problem as follows:

$$X(t) = G.S(t) \quad (1)$$

where $S(t)$ represents the cortical timeseries, and G the lead field matrix. We used only the lead field vectors reflecting the contribution of the sources located at the centroid of the regions of interest defined on the basis of the Desikan–Killiany atlas (Desikan et al. 2006) (right and left insula were excluded, leaving 66 regions of interest).

Finally, in order to simulate measurement noise, spatially and temporally uncorrelated signals were added to the scalp EEG as follows (Anzolin et al. 2019):

$$X_{noisy}(t) = \gamma \times \frac{X(t)}{\|X(t)\|_F} + (1 - \gamma) \times \frac{n(t)}{\|n(t)\|_F} \quad (2)$$

where $X(t)$ are the scalp EEG and $n(t)$ is the white uncorrelated noise. $\|X(t)\|_F$ and $\|n(t)\|_F$ refers to the Frobenius norm of the multivariate time series $X(t)$ and $n(t)$ respectively. First, γ was fixed to 1 (i.e., no measurement noise was added). Second, for evaluating the different methods in the presence of noise, γ was varied between 0.85 and 0.95 with a 0.01 step.

EEG Inverse Problem

Solving the EEG inverse problem consists of estimating the position, orientation and magnitude of dipolar sources $\hat{S}(t)$. Cortical sources were positioned at the centroids of Desikan–Killiany regions, and oriented normally to the cortical surface. Thus, the inverse problem was reduced to the computation of the magnitude of dipolar sources $\hat{S}(t)$:

$$\hat{S}(t) = W.X(t) \quad (3)$$

where $X(t)$ is the scalp EEG. Several algorithms have been proposed to solve this problem and estimate W based on different assumptions related to the spatiotemporal properties of the sources and regularization constraints [see (Awan et al. 2019; Baillet et al. 2001; Grech et al. 2008) for a review]. Here, we used two methods widely used in EEG source connectivity analysis: the weighted minimum norm estimate (wMNE) and the exact low-resolution electromagnetic tomography (eLORETA).

Weighted Minimum Norm Estimate (wMNE)

The minimum norm estimate (MNE) originally proposed by (Hämäläinen and Ilmoniemi 1994) searches for a solution that fits the measurements with a least square error. The wMNE (Fuchs et al. 1999; Lin et al. 2006) compensates for the tendency of MNE to favor weak and surface sources:

$$W_{wMNE} = BG^T(GBG^T + \lambda C)^{-1} \quad (4)$$

where λ is the regularization parameter and C is the noise covariance matrix computed, in our case, from the pre-spikes baselines extracted from all trials and concatenated (4 s * 30 trials). The matrix B is a diagonal matrix built from matrix G with non-zero terms inversely proportional to the norm of lead field vectors. It adjusts the properties of the solution by reducing the bias inherent to the standard MNE solution:

$$B_{ij} = \begin{cases} (G_i^T G_i)^{1/2} & \text{if } i = j \\ 0 & \text{if } i \neq j \end{cases} \quad (5)$$

Exact Low-Resolution Brain Electromagnetic Tomography (eLORETA)

The exact low-resolution electromagnetic tomography (eLORETA) belongs to the family of weighted minimum norm inverse solutions. However, it does not only account for depth bias, it also has exact zero error localization in the presence of measurement and structured biological noise (Pascual-Marqui 2007):

$$B_{ij} = \begin{cases} \left(G_i^T (G_i B G_i^T + \lambda C)^{-1} G_i \right)^{1/2} & \text{if } i = j \\ 0 & \text{if } i \neq j \end{cases} \quad (6)$$

eLORETA was originally described using the whole brain volume as source space. However, in the present study, in order to facilitate the comparison with other methods, we restricted the source space to the cortical surface. Regarding the regularization parameters of wMNE and eLORETA, we used default values included in Brainstorm and fieldtrip toolboxes.

Connectivity Measures

We evaluated in this study two of the most popular connectivity metrics, both based on the assessment of the phase synchrony between regional time-courses, namely PLV (phase-locking value) and PLI (phase-lag index), as detailed below.

Phase-Locking Value

For two signals $x(t)$ and $y(t)$, the phase-locking value (Lachaux et al. 2000) is defined as:

$$PLV = \left| E\{e^{i|\varphi_x(t) - \varphi_y(t)|}\} \right| \quad (7)$$

Where $E\{\cdot\}$ is the expected value operator and $\varphi(t)$ is the instantaneous phase derived from the Hilbert transform.

Weighted Phase-Lag Index

While the phase-lag index (PLI) quantifies the asymmetry of the phase difference, rendering it insensitive to shared signals at zero phase lag (Stam et al. 2007) that supposedly induce spurious volume conduction effects, the weighted

$$wPLI = \frac{|E\{|Im\{X\}| sign(Im\{X\})\}|}{E\{|Im\{X\}|\}} \quad (8)$$

where $Im\{X\}$ denotes the imaginary part of the signal's cross-spectrum.

Connectivity matrices were computed in broadband [1–45 Hz] for all considered electrode densities and possible inverse solution/connectivity combinations, resulting in 20 connectivity matrices for each epoch. The resulting matrices were thresholded by keeping nodes with the highest 12% strength values, corresponding to the proportion of nodes originally used to simulate the 2 subnetworks. A node's strength was defined as the sum of the weights of its corresponding edges.

Results Quantification

In order to assess the performance of each investigated parameter (i.e., electrodes number, inverse solution, connectivity measure), the accuracy of the estimated networks with respect to the ground truth was computed as follows:

$$\text{accuracy} = \frac{TP + TN}{TP + TN + FP + FN} \quad (9)$$

where TP (i.e., true positive) represents the connections present in the reference as well as in the estimated network, TN (i.e., true negative) refers to the absent connections in both the reference and estimated networks, FP (i.e., false positive) represents the connections obtained in the estimated network exclusively, and FN stands for the links missing in the estimated network. Accuracy values range between 0 and 1.

Statistical Analysis

Statistical analyses were performed using R (R Core Team 2020). We used linear mixed model analyses to investigate the effects of electrode number, inverse solution method, and connectivity measure on the accuracy of the estimated networks. Mixed models have several advantages, such as the ability to account for the dependence between the different measures, and to model random effects [see (Gueorguieva and Krystal 2004)]. We used the *lmer* function of the *{lme4}* package (Bates et al. 2015) with the following model that includes, epoch, electrode number, inverse solution method and connectivity measures as interacting fixed effects, and also a random intercept for epochs:

$$\begin{aligned} \text{model} = \text{lmer}(\text{Accuracy} \sim \text{Epoch} * \text{Electrode number} * \text{Inverse solution} \\ \text{method} * \text{Connectivity measure} + (1/\text{Epoch}) \text{ data} = \text{data}) \end{aligned} \quad (10)$$

PLI (wPLI) attempts to further weight the metric away from zero-lag contributions (Vinck et al. 2011).

We applied a square root transform to the data, since this led to a better compliance of the model with the assumptions

of normality and homoscedasticity of model's residuals than for raw data. Calculation of the significance of the fixed effects was performed using the *anova* function of the *{car}* package that computes ANOVA F-tests (Fox and Weisberg 2019). In order to assess the quality of the model, we computed marginal and conditional R^2 that were obtained from the *{MuMin}* package. In case of significant main effects, we performed post-hoc analyses using the *glht* function of the *{multcomp}* package that calculates adjusted p-values using individual z-tests (Hothorn et al. 2008). The significance threshold was set to $p = 0.05$.

Results

First, γ was fixed to 1 (i.e., no measurement noise was added). For each sensor density and inverse solution connectivity measure, estimated networks averaged over trials were illustrated in Fig. 2. Those results illustrated that the accuracy of the estimated networks was dramatically

influenced by scalp sensors density. The higher the number of electrodes, the more accurate the reconstructed networks were. Also, the inverse solution/connectivity measures combinations performed distinctively. The best performance was obtained using wMNE/wPLI at 64, 128, and 256 electrodes. wMNE/PLV and eLORETA/PLV performed similarly and were slightly less accurate than wMNE/wPLI at a high sensor density. However, eLORETA/wPLI exhibited the least estimation accuracy even with a high number of electrodes. The accuracy values for all electrodes montage and inverse solution/connectivity measures combinations were plotted in Fig. 3. The influence of the sensor density was confirmed by the statistical analysis with a significant sensor density effect ($F_{(4,532)} = 333.53, p < 0.001$, conditional $R^2 = 0.84$, marginal $R^2 = 0.82$). Post-hoc analyses showed significant accuracy improvement when using 256 electrodes as compared to 64 ($p < 0.05$), 32 ($p < 0.001$), and 19 ($p < 0.01$) electrodes. Increasing the sensor density from 128 to 256 electrodes did not provide further benefit.

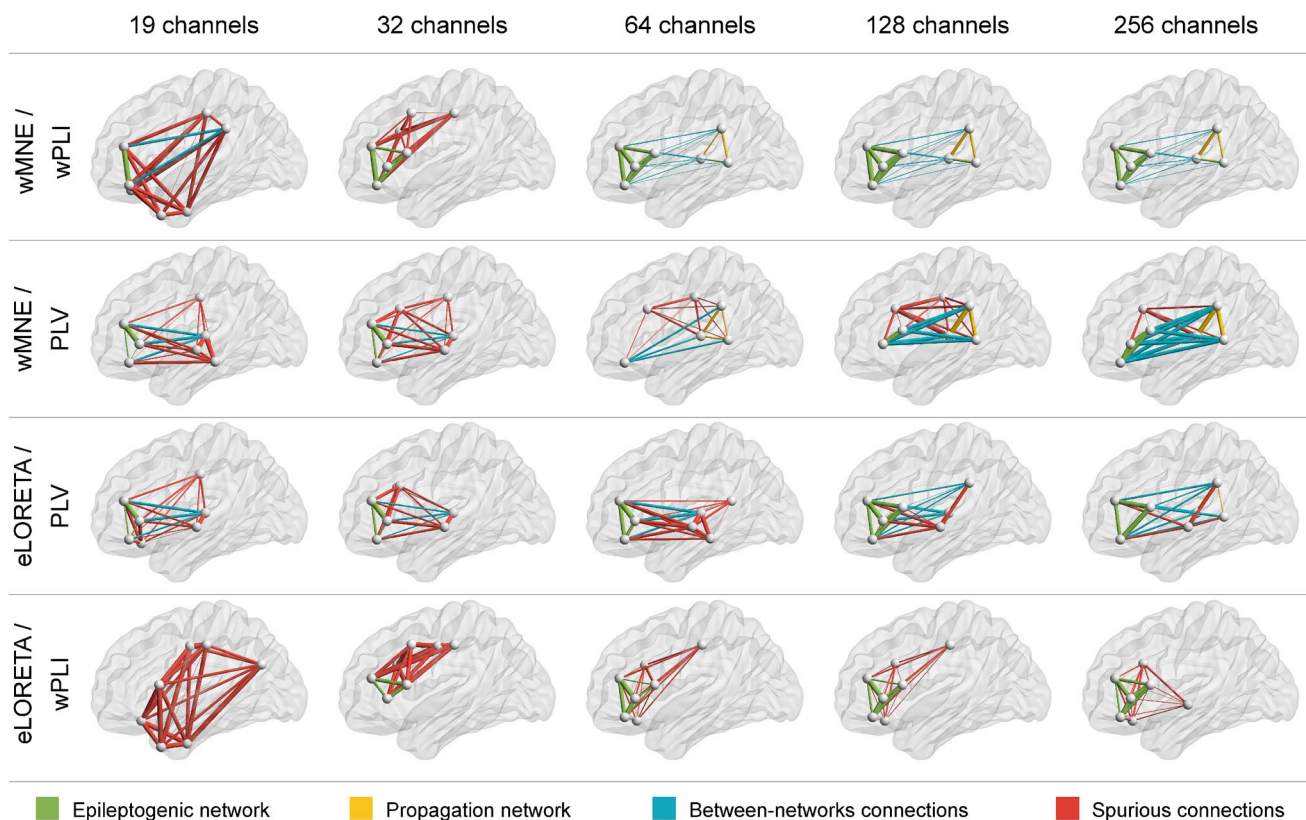


Fig. 2 Average networks over trials for all electrode montages and inverse solution/connectivity measure combinations. Networks were thresholded by keeping nodes with the highest 12% strength values, which corresponds to the proportion of nodes originally present in the reference network. γ was fixed to 1 (i.e., no measurement noise was added). Connections in green and yellow belong to the epile-

togenic and propagation subnetworks respectively. Connections in blue represent the connectivity between the two subnetworks. Connections in red are spurious connections, that do not exist in the reference network. *wMNE* weighted minimum norm estimate; *eLORETA* exact low-resolution electromagnetic tomography; *PLV* phase-locking value; *wPLI* weighted phase lag index

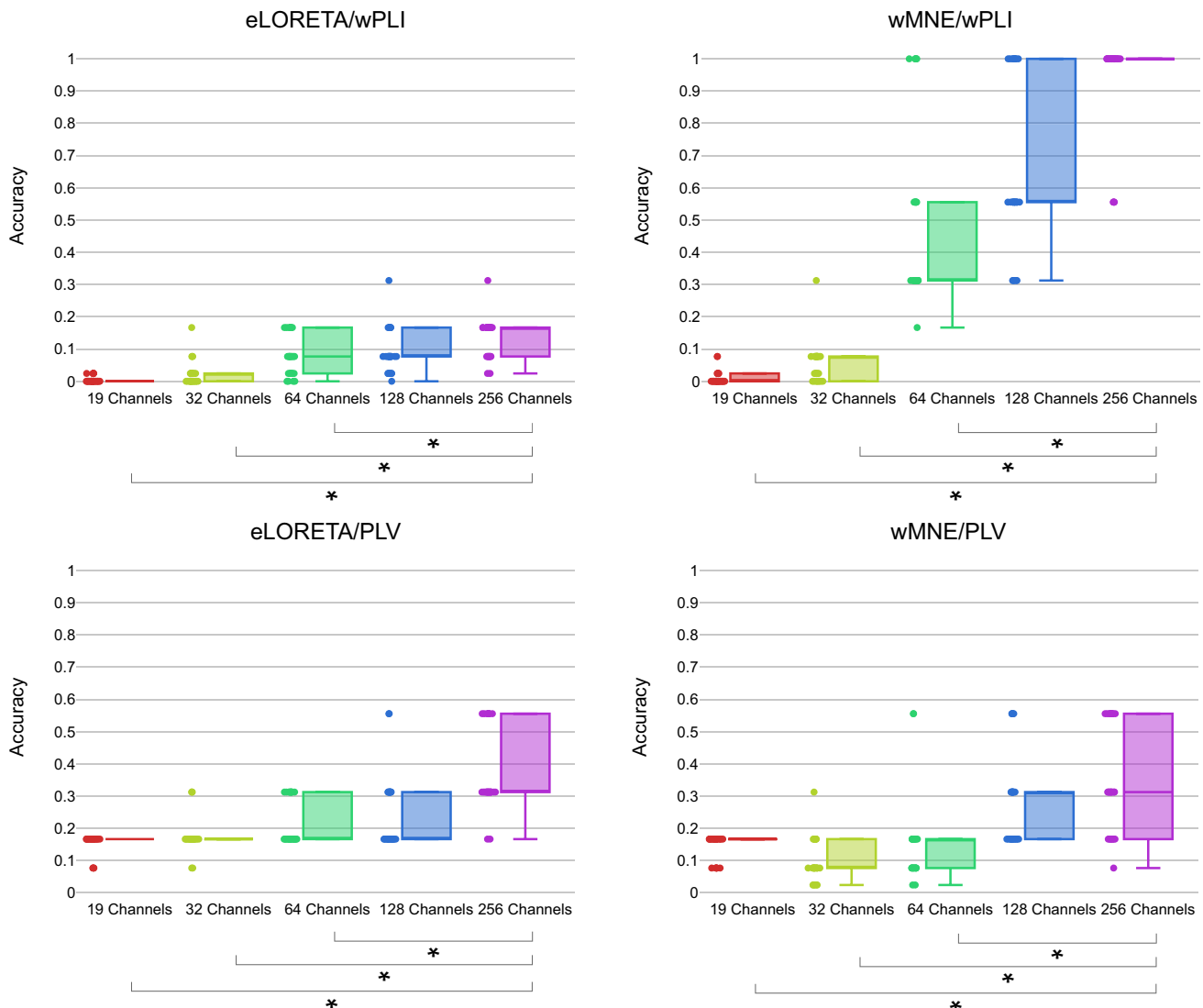


Fig. 3 Accuracy of the estimated networks based on different electrode montages for each inverse solution/connectivity measure. γ was fixed to 1 (i.e., no measurement noise was added). *Denotes signifi-

cant difference. *wMNE* weighted minimum norm estimate; *eLORETA* exact low-resolution electromagnetic tomography; *PLV* phase-locking value; *wPLI* weighted phase lag index

Differences between all others montages were non-significant. Indeed, differences between results obtained with 19 electrodes and those obtained with 32, 64, or 128 electrodes were all non-significant. Similarly, no differences were detected between 32 and 64, 32 and 128, 64 and 128 electrode montages. Regarding the inverse solution, wMNE significantly outperformed eLORETA ($F_{(1,532)} = 281.75, p < 0.001$, conditional $R^2 = 0.84$, marginal $R^2 = 0.82$). Also, statistical analyses showed a significant effect of the connectivity measure ($F_{(1,532)} = 83.19, p < 0.001$, conditional $R^2 = 0.84$, marginal $R^2 = 0.82$). The accuracy of the estimated networks was slightly higher with wPLI than with PLV. Interestingly, the combination inverse solution/connectivity measure combination had also a significant effect on the

network estimation accuracy ($F_{(1,532)} = 478.91, p < 0.001$, conditional $R^2 = 0.84$, marginal $R^2 = 0.82$).

The highest network estimation accuracy was reached using wMNE/wPLI, while the worst performance was obtained with eLORETA/wPLI. eLORETA/PLV and wMNE/PLV had similar average accuracy values. Post-hoc analyses showed significant difference between wMNE/wPLI and both eLORETA/PLV ($p < 0.001$) and wMNE/PLV ($p < 0.001$). Similarly, results obtained with eLORETA/wPLI were significantly different from those obtained with eLORETA/PLV ($p < 0.001$) and wMNE/PLV ($p < 0.001$). On the other hand, differences between eLORETA/PLV and wMNE/PLV and between eLORETA/wPLI and wMNE/wPLI were not statistically significant. All the detailed

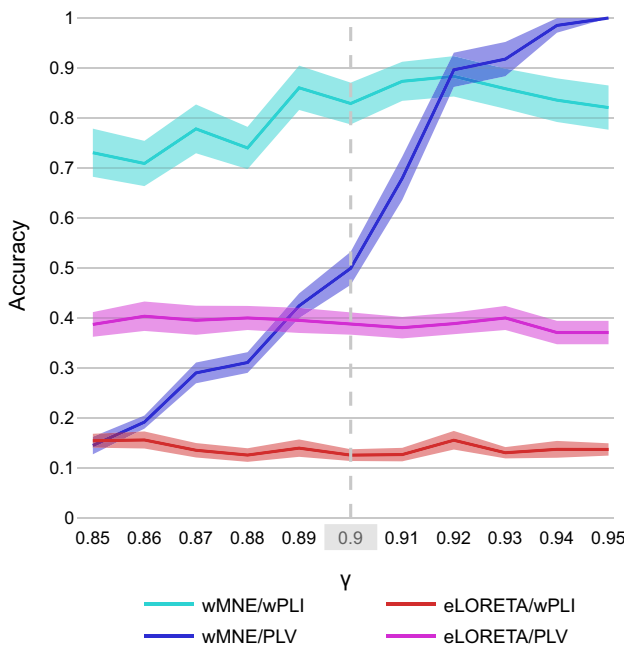


Fig. 4 Mean accuracy and standard error of each inverse solution/connectivity measure combination plotted against different levels of noise for the case of 256 electrodes. *wMNE* weighted minimum norm estimate; *eLORETA* exact low-resolution electromagnetic tomography; *PLV* phase-locking value; *wPLI* weighted phase lag index

results of the statistical analysis can be found in the Supplementary Materials (See Tables S2–S4).

In Fig. 4, the mean accuracy and standard error of each inverse solution/connectivity measure combination were plotted against different levels of noise (see Materials and Methods) for the case of 256 electrodes. With the exception of wMNE/PLV, the different combination methods maintained a relatively stable performance at different levels of noise. In (Anzolin et al. 2019; Haufe and Ewald 2016), γ was fixed at 0.9. At this specific value, wMNE/PLV reached a good performance (mean = 0.50) as compared to wMNE/wPLI (mean = 0.83), eLORETA/PLV (mean = 0.39), and eLORETA/wPLI (mean = 0.13). Plots relative to other electrode montages were also included in the Supplementary Materials (See Figs. S1–S4).

Discussion

To the best of our knowledge, there is still no consensus on the most optimized pipeline for reconstructing EEG source-space networks. At each step of this pipeline, several methods have indeed been proposed and many parameters need to be defined. Several comparative studies have investigated different methods/parameters affecting the estimation of functional networks. A key challenge in such studies (i.e., when dealing with real EEG data) is the difficulty to obtain

a ground truth, which prevents the exact evaluation of the performance of each considered method. In order to overcome this issue, in this paper we propose to use a recently developed, physiologically-grounded computational model, and highlight its potential use in optimizing the EEG network estimation procedure. Our objective was to provide a proof-of-concept regarding the use of COALIA for testing methods and parameters included in the source connectivity estimation. We believe that it can be used to address many of the methodological considerations related to EEG source connectivity estimation, and, consequently, to their effect on the properties of the obtained brain networks (Bassett and Sporns 2017). In this study, we used the COALIA model to simulate cortical-level activity. Through solving the forward problem, we computed the EEG signals. Then, we evaluated the effects of EEG channels density, two source reconstruction algorithms, and connectivity measures. Specifically, as a first step of this strategy to provide a ground truth using COALIA, we considered a scenario consisting of an epileptogenic and propagation network where epileptiform activity is present.

Overall, results obtained for the five considered electrode montages demonstrate clearly that the spatial resolution of the sensor array dramatically affects the accuracy of network estimation: as expected, increasing spatial resolution involves a higher accuracy of reconstructed networks. These results were expected theoretically, and are in line with previous studies (Lantz et al. 2003; Sohrabpour et al. 2015; Song et al. 2015). Recording EEG data with a low sensor density array can indeed contribute to a misrepresentation of high spatial frequency signal as a low spatial frequency signal. Therefore, to avoid aliasing the Nyquist criteria ($F_s > 2 * F_{max}$) should be respected and high spatial resolution is required (i.e., small interelectrode distance) (Song et al. 2015; Srinivasan et al. 1998). Interestingly, increasing the number of electrodes from 128 to 256 did not provide a significant improvement. On a different note, (Song et al. 2015) found that adding sensors on the inferior surface of the head (including the neck and the face) improves localization accuracy, even with sparse arrays. Therefore, it may be interesting to study the effect of the head coverage provided by different sensor array layouts, and not only the number of electrodes in each array.

Comparing inverse solutions and connectivity measures showed that wMNE performed better than eLORETA, and wPLI performed better than PLV. In contrast to our results, in (Tait et al. 2021), eLORETA outperformed wMNE at both voxel and ROI level. Even though (Colclough et al. 2016) did not recommend phase-based metrics as a first choice for assessing MEG functional connectivity, they were in favor of using measures that are not affected by zero-lag phase coupling. Interestingly, our study showed that a more crucial parameter is the combination of inverse method and

connectivity measure. Although wMNE/wPLI performed better than eLORETA/wPLI, the PLV connectivity measure performed similarly with both eLORETA and wMNE methods. Thus, the choice of the inverse solution and connectivity measure is recommended to be made simultaneously. In a previous study (Hassan et al. 2014), wMNE/PLV combination had the best performance in the context of a picture naming task. This combination has also showed better performance than other combinations (eLORETA and wPLI were not included) when applied to simulated epileptic spikes (Hassan et al. 2017). A possible difference between the current simulations and (Hassan et al. 2017) is that, in the latter, the reference network were very dense locally with a very high number of zero-lag correlations which may favor methods that do not remove these connections (such as PLV). Moreover, neither eLORETA nor wPLI were investigated in that study. It is therefore worth noting that the results obtained in this study are specific to the analyzed condition, i.e., epileptic spikes: therefore, we cannot be certain that the same combination of methods will provide the best network estimation accuracy when analyzing networks related to cognitive tasks or resting state, such as the alpha/beta DMN for instance (i.e., physiological activity), which is the main objective of the future steps of this work.

Finally, we varied γ between 0.85 and 0.95 to evaluate the effect of different noise levels on the performance of the inverse solutions and connectivity estimates. Our results have showed that the additive scalp-level noise mostly affected wMNE/PLV, while other methods had a more stable performance. One can also notice that at higher SNR ($\gamma > 0.9$), wMNE/PLV outperforms other combinations. These observations highlight the importance of applying an effective preprocessing of EEG signals before reconstructing the cortical networks, as well as a robust source connectivity method to correctly estimate functional connectivity. However, it is worth mentioning that the range of SNR considered here does not cover the case of highly noisy signals. A more detailed assessment of the effect of noise levels on the performance of source connectivity algorithms is a possible future avenue of research.

Methodological Considerations

Here, our objective was to provide a typical example of the use of the COALIA model to investigate the effect of different pipeline-related parameters on EEG source-space network analysis. With our approach, we aimed at promoting the use of computational modeling as a ground-truth to evaluate parameters of EEG source connectivity methods. Using this approach, other parameters could be also evaluated and other scenarios could be also generated, and we suggest hereafter possible extensions for this work. First, we

simulated in this study a network with 7 regions generating spike activity, while background brain activity was attributed to all other regions. However, it would be even more realistic for the network neuroscience field to use the model to simulate different rhythms of resting-state data (alpha/beta-band activity in the DMN network, for instance) and then evaluate the desired techniques in such context, rather than restricting the study to spikes/background activity scenarios. Second, the inverse solutions compared in this paper both belong to the family of minimum norm estimates methods. Other algorithms based on beamformers, such as the widely used linearly constrained minimum variance (LCMV) were not tested here. Moreover, it is worthy to mention that the two connectivity measures included in this study estimate phase synchrony between regional time-series. Other existing methods investigate instead the amplitude correlation between signals, such as the amplitude envelope correlation (AEC), which is widely used in the context of MEG functional connectivity. In a large study investigating the reliability of different connectivity metrics (Colclough et al. 2016), Colclough et al. have suggested that AEC between orthogonalized signals is the most consistent connectivity measure to employ in the context of resting-state recordings. Thus, it is noteworthy that the results obtained here do not necessarily extend to other inverse solutions or connectivity measures, nor they are generalized to all experimental context. Moreover, the connectivity assessed here using PLV and wPLI is bidirectional, however, since we introduced a time delay between the two subnetworks, we propose that studying directional connectivity metrics (e.g., Granger causality) may also lead to additional insights specifically related to Bartolomei's model, where epileptic activity is transferred from the epileptogenic network to the propagation network (Bartolomei et al. 2013). An additional parameter related to the connectivity estimation is the choice of the window length, i.e., the number of samples used to compute the connectivity value (Fraschini et al. 2016). Here, we did not investigate the effect of the window size on the accuracy of the network estimation. This factor could be considered in future works.

In order to threshold connectivity matrices, only the nodes with the highest 12% strength were kept. This proportional threshold was chosen to ensure that the number of nodes in the estimated networks matches the number of nodes within the reference network ($7/66 = 12\%$). Obviously, this choice is not completely realistic, since we cannot have any a priori in terms of experimental data on the exact number of activated brain regions. However, adopting a proportional, rather than a statistical thresholding for example, ensures that the density of estimated networks matches that of the ground truth, which is necessary for the correct assessment of the accuracy of estimated networks in our case (van den Heuvel et al. 2017).

Let us mention that we used in this study the accuracy to quantify the difference between estimated and reference networks. Other network-based metrics can be also useful to compute the similarities between these networks (Mheich et al. 2018, 2020). Also, the present study is limited to cortical regions based on the assumption that sub-cortical regions are not easily accessible from scalp EEG recordings. However, it has been proved that the performance of some inverse algorithms and connectivity estimators depends on the position of the reconstructed sources (Anzolin et al. 2019). Thus, a more extensive study comparing source connectivity approaches should include the effect of the location of sources.

In terms of head model, we have built for the purpose of this study a realistic head model for the ICBM152 MRI template that consisted in three nested homogeneous mesh surfaces shaping the brain (642 vertices), skull (642 vertices) and scalp (1082 vertices) with conductivity values of 0.33 Sm^{-1} , 0.0042 Sm^{-1} and 0.33 Sm^{-1} , respectively. However, source connectivity analysis in EEG/MEG are usually affected by the choice of the head model describing electrical and geometrical characteristics of the head (simplified/realistic head models, individual/template MRI, tissue types, tissue conductivity) (Cho et al. 2015; Wolters et al. 2006). Thus, it may be worthy to use COALIA and benefit from the presence of a ground truth to examine the influence of the head model on EEG source connectivity analysis. Finally, functional connectivity was estimated in broadband [1–45] Hz. However, it can be also computed in each of the classical EEG frequency sub-bands (i.e., delta, theta, alpha, beta, gamma) separately (Bettus et al. 2008; Canuet et al. 2011) which could be done in a more exhaustive study.

Conclusion

In this work, we have provided evidence that COALIA, a recently developed, physiologically-inspired computational model can provide a ground-truth for comparative studies aiming at optimizing the EEG-source connectivity pipeline. Using this model-based approach, several methodological questions can be addressed. Here, we assessed the effect of the number of EEG electrodes, as well as the inverse solution/connectivity measure combination in the context of simulated epileptic activity. Our results suggest that a higher network estimation accuracy requires a high number of EEG electrodes, and suggest a careful choice of an efficient inverse solution/connectivity measure combination.

Supplementary Information The online version contains supplementary material available at <https://doi.org/10.1007/s10548-021-00859-9>.

Acknowledgements This work was financed by the Rennes University, the Institute of Clinical Neuroscience of Rennes (project named EEG-Cog). Authors would also like to thank the Lebanese Association for Scientific Research (LASER) and Campus France, Programme Hubert Curien CEDRE (PROJECT No. 42257YA), for supporting this study. The authors would like to acknowledge the Lebanese National Council for Scientific Research (CNRS-L), the Agence Universitaire de la Francophonie (AUF) and the Lebanese university for granting Ms. Allouch a doctoral scholarship.

Funding This work was funded by Rennes University, the Institute of Clinical Neurosciences of Rennes (project named EEGCog). It was also supported by the Programme Hubert Curien CEDRE (PROJECT No. 42257YA), the National Council for Scientific Research (CNRS-L) and the Agence Universitaire de la Francophonie (AUF) and the Lebanese University.

Availability of Data and Materials Data used in this work can be found at <https://drive.google.com/drive/folders/1yDwdoLwSOg9UZrdDf6AzpT78Ve5HJRxD?usp=sharing>.

Code Availability Data and Codes supporting the results of this study are available at <https://github.com/sahar-allouch/comp-epi.git>. We used Matlab (The Mathworks, USA, version 2018b), Brainstorm toolbox (Tadel et al. 2011), Fieldtrip toolbox ((Oostenveld et al. 2011); <http://fieldtriptoolbox.org>), OpenMEG (Gramfort et al. 2010) implemented in Brainstorm, and BrainNet Viewer (Xia et al. 2013).

Declarations

Conflict of interest The authors have no conflicts of interest to declare that are relevant to the content of this article.

References

- Allen EA, Damaraju E, Plis SM, Erhardt EB, Eichele T, Calhoun VD (2014) Tracking whole-brain connectivity dynamics in the resting state. *Cereb Cortex* 24:663–676. <https://doi.org/10.1093/cercor/bhs352>
- Anzolin A, Presti P, Van De Steen F, Astolfi L, Haufe S, Marinazzo D (2019) Quantifying the effect of demixing approaches on directed connectivity estimated between reconstructed EEG sources. *Brain Topogr*. <https://doi.org/10.1007/s10548-019-00705-z>
- Awan FG, Saleem O, Kiran A (2019) Recent trends and advances in solving the inverse problem for EEG source localization. *Inverse Probl Sci Eng* 27(11):1521–1536. <https://doi.org/10.1080/1741977.2018.1490279>
- Baillet S, Mosher JC, Leahy RM (2001) Electromagnetic brain mapping. *IEEE Signal Process Mag* 18:14–30
- Bartolomei F, Guye M, Wendling F (2013) Abnormal binding and disruption in large scale networks involved in human partial seizures. *EJN Nonlinear Biomed Phys* 1(4):1–16. <https://doi.org/10.1140/epjnbp11>
- Bassett DS, Sporns O (2017) Network neuroscience. *Nat Neurosci* 20(3):353–364. <https://doi.org/10.1038/nn.4502>
- Bates D, Mächler M, Bolker BM, Walker SC (2015) Fitting linear mixed-effects models using lme4. *J Stat Softw*. <https://doi.org/10.18637/jss.v067.i01>
- Bensaid S, Modolo J, Merlet I, Wendling F, Benquet P (2019) COALIA: a computational model of human EEG for consciousness research. *Front Syst Neurosci* 13:1–18. <https://doi.org/10.3389/fnsys.2019.00059>

- Bettus G, Wendling F, Guye M, Valton L, Régis J, Chauvel P, Bartolomei F (2008) Enhanced EEG functional connectivity in mesial temporal lobe epilepsy. *Epilepsy Res* 81(1):58–68. <https://doi.org/10.1016/j.epilepsyres.2008.04.020>
- Bradley A, Yao J, Dewald J, Richter CP (2016) Evaluation of electroencephalography source localization algorithms with multiple cortical sources. *PLoS ONE* 11(1):1–14. <https://doi.org/10.1371/journal.pone.0147266>
- Canuet L, Ishii R, Pascual-Marqui RD, Iwase M, Kurimoto R, Aoki Y, Ikeda S, Takahashi H, Nakahachi T, Takeda M (2011) Resting-state EEG source localization and functional connectivity in schizophrenia-like psychosis of epilepsy. *PLoS ONE*. <https://doi.org/10.1371/journal.pone.0027863>
- Cho JH, Vorwerk J, Wolters CH, Knösche TR (2015) Influence of the head model on EEG and MEG source connectivity analyses. *Neuroimage* 110:60–77. <https://doi.org/10.1016/j.neuroimage.2015.01.043>
- Colclough GL, Woolrich MW, Tewarie PK, Brookes MJ, Quinn AJ, Smith SM (2016) How reliable are MEG resting-state connectivity metrics? *Neuroimage* 138:284–293. <https://doi.org/10.1016/j.neuroimage.2016.05.070>
- Desikan RS, Ségonne F, Fischl B, Quinn BT, Dickerson BC, Blacker D, Buckner RL, Dale AM, Maguire RP, Hyman BT, Albert MS, Killiany RJ (2006) An automated labeling system for subdividing the human cerebral cortex on MRI scans into gyral based regions of interest. *Neuroimage* 31:968–980. <https://doi.org/10.1016/j.neuroimage.2006.01.021>
- Fornito A, Zalesky A, Bullmore ET (2010) Network scaling effects in graph analytic studies of human resting-state fMRI data. *Front Syst Neurosci* 4:1–16. <https://doi.org/10.3389/fnsys.2010.00022>
- Fox J, Weisberg S (2019) An R companion to applied regression (third). Sage, Thousand Oaks. <https://doi.org/10.1177/0049124105277200>
- Fraschini M, Demuru M, Crobe A, Marrosu F, Stam CJ, Hillebrand A (2016) The effect of epoch length on estimated EEG functional connectivity and brain network organisation. *J Neural Eng* 13(3):1–10. <https://doi.org/10.1088/1741-2560/13/3/036015>
- Fuchs M, Wagner M, Köhler T, Wischmann HA (1999) Linear and nonlinear current density reconstructions. *J Clin Neurophysiol* 16(3):267–295. <https://doi.org/10.1097/00004691-199905000-00006>
- Gramfort A, Papadopoulou T, Olivi E, Clerc M (2010) OpenMEEG: opensource software for quasistatic bioelectromagnetics. *Biomed Eng Online*. <https://doi.org/10.1186/1475-925X-8-1>
- Grech R, Cassar T, Muscat J, Camilleri KP, Fabri SG, Zervakis M, Xanthopoulos P, Sakkalis V, Vanrumste B (2008) Review on solving the inverse problem in EEG source analysis. *J Neuroeng Rehabil*. <https://doi.org/10.1186/1743-0003-5-25>
- Grova C, Daunizeau J, Lina JM, Bénar CG, Benali H, Gotman J (2006) Evaluation of EEG localization methods using realistic simulations of interictal spikes. *Neuroimage* 29:734–753. <https://doi.org/10.1016/j.neuroimage.2005.08.053>
- Gueorguieva R, Krystal JH (2004) Move over ANOVA? Progress in analyzing repeated-measures data and its reflection in papers published in the Archives of General Psychiatry. *Arch Gen Psychiatry* 61:310–317
- Halder T, Talwar S, Jaiswal AK, Banerjee A (2019) Quantitative evaluation in estimating sources underlying brain oscillations using current source density methods and beamformer approaches. *Eneuro* 6(4):1–14. <https://doi.org/10.1523/ENEURO.0170-19.2019>
- Hämäläinen MS, Ilmoniemi RJ (1994) Inetrpreting magnetic fields of the brain: minimum norm estimates. *Med Biol Eng Comput* 32:35–42
- Hassan M, Dufor O, Merlet I, Berrou C, Wendling F (2014) EEG source connectivity analysis: from dense array recordings to brain networks. *PLoS ONE*. <https://doi.org/10.1371/journal.pone.0105041>
- Hassan M, Benquet P, Biraben A, Berrou C, Dufor O, Wendling F (2015) Dynamic reorganization of functional brain networks during picture naming. *Cortex* 73:276–288. <https://doi.org/10.1016/j.cortex.2015.08.019>
- Hassan M, Merlet I, Mheich A, Kabbara A, Biraben A, Nica A, Wendling F (2017) Identification of interictal epileptic networks from dense-EEG. *Brain Topogr* 30(1):60–76. <https://doi.org/10.1007/s10548-016-0517-z>
- Haufe S, Ewald A (2016) A simulation framework for benchmarking EEG-based brain connectivity estimation methodologies. *Brain Topogr* 32(4):625–642. <https://doi.org/10.1007/s10548-016-0498-y>
- Hothorn T, Bretz F, Westfall P (2008) Simultaneous inference in general parametric models. *Biom J* 50(3):346–363. <https://doi.org/10.1002/bimj.200810425>
- Kabbara A, Falou WEL, Khalil M, Wendling F, Hassan M (2017) The dynamic functional core network of the human brain at rest. *Sci Rep*. <https://doi.org/10.1038/s41598-017-03420-6>
- Klem GH, Lüders HO, Jasper HH, Elger C (1999) The ten-twenty electrode system of the International Federation. *The International Federation of Clinical Neurophysiology. Electroencephalogr Clin Neurophysiol Suppl* 52:3–6
- Lachaux J-P, Rodriguez E, Le Van Quyen M, Lutz A, Martinerie J, Varola FJ (2000) Studying single-trials of phase synchronous activity in the brain. *Int J Bifurc Chaos* 10(10):2429–2439. <https://doi.org/10.1142/s0218127400001560>
- Lantz G, Gravé de Peralta R, Spinelli L, Seeck M, Michel CM (2003) Epileptic source localization with high density EEG: how many electrodes are needed? *Clin Neurophysiol* 114(1):63–69. [https://doi.org/10.1016/S1388-2457\(02\)00337-1](https://doi.org/10.1016/S1388-2457(02)00337-1)
- Lin FH, Witzel T, Ahlfors SP, Stufflebeam SM, Belliveau JW, Hämäläinen MS (2006) Assessing and improving the spatial accuracy in MEG source localization by depth-weighted minimum-norm estimates. *Neuroimage* 31:160–171. <https://doi.org/10.1016/j.neuroimage.2005.11.054>
- Mheich A, Hassan M, Khalil M, Gripon V, Dufor O, Wendling F (2018) SimiNet: a novel method for quantifying brain network similarity. *IEEE Trans Pattern Anal Mach Intell* 40(9):2238–2249. <https://doi.org/10.1109/TPAMI.2017.2750160>
- Mheich A, Wendling F, Hassan M (2020) Brain network similarity: methods and applications. *Network Neurosci* 4(3):507–527. https://doi.org/10.1162/netn_a_00133
- O'Neill GC, Tewarie PK, Colclough GL, Gascoyne LE, Hunt BAE, Morris PG, Woolrich MW, Brookes MJ (2017) Measurement of dynamic task related functional networks using MEG. *Neuroimage* 146:667–678. <https://doi.org/10.1016/j.neuroimage.2016.08.061>
- Oostenveld R, Fries P, Maris E, Schoffelen JM (2011) FieldTrip: open source software for advanced analysis of MEG, EEG, and invasive electrophysiological data. *Comput Intell Neurosci*. <https://doi.org/10.1155/2011/156869>
- Pascual-Marqui RD (2007) Discrete, 3D distributed, linear imaging methods of electric neuronal activity. Part 1: exact, zero error localization. *arxiv: 0710.3341*
- R Core Team (2020) R: a language and environment for statistical computing. R Foundation for Statistical Computing, Vienna, Austria. <https://www.R-project.org/>
- Schelter B, Winterhalder M, Hellwig B, Guschlbauer B, Lücking CH, Timmer J (2006) Direct or indirect? Graphical models for neural oscillators. *J Physiol Paris* 99(1):37–46. <https://doi.org/10.1016/j.jphysparis.2005.06.006>
- Sohrabpour A, Lu Y, Kankirawatana P, Blount J, Kim H, He B (2015) Effect of EEG electrode number on epileptic source localization

- in pediatric patients. *Clin Neurophysiol* 126:472–480. <https://doi.org/10.1016/j.clinph.2014.05.038>
- Song J, Davey C, Poulsen C, Luu P, Turovets S, Anderson E, Li K, Tucker D (2015) EEG source localization: sensor density and head surface coverage. *J Neurosci Methods* 256:9–21. <https://doi.org/10.1016/j.jneumeth.2015.08.015>
- Srinivasan R, Tucker DM, Murias M (1998) Estimating the spatial Nyquist of the human EEG. *Behav Res Methods Instrum Comput* 30(1):8–19. <https://doi.org/10.3758/BF03209412>
- Stam CJ, Nolte G, Daffertshofer A (2007) Phase lag index: assessment of functional connectivity from multi channel EEG and MEG with diminished bias from common sources. *Hum Brain Mapp* 28:1178–1193. <https://doi.org/10.1002/hbm.20346>
- Tadel F, Baillet S, Mosher JC, Pantazis D, Leahy RM (2011) Brainstorm: a user-friendly application for MEG/EEG analysis. *Comput Intell Neurosci*. <https://doi.org/10.1155/2011/879716>
- Tait L, Özkan A, Szul MJ, Zhang J (2021) A systematic evaluation of source reconstruction of resting MEG of the human brain with a new high-resolution atlas: performance, precision, and parcellation. *Hum Brain Mapp*. <https://doi.org/10.1002/hbm.25578>
- van den Heuvel MP, de Lange SC, Zalesky A, Seguin C, Yeo BTT, Schmidt R (2017) Proportional thresholding in resting-state fMRI functional connectivity networks and consequences for patient-control connectome studies: issues and recommendations. *Neuroimage* 152(February):437–449. <https://doi.org/10.1016/j.neuroimage.2017.02.005>
- Vinck M, Oostenveld R, Van Wingerden M, Battaglia F, Pennartz CMA (2011) An improved index of phase-synchronization for electrophysiological data in the presence of volume-conduction, noise and sample-size bias. *Neuroimage* 55(4):1548–1565. <https://doi.org/10.1016/j.neuroimage.2011.01.055>
- Wang J, Wang L, Zang Y, Yang H, Tang H, Gong Q, Chen Z, Zhu C, He Y (2009) Parcellation-dependent small-world brain functional networks: a resting-state fmri study. *Hum Brain Mapp* 30:1511–1523. <https://doi.org/10.1002/hbm.20623>
- Wang HE, Bénar CG, Quilichini PP, Friston KJ, Jirsa VK, Bernard C (2014) A systematic framework for functional connectivity measures. *Front Neurosci*. <https://doi.org/10.3389/fnins.2014.00405>
- Wendling F, Ansari-Asl K, Bartolomei F, Senhadji L (2009) From EEG signals to brain connectivity: a model-based evaluation of interdependence measures. *J Neurosci Methods* 183:9–18. <https://doi.org/10.1016/j.jneumeth.2009.04.021>
- Wolters CH, Anwander A, Tricoche X, Weinstein D, Koch MA, MacLeod RS (2006) Influence of tissue conductivity anisotropy on EEG/MEG field and return current computation in a realistic head model: a simulation and visualization study using high-resolution finite element modeling. *Neuroimage* 30(3):813–826. <https://doi.org/10.1016/j.neuroimage.2005.10.014>
- Xia M, Wang J, He Y (2013) BrainNet viewer: a network visualization tool for human brain connectomics. *PLoS ONE*. <https://doi.org/10.1371/journal.pone.0068910>

Publisher's Note Springer Nature remains neutral with regard to jurisdictional claims in published maps and institutional affiliations.

Supplementary Materials

Mean-field modeling of brain-scale dynamics for the evaluation of EEG source-space networks

Sahar Allouch^{1,2}, Maxime Yochum¹, Aya Kabbara¹, Joan Duprez¹, Mohamad Khalil^{2,4}, Fabrice Wendling¹, Mahmoud Hassan^{3,*}, Julien Modolo^{1,*}

¹ Univ Rennes, LTSI - INSERM U1099, F-35000 Rennes, France

² Azm Center for Research in Biotechnology and Its Applications, EDST, Tripoli, Lebanon.

³ NeuroKyma, F-35000 Rennes, France

⁴ CRSI research center, Faculty of Engineering, Lebanese University, Beirut, Lebanon

* Equally contributed

1. Materials and methods

1.1. COALIA: a physiologically-inspired computational model

COALIA is a recently developed physiologically-grounded computational model (Bensaid, Modolo, Merlet, Wendling, & Benquet, 2019) of large-scale brain activity. Using a bottom-up approach taking account the detailed circuitry between the main neuronal subtypes, and anatomical regions from a widely used atlas, COALIA generates brain-scale electrophysiological activity while accounting for the macro- (between-regions) as well as the micro- (within-regions) circuitry of the brain. The basic unit of the model is the neural mass, a local network involving different neuronal types in which the electrical activity is averaged over the cells of a similar type, instead of describing individual cell dynamics as in microscopic models. Therefore, the neural mass model (NMM) is a mesoscopic model describing synchronized activity in local networks in which the micro-circuitry can be taken into account. At the level of a single neural mass (approximating a specific brain region, as done in (Bensaid et al., 2019)), the model includes glutamatergic pyramidal neurons and three different types of GABAergic interneurons with physiologically-based kinetics (fast vs. slow). At the brain-scale level, each neural mass represents the local field activity of one region of the Desikan-Killiany atlas (66 regions, since the right and left insula were excluded, (Desikan et al., 2006)). Given that each neural mass simulates the activity of one specific brain region, neural masses are then synaptically connected through long-range glutamatergic projections. This neuro-inspired model can simulate both cortical and thalamic activity. In the following, a brief description of the local NMM of neocortical and thalamic activity is presented.

The neocortical module involved pyramidal cells (PCs) and three types of inhibitory GABAergic interneurons, namely, (1) somatic-targeting parvalbumin-positive (PV+) basket cells (BC); (2) the dendritic-targeting somatostatin positive (SST) interneurons; and (3) vasoactive intestinal-peptide (VIP) expressing interneurons. BC and SST received excitatory inputs from PCs, that are reciprocally inhibited by both of them. Pyramidal collateral excitation was implemented *via* an excitatory feedback loop passed by a supplementary excitatory population (PC') analogous to PC, except that it projected only to the subpopulation PC and receives projection from PC as well. An inhibitory feedback loop was implemented to account for direct PV+/PV+ coupling through electrical gap-junctions. Communication through disinhibition was modeled by inhibitory projections first from VIP to SST, then from SST to

BC. The non-specific influence from neighboring and distant populations was modeled by a Gaussian input noise corresponding to an excitatory input $p_c^n(t)$ that globally described the average density of afferent action potentials. The thalamic module included one population of excitatory glutamatergic neurons (TCs, i.e., thalamic cells), and two thalamic reticular nuclei (TRN) GABAergic interneurons. TCs received GABAergic IPSPs with slow and fast kinetics from the TRNs, whereas the latter received excitatory inputs from the former. As in the cortical module, a Gaussian input noise corresponding to excitatory input $p_c^n(t)$ was used to represent non-specific inputs on TCs.

At the brain-scale, glutamatergic PCs originating from a single cortical column targeted PCs of other cortical columns by common feedforward excitation and GABAergic cells by disynaptic cortico-cortical feedforward inhibition. Variable time delays between NMMs were introduced in order to account for activity propagation delays caused by long-range connections. Regarding thalamo-cortical connectivity, TCs received glutamatergic excitatory postsynaptic potentials (EPSPs) from PCs which, in turn, received excitatory input from TCs. Similarly, TRNs received excitatory cortical projections. In terms of GABAergic cortical targets, thalamic projections targeted PV+ basket cells, SST neurons as well as VIP neurons, which in turn inhibit SST neurons, and disinhibit PCs dendrites. The model output corresponds to the total input onto PCs in the cortical modules (i.e., sum of excitatory and inhibitory PSPs).

Here, the thalamic module was used to generate epileptic spikes. Background activity was generated in all cortical populations. At the desired moment, spikes were generated in the epileptogenic and propagation network 50 between the thalamic modules and the desired cortical regions. All sources belonging to a single patch were synchronized at zero lag, while a delay of 30 ms was introduced between the two subnetworks to reflect the propagation of spikes between relatively distant brain regions.

Table S1 COALIA simulation parameters (values and interpretation)

Cortical module		
Parameter	Value	Interpretation
A_c	305 mV	Amplitude of the cortical average EPSP
B_c	30 mV	Amplitude of the cortical average IPSP (GABA _{A, slow} mediated currents)
G_c	20 mV	Amplitude of the cortical average IPSP (GABA _{A, fast} mediated currents)
D_c	0 mV	Amplitude of the cortical average IPSP (GABA _{A, slow} mediated currents)
$1/\alpha_c$	1/100 s	Time constant of cortical glutamate-mediated synaptic transmission

$1/b_c$	1/50 s	Time constant of cortical GABA-mediated synaptic transmission ($GABA_{A, slow}$ receptors)
$1/g_c$	1/500 s	Time constant of cortical GABA-mediated synaptic transmission ($GABA_{A, fast}$ receptors)
$1/d_c$	1/20 s	Time constant of cortical GABA-mediated synaptic transmission ($GABA_{A, slow}$ receptors)
μ_c, σ_c	$90\text{s}^{-1}, 60\text{s}^{-1}$	Mean and standard deviation of nonspecific cortical input
$C_{P,P}^n$	135	Collateral excitation connectivity constant of n^{th} cortical population
$C_{P,P}^n$	108	Collateral excitation connectivity constant of n^{th} cortical population
$C_{BC,P}^n$	13.5	BC to PC connectivity constant of n^{th} cortical population
$C_{SST,P}^n$	33.75	SST to PC connectivity constant of n^{th} cortical population
$C_{P,BC}^n$	40.5	PC to BC connectivity constant of n^{th} cortical population
$C_{P,SST}^n$	33.75	PC to SST connectivity constant of n^{th} cortical population
$C_{SST,BC}^n$	108	SST to BC connectivity constant of n^{th} cortical population
$C_{SST,VIP}^n$	0	SST to VIP connectivity constant of n^{th} cortical population
$C_{VIP,SST}^n$	0	VIP to SST connectivity constant of n^{th} cortical population
C_{BC}^n	0	BC to BC connectivity constant of n^{th} cortical population

Thalamic module

Parameter	Value	Interpretation
A_{Th}	5 mV	Amplitude of the thalamic average EPSP
B_{Th}	50 mV	Amplitude of the thalamic average IPSP ($GABA_{A, slow}$ and $GABA_B$ receptors)
G_{Th}	30 mV	Amplitude of the thalamic average IPSP ($GABA_{A, fast}$ receptors)
$1/a_{Th}$	1/100 s	Time constant of thalamic glutamate-mediated synaptic transmission
$1/b_{Th}$	1/30 s	Time constant of thalamic GABA-mediated synaptic transmission ($GABA_{A, slow}$ and $GABA_B$ receptors)
$1/g_{Th}$	1/150 s	Time constant of thalamic GABA-mediated synaptic transmission ($GABA_{A, fast}$ receptors)
μ_{Th}, σ_{Th}	$120\text{s}^{-1}, 1\text{s}^{-1}$	Mean and standard deviation of nonspecific subcortical input
C_{Th,TRN_1}	50	TC to TRN ₁ connectivity constant
C_{Th,TRN_2}	20	TC to TRN ₂ connectivity constant
$C_{TRN_1,Th}$	50	TRN ₁ to TC connectivity constant
$C_{TRN_2,Th}$	20	TRN ₂ to TC connectivity constant
C_{Th}	0	Collateral excitation connectivity constant

2. Results

2.1. Statistical analysis

Mixed Model Analysis

Table S2 Results of the applied ANOVA function.

Factors	F	Pr(>F)
Montage (4, 532)	333.5300	<2e-16 ***
Inverse solution (1, 532)	281.7463	<2e-16 ***
Connectivity measure (1,532)	83.1897	<2e-16 ***
Inverse solution * Connectivity measure (1, 532)	478.9063	<2e-16 ***

In the column “Factors”, the degrees of freedom are also reported

- R-squared Values
 - Marginal R-squared $R^2 = 0.8179461$
 - Conditional R-squared $R^2 = 0.835997$

Table S3 Mean and standard deviation of each electrode montage, inverse solution, connectivity measure, and inverse solution/connectivity measure combination

		Mean	Standard deviation
Electrodes number	19	0.07882791	0.07666976
	32	0.08949050	0.07897032
	64	0.23688536	0.22433564
	128	0.3224623	0.26276491
	256	0.44958296	0.32680356
Inverse solution	eLORETA	0.1508845	0.1263843
	wMNE	0.3200152	0.3230330
Connectivity measure	PLV	0.2202468	0.1326610
	wPLI	0.25065282	0.3414835
Inverse solution * Connectivity measure	eLORETA.PLV	0.23437322	0.11469367
	wMNE.PLV	0.20612041	0.14751131
	eLORETA.wPLI	0.06739577	0.06974413
	wMNE.wPLI	0.43390991	0.40189956

Table S4 Post-hoc comparison for electrodes number and inverse solution/connectivity measure combination

	Estimate	Std. error	z value	Pr (> z)
32 - 19	-0.01885	0.05575	-0.338	0.99719
64 - 19	0.03689	0.05575	0.662	0.96445
128 - 19	0.08077	0.05575	1.449	0.59584
256 - 19	0.20956	0.05575	3.759	0.00168 **
64 – 32	0.05574	0.05575	1.000	0.85550
128 - 32	0.09962	0.05575	1.787	0.38115
256 - 32	0.22841	0.05575	4.097	<0.001 ***

128 - 64	0.04388	0.05575	0.787	0.93444
256 - 64	0.17266	0.05575	3.097	0.01677 *
256 - 128	0.12879	0.05575	2.310	0.14162
wMNE.PLV - eLORETA.PLV	-0.0009027	0.0557457	-0.016	1.000
eLORETA.wPLI	-	-0.3717071	0.0557457	<1e-07 ***
eLORETA.PLV				
wMNE.wPLI - eLORETA.PLV	-0.3571905	0.0557457	-6.408	<1e-07 ***
eLORETA.wPLI - wMNE.PLV	-0.3708044	0.0557457	-6.652	<1e-07 ***
wMNE.wPLI - wMNE.PLV	-0.3562878	0.0557457	-6.391	<1e-07 ***
wMNE.wPLI - eLORETA.wPLI	0.0145166	0.0557457	0.260	0.994

2.2. Effect of added measurement noise

The mean accuracy and standard error of each inverse solution/connectivity measure combination were plotted against different levels of noise (see Materials and Methods) for the case of 128, 64, 32, and 19 electrodes in Fig. S1, Fig. S2, Fig. S3, and Fig. S4 respectively. In the case of 128 electrodes, with the exception of wMNE/PLV, the different combination methods maintained a relatively stable performance at different levels of noise. With 64 electrodes, only wMNE/wPLI maintained an acceptable accuracy. With 32 and 19 electrodes, all four combinations led to a low accuracy.

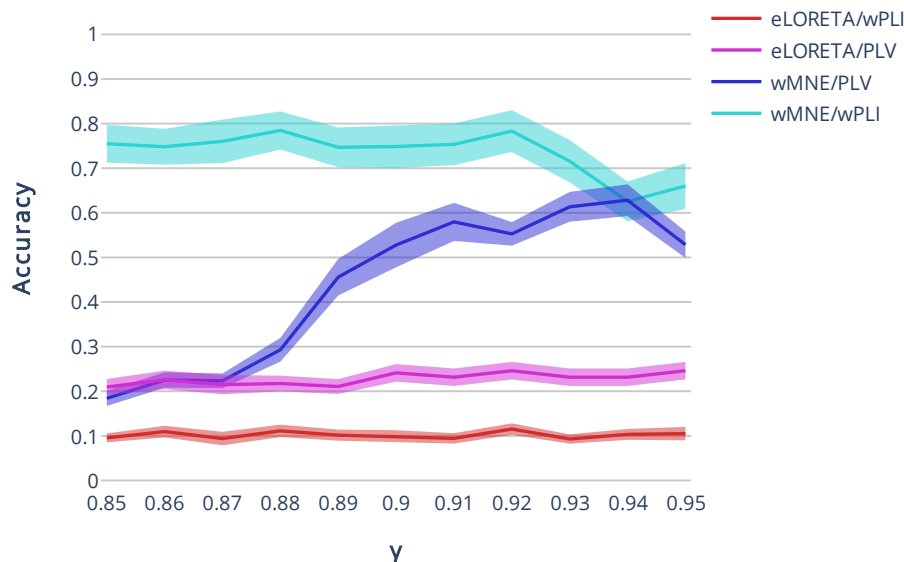


Fig. S1 Mean accuracy and standard error of each inverse solution/connectivity measure combination plotted against different levels noise for the case of 128 electrodes

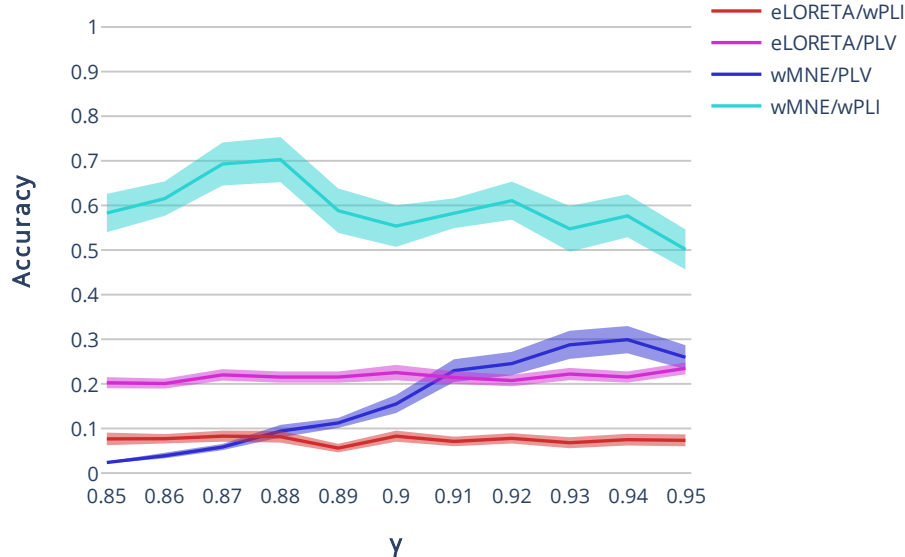


Fig. S2 Mean accuracy and standard error of each inverse solution/connectivity measure combination plotted against different levels noise for the case of 64 electrodes.

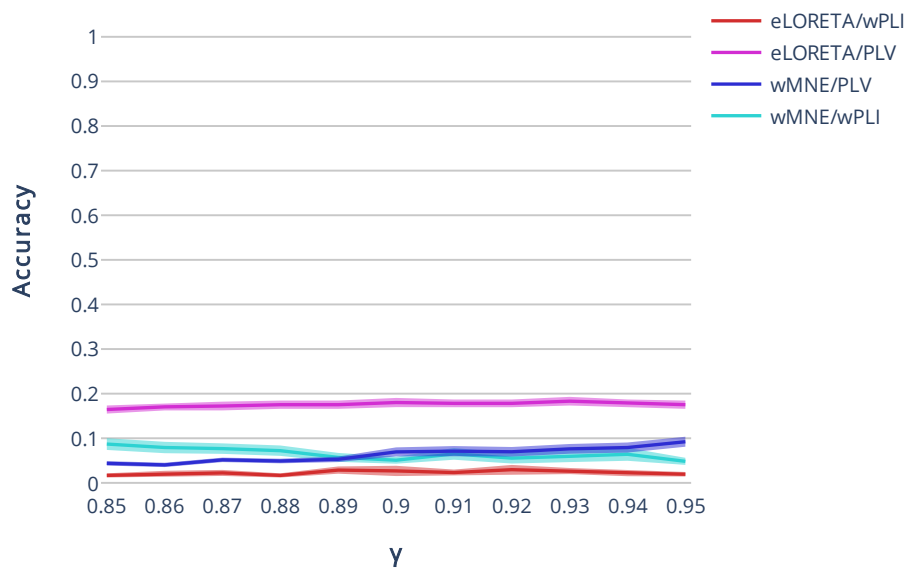


Fig. S3 Mean accuracy and standard error of each inverse solution/connectivity measure combination plotted against different levels noise for the case of 32 electrodes

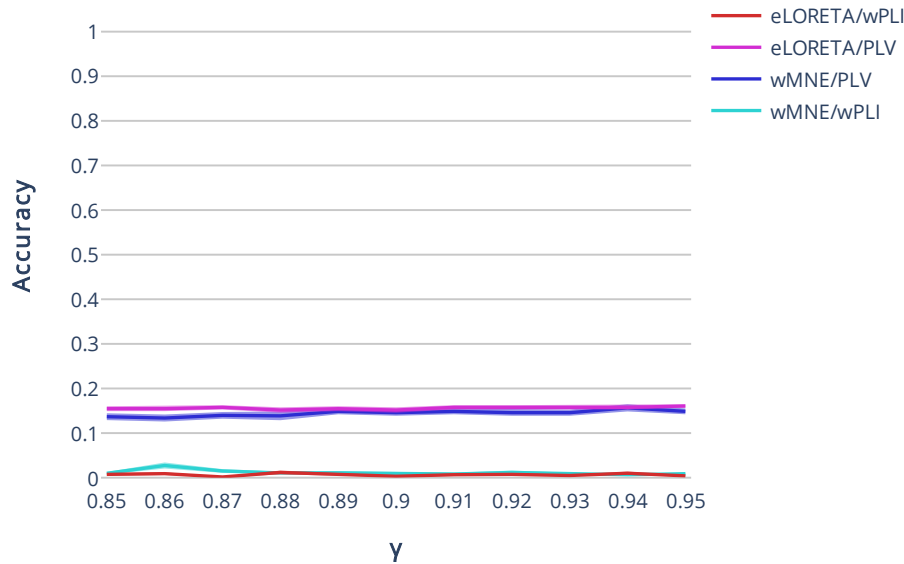


Fig. S4 Mean accuracy and standard error of each inverse solution/connectivity measure combination plotted against different levels noise for the case of 19 electrodes

References

- Bensaid, S., Modolo, J., Merlet, I., Wendling, F., & Benquet, P. (2019). COALIA: A Computational Model of Human EEG for Consciousness Research. *Frontiers in Systems Neuroscience*, 13, 1–18. <https://doi.org/10.3389/fnsys.2019.00059>
- Desikan, R. S., Ségonne, F., Fischl, B., Quinn, B. T., Dickerson, B. C., Blacker, D., ... Killiany, R. J. (2006). An automated labeling system for subdividing the human cerebral cortex on MRI scans into gyral based regions of interest. *NeuroImage*, 31, 968–980. <https://doi.org/10.1016/j.neuroimage.2006.01.021>

3.2 Study II: Effect of channel density, inverse solutions and connectivity measures on EEG resting-state networks: a simulation study

Study status: **Submitted** to *NeuroImage*.

Preprint: <https://www.biorxiv.org/content/10.1101/2022.06.01.494301v1>

Effect of channel density, inverse solutions and connectivity measures on EEG resting-state networks reconstruction: a simulation study

Sahar Allouch^{1,2}, Aya Kabbara^{3,4}, Joan Duprez¹, Mohamad Khalil^{2,5}, Julien Modolo^{1*}, Mahmoud Hassan^{3,6*},

¹ Univ Rennes, INSERM, LTSI - UMR 1099, F-35000 Rennes, France

² Azm Center for Research in Biotechnology and Its Applications, EDST, Tripoli, Lebanon

³ MINDig, F-35000 Rennes, France

⁴ LASER - Lebanese Association for Scientific Research, Tripoli, Lebanon

⁵ CRSI research center, Faculty of Engineering, Lebanese University, Beirut, Lebanon

⁶ School of Science and Engineering, Reykjavik University, Reykjavik, Iceland

* Equally contributed

Corresponding author: saharallouch@gmail.com

Highlights

- Analytical variability and absence of consensus over analytical approaches is a critical issue in neuroimaging analyses.
- Analytical variability related to the number of electrodes, source reconstruction algorithms, and functional connectivity measures in the EEG source connectivity analysis has a substantial impact on the outcomes.
- A high number of electrodes (at least 64) is needed to accurately infer cortical resting-state networks from recorded scalp signals.
- A very careful choice of the inverse solution/connectivity measure combination is needed, since our results showed a significant variability in the networks reconstructed using different inverse solutions and connectivity measures.

Abstract

Along with the study of brain activity evoked by external stimuli, the past two decades witnessed an increased interest in characterizing the spontaneous brain activity occurring during resting conditions. The identification of connectivity patterns in this so-called "resting-state" has been the subject of a great number of electrophysiology-based studies, using the Electro/Magneto-Encephalography (EEG/MEG) source connectivity method. However, no consensus has been reached yet regarding a unified (if possible) analysis pipeline, and several involved parameters and methods require cautious tuning. This is particularly challenging when different analytical choices induce significant discrepancies in results and drawn conclusions, thereby hindering the reproducibility of neuroimaging research. Hence, our objective in this study was to shed light on the effect of analytical variability on the outcome consistency by evaluating the implications of parameters involved in the EEG source connectivity analysis on the accuracy of resting-state networks (RSNs) reconstruction. We simulated, using neural mass models, EEG data corresponding to two RSNs, namely the default mode network (DMN) and dorsal attentional network (DAN). We investigated the impact of five channel densities (19, 32, 64, 128, 256), three inverse solutions (weighted minimum norm estimate (wMNE), exact low-resolution brain electromagnetic tomography (eLORETA), and linearly constrained minimum variance (LCMV) beamforming) and four functional connectivity measures (phase-locking value (PLV), phase-lag index (PLI), and amplitude envelope correlation (AEC) with and without source leakage correction), on the correspondence between reconstructed and reference networks. We showed that, with different analytical choices related to the number of electrodes, source reconstruction algorithm, and functional connectivity measure, high variability is present in the results. More specifically, our results show that a higher number of EEG channels significantly increased the accuracy of the reconstructed networks. Additionally, our results showed significant variability in the performance of the tested inverse solutions and connectivity measures. Such methodological variability and absence of analysis standardization represent a critical issue for neuroimaging studies that should be prioritized. We believe that this work could be useful for the field of electrophysiology connectomics, by increasing awareness regarding the challenge of variability in methodological approaches and its implications on reported results.

Keywords: EEG resting-state networks, channel density, inverse solution, functional connectivity, neural mass model, analytical variability.

1. Introduction

Over the past two decades, there has been a considerable growth in the number of studies investigating human brain activity at rest (Damoiseaux et al., 2006; Raichle et al., 2001; Raichle & Snyder, 2007; van den Heuvel et al., 2008). Characterizing synchronous activity across spatially distributed regions, using either functional magnetic resonance imaging (fMRI) or magneto/electro-encephalography (M/EEG) has revealed consistent patterns of brain connectivity in the absence of a goal-directed task, with a preserved consistency across subjects as well as across different neuroimaging modalities (Matthew J. Brookes et al., 2011; Damoiseaux et al., 2006; de Pasquale et al., 2012; A. Kabbara et al., 2021). Interestingly, accurate identification of the so-called resting-state networks (RSNs) has been found to be primordial for both cognitive (Keller et al. 2015; Jockwitz et al. 2017; Shen et al. 2018; Alavash et al. 2015) and clinical studies (Gratton et al., 2018; Hassan, Chaton, et al., 2017; Jimenez et al., 2019; A. Kabbara et al., 2018; Sheline & Raichle, 2013).

In this context, the EEG source connectivity method enables inferring functional brain networks at the cortical level with high temporal resolution (Hassan & Wendling, 2018). However, due to the complexity of the analysis workflow, many methodological questions related to the EEG source connectivity pipeline remain unanswered. In fact, each step of the analysis involves different choices that might significantly affect the resulting functional network. Hence, the effect of several factors needs to be investigated and quantified for more consistent and reliable use of this method.

One major factor in terms of impact on the EEG source connectivity analysis is the number of EEG electrodes (electrodes density). In fact, several studies investigated the effect of electrodes density on EEG source localization in simulations in the context of epilepsy (Goran Lantz et al., 2003; Sohrabpour et al., 2015; Song et al., 2015). More specifically, it has been shown that EEG electrodes density has a direct influence on the localization error: as intuitively expected, a higher number of electrodes is associated with a significant decrease in localization error (Goran Lantz et al., 2003; Sohrabpour et al., 2015; Song et al., 2015). In both studies by (Goran Lantz et al., 2003) and (Sohrabpour et al., 2015), a dramatic decrease in localization error occurred when increasing the number of electrodes from 32 to 64.

Another critical influencing factor in the EEG source connectivity pipeline is the algorithm chosen to solve the inverse problem, which is ill-posed due to its non-uniqueness and the instability of its solution (see (Grech et al., 2008) for a review). Several studies quantifying

the performance of different inverse methods, in simulated and experimental EEG/MEG data, concluded that the choice of the inverse method significantly influences source estimation results (Allouch et al., 2022; Anzolin et al., 2019; Bradley et al., 2016; Grova et al., 2006; Halder et al., 2019; Hedrich et al., 2017; Mahjoory et al., 2017; Tait et al., 2021). However, no consistent conclusions have been made regarding one method that would stand apart from the others in terms of performance, which can also be related to the analyzed conditions.

The choice of the functional connectivity metric is also a critical step. A wide range of measures are used in the field, and each differs in the aspect of the data being investigated (amplitude-*vs* phase-based measures / directional *vs* non-directional connectivity, prone/robust to source leakage), (see (Cao et al., 2022; Friston, 2011; Pereda et al., 2005) for a review), resulting in significant variability of performance and interpretations (Allouch et al., 2022; Colclough et al., 2016; Hassan, Merlet, et al., 2017; H. E. Wang et al., 2014; Wendling et al., 2009).

In this context, simulation studies are of utmost interest, since they provide an accessible ground truth that enables an objective evaluation of the methods/techniques under investigation. Here, we used a model for cortical dynamics, namely neural mass models (NMMs), to simulate resting state networks (RSNs), and more specifically the default mode network (DMN) and dorsal attentional network (DAN). Then, we quantified the effect of three key factors involved in the EEG source connectivity analysis:

- 1) EEG channel density (from 19,32,64,128 to 256 channels).
- 2) Inverse solution method used to reconstruct EEG sources. We selected three of the widely used algorithms in the EEG/MEG community, namely i) weighted minimum norm estimate (wMNE) (Fuchs et al., 1999; Lin et al., 2006), ii) exact low-resolution brain electromagnetic tomography (eLORETA) (Pascual-Marqui, 2007), and iii) linearly constrained minimum variance (LCMV) beamformer (Van Veen et al., 1997).
- 3) Functional connectivity metric. We selected two phase-based and two amplitude-based metrics: the phase-locking value (PLV) (Lachaux et al., 2000), phase-lag index (PLI) (Stam et al., 2007), and amplitude envelope correlation (AEC) with and without source leakage correction (Colclough et al., 2015, 2016; Hipp et al., 2012).

Finally, cortical networks obtained for each combination (number of electrodes \times inverse solution \times connectivity measure) were quantitatively compared to the reference simulated networks.

2. Materials and Methods

A schematic diagram of the analysis pipeline is presented in Fig. 1.

2.1. Simulations

The simulated cortical networks (DMN and DAN) each included six regions based on the Desikan-Killiany atlas (Desikan et al., 2006) in terms of region parcellation. The DMN consisted of the right and left posterior cingulate cortex (PCC), medial orbitofrontal (MOF) gyrus, and inferior parietal lobe (IPL). Regarding the DAN, this network consisted of the right and left inferior parietal lobe (IPL), caudal middle frontal gyrus (cMFG), and superior parietal lobe (SPL). The choice of those regions was based on their frequent occurrence in previous resting-state studies (E. A. Allen et al., 2018; Elena A. Allen et al., 2014; Baker et al., 2014; Damoiseaux et al., 2006; M. D. Fox & Raichle, 2007; Greicius et al., 2003; A. Kabbara et al., 2017, 2021; Shirer et al., 2012). Cortical-level activity was generated using a flexible neural mass model framework, named COALIA (Bensaid et al. 2019). This multi-population neural mass model enables the simulation of brain-scale electrophysiological activity while accounting for the macro- (between regions) and micro-circuitry (within a single region) of the brain, with one neural mass representing the local field potential of one Desikan-Killiany atlas region [for details, readers may refer to (Bensaid et al. 2019)]. Activity in the alpha band ([8 – 12] Hz) was attributed to reference RSNs regions, while background activity was assigned to remaining cortical regions. To account for variability between simulated data segments, each “virtual subject” had different connectivity matrices provided to the model, while each epoch for the same subject had a different randomly generated input noise (*mean* = 90 Hz, *standard deviation* = 30 Hz). More specifically, for each subject, a different fractional anisotropy matrix of the HCP dataset was used (Van Essen et al. 2013), and the weights corresponding to an RSN-connection were modified and set to a value of (1 ± 20%). A corresponding scaling of the matrices followed in accordance with COALIA’s requisites and the type of each input matrix (inhibitory/excitatory). A total of 50 “virtual subjects”, 4 epochs per subject (i.e., 200 data segments) were simulated; with a duration of 40 seconds each and a sampling rate of 2048 Hz. The time delay between NMMs was determined by the euclidean distance between the centroids of Desikan-Killiany’s regions divided by the velocity of action potentials propagation, which was set as 100 cm/s. An example of simulated cortical signals is shown in Supplementary Materials, Fig. S1 (A).

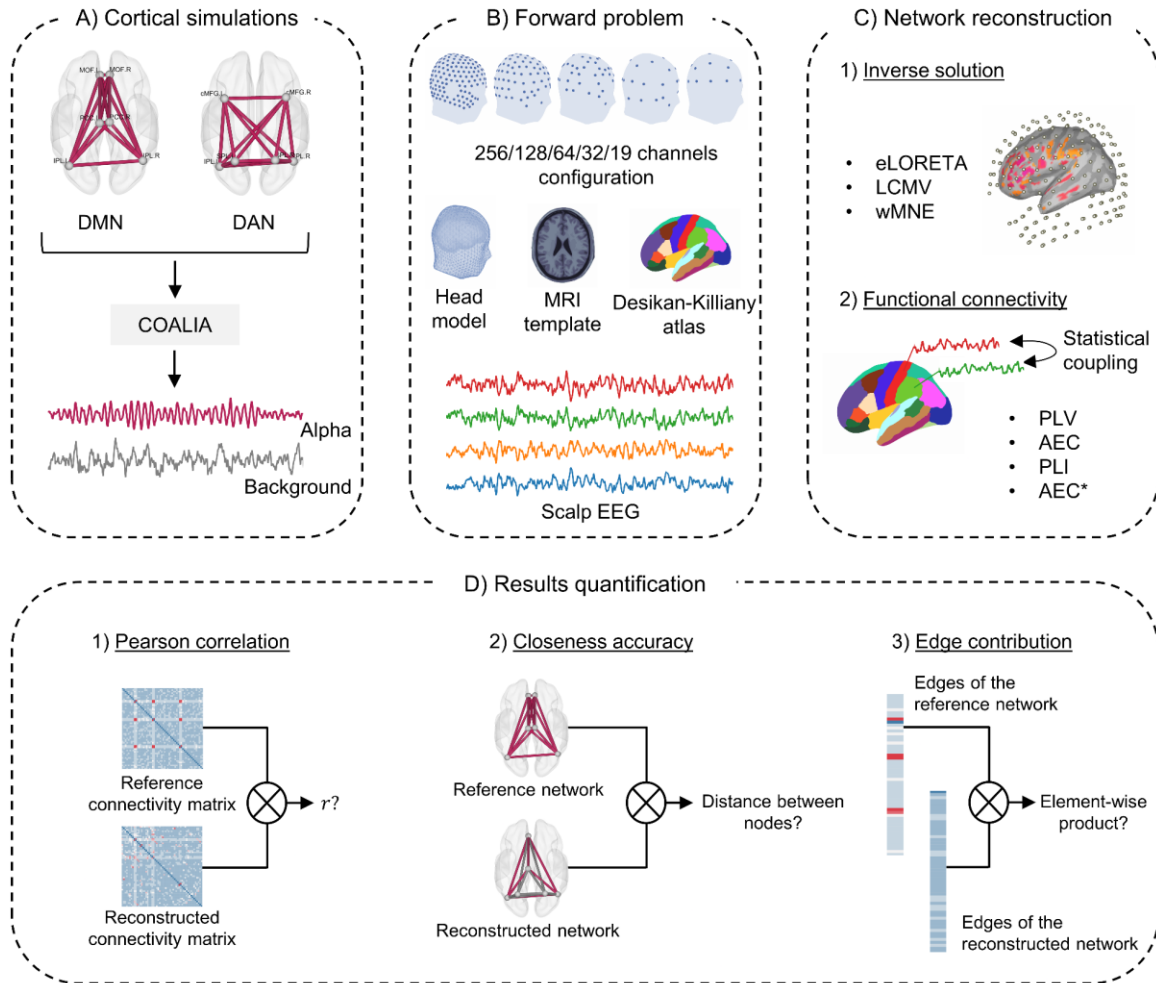


Fig. 1. Processing pipeline used in the present study. (A) Generation of reference, ground-truth cortical-level electrophysiological signals using a realistic model of neuronal activity. (B) Projection of source-level activity on scalp-level EEG sensors by using an anatomically accurate head model. (C) Network reconstruction using different methods of source reconstruction based on scalp-level signals, and of statistical coupling between signals (functional connectivity metrics). (D) Quantification of the level of matching between estimated and reference networks. *DMN* - default mode network. *DAN* - Dorsal attentional network. *eLORETA* - exact low-resolution electromagnetic tomography. *LCMV* - linearly constrained minimum norm beamforming. *wMNE* - weighted minimum norm estimate. *PLV* - phase-locking value. *AEC* - amplitude envelope correlation. *PLI* - phase-lag index. *AEC** - amplitude envelope correlation with source leakage correction.

2.2. Forward problem

Scalp EEG signals were estimated from simulated cortical activity by solving the forward problem as follows:

$$X(t) = (x_1(t) \dots x_M(t))^T = G \cdot (s_1(t) \dots s_P(t))^T = G \cdot S(t) \quad (1)$$

where $X(t)$ represents scalp EEG signals, $S(t)$ simulated cortical time series, and G the $(M \times P)$ Gain (lead field) matrix. More specifically, G quantifies the contribution of each cortical source to the generation of scalp signals by taking into account the geometrical and electrical characteristics of the head. Here, the gain matrix was computed using a realistic head model (Colin27 MRI template) using the boundary element method (BEM), implemented within the OpenMEEG package (Gramfort et al., 2010) in the Fieldtrip toolbox (Oostenveld et al. 2011). The sensor space was defined based on the GSN HydroCel electrodes configuration (EGI, Electrical geodesic Inc) with 256, 128, 64, and 32 channels, as well as the international 10-20 system with 19 channels. The lead field matrix used for solving the forward problem, as well as the inverse problem, was constrained to 66 lead field vectors representing the contribution of sources located at the centroid of the regions of interest defined by the Desikan-Killiany atlas (Desikan et al., 2006) (right and left insula were excluded, leaving 66 regions of interest).

To mimic measurement noise, white gaussian noise was added to scalp EEG (Anzolin et al., 2019) as follows:

$$X_{noisy}(t) = \gamma \times \frac{X(t)}{\|X(t)\|_F} + (1 - \gamma) \times \frac{n(t)}{\|n(t)\|_F} \quad (2)$$

where $X(t)$ and $n(t)$ represent the scalp EEG signals and white uncorrelated noise signals, respectively; and $\|\cdot\|_F$ denotes their Frobenius norm. γ ranges from 0.1 to 1. An example of scalp EEG signals obtained for different γ values is shown in Supplementary Materials, Fig. S1 (B). Results shown in the main manuscript correspond to $\gamma = 1$, i.e., no added measurement noise.

2.3. Inverse problem

The first step to reconstruct cortical networks was to estimate the dynamics of cortical sources from scalp EEG data, i.e., determining the position, orientation, and magnitude of dipolar sources $\hat{S}(t)$. Cortical sources were located at the centroids of Desikan-Killiany regions and oriented normally to the cortical sheet. Thus, the inverse problem was reduced to computing the magnitude of dipolar sources $\hat{S}(t)$:

$$\hat{S}(t) = W \cdot X(t) \quad (3)$$

Several algorithms have been proposed to solve this problem, and estimate W based on different assumptions related to the spatiotemporal properties of sources and regularization

constraints (see (Awan et al., 2019; Baillet et al., 2001; Grech et al., 2008) for a review). Inverse solutions can be classified into two major families: minimum norm estimates and beamformers. The former reconstructs all sources simultaneously by minimizing the difference between the data $X(t)$ and predicted data $G \cdot \hat{S}(t)$, while beamformers take an adaptive spatial-filtering approach in which each source is scanned independently. In this study, we focused on three commonly used solutions in EEG source reconstruction, as detailed below.

2.3.1. Weighted minimum norm estimate (wMNE)

wMNE (Fuchs et al., 1999; Lin et al., 2006) is a derivative of the minimum norm estimate (MNE) (Hämäläinen & Ilmoniemi, 1994), which proposes a solution that fits the measurements with a least square error. However, wMNE compensates further for the tendency of MNE to favor weak and surface sources:

$$W_{wMNE} = BG^T(GBG^T + \lambda C)^{-1} \quad (4)$$

where λ is the regularization parameter and C is the noise covariance matrix (set to the identity matrix in our case). The matrix B is a diagonal matrix built from matrix G with non-zero terms inversely proportional to the norm of lead field vectors. This matrix adjusts the properties of the solution by reducing the bias inherent to the standard MNE solution:

$$B_{ij} = \begin{cases} (G_i^T G_i)^{\frac{1}{2}} & \text{if } i = j; \\ 0 & \text{if } i \neq j; \end{cases} \quad (5)$$

Regarding the regularization parameter λ , we used the recommended default value ($1/SNR$; $SNR = 3$) included in the Brainstorm toolbox (Tadel et al. 2011).

2.3.2. Exact low-resolution brain electromagnetic tomography (eLORETA)

eLORETA belongs to the family of weighted minimum norm inverse solutions. However, in addition to compensating for depth bias, it also has exact-zero error localization in the presence of measurement and structured biological noise (Pascual-Marqui, 2007):

$$B_{ij} = \begin{cases} (G_i^T (G_i B G_i^T + \lambda C)^{-1})^{\frac{1}{2}} & \text{if } i = j; \\ 0 & \text{if } i \neq j; \end{cases} \quad (6)$$

Regarding the regularization parameter λ , we used the default value (0.05) of the Fieldtrip toolbox (Oostenveld et al. 2011).

2.3.3. Linearly constrained minimum-variance (LCMV) beamformer

The LCMV beamformer (Van Veen et al., 1997) takes an adaptive spatial-filtering approach and estimates the activity for a source at a given location while simultaneously suppressing contributions from all other sources and noise captured in the data covariance.

$$W_{LCMV} = ((G^T \cdot (C + \lambda \cdot I)^{-1}) \cdot G)^{-1} \cdot (G^T \cdot (C + \lambda \cdot I)^{-1}) \quad (7)$$

The regularization parameter λ was set to 0.05.

2.4. Functional connectivity

Following the reconstruction of cortical dynamics, functional connectivity was assessed to estimate cortical networks. Two distinct approaches can be adopted to compute functional connectivity: phase-based and amplitude-based techniques. We tested here four different connectivity measures:

2.4.1. Phase-locking value (PLV)

For two signals $x(t)$ and $y(t)$, the phase-locking value (Lachaux et al., 2000) is defined as:

$$PLV = |E\{e^{i(\phi_x(t)-\phi_y(t))}\}| \quad (8)$$

where $E\{\cdot\}$ is the expected value operator, and $\phi(t)$ is the instantaneous phase derived from the Hilbert transform. PLV was computed over consecutive non-overlapping sliding windows, with the length of the window δ set to $\frac{6}{central\ frequency}$ as recommended in (Lachaux et al., 2000), and where 6 is the number of cycles in a given frequency band. Thus, δ equals 600 ms in the considered alpha band ([8 – 12] Hz) where the central frequency was equal to 10 Hz. PLV values were then averaged over all sliding windows.

2.4.2. Phase-lag index (PLI)

The PLI originally proposed in (Stam et al., 2007) is a measure of the asymmetry of the distribution of phase differences between two signals. It aims at overcoming source leakage by discarding phase differences centered around 0 and π , i.e., removing zero-lag connections. For two signals $x(t)$ and $y(t)$, PLI is defined as follows:

$$PLI = |E\{sign(\phi_x(t) - \phi_y(t))\}| \quad (9)$$

where $E\{\cdot\}$ is the expected value operator, and $\phi(t)$ the instantaneous phase derived from the Hilbert transform. Similar to PLV computation, PLI was assessed over consecutive non-

overlapping sliding windows (600 ms). PLI values were then averaged over all sliding windows.

2.4.3. Amplitude envelope correlation (AEC)

AEC was computed as the Pearson correlation between signals' envelopes derived from the Hilbert transform (Matthew J. Brookes et al., 2011; Hipp et al., 2012). Similar to PLV and PLI computation, a sliding window approach was adopted. Based on (O'Neill et al., 2017), the window length was set to 6 s with an overlap of 0.5 s.

2.4.4. Amplitude envelope correlation with source leakage correction (AEC*)

Zero-lag signal overlaps caused by spatial leakage were removed using a multivariate symmetric orthogonalization approach (Colclough et al., 2015). Briefly, the closest orthonormal matrix to the uncorrected regional time courses is first computed; then the magnitudes of the orthogonalized vectors are adjusted iteratively to minimize the least-squares distances between corrected and uncorrected signals. Orthogonalization was applied over the entire data segment. Following the orthogonalization procedure, AEC was computed as previously described in section 2.4.3.

2.5. Results quantification and statistical testing

We used three metrics, detailed below, to assess the performance of different channel densities and the tested inverse solutions and connectivity measures.

2.5.1. Pearson correlation

First, the Pearson correlation between the reference and reconstructed connectivity matrices was computed as a global measure of the similarity between networks. Matrices were not thresholded nor binarized.

2.5.2. Closeness accuracy

Second, closeness accuracy (*CA*), defined as follows, was used for a node-wise comparison between the reference and reconstructed networks:

$$CA = \frac{1}{1+AD} \quad (9)$$

where AD is the average distance (in cm) between the reference and reconstructed networks given by:

$$AD = \frac{\sum_k d(N_k, N_v)}{M} \quad k \in [1, M]; v \in [1, W] \quad (10)$$

where $d(N_k, N_v)$ denotes the Euclidean distance between the node N_k in the reconstructed network, and the nearest node N_v in the reference simulated network. M and W represent the total number of nodes detected in reconstructed and reference networks, respectively. Before computing the CA , networks were thresholded by keeping the edges with the highest 0.7% weight values, the choice of this proportion corresponding to the number of edges in the simulated RSNs (30 edges).

2.5.3. Edge contribution

Finally, we investigated the contribution of individual edges to the correlation values obtained between the reference and reconstructed networks (Colclough et al., 2016; Finn et al., 2015). The set of edges of reference and reconstructed (non-thresholded) networks were first z-score normalized ($mean = 0, std = 1$). Second, the edge contribution φ was calculated as the element-wise product between the two normalized edge vectors. Suppose that $[X_i^{Ref}]$ and $[X_i^{Rec}]$ are the set of edges of the reference and reconstructed networks for an epoch i , after z-score normalization, then:

$$\varphi_i(e) = X_i^{Ref}(e) * X_i^{Rec}(e), e \in [1, E] \quad (11)$$

where i is the epoch index, e the edge index, and E the total number of edges. The average of φ_i across all subjects and all epochs is denoted ϕ . High positive ϕ values correspond to the edges that are consistent within- and between- subjects.

All statistical analyses were performed using R (R Core Team 2020). Linear mixed models implemented using the `{lme4}` package (Bates et al. 2015) were used to assess the effect of (i) number of electrodes, (ii) inverse solution, and (iii) functional connectivity metric as fixed effects on correlation and closeness accuracy. The “subject” was added as a random intercept to account for simulation-related variability (we had 50 subjects and 4 epochs per subject). Assumptions of normality and homoscedasticity of the model’s residuals were graphically checked. Regarding correlation, the following model was used:

$$Model = lmer(pearson_correlation \sim inverse_solution * connectivity_measure * channels + (1|subject_id), data = data) \quad (12)$$

The same model was used for closeness accuracy with the difference that closeness accuracy was inverse-transformed because of better compliance with the model's assumptions in that case. Calculation of the significance of fixed effects was performed with F tests using the *Anova* function of the *{car}* package (J. Fox and Weisberg 2019), and *post-hoc* analyses were performed using z -tests with the *glht* function of the *{multcomp}* package (Hothorn, Bretz, and Westfall 2008) that provides corrected p -values. Marginal and conditional R^2 were calculated with the *{MuMin}* package (Barton 2009) to estimate the variance explained by models. The significance threshold was set at its usual value of $p = 0.05$.

3. Results

Fig. 2 and Fig. 3 present, respectively, the distributions of correlation and closeness accuracy values, for all tested conditions (number of channels \times inverse solution \times connectivity measure) (results obtained for DAN can be found in the Supplementary Materials, Fig. S2, S3). Since the orthogonalization procedure used here is limited by the rank of data matrix (Colclough et al., 2015), it can only be applied to 128- and 256-electrodes configurations. Therefore, the statistical tests were repeated twice:

- Case 1: comparing all electrodes configurations (19, 32, 64, 128, 256), inverse solutions (eLORETA, LCMV, wMNE), and three connectivity measures (PLV, AEC, PLI) where no orthogonalization is applied.
- Case 2: comparing two electrode configurations (128, 256), all inverse solutions (eLORETA, LCMV, wMNE), and all connectivity metrics (PLV, AEC, PLI, AEC*).

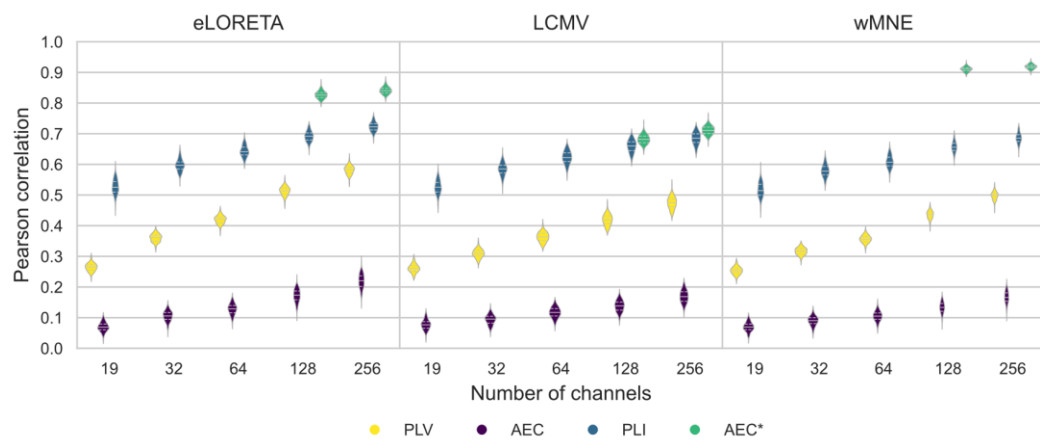


Fig. 2. Violin plots of the Pearson correlation values computed between reference and reconstructed DMNs for all electrode montages and inverse methods/connectivity metrics combinations. *eLORETA* - exact low-resolution electromagnetic tomography. *LCMV* - linearly constrained minimum norm

beamforming. wMNE - weighted minimum norm estimate. PLV - phase-locking value. AEC - amplitude envelope correlation. PLI - phase-lag index. AEC - amplitude envelope correlation with source leakage correction.*

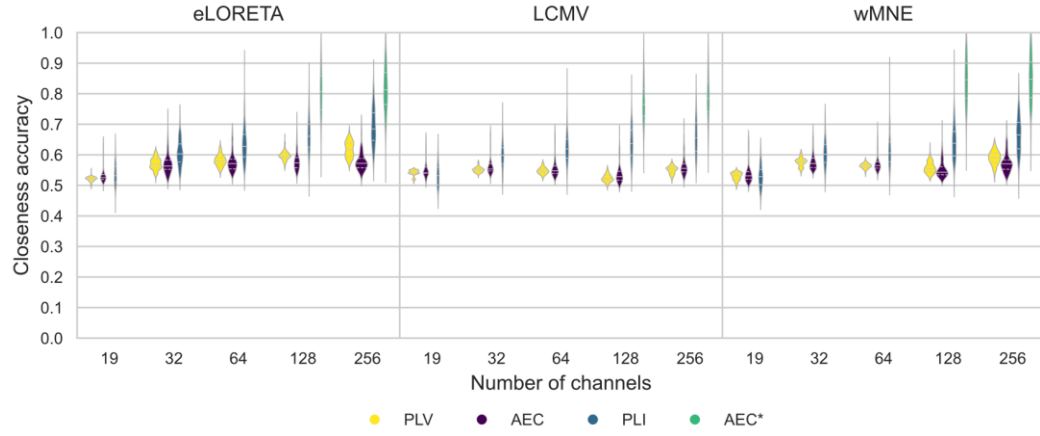


Fig. 3. Violin plots of closeness accuracy values computed between the reference and reconstructed DMNs for all electrode montages and inverse methods/connectivity metrics combinations. *eLORETA* - exact low-resolution electromagnetic tomography. *LCMV* - linearly constrained minimum norm beamforming. *wMNE* - weighted minimum norm estimate. *PLV* - phase-locking value. *AEC* - amplitude envelope correlation. *PLI* - phase-lag index. *AEC** - amplitude envelope correlation with source leakage correction.

3.1. Pearson Correlation

For all inverse methods and connectivity metrics, the trend in correlation values was similar as the number of electrodes increased, for both DMN and DAN: a greater number of channels was associated with higher correlation values. Pearson correlation results demonstrate a drastic effect of increasing the number of electrodes on enhancing the accuracy of reconstructed networks, regardless of the chosen inverse solution/connectivity measure. Statistical tests comparing all channels configurations, inverse solutions, and connectivity measures (PLV, AEC, PLI) (case 1) revealed that the effect of channel density was significant ($F(4, 8906) = 32256, p < 0.0001$; *full model marginal R*² = 0.99; *conditional R*² = 0.99) as well as all pairwise comparisons ($p < 0.0001$). Similarly, comparing all inverse solutions and connectivity measures (PLV, AEC, PLI, AEC*) at 128 and 256 channels (case 2) revealed a significant effect of electrodes density ($F(1, 4727) = 6142, p < 0.0001$; *full model marginal R*² = 0.99; *conditional R*² = 0.99). Significant effects of the inverse method (case 1: $F(2, 8906) = 4388, p < 0.0001$; case 2: $F(2, 4727) = 10396, p < 0.0001$) and functional connectivity measure (case 1: $F(2, 8906) = 651672, p <$

0.0001 ; case 2: $F(3,4727) = 371598, p < 0.0001$) were also identified. Moreover, reconstructed networks differed as a function of the inverse solution/connectivity metric combination (case 1: $F(4,8906) = 548, p < 0.0001$; case 2: $F(6,4727) = 4858, p < 0.0001$). *Post-hoc* analysis showed significant differences between inverse solution algorithms (case 1: $p < 0.001$, except for eLORETA vs wMNE: $p = 0.17$; case 2: $p < 0.001$ except for LCMV vs wMNE: $p = 0.01$), as well as connectivity measures ($p < 0.001$). Pairwise comparisons of the different combinations of inverse solution and functional connectivity methods also revealed significant differences between combinations (case 1: $p < 0.001$ except for wMNE/AEC vs eLORETA/AEC ($p = 1$), LCMV/PLI vs eLORETA/PLI ($p = 0.99$) and LCMV/PLV vs eLORETA/PLV ($p = 0.48$); case 2: $p < 0.001$ except for wMNE/AEC vs LCMV/AEC ($p = 0.13$) and wMNE/PLI vs LCMV/PLI ($p = 0.97$). At high sensor densities, AEC computed between orthogonalized time series along with wMNE and eLORETA, had the best reconstruction accuracy. PLI and corrected AEC, which discards zero-lag connections, came second with all three inverse solutions regardless of channel density. Regarding measures that do not compensate for spatial leakage, PLV had moderate performance, whereas AEC values were systematically low, regardless of the inverse method and number of electrodes.

3.2. Closeness accuracy

Differences in closeness accuracy values between evaluated electrode configurations were not as clear as with the Pearson correlation values, except for PLI and AEC*, which were associated with higher between-epochs variability. Similar to correlation results, closeness accuracy values were significantly affected by electrodes density (case 1: $F(4,8906) = 1278, p < 0.001$; *full model marginal R*² = 0.43; *conditional R*² = 0.44 ; case 2: $F(1,4727) = 267, p < 0.001$; *full model marginal R*² = 0.81; *conditional R*² = 0.82), inverse method (case 1: $F(2,8906) = 304, p < 0.001$; case 2: $F(2,4727) = 395, p < 0.001$), connectivity metric (case 1: $F(2,8906) = 2167, p < 0.001$; case 2: $F(3,4727) = 6696, p < 0.001$), and inverse method/connectivity metric combination (case 1: $F(4,8906) = 53, p < 0.001$; case 2: $F(6,4727) = 74, p < 0.001$). Pairwise comparisons of channel density showed significant differences between results obtained with 19 and (32, 64, 128, 256) channels ($p < 0.001$), as well as between 32 and 128 electrodes ($p = 0.01$). Other pairwise comparisons of electrode configurations were not significant. When comparing all electrodes configurations, inverse solutions, and (PLV, AEC, PLI), *post-hoc* analysis showed significant differences between inverse solutions ($p < 0.001$) except for

wMNE vs eLORETA ($p = 0.17$), as well as between connectivity metrics ($p < 0.001$) except for PLI vs AEC ($p = 1$). Regarding the inverse solution/connectivity measure combination, differences were not all significant. When comparing results obtained with 128 and 256 electrodes, all inverse solutions and connectivity metrics, significant differences were obtained for all inverse solutions ($p < 0.001$), connectivity measures ($p < 0.001$), and inverse solution/connectivity measure combinations ($p < 0.001$ except for wMNE/PLV vs WMNE/AEC ($p = 0.89$) and wMNE/PLI vs LCMV/PLI ($p = 1$).

3.3. Edge contribution

In Fig. 4 and Fig. 5, the contribution of DMN edges averaged across all subjects and epochs are presented for all sensor densities and inverse method/connectivity metric combinations (results for the DAN are shown in Fig. S4 and Fig. S5 in Supplementary Materials). The contribution of DMN connections to the correlation value computed between the reference and reconstructed networks increased when increasing the number of electrodes. High averaged edge contribution values can be seen as an indication of the consistency of DMN connections in the reconstructed networks across all data segments, i.e., a higher number of electrodes is associated with greater consistency of DMN edges. This trend was clearer with phase-based connectivity measures (PLV and PLI) than with AEC.

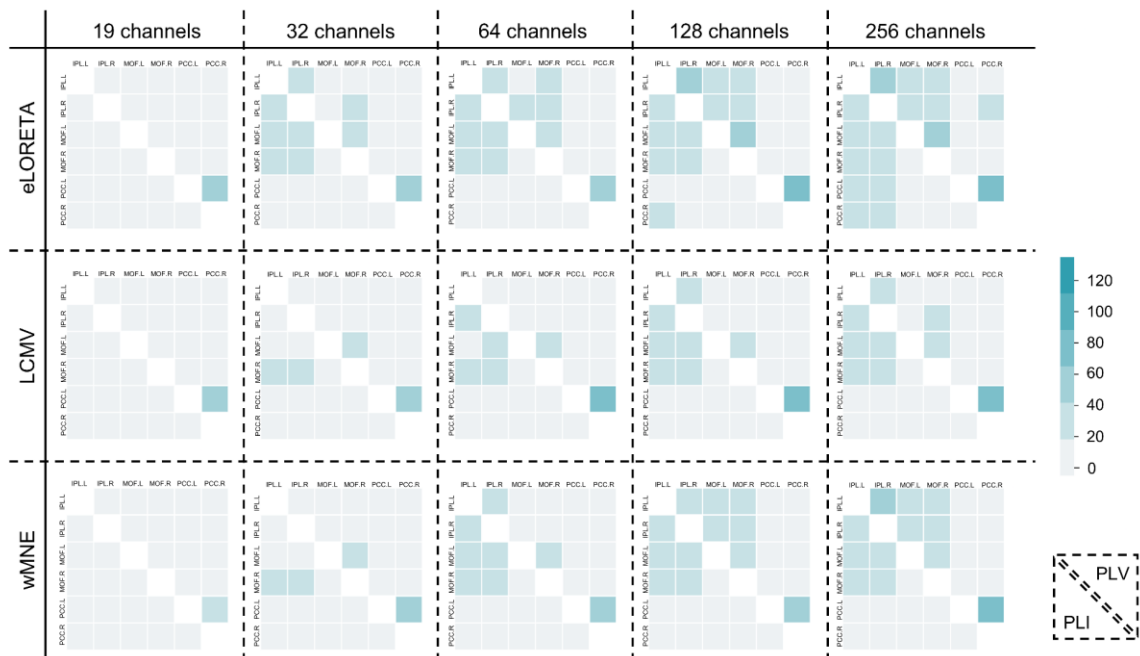


Fig. 4. Heatmaps of the contribution of DMN edges (see Materials and Methods section) averaged across all subjects and epochs are shown for all sensor densities and inverse method/connectivity measures (PLV, PLI) combinations. *eLORETA* - exact low-resolution electromagnetic tomography. *LCMV* - linearly constrained minimum norm beamforming. *wMNE* - weighted minimum norm estimate. *PLV* - phase-locking value. *AEC* - amplitude envelope correlation. *PLI* - phase-lag index. *AEC** - amplitude envelope correlation with source leakage correction.

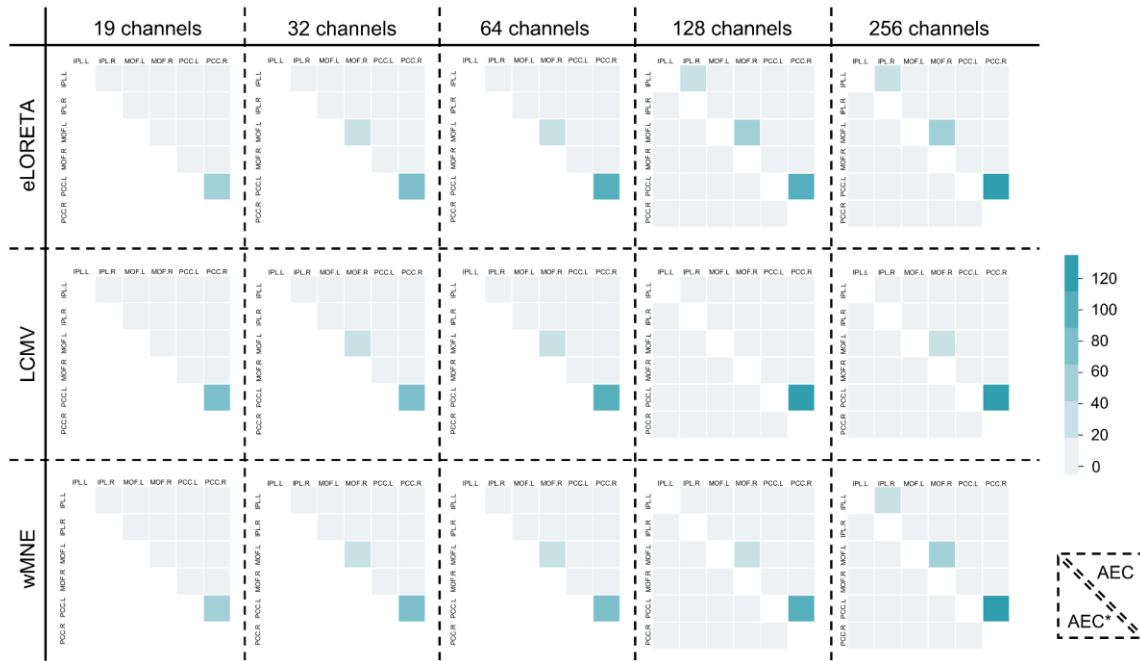


Fig. 5. Heatmaps of the contribution of the DMN edges averaged across all subjects and epochs are shown for all sensor densities and inverse method/connectivity measure (AEC, AEC*) combinations. *eLORETA* - exact low-resolution electromagnetic tomography. *LCMV* - linearly constrained minimum norm beamforming. *wMNE* - weighted minimum norm estimate. *PLV* - phase-locking value. *AEC* - amplitude envelope correlation. *PLI* - phase-lag index. *AEC** - amplitude envelope correlation with source leakage correction.

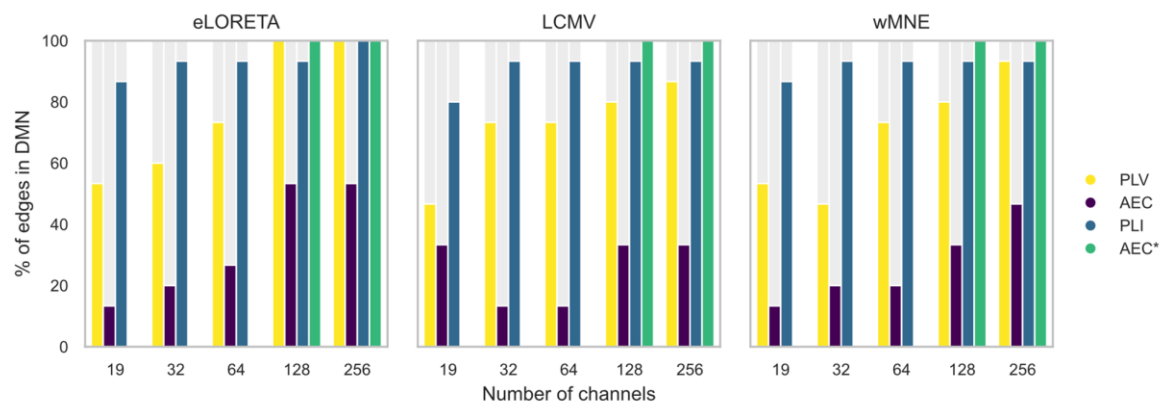


Fig. 6. Bar plots of the percentage of edges located within the DMN among the 30 edges having the highest contribution values. *eLORETA* - exact low-resolution electromagnetic tomography. *LCMV* - linearly constrained minimum norm beamforming. *wMNE* - weighted minimum norm estimate. *PLV* -

phase-locking value. AEC - amplitude envelope correlation. PLI - phase-lag index. AEC - amplitude envelope correlation with source leakage correction.*

We then thresholded the averaged edge contribution matrices and kept only the 30 edges (= number of edges in the reference RSNs) having the highest contribution values. The percentile of edges (among those having the highest contribution value) belonging to DMN (DAN) are thus shown in Fig. 6 (Fig. S6 in Supplementary Materials). With PLV and AEC, the percentage of edges within the DMN increased at higher channel density. With AEC, the percentage did not exceed 50%. In contrast, the majority of edges having the highest contribution were within the DMN when using PLI or AEC with source leakage correction, regardless of the number of channels.

3.4. Effect of white measurement noise

In Fig. 7, we plotted the Pearson correlation (mean + standard deviation) as a function of the measurement noise level (number of channels = 256). eLORETA and wMNE had similar performances. They both exhibited stable correlation values (≈ 0.7) for $\gamma \geq 0.4$ with PLV and $\gamma \geq 0.6$ with PLI. In contrast, LCMV combined with PLV and PLI had a linear trend where correlation values increased when measurement noise level decreased. Interestingly, AEC* had the highest performance in the absence of noise ($\gamma = 1$). However, its performance degraded drastically when white noise was added. eLORETA/AEC, wMNE/AEC, and LCMV/AEC were also stable in terms of performance, albeit performance being low. (Results corresponding to DAN are shown in Fig. S7 in Supplementary Materials).

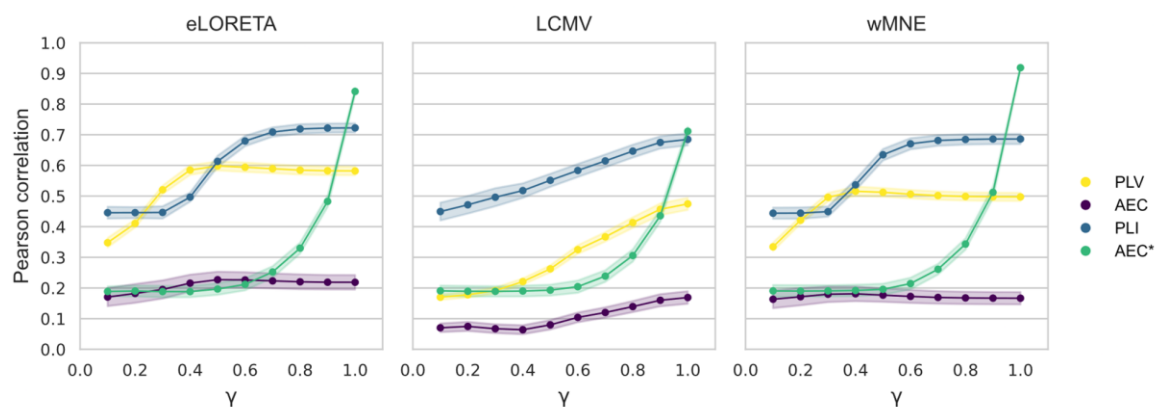


Fig. 7. The mean and standard deviation of the Pearson correlation computed between reference and reconstructed DMNs for different levels of measurement noise using 256 channels. *eLORETA* - exact low-resolution electromagnetic tomography. *LCMV* - linearly constrained minimum norm beamforming. *wMNE* - weighted minimum norm estimate. *PLV* - phase-locking value. *AEC* - amplitude

envelope correlation. PLI - phase-lag index. AEC - amplitude envelope correlation with source leakage correction.*

4. Discussion

The EEG/MEG source connectivity technique has gained increased interest due to its ability to reconstruct functional networks in the cortical space with a high temporal resolution. However, as aforementioned, there is still no agreement to date over a unified detailed EEG source connectivity pipeline, and several involved parameters/methods require cautious tuning. Such analytical variability is potentially problematic when associated with substantial variability in the outcomes. Here, our objective was to evaluate some of the parameters related to the EEG source connectivity analysis in the context of simulated RSNs and investigate results variability caused by different choices in the analysis pipeline. We mainly focused on the effect of electrodes density, inverse method, and functional connectivity metric. In a recent study, we tested the effect of electrodes density and tested wMNE and eLORETA along with PLV and wPLI in the context of simulated epileptiform activity (Allouch et al. 2022). In this specific case, epileptiform signals had a sufficiently high signal-to-noise-ratio (SNR) to be distinguished from background noise (Wa 1983; Iwasaki et al. 2005), which might have facilitated the identification of underlying networks. However, a growing interest since the last two decades has led to an increased number of resting-state studies where the significantly lower SNR could be in favor of different methods/parameter tuning in EEG source connectivity analysis. Therefore, in the present study, we used neural mass models to simulate resting-state brain activity (DMN and DAN) in the cortical space and derived the corresponding scalp EEG signals by solving the forward problem. Then, we reconstructed the corresponding cortical networks. This pipeline was repeated using different electrode densities (19, 32, 64, 128, and 256 channels) to solve the forward problem, three algorithms to solve the inverse problem (wMNE, eLORETA, LCMV), and four metrics to assess functional connectivity (PLV, AEC, PLI, leakage-corrected AEC (AEC*)), at different levels of measurement noise.

4.1. Number of electrodes

To the best of our knowledge, the effect of the number of electrodes on the reconstruction of EEG-based resting-state cortical networks has never been studied before, especially in the presence of a ground truth enabling an objective comparison of the tested electrode configurations. Our results demonstrate a key role of electrodes density on the EEG source

connectivity analysis: a more accurate reconstruction of cortical activity was achieved using high-density EEG (hd-EEG). This result is in line with previous simulations and empirical evidence (Goran Lantz et al., 2003; Sohrabpour et al., 2015; Song et al., 2015), as well as with the theoretical foundation (Song et al., 2015; Srinivasan et al., 1998). As established in (Srinivasan et al., 1998), an accurate characterization of spatial electrophysiological information requires a higher number of electrodes. A high inter-electrode distance (i.e., corresponding to a low number of EEG electrodes) can induce aliasing, and therefore high spatial frequency signals are misrepresented as low spatial frequency signals due to violation of the Nyquist criteria ($F_s > 2 \times F_{max}$) (Song et al., 2015; Srinivasan et al., 1998). In (Song et al., 2015) results were found to be independent of the inverse method (minimum norm/standardized low resolution brain electromagnetic tomography). On the other hand, (Goran Lantz et al., 2003) showed that 63 electrodes were sufficient for decent source localization with EPIFOCUS (a linear inverse solution that optimally localizes single focal sources (Grave de Peralta Menendez et al., 2001; G. Lantz et al., 2001)), however 100 electrodes were required when using wMNE. Consistently, (Goran Lantz et al., 2003) and (Sohrabpour et al., 2015) showed that a dramatic decrease in localization error was achieved when increasing the number of electrodes from 32 to 64 electrodes. Taken together, those studies and the present study support that the number of electrodes has a substantial effect on network reconstruction. Based on our results, we recommend a minimum of 64 electrodes to be used in the course of EEG source reconstruction in the specific context of RSNs.

4.2. Inverse solution and connectivity measures

Regarding the source connectivity estimation, a plethora of methods offers the possibility to 1) reconstruct cortical activity dynamics, and 2) assess functional connectivity between reconstructed sources. However, there is no consensus over an optimal approach, nor on whether such a “best” technique exists. Testing different combinations of inverse methods and connectivity measures with different measurement noise levels, we observed significant discrepancies in the results which was also observed in other comparative studies. In general, there is a lack of consistency across studies comparing inverse methods and connectivity measures. For example, (Anzolin et al., 2019) showed that LCMV had a better performance globally as compared to eLORETA. Similarly, in (Mahjoory et al., 2017), a relatively strong difference was found between LCMV beamformer on one hand, and eLORETA/wMNE solutions on the other hand. In (Bishop et al., 2015) the coherent maximum entropy on the

mean (cMEM) showed similar localization error to MNE, dynamic statistical parametric mapping (DSPM), sLORETA, but lower spatial spread and reduced crosstalk. In (Bradley et al., 2016), the use of LORETA for source localization outperformed sLORETA and minimum norm least square (MNLS). Following an extensive comparison between six inverse methods, (Bishop et al., 2015) recommended taking into account results from different methods when localizing actual interictal spikes. Results of source localization in (Halder et al., 2019) did not identify a clear winner between LCMV, eLORETA, MNE, DISC. (Bishop et al., 2015) summarized the conditions where each method can be recommended, following comparison of six inverse methods in resting-state MEG data. It is noteworthy to mention that the discrepancy in results could be probably related to the mathematical and physical constraints imposed by each inverse solution. More precisely, wMNE searches for a solution with minimum power (Hämäläinen & Ilmoniemi, 1994), while eLORETA tends to achieve exact zero error localization in the presence of measurement and structured biological noise (Pascual-Marqui, 2007). On the other hand, LCMV beamformer assumes that only one dipole is active at a time, and tries to minimize the corresponding output energy (Bishop et al., 2015).

In terms of functional connectivity metrics, (Colclough et al., 2016) assessed the consistency of different measures in experimental MEG resting-state data and recommended using the correlation between orthogonalized, band-limited, power envelopes (AEC). On the other hand, following extensive simulation studies, (Bishop et al., 2015) and (Wendling et al., 2009) both concluded that there is no ideal “one-fits-all” method for all data types: it is rather suggested to evaluate which conditions are appropriate for each method. In (Bishop et al., 2015) and (Hassan, Merlet, et al., 2017) in the context of epileptic spikes, wMNE combined with PLV had better accuracy as compared to other algorithms. Let us note that, in (Allouch et al. 2022), wMNE combined with wPLI performed better in the context of epileptiform activity simulations.

A key limitation of those numerous studies, and ours is no exception, is that different methods were tested in different contexts and using different data types, which complicates further the identification of clear and concise guidelines on the topic. Thus, we are aware that, even with our additional contribution, we are still far from a generalization of the results obtained in the specific context tested here (simulated signals, resting state activity, alpha rhythms, number/location of cortical sources, etc...). In fact, it is entirely possible (and even probable) that the inverse solution/connectivity measure combination is context-specific, and that no ideal method can account for all data types or all research questions. However, this raises the

question of whether it is possible to determine the method that is the most adapted in each context, which requests extensive investigation far beyond simple comparative studies. Meanwhile, cross-validation of the results using several methods/measures could be a reasonable compromise to avoid false positives induced by such substantial analytical variability.

4.3. Methodological considerations

Taking together the conclusions from the vast majority of analysis and modeling choices, the identified networks might be also sensitive to other factors that were not investigated in this study. For instance, spatial resolution in the cortical space (i.e., number/size of parcellated ROIs) could affect the accuracy of reconstructed networks. Our simulations were all restricted to 66 ROIs (Desikan-Killiany atlas) due to the model design. Many graph-based studies have reported that different parcellation scales resulted in significant differences in network parameters (clustering coefficient, characteristic path length, local and global efficiency, degree distribution, etc...), while inferences about small-world and scale-free properties were maintained across different scales (Bishop et al., 2015). In this study, we did not investigate how analytical variability related spatial resolution in the source space (i.e., number/size of ROIs) could affect the results. Therefore, it would be interesting to evaluate if the optimal number of ROIs depends on the number of recording electrodes and *vice versa*, i.e., whether there exists an optimal ratio (number of electrodes/number of ROIs) that exhibits higher accuracy regarding source connectivity. Moreover, the effect of parcellation is not limited to the number of regions, but also involves the algorithms by which sources belonging to the same ROI are aggregated (averaging signals across all vertices, averaging their absolute values, power signals, keeping the first mode of PCA decomposition, choosing the maximum value among vertices at each time point...).

Here, we simulated two widely studied RSNs (DMN and DAN). The major difference between those two networks is the position of simulated sources (i.e., the DMN/DAN's regions). While the DMN exhibits a less distributed architecture with small to moderate distance between regions (especially the right and left MPFC and PCC), DAN regions are widespread across the cortex with higher inter-region distances. Due to this difference, we were able to test whether the results are affected by the specific spatial location of sources. However, the similarity of results obtained with both networks confirms, to some extent, the absence of a bias caused by the position of sources. For simplicity, we restricted the number of DMN and DAN regions in

our simulations to six and focused on the most consistent regions reported in the literature. However, other regions could be involved in the simulated DMN, such as the precuneus, isthmus cingulate, rostral anterior cingulate, and lateral orbitofrontal cortex. The DAN could also include the middle temporal gyrus and frontal regions, such as the *pars opercularis*, *pars orbitalis*, and *pars triangularis* of the inferior frontal cortex (A. Kabbara et al., 2017, 2021). An interesting prospect would be testing the consistency of results when more complex networks are involved.

In the simulations used for this study, alpha activity [8-12] Hz was assigned to RSN, while background activity was attributed to the remaining regions. We acknowledge that such contrast between those two types of activity is not completely realistic. Despite a potential significant interest, we were not able to simulate brain-like broadband signals covering all frequency bands, due to intrinsic model limitations. In addition to broadband simulations, frequency bands other than alpha could be tested to replicate those results. Another limitation of our study is our “static” approach for brain networks’ identification (i.e., one network estimated per epoch), which we could improve upon by investigating the accuracy of brain networks’ dynamics. Importantly, understanding the dynamics of brain networks provides crucial insights regarding brain functions both in resting-state (Bishop et al., 2015) and task-related paradigms (Braun et al., 2015; Elton & Gao, 2015; Fong et al., 2019; Hassan et al., 2015; Krienen et al., 2014; O’Neill et al., 2017; Shine et al., 2016).

As aforementioned, inverse solutions and connectivity algorithms require tuning several parameters, such as the regularization parameter in wMNE, eLORETA, LCMV, and the time window over which connectivity measures are computed. Here, we applied either default or usually used values proposed by the Fieldtrip and Brainstorm toolboxes, or values proposed in previous studies. To test the stability of reconstructed networks across different regularization values, we computed the Pearson correlation between the reference and reconstructed networks for different regularization values (PLV, 256 channels) and presented the results in Fig. S8 in the Supplementary Materials. A decrease in the correlation values was observed when increasing the regularization of the inverse solution, emphasizing the importance of tuning the regularization parameter rather than using default values. Several methods are available to address this issue, falling into two general categories: those based on the estimation of the measurement noise, and those which are not (L-curve method, general-cross validation method, composite residual and smoothing operator, minimal product method, zero crossing) (Grech et al., 2008). An additional crucial factor that may introduce variability between results, and that

emerges when dealing with experimental EEG data, is the pre-processing procedure that precedes network reconstruction. EEG signals are indeed usually contaminated by several artifacts and noise sources, that may each introduce undesired changes in the measurements and affect the signal of interest (Urigüen and Garcia-Zapirain 2015), especially in clinical, pediatric, and aging populations (Pedroni, Bahreini, and Langer 2019). To “clean” EEG signals, pre-processing algorithms usually impose different constraints for accepting and rejecting artifactual epochs and propose different techniques to eliminate artifacts. Hence, an important methodological consideration would be to investigate and systematically quantify the variability induced by different data preprocessing techniques.

The choice of the most convenient metric for quantifying the results is also a challenge. Here, to quantify the performance of the tested parameters, we used the (1) Pearson correlation computed between the reference and reconstructed networks, (2) closeness accuracy reflecting the distance between the nodes detected in the reconstructed and reference networks, and (3) averaged contribution of network edges to the correlation between connectivity matrices (i.e., consistency of DMN/DAN connections across all simulation epochs) and the percentage of edges having the highest contributions and falling within the simulated RSN. It should be noted that each metric measures different aspects of data, and it is important in the context of comparative studies to address the relevant aspect of data to prevent biases. In our case, the general trend in the results was preserved across all used metrics. While both Pearson correlation and closeness accuracy showed significant differences between tested parameters, the latter exhibited higher variability between epochs. Other metrics such as networks-based metrics have also been developed to evaluate the distance/similarity between networks, and a promising approach would be testing whether the differences between networks are maintained across different aspects investigated by such metrics (global analysis, edge-wise, node-wise, spectral graph analysis, edit distance, kernel methods) (Mheich, Wendling, and Hassan 2020).

Importantly, correlation results presented in this article were computed between unthresholded weighted connectivity matrices. However, selecting a set of network edges for subsequent analysis while discarding others remains a debatable subject in the network neuroscience community. We usually face two main questions: 1) what method to use to perform thresholding, and 2) the choice of the threshold value when needed. Since we aimed to reduce further data manipulation and subjective intervention in the analysis, no threshold was applied before computing the Pearson correlation and edge contribution matrices in our study. However, we also tested the effect of a proportional threshold (1%) on correlation values and

reported the results in Fig. S9 in Supplementary materials. Although lower correlation values and higher between-epochs variability were obtained, the general trend was similar to that of unthresholded matrices.

5. Conclusion

To summarize, we simulated EEG data corresponding to RSNs and tested the effect of several key parameters (number of EEG electrodes and inverse solution/connectivity measure combination) on network reconstruction accuracy. Different analytical choices led to high variability in the resulting networks. In the context of RSN simulations, our results demonstrate, as expected, that an accurate cortical network reconstruction requires a high number of EEG electrodes. Therefore, we recommend using hd-EEG (≥ 64 channels) to infer cortical dynamics from recorded scalp EEG signals. In addition, we suggest a very careful choice of the inverse solution/connectivity measure combination, since our results highlight a significant variability in the networks reconstructed using different inverse solutions and connectivity measures. Such methodological variability and absence of analysis standardization represent a critical issue for neuroimaging studies that should be prioritized.

Data and codes availability

Data simulated for this study are available at <https://doi.org/10.5281/zenodo.6597385>. Codes supporting the results of this study are available at <https://github.com/sahar-allouch/var-RSNs>. We used Matlab (Matlab 2018), Brainstorm toolbox (Tadel et al. 2011), Fieldtrip toolbox ((Oostenveld et al. 2011); <http://fieldtriptoolbox.org>), OpenMEEG (Gramfort et al., 2010) implemented in fieldtrip, R (R Core Team 2020) for statistical analysis, and Seaborn (Waskom 2021) and Matplotlib (Hunter 2007) for visualization.

Acknowledgments

The authors would like to acknowledge the Lebanese National Council for Scientific Research (CNRS-L), the Agence Universitaire de la Francophonie (AUF), and the Lebanese University for granting Ms. Allouch a doctoral scholarship. This work was also supported by the Labex Cominlabs project PKSTIM and by the Institute of Clinical Neuroscience of Rennes (Projects EEGCog and EENET3). The authors would also like to thank Campus France, Programme

Hubert Curien CEDRE (PROJET N° 42257YA), and the Lebanese Association for Scientific Research (LASER) for their support.

Competing Interests

The authors declare that they have no competing interests.

References

- Alavash, Mohsen, Philipp Doebler, Heinz Holling, Christiane M. Thiel, and Carsten Gießing. 2015. “Is Functional Integration of Resting State Brain Networks an Unspecific Biomarker for Working Memory Performance?” *NeuroImage* 108 (March): 182–93.
- Allen, E. A., E. Damaraju, T. Eichele, L. Wu, and V. D. Calhoun. 2018. “EEG Signatures of Dynamic Functional Network Connectivity States.” *Brain Topography* 31 (1): 101–16.
- Allen, Elena A., Eswar Damaraju, Sergey M. Plis, Erik B. Erhardt, Tom Eichele, and Vince D. Calhoun. 2014. “Tracking Whole-Brain Connectivity Dynamics in the Resting State.” *Cerebral Cortex* 24: 663–76.
- Allouch, Sahar, Maxime Yochum, Aya Kabbara, Joan Duprez, Mohamad Khalil, Fabrice Wendling, Mahmoud Hassan, and Julien Modolo. 2022. “Mean-Field Modeling of Brain-Scale Dynamics for the Evaluation of EEG Source-Space Networks.” *Brain Topography* 35 (1): 54–65.
- Anzolin, Alessandra, Paolo Presti, Frederik Van De Steen, Laura Astolfi, Stefan Haufe, and Daniele Marinazzo. 2019. “Quantifying the Effect of Demixing Approaches on Directed Connectivity Estimated Between Reconstructed EEG Sources.” *Brain Topography*. <https://doi.org/10.1007/s10548-019-00705-z>.
- Awan, Fahim Gohar, Omer Saleem, and Asima Kiran. 2019. “Recent Trends and Advances in Solving the Inverse Problem for EEG Source Localization.” *Inverse Problems in Science & Engineering* 27 (11): 1521–36.
- Baillet, Sylvain, John C. Mosher, and Richard M. Leahy. 2001. “Electromagnetic Brain Mapping.” *IEEE Signal Processing Magazine*, no. November: 14–30.
- Baker, Adam P., Matthew J. Brookes, Iead A. Rezek, Stephen M. Smith, Timothy Behrens, Penny J. Probert Smith, and Mark Woolrich. 2014. “Fast Transient Networks in Spontaneous Human Brain Activity.” *ELife* 3 (March): e01867.
- Barton, K. 2009. “MuMIn: Multi-Model Inference.” *Http://R-Forge. r-Project. Org/Projects/Mumin/*. <https://ci.nii.ac.jp/naid/20001420752/>.
- Bates, Douglas, Martin Mächler, Benjamin M. Bolker, and Steven C. Walker. 2015. “Fitting Linear Mixed-Effects Models Using Lme4.” *Journal of Statistical Software* 67 (1). <https://doi.org/10.18637/jss.v067.i01>.
- Bensaid, Siouar, Julien Modolo, Isabelle Merlet, Fabrice Wendling, and Pascal Benquet. 2019. “COALIA: A Computational Model of Human EEG for Consciousness Research.” *Frontiers in Systems Neuroscience* 13: 1–18.
- Bradley, Allison, Jun Yao, Jules Dewald, and Claus Peter Richter. 2016. “Evaluation of Electroencephalography Source Localization Algorithms with Multiple Cortical Sources.” *PloS One* 11 (1): 1–14.

- Braun, Urs, Axel Schäfer, Henrik Walter, Susanne Erk, Nina Romanczuk-Seiferth, Leila Haddad, Janina I. Schweiger, et al. 2015. “Dynamic Reconfiguration of Frontal Brain Networks during Executive Cognition in Humans.” *Proceedings of the National Academy of Sciences of the United States of America* 112 (37): 11678–83.
- Brookes, Matthew J., Joanne R. Hale, Johanna M. Zumer, Claire M. Stevenson, Susan T. Francis, Gareth R. Barnes, Julia P. Owen, Peter G. Morris, and Srikantan S. Nagarajan. 2011. “NeuroImage Measuring Functional Connectivity Using MEG : Methodology and Comparison with FcMRI.” *NeuroImage* 56 (3): 1082–1104.
- Cao, Jun, Yifan Zhao, Xiaocai Shan, Hua-Liang Wei, Yuzhu Guo, Liangyu Chen, John Ahmet Erkoyuncu, and Ptolemaios Georgios Sarrigiannis. 2022. “Brain Functional and Effective Connectivity Based on Electroencephalography Recordings: A Review.” *Human Brain Mapping* 43 (2): 860–79.
- Colclough, G. L., M. J. Brookes, S. M. Smith, and M. W. Woolrich. 2015. “A Symmetric Multivariate Leakage Correction for MEG Connectomes.” *NeuroImage* 117 (August): 439–48.
- Colclough, G. L., M. W. Woolrich, P. K. Tewarie, M. J. Brookes, A. J. Quinn, and S. M. Smith. 2016. “How Reliable Are MEG Resting-State Connectivity Metrics?” *NeuroImage* 138: 284–93.
- Damoiseaux, J. S., S. A. R. B. Rombouts, F. Barkhof, P. Scheltens, C. J. Stam, S. M. Smith, and C. F. Beckmann. 2006. “Consistent Resting-State Networks across Healthy Subjects.” *Proceedings of the National Academy of Sciences of the United States of America* 13 (37): 13848–53.
- De Pasquale, Francesco, Stefania Della Penna, O. Sporns, Gian Luca Romani, and M. Corbetta. 2016. “A Dynamic Core Network and Global Efficiency in the Resting Human Brain.” *Cerebral Cortex* 26 (10): 4015–33.
- Desikan, Rahul S., Florent Ségonne, Bruce Fischl, Brian T. Quinn, Bradford C. Dickerson, Deborah Blacker, Randy L. Buckner, et al. 2006. “An Automated Labeling System for Subdividing the Human Cerebral Cortex on MRI Scans into Gyral Based Regions of Interest.” *NeuroImage* 31: 968–80.
- Elton, Amanda, and Wei Gao. 2015. “Task-Related Modulation of Functional Connectivity Variability and Its Behavioral Correlations.” *Human Brain Mapping* 36 (8): 3260–72.
- Finn, Emily S., Xilin Shen, Dustin Scheinost, Monica D. Rosenberg, Jessica Huang, Marvin M. Chun, Xenophon Papademetris, and R. Todd Constable. 2015. “Functional Connectome Fingerprinting: Identifying Individuals Using Patterns of Brain Connectivity.” *Nature Neuroscience* 18 (11): 1664–71.
- Fong, Angus Ho Ching, Kwangsun Yoo, Monica D. Rosenberg, Sheng Zhang, Chiang-Shan R. Li, Dustin Scheinost, R. Todd Constable, and Marvin M. Chun. 2019. “Dynamic Functional Connectivity during Task Performance and Rest Predicts Individual Differences in Attention across Studies.” *NeuroImage* 188 (March): 14–25.
- Fornito, Alex, Andrew Zalesky, and Edward T. Bullmore. 2010. “Network Scaling Effects in Graph Analytic Studies of Human Resting-State FMRI Data.” *Frontiers in Systems Neuroscience* 4: 1–16.
- Fox, John, and Sanford Weisberg. 2019. *An R Companion to Applied Regression (Third)*. Sage. <https://doi.org/10.1177/0049124105277200>.
- Fox, Michael D., and Marcus E. Raichle. 2007. “Spontaneous Fluctuations in Brain Activity Observed with Functional Magnetic Resonance Imaging.” *Nature Reviews Neuroscience* 8 (9): 700–711.
- Friston, Karl J. 2011. “Functional and Effective Connectivity: A Review.” *Brain Connectivity* 1 (1): 13–36.
- Fuchs, Manfred, Michael Wagner, Thomas Köhler, and Hans Aloys Wischmann. 1999. “Linear and Nonlinear Current Density Reconstructions.” *Journal of Clinical Neurophysiology: Official Publication of the American Electroencephalographic Society* 16 (3): 267–95.

- Gramfort, Alexandre, Théodore Papadopulo, Emmanuel Olivi, and Maureen Clerc. 2010. “OpenMEEG: Opensource Software for Quasistatic Bioelectromagnetics.” *Biomedical Engineering Online* 9 (45). <https://doi.org/10.1186/1475-925X-8-1>.
- Gratton, Caterina, Jonathan M. Koller, William Shannon, Deanna J. Greene, Baijayanta Maiti, Abraham Z. Snyder, Steven E. Petersen, Joel S. Perlmutter, and Meghan C. Campbell. 2018. “Emergent Functional Network Effects in Parkinson Disease.” *Cerebral Cortex* 29 (6): 2509–23.
- Grave de Peralta Menendez, R., S. Gonzalez Andino, G. Lantz, C. M. Michel, and T. Landis. 2001. “Noninvasive Localization of Electromagnetic Epileptic Activity. I. Method Descriptions and Simulations.” *Brain Topography* 14 (2): 131–37.
- Grech, Roberta, Tracey Cassar, Joseph Muscat, Kenneth P. Camilleri, Simon G. Fabri, Michalis Zervakis, Petros Xanthopoulos, Vangelis Sakkalis, and Bart Vanrumste. 2008. “Review on Solving the Inverse Problem in EEG Source Analysis.” *Journal of Neuroengineering and Rehabilitation* 5 (25). <https://doi.org/10.1186/1743-0003-5-25>.
- Greicius, Michael D., Ben Krasnow, Allan L. Reiss, and Vinod Menon. 2003. “Functional Connectivity in the Resting Brain: A Network Analysis of the Default Mode Hypothesis.” *Proceedings of the National Academy of Sciences of the United States of America* 100 (1): 253–58.
- Grova, C., J. Daunizeau, J. M. Lina, C. G. Bénar, H. Benali, and J. Gotman. 2006. “Evaluation of EEG Localization Methods Using Realistic Simulations of Interictal Spikes.” *NeuroImage* 29: 734–53.
- Halder, Tamesh, Siddharth Talwar, Amit Kumar Jaiswal, and Arpan Banerjee. 2019. “Quantitative Evaluation in Estimating Sources Underlying Brain Oscillations Using Current Source Density Methods and Beamformer Approaches.” *ENeuro* 6 (4): 1–14.
- Hämäläinen, M. S., and R. J. Ilmoniemi. 1994. “Interpreting Magnetic Fields of the Brain: Minimum Norm Estimates.” *Medical & Biological Engineering & Computing* 32: 35–42.
- Hassan, M., P. Benquet, A. Biraben, C. Berrou, O. Dufor, and F. Wendling. 2015. “Dynamic Reorganization of Functional Brain Networks during Picture Naming.” *Cortex; a Journal Devoted to the Study of the Nervous System and Behavior* 73: 276–88.
- Hassan, M., L. Chaton, P. Benquet, A. Delval, C. Leroy, L. Plomhause, A. J. H. Moonen, et al. 2017. “Functional Connectivity Disruptions Correlate with Cognitive Phenotypes in Parkinson’s Disease.” *NeuroImage. Clinical* 14 (March): 591–601.
- Hassan, M., O. Dufor, I. Merlet, C. Berrou, and F. Wendling. 2014. “EEG Source Connectivity Analysis: From Dense Array Recordings to Brain Networks.” *PloS One* 9 (8): e105041.
- Hassan, M., I. Merlet, A. Mheich, A. Kabbara, A. Biraben, A. Nica, and F. Wendling. 2017. “Identification of Interictal Epileptic Networks from Dense-EEG.” *Brain Topography* 30 (1): 60–76.
- Hassan, M., and F. Wendling. 2018. “Electroencephalography Source Connectivity: Aiming for High Resolution of Brain Networks in Time and Space.” *IEEE Signal Processing Magazine* 35 (3): 81–96.
- Hayasaka, Satoru, and Paul J. Laurienti. 2010. “Comparison of Characteristics between Region-and Voxel-Based Network Analyses in Resting-State fMRI Data.” *NeuroImage* 50: 499–508.
- Hedrich, T., G. Pellegrino, E. Kobayashi, J. M. Lina, and C. Grova. 2017. “Comparison of the Spatial Resolution of Source Imaging Techniques in High-Density EEG and MEG.” *NeuroImage* 157 (August): 531–44.
- Heuvel, Martijn van den, Rene Mandl, and Hilleke Hulshoff Pol. 2008. “Normalized Cut Group Clustering of Resting-State fMRI Data.” *PloS One* 3 (4). <https://doi.org/10.1371/journal.pone.0002001>.

- Hipp, Joerg F., David J. Hawellek, Maurizio Corbetta, Markus Siegel, and Andreas K. Engel. 2012. “Large-Scale Cortical Correlation Structure of Spontaneous Oscillatory Activity.” *Nature Neuroscience* 15 (6): 884–90.
- Hothorn, Torsten, Frank Bretz, and Peter Westfall. 2008. “Simultaneous Inference in General Parametric Models.” *Biometrical Journal. Biometrische Zeitschrift* 50 (3): 346–63.
- Hunter. 2007. “Matplotlib: A 2D Graphics Environment.” *Computing in Science & Engineering* 9 (May): 90–95.
- Iwasaki, Masaki, Elia Pestana, Richard C. Burgess, Hans O. Lüders, Hiroshi Shamoto, and Nobukazu Nakasato. 2005. “Detection of Epileptiform Activity by Human Interpreters: Blinded Comparison between Electroencephalography and Magnetoencephalography.” *Epilepsia* 46 (1): 59–68.
- Jimenez, Amy M., Philipp Riedel, Junghee Lee, Eric A. Reavis, and Michael F. Green. 2019. “Linking Resting-State Networks and Social Cognition in Schizophrenia and Bipolar Disorder.” *Human Brain Mapping* 40 (16): 4703–15.
- Jockwitz, Christiane, Svenja Caspers, Silke Lux, Simon B. Eickhoff, Kerstin Jütten, Stefan Lenzen, Susanne Moebus, et al. 2017. “Influence of Age and Cognitive Performance on Resting-State Brain Networks of Older Adults in a Population-Based Cohort.” *Cortex; a Journal Devoted to the Study of the Nervous System and Behavior* 89 (April): 28–44.
- Kabbara, A., H. Eid, W. El Falou, M. Khalil, F. Wendling, and M. Hassan. 2018. “Reduced Integration and Improved Segregation of Functional Brain Networks in Alzheimer’s Disease.” *Journal of Neural Engineering* 15 (2): 026023.
- Kabbara, A., W. El Falou, M. Khalil, F. Wendling, and M. Hassan. 2017. “The Dynamic Functional Core Network of the Human Brain at Rest.” *Scientific Reports* 7 (1): 2936.
- Kabbara, A., V. Paban, and M. Hassan. 2021. “The Dynamic Modular Fingerprints of the Human Brain at Rest.” *NeuroImage* 227 (February): 117674.
- Keller, Joseph B., Trey Hedden, Todd W. Thompson, Sheeba A. Anteraper, John D. E. Gabrieli, and Susan Whitfield-Gabrieli. 2015. “Resting-State Anticorrelations between Medial and Lateral Prefrontal Cortex: Association with Working Memory, Aging, and Individual Differences.” *Cortex; a Journal Devoted to the Study of the Nervous System and Behavior* 64 (March): 271–80.
- Krienen, Fenna M., B. T. Thomas Yeo, and Randy L. Buckner. 2014. “Reconfigurable Task-Dependent Functional Coupling Modes Cluster around a Core Functional Architecture.” *Philosophical Transactions of the Royal Society of London. Series B, Biological Sciences* 369 (1653). <https://doi.org/10.1098/rstb.2013.0526>.
- Lachaux, Jean-Philippe, Eugenio Rodriguez, Michel Le Van Quyen, Antoine Lutz, Jacques Martinerie, and Francisco J. Varela. 2000. “Studying Single-Trials of Phase Synchronous Activity in the Brain.” *International Journal of Bifurcation and Chaos in Applied Sciences and Engineering* 10 (10): 2429–39.
- Lantz, G., R. Grave de Peralta Menendez, S. Gonzalez Andino, and C. M. Michel. 2001. “Noninvasive Localization of Electromagnetic Epileptic Activity. II. Demonstration of Sublobar Accuracy in Patients with Simultaneous Surface and Depth Recordings.” *Brain Topography* 14 (2): 139–47.
- Lantz, Goran, R. Grave de Peralta, L. Spinelli, M. Seeck, and C. M. Michel. 2003. “Epileptic Source Localization with High Density EEG: How Many Electrodes Are Needed?” *Clinical Neurophysiology: Official Journal of the International Federation of Clinical Neurophysiology* 114 (1): 63–69.

- Lin, Fa Hsuan, Thomas Witzel, Seppo P. Ahlfors, Steven M. Stufflebeam, John W. Belliveau, and Matti S. Härmäläinen. 2006. “Assessing and Improving the Spatial Accuracy in MEG Source Localization by Depth-Weighted Minimum-Norm Estimates.” *NeuroImage* 31: 160–71.
- Mahjoory, Keyvan, Vadim V. Nikulin, Loïc Botrel, Klaus Linkenkaer-Hansen, Marco M. Fato, and Stefan Haufe. 2017. “Consistency of EEG Source Localization and Connectivity Estimates.” *NeuroImage* 152 (May): 590–601.
- Matlab. 2018. “9.5.0.944444 (R2018b).” Natick, Massachusetts: The MathWorks Inc.
- Mheich, A., F. Wendling, and M. Hassan. 2020. “Brain Network Similarity: Methods and Applications.” *Network Neuroscience* 4 (3): 507–27.
- O’Neill, George C., Prejaas K. Tewarie, Giles L. Colclough, Lauren E. Gascoyne, Benjamin A. E. Hunt, Peter G. Morris, Mark W. Woolrich, and Matthew J. Brookes. 2017. “Measurement of Dynamic Task Related Functional Networks Using MEG.” *NeuroImage* 146: 667–78.
- Oostenveld, Robert, Pascal Fries, Eric Maris, and Jan Mathijs Schoffelen. 2011. “FieldTrip: Open Source Software for Advanced Analysis of MEG, EEG, and Invasive Electrophysiological Data.” *Computational Intelligence and Neuroscience* 2011. <https://doi.org/10.1155/2011/156869>.
- Pascual-Marqui, Roberto D. 2007. “Discrete, 3D Distributed, Linear Imaging Methods of Electric Neuronal Activity. Part 1: Exact, Zero Error Localization.” <http://arxiv.org/abs/0710.3341>.
- Pasquale, F. de, M. Corbetta, V. Betti, and S. Della Penna. 2018. “Cortical Cores in Network Dynamics.” *NeuroImage* 180 (Pt B): 370–82.
- Pasquale, Francesco de, Stefania Della Penna, Abraham Z. Snyder, Laura Marzetti, Vittorio Pizzella, Gian Luca Romani, and Maurizio Corbetta. 2012. “A Cortical Core for Dynamic Integration of Functional Networks in the Resting Human Brain.” *Neuron* 74 (4): 753–64.
- Pedroni, Andreas, Amirreza Bahreini, and Nicolas Langer. 2019. “Automagic: Standardized Preprocessing of Big EEG Data.” *NeuroImage* 200 (October): 460–73.
- Pereda, Ernesto, Rodrigo Quiroga, and Joydeep Bhattacharya. 2005. “Nonlinear Multivariate Analysis of Neurophysiological Signals.” *Progress in Neurobiology* 77: 1–37.
- R Core Team. 2020. *R: A Language and Environment for Statistical Computing*. Vienna, Austria: R Foundation for Statistical Computing. <https://www.R-project.org/>.
- Raichle, Marcus E., Ann Mary MacLeod, Abraham Z. Snyder, William J. Powers, Debra A. Gusnard, and Gordon L. Shulman. 2001. “A Default Mode of Brain Function.” *Proceedings of the National Academy of Sciences of the United States of America* 98 (2): 676–82.
- Raichle, Marcus E., and Abraham Z. Snyder. 2007. “A Default Mode of Brain Function: A Brief History of an Evolving Idea.” *NeuroImage* 37 (4): 1083–90.
- Sheline, Yvette I., and Marcus E. Raichle. 2013. “Resting State Functional Connectivity in Preclinical Alzheimer’s Disease.” *Biological Psychiatry* 74 (5): 340–47.
- Shen, Xueyi, Simon R. Cox, Mark J. Adams, David M. Howard, Stephen M. Lawrie, Stuart J. Ritchie, Mark E. Bastin, Ian J. Deary, Andrew M. McIntosh, and Heather C. Whalley. 2018. “Resting-State Connectivity and Its Association With Cognitive Performance, Educational Attainment, and Household Income in the UK Biobank.” *Biological Psychiatry. Cognitive Neuroscience and Neuroimaging* 3 (10): 878–86.
- Shine, James M., Patrick G. Bissett, Peter T. Bell, Oluwasanmi Koyejo, Joshua H. Balsters, Krzysztof J. Gorgolewski, Craig A. Moodie, and Russell A. Poldrack. 2016. “The Dynamics of Functional Brain Networks: Integrated Network States during Cognitive Task Performance.” *Neuron* 92 (2): 544–54.

- Shirer, W. R., S. Ryali, E. Rykhlevskaia, V. Menon, and M. D. Greicius. 2012. “Decoding Subject-Driven Cognitive States with Whole-Brain Connectivity Patterns.” *Cerebral Cortex* 22 (1): 158–65.
- Sohrabi, Abbas, Yunfeng Lu, Pongkiat Kankirawatana, Jeffrey Blount, Hyunmi Kim, and Bin He. 2015. “Effect of EEG Electrode Number on Epileptic Source Localization in Pediatric Patients.” *Clinical Neurophysiology: Official Journal of the International Federation of Clinical Neurophysiology* 126: 472–80.
- Song, J., C. Davey, C. Poulsen, P. Luu, S. Turovets, E. Anderson, K. Li, and D. Tucker. 2015. “EEG Source Localization: Sensor Density and Head Surface Coverage.” *Journal of Neuroscience Methods* 256: 9–21.
- Srinivasan, Ramesh, Don M. Tucker, and Michael Murias. 1998. “Estimating the Spatial Nyquist of the Human EEG.” *Behavior Research Methods, Instruments, & Computers: A Journal of the Psychonomic Society, Inc* 30 (1): 8–19.
- Stam, Cornelis J., Guido Nolte, and Andreas Daffertshofer. 2007. “Phase Lag Index: Assessment of Functional Connectivity from Multi Channel EEG and MEG with Diminished Bias from Common Sources.” *Human Brain Mapping* 28: 1178–93.
- Tadel, Franois, Sylvain Baillet, John C. Mosher, Dimitrios Pantazis, and Richard M. Leahy. 2011. “Brainstorm: A User-Friendly Application for MEG/EEG Analysis.” *Computational Intelligence and Neuroscience* 2011. <https://doi.org/10.1155/2011/879716>.
- Tait, Luke, Aysegül Özkan, Maciej J. Szul, and Jiaxiang Zhang. 2021. “A Systematic Evaluation of Source Reconstruction of Resting MEG of the Human Brain with a New High-Resolution Atlas: Performance, Precision, and Parcellation.” *Human Brain Mapping* 42 (14): 4685–4707.
- Urigüen, Jose Antonio, and Begoña Garcia-Zapirain. 2015. “EEG Artifact Removal - State-of-the-Art and Guidelines.” *Journal of Neural Engineering* 12: 1–23.
- Van Essen, David C., Stephen M. Smith, Deanna M. Barch, Timothy E. J. Behrens, Essa Yacoub, Kamil Ugurbil, and WU-Minn HCP Consortium. 2013. “The WU-Minn Human Connectome Project: An Overview.” *NeuroImage* 80 (October): 62–79.
- Van Veen, B. D., W. van Drongelen, M. Yuchtman, and A. Suzuki. 1997. “Localization of Brain Electrical Activity via Linearly Constrained Minimum Variance Spatial Filtering.” *IEEE Transactions on Bio-Medical Engineering* 44 (9): 867–80.
- Wa, C. 1983. “IFCN Recommendations for the Practice of Clinical Neurophysiology Amsterdam.” New York, NY: Elsevier.
- Wang, Huifang E., Christian G. Bénar, Pascale P. Quilichini, Karl J. Friston, Viktor K. Jirsa, and Christophe Bernard. 2014. “A Systematic Framework for Functional Connectivity Measures.” *Frontiers in Neuroscience* 8. <https://doi.org/10.3389/fnins.2014.00405>.
- Wang, Jinhuai, Liang Wang, Yufeng Zang, Hong Yang, Hehan Tang, Qiyong Gong, Zhang Chen, Chaozhe Zhu, and Yong He. 2009. “Parcellation-Dependent Small-World Brain Functional Networks: A Resting-State Fmri Study.” *Human Brain Mapping* 30: 1511–23.
- Waskom, Michael. 2021. “Seaborn: Statistical Data Visualization.” *Journal of Open Source Software* 6 (60): 3021.
- Wendling, Fabrice, Karim Ansari-Asl, Fabrice Bartolomei, and Lotfi Senhadji. 2009. “From EEG Signals to Brain Connectivity: A Model-Based Evaluation of Interdependence Measures.” *Journal of Neuroscience Methods* 183: 9–18.
- Zalesky, Andrew, Alex Fornito, Ian H. Harding, Luca Cocchi, Murat Yücel, Christos Pantelis, and Edward T. Bullmore. 2010. “Whole-Brain Anatomical Networks: Does the Choice of Nodes Matter?” *NeuroImage* 50: 970–83.

Supplementary Materials

Effect of channel density, inverse solutions and connectivity measures on EEG resting-state networks reconstruction: a simulation study

Sahar Allouch^{1,2}, Aya Kabbara^{3,4}, Joan Duprez¹, Mohamad Khalil^{2,5}, Julien Modolo^{1*}, Mahmoud Hassan^{3,6*},

¹ Univ Rennes, INSERM, LTSI - UMR 1099, F-35000 Rennes, France

² Azm Center for Research in Biotechnology and Its Applications, EDST, Tripoli, Lebanon

³ MINDig, F-35000 Rennes, France

⁴ LASER - Lebanese Association for Scientific Research, Tripoli, Lebanon

⁵ CRSI research center, Faculty of Engineering, Lebanese University, Beirut, Lebanon

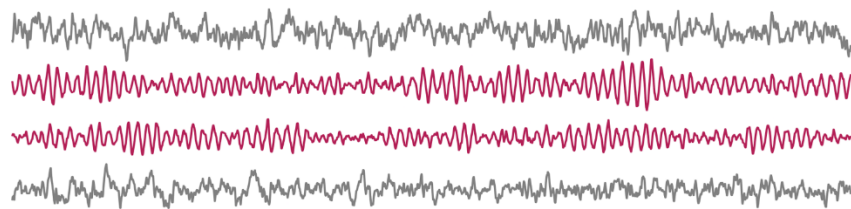
⁶ School of Science and Engineering, Reykjavik University, Reykjavik, Iceland

* Equally contributed

Corresponding author: saharallouch@gmail.com

1. Materials and Methods

A) Cortical simulations



B) Scalp EEG

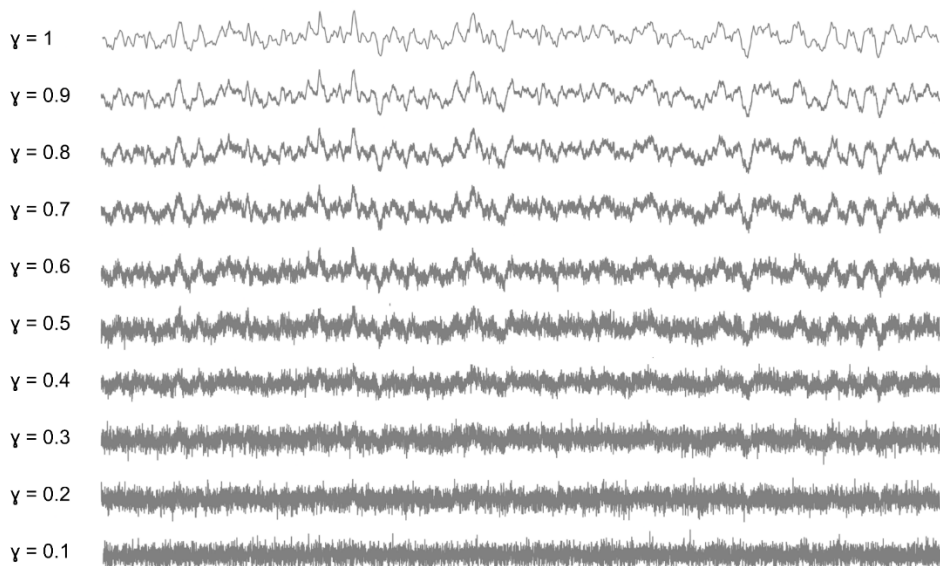


Fig. S1. A) An example of simulated cortical signals. B) Scalp EEG signals for different measurement noise levels (i.e., different gamma values).

2. Results

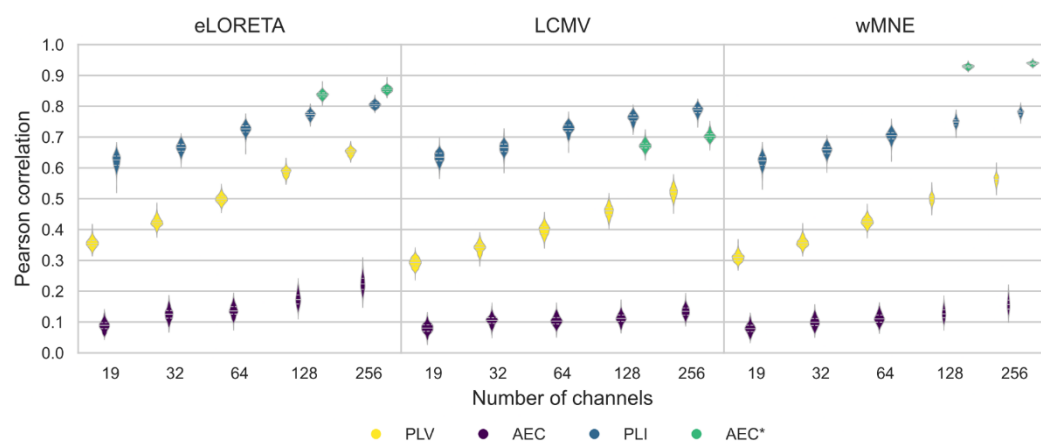


Fig. S2. Violin plots of the Pearson correlation values computed between the reference and reconstructed DANs for all electrode montages and inverse methods/connectivity metrics combinations. *eLORETA* - exact low-resolution electromagnetic tomography. *LCMV* - linearly constrained minimum norm beamforming. *wMNE* - weighted minimum norm estimate. *PLV* - phase-locking value. *AEC* - amplitude envelope correlation. *PLI* - phase-lag index. *AEC** - amplitude envelope correlation with source leakage correction.

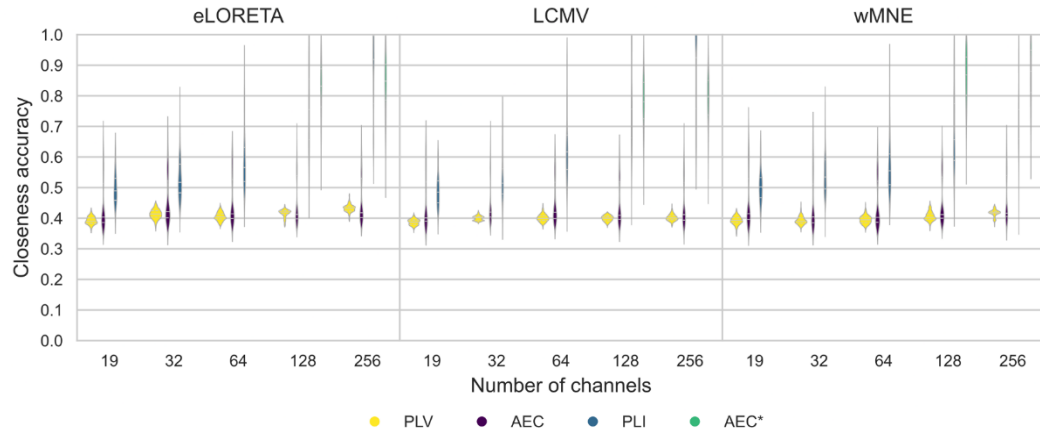


Fig. S3. Violin plots of the closeness accuracy values computed between the reference and reconstructed DANs for all electrode montages and inverse methods/connectivity metrics combinations. *eLORETA* - exact low-resolution electromagnetic tomography. *LCMV* - linearly constrained minimum norm beamforming. *wMNE* - weighted minimum norm estimate. *PLV* - phase-locking value. *AEC* - amplitude envelope correlation. *PLI* - phase-lag index. *AEC** - amplitude envelope correlation with source leakage correction.

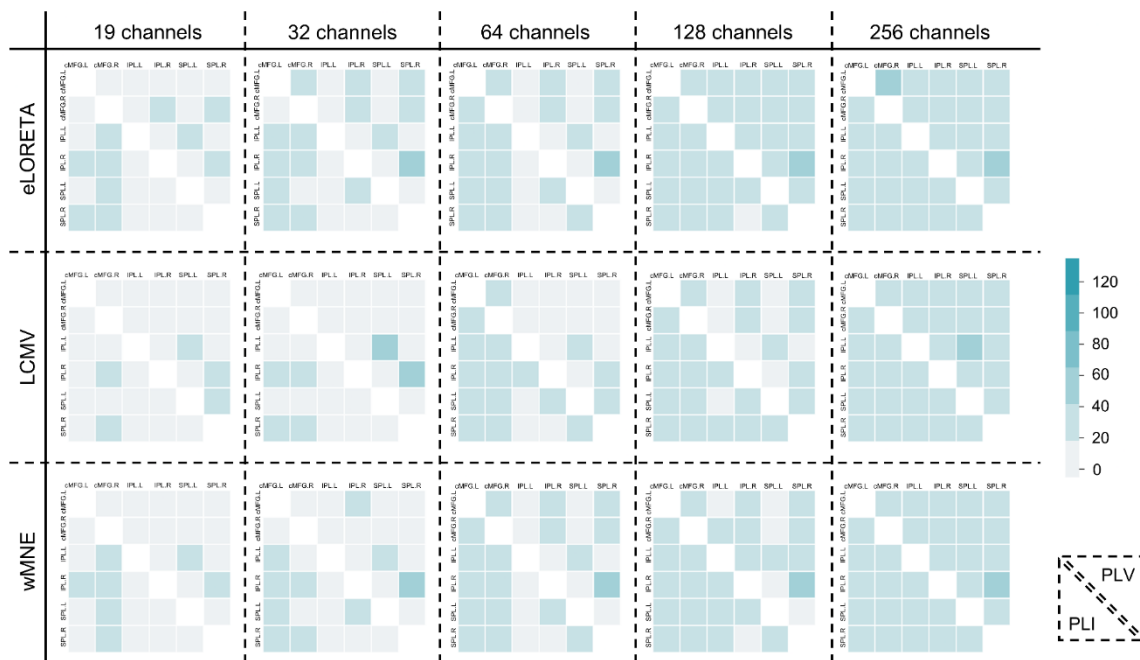


Fig. S4. Heatmaps of the contribution of DAN edges (see Materials and Methods section) averaged across all subjects and epochs are shown for all sensor densities and inverse method/connectivity measures (PLV, PLI) combinations. *eLORETA* - exact low-resolution electromagnetic tomography.

LCMV - linearly constrained minimum norm beamforming. wMNE - weighted minimum norm estimate. PLV - phase-locking value. AEC - amplitude envelope correlation. PLI - phase-lag index. AEC - amplitude envelope correlation with source leakage correction.*

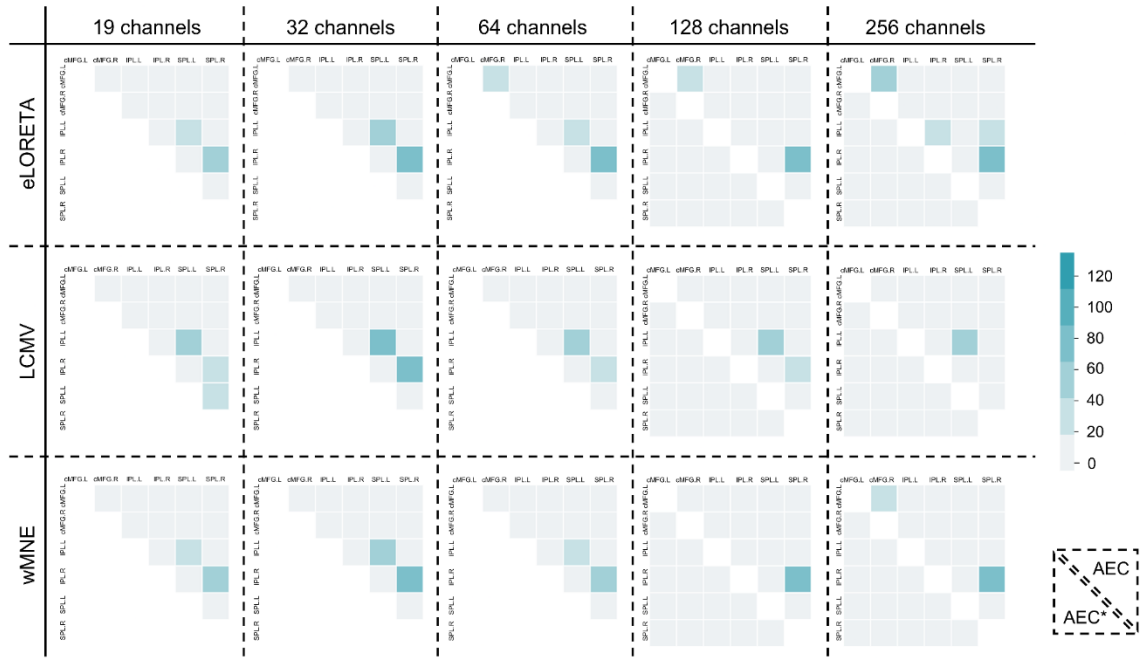


Fig. S5. Heatmaps of the contribution of DAN edges averaged across all subjects and epochs are shown for all sensor densities and inverse method/connectivity measures (AEC, AEC*) combinations. *eLORETA* - exact low-resolution electromagnetic tomography. *LCMV* - linearly constrained minimum norm beamforming. *wMNE* - weighted minimum norm estimate. *PLV* - phase-locking value. *AEC* - amplitude envelope correlation. *PLI* - phase-lag index. *AEC** - amplitude envelope correlation with source leakage correction.

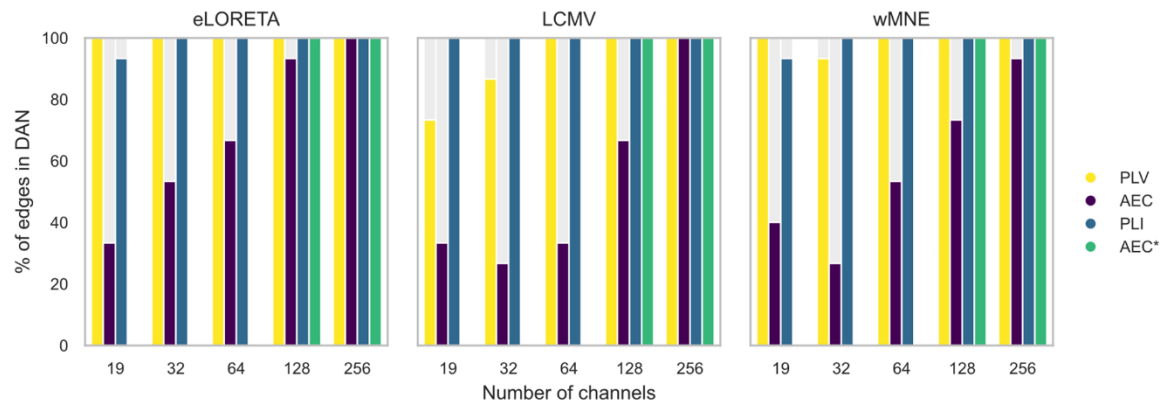


Fig. S6. Barplots of the percentage of edges located within the DAN among the edges having the $\approx 0.7\%$ highest contribution values. *eLORETA* - exact low-resolution electromagnetic tomography. *LCMV* - linearly constrained minimum norm beamforming. *wMNE* - weighted minimum norm estimate. *PLV* - phase-locking value. *AEC* - amplitude envelope correlation. *PLI* - phase-lag index. *AEC** - amplitude envelope correlation with source leakage correction.

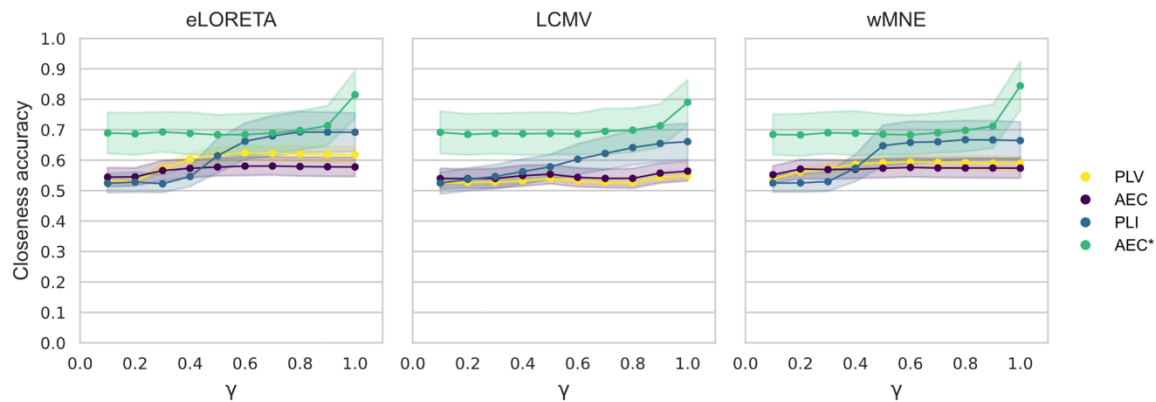


Fig. S7. Mean and standard deviation of closeness accuracy computed between the reference and reconstructed DMNs for different levels of measurement noise using 256 channels. *eLORETA* - exact low-resolution electromagnetic tomography. *LCMV* - linearly constrained minimum norm beamforming. *wMNE* - weighted minimum norm estimate. *PLV* - phase-locking value. *AEC* - amplitude envelope correlation. *PLI* - phase-lag index. *AEC** - amplitude envelope correlation with source leakage correction.

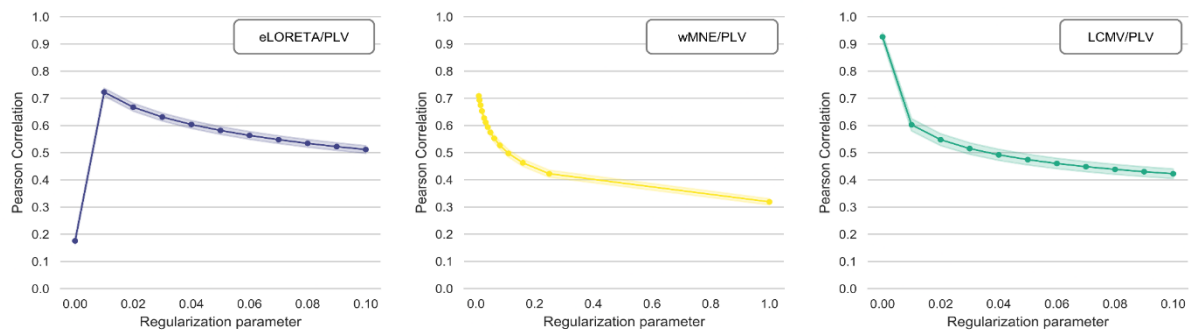


Fig. S8. Mean and standard deviation of the Pearson correlation computed between the reference and reconstructed DMNs for different regularization values using 256 channels. *eLORETA* - exact low-resolution electromagnetic tomography. *wMNE* - weighted minimum norm estimate. *LCMV* - linearly constrained minimum norm beamforming. *PLV* - phase-locking value.

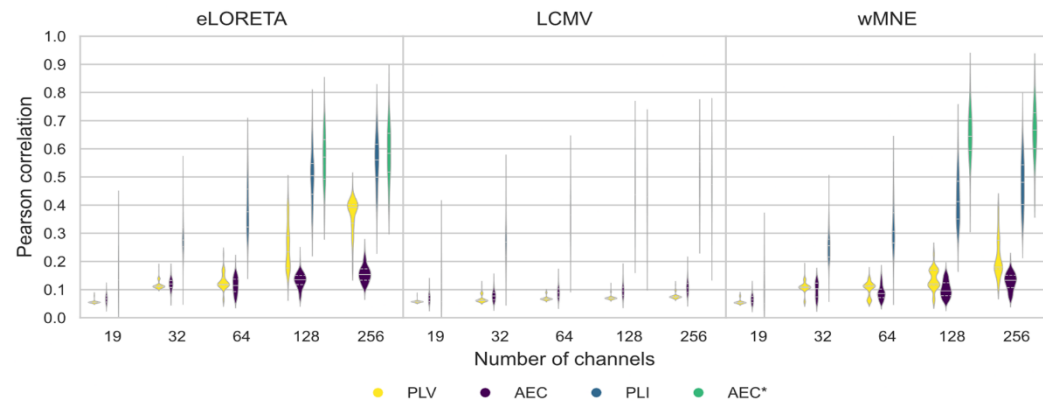


Fig. S9. Violin plots of the Pearson correlation values computed between the reference and reconstructed DMNs (threshold = 1%) for all electrode montages and inverse methods/connectivity metrics combinations. *eLORETA* - exact low-resolution electromagnetic tomography. *LCMV* - linearly constrained minimum norm beamforming. *wMNE* - weighted minimum norm estimate. *PLV* - phase-

locking value. AEC - amplitude envelope correlation. PLI - phase-lag index. AEC - amplitude envelope correlation with source leakage correction.*

3.3 Study III: Effect of analytical variability in estimating EEG-based functional connectivity

Study status: **To be submitted** to *NeuroImage*.

Effect of analytical variability in estimating EEG-based functional connectivity

Sahar Allouch^{1,2}, Aya Kabbara^{3,4}, Joan Duprez¹, Véronique Paban⁵, Mohamad Khalil^{2,6}, Julien Modolo¹, Mahmoud Hassan^{3,7}

¹ Univ Rennes, INSERM, LTSI - UMR 1099, F-35000 Rennes, France

² Azm Center for Research in Biotechnology and Its Applications, EDST, Tripoli, Lebanon

³ MINDig, F-35000 Rennes, France

⁴ LASer - Lebanese Association for Scientific Research, Tripoli, Lebanon

⁵ CRSI research center, Faculty of Engineering, Lebanese University, Beirut, Lebanon

⁶ Aix Marseille University, CNRS, LNSC, Marseille, France

⁷ School of Science and Engineering, Reykjavik University, Reykjavik, Iceland

Corresponding author: saharallouch@gmail.com

Highlights

- The significant impact of methodological variability represents a critical issue for neuroimaging studies that should be prioritized.
- Analytical variability related to the number of electrodes, the source reconstruction algorithm, and the functional connectivity measure is a prominent issue in the EEG source connectivity analysis.
- Group-level consistency, between-, and within-subjects similarity are substantially affected by the issue of analytical variability in the EEG source connectivity analysis.

Abstract

The significant degree of variability and flexibility in neuroimaging analysis approaches has recently raised concerns. When running any neuroimaging study, the researcher is faced with a large number of methodological choices, often made arbitrarily. This can produce substantial variability in results, ultimately hindering research replicability, and thus, robust conclusions. Here, we addressed the analytical variability in the EEG source connectivity pipeline and its

effects on the consistency of the outcomes. Like most neuroimaging analyses, the EEG source connectivity analysis involves the processing of high-dimensional data and is characterized by a complex workflow that promotes high analytical variability. In this study, we focused on source functional connectivity variability induced by three factors along the analysis pipeline: 1) number of EEG electrodes, 2) inverse solution algorithms, and 3) functional connectivity metrics. Variability of the outcomes was assessed in terms of group-level consistency, inter-, and intra-subjects similarity, using resting-state EEG data ($n = 88$). As expected, our results showed that different choices related to the number of electrodes, source reconstruction algorithm, and functional connectivity measure substantially affect group-level consistency, between-, and within-subjects similarity. We believe that the significant impact of such methodological variability represents a critical issue for neuroimaging studies that should be prioritized.

1. Introduction

1.1. Analytical variability in neuroimaging research

In the course of running a study, the researcher is faced with a large number of choices often made arbitrarily. Those choices are known as the researcher's "degree of freedom" (Simmons, Nelson, and Simonsohn 2011), and are spread out across all research phases (Wicherts et al. 2016). Recently, the question of analytical flexibility has received much attention in many scientific fields as a potential source of poor reproducibility (Botvinik-Nezer et al. 2020; Wicherts et al. 2016; Simmons, Nelson, and Simonsohn 2011; Silberzahn et al. 2018; Carp 2012). The risks of high variability in analytical approaches are twofold. First, one may chase statistical significance by taking advantage of the researcher's degrees of freedom, i.e., run several analyses and modify the study while progressing until finding a significant positive result, and then only reporting the positive result and the corresponding analysis (Bishop et al. 2015; Simmons, Nelson, and Simonsohn 2011; Carp 2012). Second, interestingly, the researcher may run only one analysis, and that analysis yields significant positive results, but only due to certain choices along the analysis pipeline. Hence, analytic decisions made without direct attempts to achieve statistical significance can still produce high variability in results (Simmons, Nelson, and Simonsohn 2011; Carp 2012; Silberzahn et al. 2018; Botvinik-Nezer et al. 2020), affecting, thus, conclusions that could be drawn from a study (Botvinik-Nezer et

al., 2020), and ultimately hindering the reproducibility of scientific research (Wicherts et al., 2016).

Due to the high dimensionality of the data and complexity of analysis workflows, analytical variability issues are thought to be prominent in neuroimaging research (Botvinik-Nezer et al. 2020). Recently, those issues were addressed, in fMRI (Botvinik-Nezer et al. 2020) and EEG (<https://www.eegmanypipelines.org>), by large collaborative initiatives where independent teams are asked to analyze the same data set and test the same hypotheses. Moreover, the sensitivity of EEG results to the variability in preprocessing strategies was investigated in (Šoškić et al. 2022; Clayson et al. 2021; Robbins et al. 2020). Different analysis software (Bowring, Maumet, and Nichols 2019; Glatard et al. 2015), software versions (Gronenschild et al. 2012), and operating systems (Glatard et al. 2015; Gronenschild et al. 2012) were also studied as substantial sources of variability in fMRI preprocessing. Similarly, (Kabbara et al. 2022) revealed that a considerable variability in results is observed when using different software tools to preprocess EEG signals.

1.2. Analytical variability in EEG source connectivity analysis

In this work, we are particularly interested in the question of analytical variability in the specific context of functional brain connectivity inferred from EEG data (Hassan and Wendling 2018; Hassan et al. 2015, 2014; A. Kabbara et al. 2017; Mehrkanoon et al. 2014). Mainly, the analysis consists of two main steps: (i) reconstructing the dynamics of cortical sources by solving the so-called EEG inverse problem, and (ii) computing functional connectivity between reconstructed sources. Although the two steps mentioned above are relatively standard in the field of EEG-based brain connectivity, combining them can be much more cumbersome than it seems in terms of choices and flexibility. Dozens of substeps are to be made, and each entails numerous choices that are often arbitrary. For instance, during the first steps of the analysis pipeline, the spatial density (i.e., number of electrodes) of the EEG system must be determined. When solving the inverse problem, a large set of mathematical methods is available, each imposing assumptions and constraints regarding the spatial and temporal properties of the reconstructed sources, without mentioning the various parameters that require tuning for each of those algorithms. This is also valid for connectivity measures, with metrics assessing various signal features such as phase synchronization, amplitude synchronization, omitting or keeping zero-lag connections, and a set of parameters that require tuning in each method. The numerous

choices to be made in the EEG source connectivity analysis pipeline have the potential to be problematic. The researcher's high degree of freedom could produce a substantial variability in reported results, ultimately hindering replicability in EEG source connectivity research. Therefore, the overall goal of the present paper is to call into question the analytical variability in the EEG source connectivity pipeline and its effects on the consistency/discrepancy of the outcomes. Mainly, we focused on three key factors along the analysis:

1.2.1. The number of EEG electrodes (i.e., electrode density):

In fact, the spatial density of standard EEG systems ranges from 19 to 256 sensors and several studies investigated the effect of the number of electrodes on EEG source localization in simulations in the context of epilepsy (Song et al. 2015; Sohrabpour et al. 2015; Lantz et al. 2003). More specifically, it has been shown that a higher number of electrodes is associated with a significant decrease in localization error (Lantz et al. 2003; Song et al. 2015; Sohrabpour et al. 2015). In two previous simulation studies (Allouch, Yochum, et al. 2022; Allouch, Kabbara, et al. 2022), we showed a significant effect of the number of electrodes (19, 32, 64, 128, 256) on the accuracy of reconstructed cortical networks and their correspondence with the reference simulated networks. In this article, we wanted to investigate if this effect stands in the experimental EEG context. Thus, we tested three electrode configurations (64, 32, 19 channels) on the outcomes' variability.

1.2.2. The source reconstruction algorithms

Another critical influencing factor in the EEG source connectivity analysis is the algorithm chosen to reconstruct the cortical sources. Several studies quantifying the performance of different inverse methods, in simulated and experimental EEG/MEG data, concluded that the choice of the inverse method significantly influences source estimation results (Anzolin et al. 2019; Mahjoory et al. 2017; Hedrich et al. 2017; Bradley et al. 2016; Grova et al. 2006; Halder et al. 2019; Tait et al. 2021; Allouch, Yochum, et al. 2022; Allouch, Kabbara, et al. 2022). In this article, we choose to test three widely used source reconstruction algorithms, specifically, the eLORETA, LCMV, and wMNE.

1.2.3. The functional connectivity metrics

The choice of the functional connectivity metric is also a critical step when reconstructing brain networks. A wide range of measures are used in the field, and each differs in the aspect of the

data that is being investigated (linear/non-linear, amplitude/phase- synchronization, time/spectral domain, prone/robust to source leakage, etc...), (see (Friston 2011; Pereda, Quiroga, and Bhattacharya 2005; Cao et al. 2022) for a review), resulting in significant variability of performance and interpretations (Colclough et al. 2016; H. E. Wang et al. 2014; Wendling et al. 2009; Hassan et al. 2017; Allouch, Yochum, et al. 2022; Allouch, Kabbara, et al. 2022). Here, tested measures included: PLV, AEC, PLI, wPLI, and corrected AEC and PLV as they are widely used in functional connectivity studies.

2. Materials and Methods

The full pipeline of the study is summarized in Fig. 1.

2.1. Dataset

2.1.1. Data acquisition

125 healthy subjects (78 Females) participated in this study. Their age ranged between 20 and 75 years old. (mean = 42, sd = 16). The study was approved by the “Comité de Protection des Personnes Sud Méditerranée” (agreement n° 10-41). After EEG acquisition, all participants have completed the resting-state questionnaire (ReSQ) (Delamillieure et al. 2010). Participants were asked to relax for 5 minutes with their eyes closed without falling asleep. EEG data were collected using a 64-channel Biosemi ActiveTwo system (Biosemi Instruments, Amsterdam, The Netherlands) positioned according to the standard 10–20 system montage. Two bilateral electrooculogram electrodes (EOG) recorded horizontal movements. Electrode impedances were kept below $20\text{ k}\Omega$. EEG data were originally sampled at 1024 or 2048 Hz.

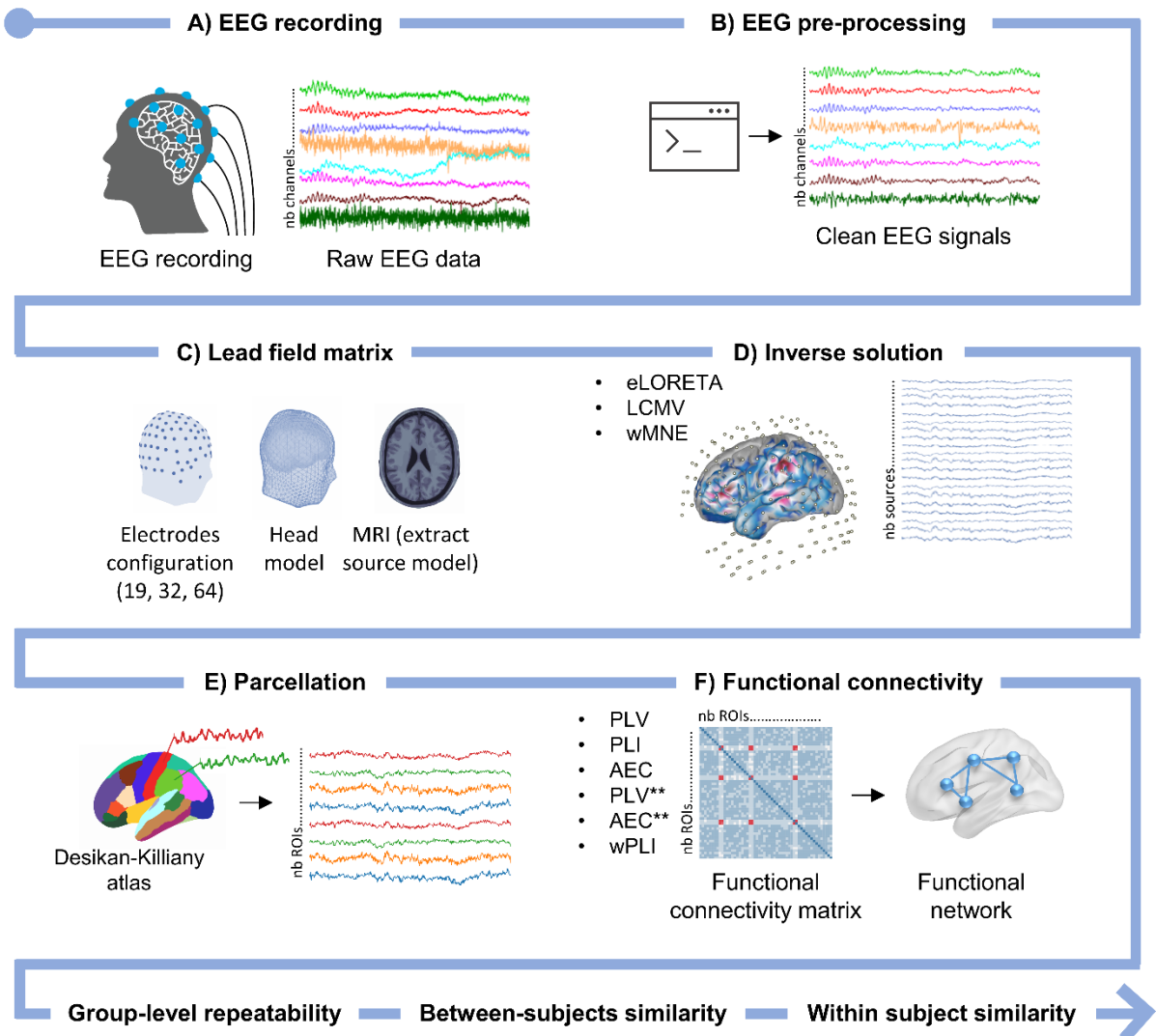


Fig. 1. Full pipeline of the study. The EEG source connectivity analysis consists of A) scalp EEG recordings. B) EEG signals pre-processing. C) Gain (lead field) matrix computation. D) solving the inverse problem to reconstruct cortical activity. E) regional time series extraction. F) functional connectivity computation. Networks reconstructed using different electrode configurations, inverse solution algorithms, and connectivity measures were compared based on group-level repeatability, between-subjects similarity, and within-subject similarity. *eLORETA* - exact low-resolution electromagnetic tomography. *LCMV* - linearly constrained minimum norm beamforming. *wMNE* - weighted minimum norm estimate. *PLV* - phase-locking value. *PLI* - phase-lag index. *AEC* - amplitude envelope correlation. *wPLI* - weighted phase-lag index. Asterisks (**) - source leakage correction.

2.1.2. Data pre-processing

Data were re-sampled to a common frequency of 512 Hz and segmented into 10-seconds epochs. Preprocessing was done using Automagic Matlab toolbox (Pedroni, Bahreini, and Langer 2019) (<https://github.com/methlabUZH/automagic>). Automagic pre-processing parameters are detailed in the Supplementary Materials. The number of interpolated channels did not exceed 15% of the total number of channels; otherwise, the epoch was rejected. For

each subject, we chose the best 30 epochs based on Automagic quality metrics (check Supplementary Materials). Subjects having less than 30 clean epochs were excluded from the analysis. After pre-processing, 88 subjects were included in the analysis.

2.2. EEG source connectivity

The “EEG source connectivity” method refers to the assessment of functional connectivity between cortical sources. It includes two main steps: 1) reconstructing the temporal dynamics of cortical sources by solving the EEG inverse problem, and 2) assessing the functional connectivity between reconstructed sources (Hassan and Wendling 2018; Hassan et al. 2015, 2014; A. Kabbara et al. 2017; Mehrkanoon et al. 2014).

2.2.1. EEG inverse solution

The source model, which provides information about the location and orientation of the dipole sources to be estimated, is computed, here, based on ICBM152 MRI template using the Boundary Element Method (BEM) in OpenMEEG (Gramfort et al. 2010) implemented in Fieldtrip toolbox (Oostenveld et al. 2011). EEG signals $X(t)$ recorded from Q channels (64, 32, or 19 channels) can therefore be expressed as a linear combination of P time-varying current dipole sources $S(t)$:

$$X(t) = G \cdot S(t) + N(t) \quad (2.1)$$

where G ($Q \times P$) is the lead field (gain) matrix and $N(t)$ is the additive noise. G reflects the contribution of each cortical source to the scalp sensors, and is computed from a multiple-layer head model and the position of the Q electrodes. In order to assess the effect of sensors' spatial resolution on the reconstructed cortical networks, the lead field matrix was computed using different electrode montages (64, 32, and 19 channels). The source model was constrained to a field of current dipoles homogeneously dispersed over the cortex and normal to the cortical surface. In this case, the inverse problem is reduced to computing the magnitude of dipolar sources $\hat{S}(t)$ as follows:

$$\hat{S}(t) = W \cdot X(t) \quad (2.2)$$

Since the problem is ill-posed (undetermined), mathematical and/or biophysical or electrophysiological assumptions need to be imposed to compute W and find a unique solution

that fits the data (see (Awan, Saleem, and Kiran 2019; Grech et al. 2008; Baillet, Mosher, and Leahy 2001) for a review).

In this study, we chose to test the variability in the networks obtained using three different source reconstruction algorithms:

i. Weighted minimum norm estimate (wMNE)

The minimum norm estimate, initially proposed by (Hämäläinen and Ilmoniemi 1994), and widely used in EEG source imaging, searches for a solution that fits the data while having the minimum energy (minimum least-square error, L2-norm). An intrinsic consequence of this constraint is a bias toward superficial sources generating strong fields with less energy due to their vicinity to electrodes (He et al. 2018; Michel and Brunet 2019). To compensate for the tendency of MNE to favor weak and surface sources, the weighted minimum norm estimate (wMNE) (Lin et al. 2006; Fuchs et al. 1999) sets the diagonals of B (eq. 2.4) inversely proportional to the norm of the lead field vectors, essentially assuming a priori that sources that only weakly influence M/EEG must have a higher variance to be measured by sensors (Tait et al. 2021).

$$W_{MNE} = BG^T(GBG^T + \lambda C)^{-1} \quad (2.3)$$

where λ is the regularization parameter, and C the noise covariance matrix.

$$B_{ij} = \begin{cases} (G_i^T G_i)^{\frac{1}{2}} & \text{if } i = j; \\ 0 & \text{if } i \neq j \end{cases} \quad (2.4)$$

ii. Exact low-resolution brain electromagnetic tomography (eLORETA)

eLORETA belongs to the family of weighted minimum norm inverse solutions. In addition to compensating for depth bias, it also has exact-zero error localization in the presence of measurement and structured biological noise (Pascual-Marqui 2007):

$$B_{ij} = \begin{cases} (G_i^T (G_i B G_i^T + \lambda C)^{-1})^{\frac{1}{2}} & \text{if } i = j; \\ 0 & \text{if } i \neq j \end{cases} \quad (2.5)$$

iii. Linearly constrained minimum-variance (LCMV) beamformer

Beamformers (a.k.a. spatial filters or virtual sensors), originally established in radar and sonar signal processing, are now widely used in source imaging, mainly with MEG data (Michel et

al. 2004). The basic idea of beamformer approaches is to discriminate between signals arriving from a location of interest and those originating elsewhere (Baillet, Mosher, and Leahy 2001). Specifically, the LCMV beamformer (Van Veen et al. 1997) estimates the activity for a source at a given location while simultaneously suppressing (i.e., setting null values) contributions from all other sources and noise captured in the data covariance.

$$W_{LCMV} = ((G^T \cdot (C + \lambda \cdot I)^{-1}) \cdot G)^{-1} \cdot (G^T \cdot (C + \lambda \cdot I)^{-1}) \quad (2.6)$$

The estimation of matrix W is done on a high-resolution surface mesh (15000 vertices). Spatially close brain sources are then clustered (average signal) into 68 regional time series $R(t)$ based on the regions of interest (ROIs) of the Desikan-Killiany atlas (Desikan et al. 2006).

2.2.2. Functional connectivity

The next step following the reconstruction of cortical dynamics, is to assess functional connectivity, i.e., statistical interdependence between spatially distant brain regions (Friston 2011). A plethora of methods are proposed in the literature which are either linear or nonlinear, parametric or nonparametric, based on phase and/or amplitude synchronization, computed in time and/or frequency domain, robust or prone to source leakage (see (Friston 2011; Pereda, Quiroga, and Bhattacharya 2005; Cao et al. 2022) for a review). At the end of this step, an $R \times R$ matrix is obtained, where each entry a_{ij} of the matrix is equal to the weight of the connection linking node (i.e., ROI) i to node j . Since our intent was not to present an exhaustive comparison between all available metrics, our study covered, in total, six frequently used metrics:

i. Phase-locking value (PLV)

For two signals $x(t)$ and $y(t)$, the phase-locking value (Lachaux et al. 2000) is defined as:

$$PLV = |E\{e^{i(\phi_x(t)-\phi_y(t))}\}| \quad (2.7)$$

where $E\{\cdot\}$ is the expected value operator and $\phi(t)$ is the instantaneous phase derived from the Hilbert transform.

ii. Phase-lag index (PLI)

The PLI originally proposed in (Stam, Nolte, and Daffertshofer 2007) is a measure of the asymmetry of the distribution of phase differences between two signals. It aims at overcoming

the issue of source leakage by discarding phase differences centered around 0 and π , i.e., removing zero-lag connections. It is an estimation of the extent on non-equiprobability of phase leads and lags between signals (Vinck et al. 2011). For two signals $x(t)$ and $y(t)$, PLI is defined as follows:

$$PLI = |E\{sign(\phi_x(t) - \phi_y(t))\}| \quad (2.8)$$

where $E\{\cdot\}$ is the expected value operator, and $\phi(t)$ is the instantaneous phase derived from the Hilbert transform.

iii. Weighted phase-lag index (wPLI)

The weighted phase-lag index attempts to further weight the metric away from zero-lag contributions (Vinck et al. 2011). The contribution of observed phase leads and lags is weighted by the magnitude of the imaginary component of the cross-spectrum. This results in reduced sensitivity to additional, uncorrelated noise sources and increased statistical power to detect changes in phase-synchronization. wPLI is defined as follows:

$$wPLI = \frac{|E\{|imag\{x\}|sign(imag\{x\})\}|}{E\{|imag\{x\}\|}} \quad (2.9)$$

Where $imag\{x\}$ denotes the imaginary part of the signal's cross-spectrum.

iv. Amplitude envelope correlation (AEC)

AEC denotes the Pearson correlation between the signals' envelopes derived from the Hilbert transform (Hipp et al. 2012; Brookes et al. 2011).

*v. PLV and AEC with source leakage correction (PLV**, AEC**)*

We computed PLV and AEC between time courses corrected for source leakage. Zero-lag signal overlaps are removed by regressing out (orthogonalizing with respect to) the linear projection of the regional time course (Brookes, Woolrich, and Barnes 2012). Since the orthogonalization can be done in two directions (x to y , y to x), we computed PLV and AEC for both directions of orthogonalized time series and then averaged the obtained values. We also tested a multivariate symmetric orthogonalization approach (Results are shown in the Supplementary Materials): the closest orthonormal matrix to the uncorrected regional time courses is first computed; then the magnitudes of the orthogonalized vectors are adjusted

iteratively to minimize least-squares distances between corrected and uncorrected signals (Colclough et al. 2015).

2.3. Results quantification

The effect of different analytical choices (number of electrodes, source reconstruction algorithm, functional connectivity measure) was estimated by assessing the:

- i. Group-level consistency/repeatability
- ii. Between-subjects similarity/variability
- iii. Within-subject similarity/variability

2.3.1. *Group-level consistency*

A split-half reliability approach was used to assess the group-level consistency (Colclough et al. 2016). The dataset (88 subjects) was randomly divided into two groups G_1 and G_2 . Group connectivity matrices (\mathbf{C}_{G_1} and \mathbf{C}_{G_2}) were obtained by averaging connectivity matrices across all subjects within a single group. Then, Pearson correlation was computed between averaged matrices \mathbf{C}_{G_1} and \mathbf{C}_{G_2} . This was repeated for 100 iterations.

To investigate the effect of source leakage on group-level consistency, we computed the correlation between the length of the edge (i.e., the distance between ROIs) and its contribution to group-level consistency. The contribution of individual edges (Finn et al. 2015; Colclough et al. 2016) to the group-level consistency was defined as the element-wise product between edge vectors of matrices \mathbf{C}_{G_1} and \mathbf{C}_{G_2} (after z-score normalization). The contribution of individual edges was averaged across all iterations and correlated with the distance separating distinct ROIs.

2.3.2. *Between-subjects similarity*

We computed the Pearson correlation between the connectivity matrices of the different subjects in the dataset (Colclough et al. 2016). The distribution of correlation values reflects the between-subjects similarity/variability obtained for different channel densities, inverse solutions, and connectivity measures.

2.3.3. *Within-subject similarity*

Pearson correlation was computed between all connectivity matrices of the different epochs within a single subject (30 epochs). We then plotted the distribution of averaged correlation values within each subject. Higher correlation values reflect thus an intra-subject similarity, that is, consistency across all epochs of the subject.

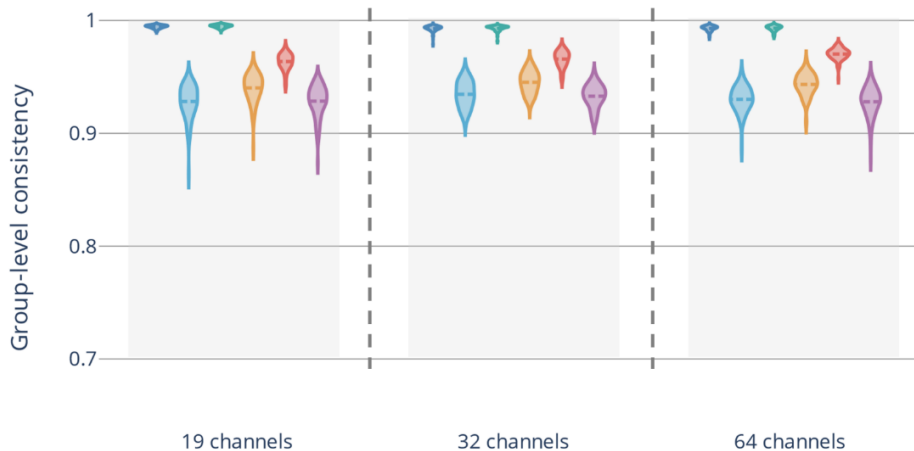
2.3.4. Statistical Tests

All statistical analyses were performed using R (R Core Team 2020). Generalized linear models were used to assess the effect of (i) number of electrodes, (ii) inverse solution, and (iii) functional connectivity metric as fixed effects on group-level repeatability and between-subjects similarity. Beta regression model was used to assess the effects of different tested factors on the absolute value of the within-subjects similarity. These models were chosen after careful inspection of the model's assumptions based on visual inspections of the model's residuals distributions. In each case, the model that best met these assumptions was chosen. *Post-hoc* analyses were performed using z-tests with the *glht* function of the *multcomp* package (Hothorn, Bretz, and Westfall 2008) that provides corrected *p*-values. Models' *R*² were calculated with the *r.squaredGLMM* function of the *MuMin* package (Barton 2009) to estimate the variance explained by models. The significance threshold was set at its usual value of 0.05.

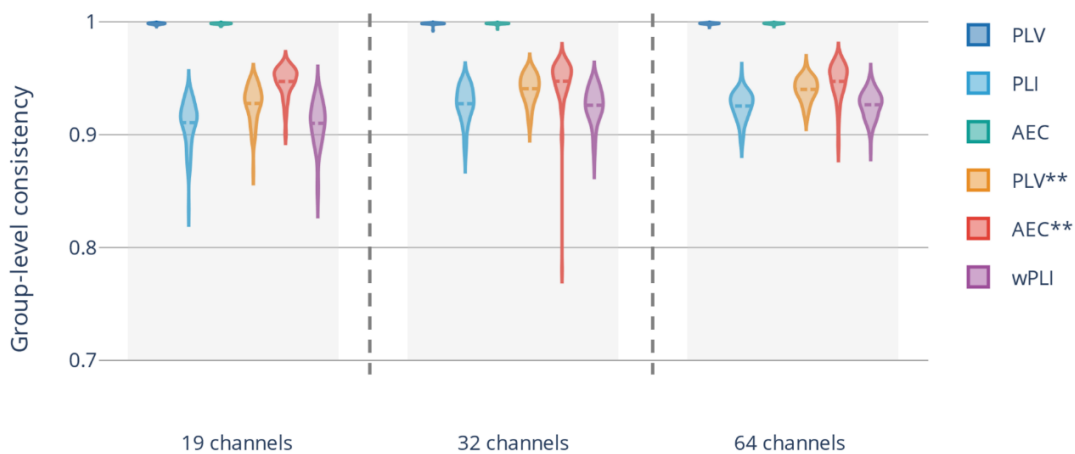
3. Results

Violin plots of the distributions of group level consistency, between-, and within-subject similarity are shown in Fig. 2, Fig. 3, and Fig., 4, respectively. The results reported here correspond to the alpha ([8-13 Hz]) frequency band, whereas results obtained for other frequency bands are shown in Fig. S1-S3 in the Supplementary Materials.

eLORETA



LCMV



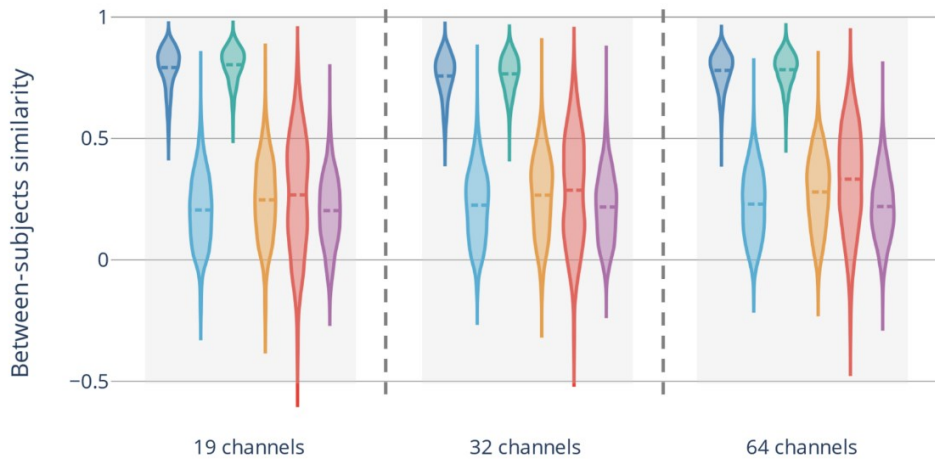
wMNE



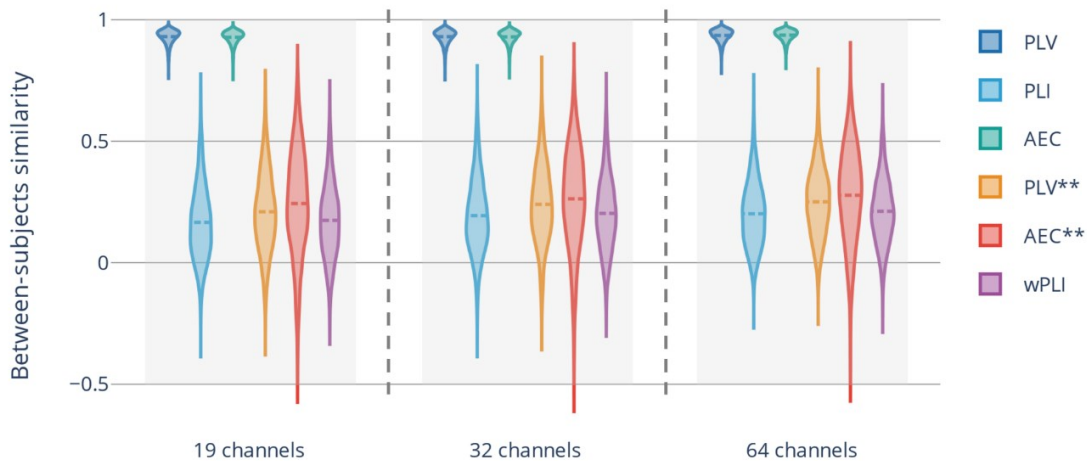
Fig. 2. Group-level consistency. The dataset was divided into two halves 100 times. For each condition (number of electrodes x inverse solution algorithm x connectivity measure), the Pearson correlation was computed between averaged connectivity matrices inferred from separate halves of the dataset. *eLORETA* - exact low-resolution electromagnetic tomography. *LCMV* - linearly constrained minimum norm beamforming. *wMNE* - weighted minimum norm estimate. *PLV* - phase-locking value. *PLI* -

*phase-lag index. AEC - amplitude envelope correlation. wPLI - weighted phase-lag index. Asterisks (***) - source leakage correction.*

eLORETA



LCMV



wMNE

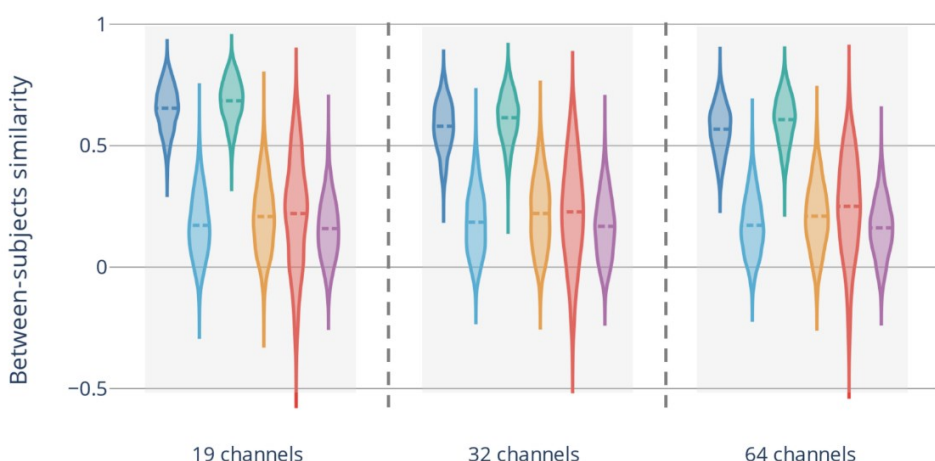


Fig. 3. Between-subjects similarity. Pearson correlation was computed between all subjects for each condition (number of electrodes x inverse solution algorithm x connectivity measure). *eLORETA* - exact low-resolution electromagnetic tomography. *LCMV* - linearly constrained minimum norm beamforming. *wMNE* - weighted minimum norm estimate. *PLV* - phase-locking value. *PLI* - phase-lag

index. AEC - amplitude envelope correlation. wPLI - weighted phase-lag index. Asterisks (**) - source leakage correction.

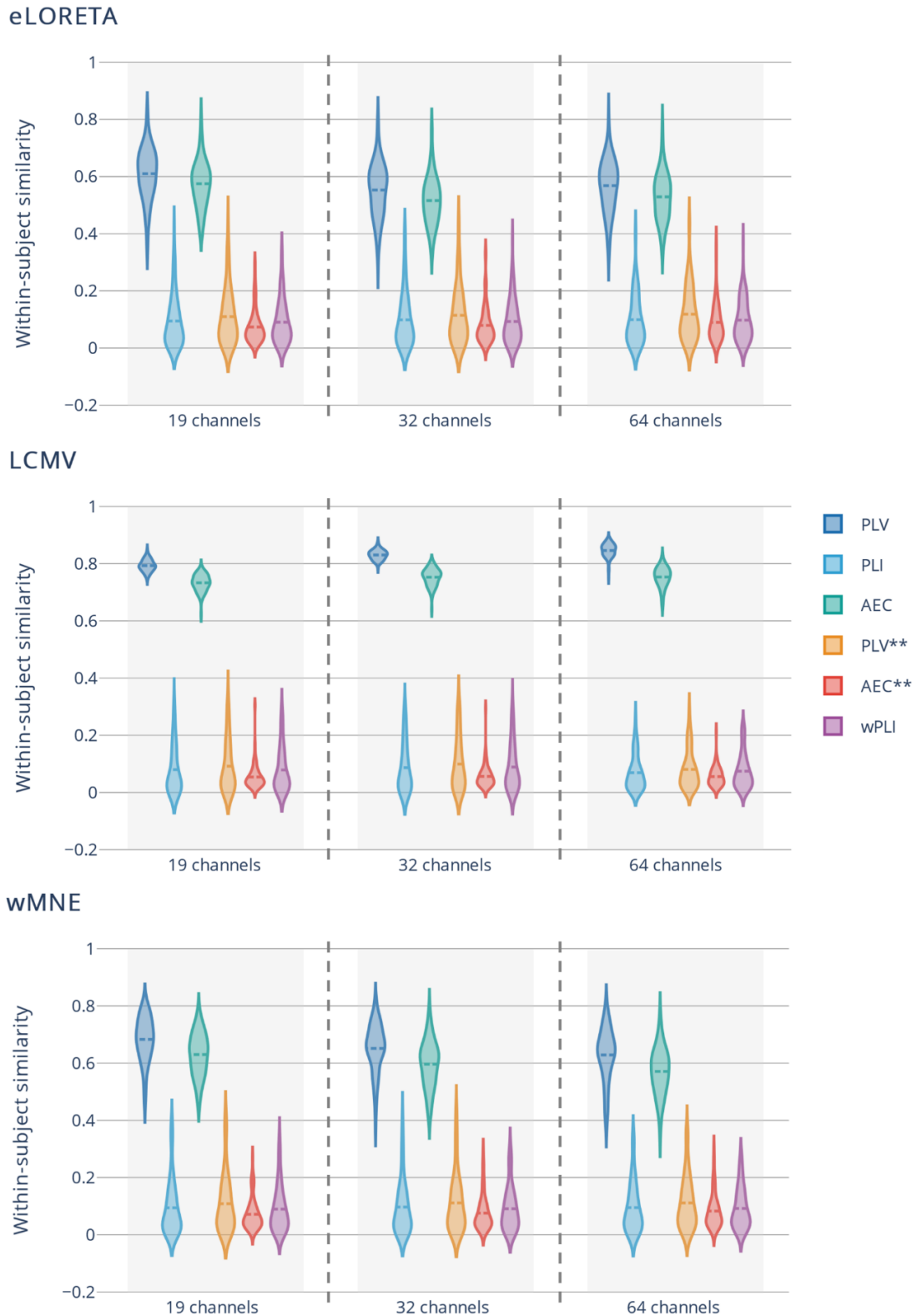


Fig. 4. Within-subject similarity. For each condition (number of electrodes x inverse solution algorithm x connectivity measure), and for each subject, Pearson correlation was computed between connectivity matrices inferred from different epochs. All correlation values for a single subject were averaged to

obtain a single value representing the degree of within-subject similarity/consistency. *eLORETA - exact low-resolution electromagnetic tomography.* *LCMV - linearly constrained minimum norm beamforming.* *wMNE - weighted minimum norm estimate.* *PLV - phase-locking value.* *PLI - phase-lag index.* *AEC - amplitude envelope correlation.* *wPLI - weighted phase-lag index.* Asterisks (**) - source leakage correction.

3.1. Effect of the number of electrodes

Group-level consistency, between-, and within-subjects similarity were investigated for different electrode densities (19, 32, 64 channels). Statistical tests showed a significant effect of the number of electrodes on the group-level consistency ($F_{(2, 5397)}=73$, $p<0.0001$, $R^2=0.36$) and between-subjects similarity ($F_{(2, 206709)}=65$, $p<0.0001$, $R^2=0.79$), whereas no significant effect on the within-subjects similarity was detected ($F_{(2, 4749)}=0.5523$, $p=0.6$, $R^2=0.75$). *Post-hoc* comparisons between group consistency values showed significant (small) differences between those obtained with 19 (0.9499 ± 0.0367) and 32 channels (0.9537 ± 0.0320) ($p<0.01$) and 19 and 64 (0.9519 ± 0.0343) channels ($p<0.01$). The difference between results obtained with 64 and 32 channels was not significant ($p=1$). Regarding the inter-subject similarity, all pairwise comparisons were significant ($p<0.0001$). Fig. 5 A) shows the distribution of consistency values at group-, inter-, and intra-subjects levels with respect to different channel densities (all source reconstruction algorithms and functional connectivity values are included). Fig. 2-5 do not show clear differences between different channel configurations in contrast to the results of statistical tests, however, these differences are more evident when looking at the distribution of group consistency and between-subjects similarity values as shown in Fig. S4. in the Supplementary materials.

3.2. Effect of the inverse solution algorithm:

In Fig. 5 B), we illustrated the distributions of the group level repeatability, between-, and within-subjects similarity values with respect to different source reconstruction algorithms (all channels configurations and connectivity measures are included). Based on the statistical tests, the choice of the source reconstruction algorithm (eLORETA, LCMV, wMNE) had a significant effect on the group consistency ($F_{(2, 5397)}=1484$, $p<0.0001$, $R^2=0.36$), the between-subjects similarity ($F_{(2, 206709)}=13303$, $p<0.0001$, $R^2=0.79$), and the within-subjects similarity ($F_{(2, 4749)}=166$, $p<0.0001$, $R^2=0.75$). All pairwise *post-hoc* comparisons were statistically significant ($p<0.0001$). For the group consistency, the mean and standard values obtained with eLORETA (0.9595 ± 0.0284) were significantly higher than those obtained with LCMV

(0.9537 ± 0.0356), and wMNE (0.9423 ± 0.0364), respectively. For the between-subjects similarity, the values obtained for LCMV (0.4567 ± 0.3627) were higher than those obtained with eLORETA (0.4259 ± 0.2926) and wMNE (0.3369 ± 0.2468). Similarly, the within-subjects similarities values were 0.2505 ± 0.2342 , 0.3123 ± 0.3402 , 0.2711 ± 0.2655 for eLORETA, LCMV, and wMNE, respectively.

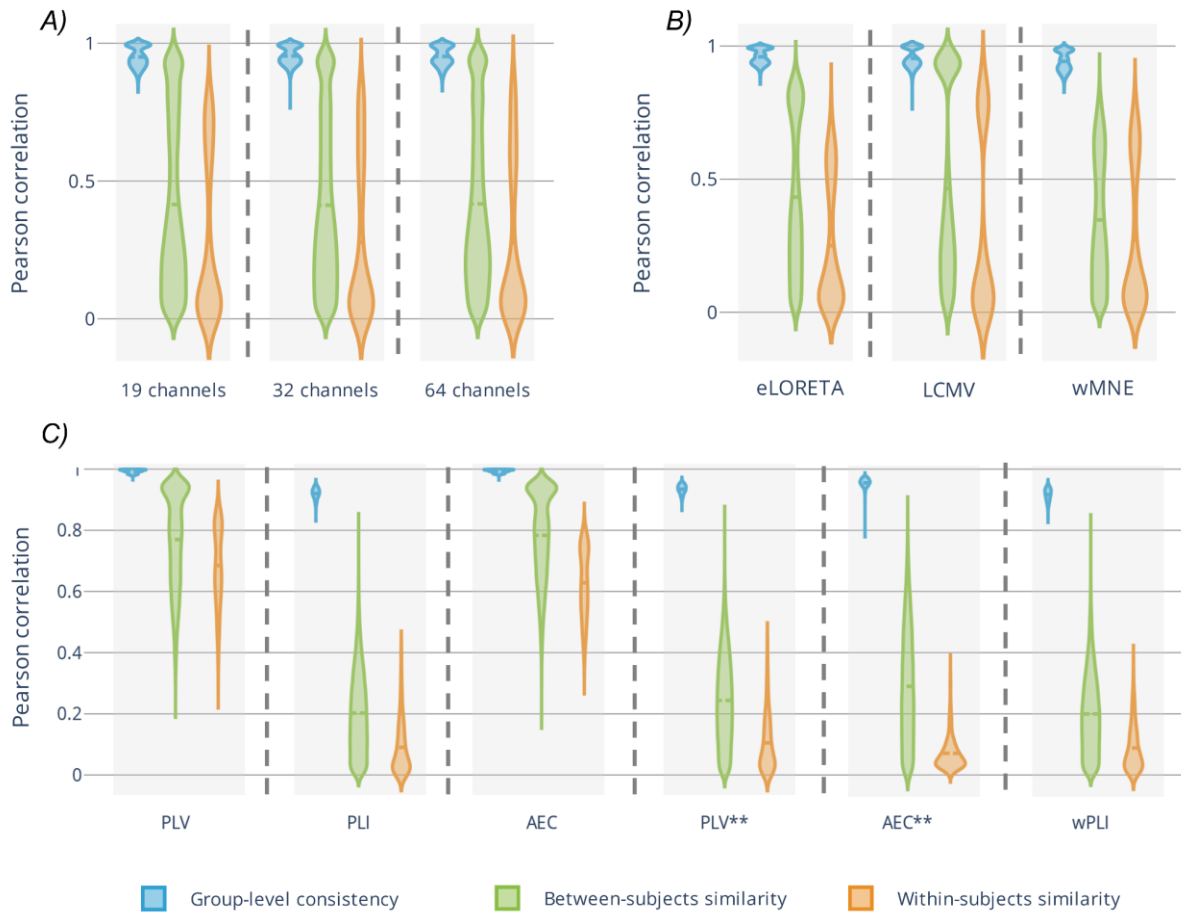


Fig. 5. Violin plots of the group-level consistency, between-, and within-subjects variability with respect to A) different electrode configurations, B) source reconstruction algorithms, and C) functional connectivity measures. *eLORETA* - exact low-resolution electromagnetic tomography. *LCMV* - linearly constrained minimum norm beamforming. *wMNE* - weighted minimum norm estimate. *PLV* - phase-locking value. *PLI* - phase-lag index. *AEC* - amplitude envelope correlation. *wPLI* - weighted phase-lag index. Asterisks (**) - source leakage correction.

3.3. Effect of the connectivity measure:

Group- and subject-level consistency values were both affected by the choice of the functional connectivity measure. Statistical tests showed a significant effect of the connectivity measure on group-level consistency ($F_{(5,5394)}=513889$, $p<0.0001$, $R^2=0.36$), the between-subjects

similarity ($F_{(5,206706)}=5142440$, $p<0.0001$, $R^2=0.79$), and the within-subject similarity ($F_{(2,4746)}=54951$, $p<0.0001$, $R^2=0.75$). At the group level, for all channel densities and source reconstruction algorithms, the highest consistency was obtained using PLV and AEC. No significant difference was observed between the two measures ($p=0.97$). Significantly lower consistency values were obtained in all methods that neglect zero lag (PLI and wPLI) or correct for source leakage (corrected AEC and PLV). Consistency values obtained with corrected AEC (0.9550 ± 0.0149), and corrected PLV (0.9342 ± 0.0151) were significantly lower than those with PLV (0.9922 ± 0.0062) and AEC (0.9929 ± 0.0054) ($p<0.0001$) and higher than those with PLI (0.9203 ± 0.0177) and wPLI (0.9166 ± 0.0202) ($p<0.0001$) who both had similar performance ($p=1$). A similar trend (higher values obtained with PLV and AEC as compared to other connectivity measures) was obtained when assessing between- and within-subjects similarity. Regarding inter-subject similarity, the mean value was 0.7696 ± 0.1570 and 0.7836 ± 0.1416 for PLV and AEC, 0.2632 ± 0.2185 and 0.2369 ± 0.1549 for corrected AEC and PLV, and 0.1946 ± 0.1439 and 0.1909 ± 0.1405 for PLI and wPLI, respectively. *Post-hoc* comparisons between different connectivity measures were all significant ($p<0.0001$; for PLV vs AEC $p=0.003$) except for PLI vs wPLI ($p=0.9$). Regarding intra-subject similarity, the mean value was 0.6848 ± 0.1283 and 0.6284 ± 0.1125 for PLV and AEC, 0.1051 ± 0.0925 and 0.0709 ± 0.0554 for corrected PLV and corrected AEC, 0.0905 ± 0.0869 and 0.0883 ± 0.0742 for PLI and wPLI, respectively. Significant statistical differences were obtained for all pairwise comparisons ($p<0.0001$; for corrected PLV vs wPLI $p=0.016$) except for corrected AEC vs PLI ($p=0.9$), corrected AEC vs wPLI ($p=0.8$), and PLI vs wpLI ($p=0.2$). In Fig. 5 C), we illustrated the distributions of the group level repeatability, between-, and within-subjects similarity values with respect to different functional connectivity measures (all channel configurations and source reconstruction algorithms). Results obtained for AEC and PLV with source leakage correction using the symmetric multivariate orthogonalization approach are shown in Fig. S5-S7. in the Supplementary Materials. It is noteworthy that the performance of those metrics was not stable across different channel densities.

4. Discussion

In neuroimaging research, the high dimensionality of the data and the complexity of analysis workflows are thought to reinforce the issue of analytical variability, defined as the innumerable steps, parameters, and decisions often made arbitrarily within an analysis workflow. The issue is that the same data set could be analyzed, in many different ways,

potentially leading to inconsistent results (Wicherts et al. 2016). Importantly, this makes research results harder to reproduce. In this work, we were interested in investigating the impact of analytical variability in the context of EEG-based brain functional connectivity analysis. We mainly focused on the effect of the choice of EEG electrode density, source reconstruction algorithm, and functional connectivity measure on the consistency/discrepancy in studies' outcomes. In simulation-based studies, the availability of a ground truth allows an objective evaluation of different analyses, whereas, the lack of such ground truth poses a serious challenge when using empirical data. Therefore, alternative approaches are usually adopted with empirical data. For instance, we used group-level repeatability, inter-, and intra-subject similarities to assess the variability of the results induced by different analytical choices. Our objective was not to propose the 'best' analytical choices, but rather to shed light on the issue of analytical variability in estimating EEG-based cortical functional networks. Specifically, we highlight how different analytical choices related to the channel density, source reconstruction algorithm, and functional connectivity measure have a substantial effect on the variability of the outcomes.

4.1. Effect of the number of electrodes

The spatial density of standard EEG systems ranges from 19 to 256 sensors. Several studies investigated the effect of the number of electrodes on EEG source localization in simulations in the context of epilepsy (Song et al. 2015; Sohrabpour et al. 2015; Lantz et al. 2003). More specifically, it has been shown that a higher number of electrodes is associated with a significant decrease in localization error (Lantz et al. 2003; Song et al. 2015; Sohrabpour et al. 2015). As established in (Srinivasan, Tucker, and Murias 1998), a high inter-electrode distance (i.e., corresponding to a low number of EEG electrodes) can induce aliasing, and therefore high spatial frequency signals are misrepresented as low spatial frequency signals due to the violation of the Nyquist criteria ($F_s > 2 \times F_{max}$) (Srinivasan, Tucker, and Murias 1998; Song et al. 2015). In two previous simulation studies (Allouch, Yochum, et al. 2022; Allouch, Kabbara, et al. 2022), a significant improvement in network reconstruction accuracy was observed when increasing the number of electrodes (19, 32, 64, 128, 256). In this article, we tested the effect of three electrode configurations (64, 32, 19 channels) on the outcomes' variability. In line with the reported studies, in this article, different channel densities resulted in significant differences in group-level repeatability, between-, and within-subjects variability.

4.2. Effect of the source reconstruction algorithm

Another critical influencing factor in the EEG source connectivity analysis is the algorithm chosen to reconstruct the cortical sources. Several studies quantifying the performance of different inverse methods, in simulated and experimental EEG/MEG data, concluded that the choice of the inverse method significantly influences source estimation results (Anzolin et al. 2019; Mahjoory et al. 2017; Hedrich et al. 2017; Bradley et al. 2016; Grova et al. 2006; Halder et al. 2019; Tait et al. 2021). However, no consistent conclusions have been made regarding one method that would stand apart from the others in terms of performance. For example, (Anzolin et al. 2019) showed that LCMV had a better performance globally as compared to eLORETA. Similarly, in (Mahjoory et al. 2017), a relatively strong difference was found between LCMV beamformer on one hand, and eLORETA/wMNE solutions on the other hand. In (Bradley et al. 2016), the use of LORETA for source localization outperformed sLORETA and minimum norm least square. Results of source localization in (Halder et al. 2019) did not identify a clear winner between LCMV, eLORETA, MNE, and dynamic imaging of coherent sources (DISC). (Tait et al. 2021) summarized the conditions where each method can be recommended, following comparison of six inverse methods in resting-state MEG data. In line with the above-mentioned studies, we showed in (Allouch, Yochum, et al. 2022; Allouch, Kabbara, et al. 2022) that the choice of the source reconstruction algorithm has a significant effect on the accuracy of reconstructed cortical networks in the context of epileptiform and resting-state simulations. This same effect was also observed in this article: group-level consistency, between-, and within subjects similarity were all substantially affected by the choice of the source reconstruction algorithm.

4.3. Effect of the connectivity measure:

The choice of the functional connectivity metric is also a critical step when reconstructing brain networks. A wide range of measures are used in the field, and each differs in the aspect of the data that is being investigated (see (Friston 2011; Pereda, Quiroga, and Bhattacharya 2005; Cao et al. 2022) for a review), resulting in significant variability of performance and interpretations (Colclough et al. 2016; H. E. Wang et al. 2014; Wendling et al. 2009; Hassan et al. 2017). For instance, (Colclough et al. 2016) assessed the consistency of different measures in experimental MEG resting state data and recommended using the correlation between orthogonalized, band-limited, power envelopes (AEC). On the other hand, following

extensive simulation studies, (H. E. Wang et al. 2014) and (Wendling et al. 2009) both concluded that there is no ideal “one-fits-all” method for all data types: it was rather suggested to evaluate which conditions are appropriate for each method. In (Hassan et al. 2014) and (Hassan et al. 2017), in the context of epileptic spikes, wMNE combined with PLV had better accuracy as compared to other algorithms. In (Allouch, Yochum, et al. 2022; Allouch, Kabbara, et al. 2022), we tested several connectivity measures and obtained a significant variability in the accuracy of reconstructed cortical networks in the context of epileptiform and resting-state simulations (Allouch, Yochum, et al. 2022; Allouch, Kabbara, et al. 2022). In line with previous findings, significant differences in group-level consistency, between-, and within-subjects similarity were obtained for different connectivity measures tested in this work.

It is noteworthy that higher group-level consistency, between-, and within-subject similarity were obtained with PLV and AEC. In contrast, connectivity metrics that are supposed to be robust to source leakage and signal spread problems (PLI, wPLI, corrected PLV, and corrected AEC) resulted in substantially lower group-level consistency, between-, and within-subject similarity. Therefore, we tested whether high consistency values are correlated with source leakage and signal spread problems or not. As illustrated in Fig. S8 in Supplementary materials., there is no correlation between the contribution of each edge to the consistency value at the group level and the edge length (i.e., the distance separating correspondent ROIs). Shown results were obtained using eLORETA as a source reconstruction algorithm and a montage with 64 electrodes. Similar results were obtained for other inverse solution algorithms and electrode configurations. Since there was no correlation between the contribution of each edge to the consistency values at the group level and the distance separating different ROIs, high group-level repeatability cannot be explained by source leakage and signal spread problem. The high group-level consistency values we obtained are not a result of repetitive connectivity patterns induced by source leakage. In contrast, in (Colclough et al. 2016), the authors found that high group-level repeatability is spurious and caused by the signal spread problem. Moreover, the low within-subject similarity values we obtained are in line with the results obtained by (Fraschini et al. 2019) where methods correcting for the source leakage problem performed the worst in terms of within-subject network-based fingerprints. The authors proposed that metrics correcting for the source leakage problem (PLI, wPLI, corrected PLV, corrected AEC) may be obscuring individual network characteristics which results in lower within-subject epochs similarity.

4.4. Other possible sources of variability

The purpose of our paper was not to present an exhaustive investigation of all sources of analytical variability in the EEG source connectivity analysis. There exist numerous factors that were not addressed in this work and are thought to produce substantial variability in reported results. For instance, in (Šoškić et al. 2022), preprocessing and data cleaning steps were shown to affect the outcomes in ERP analysis. Similar conclusions were obtained in (Clayson et al. 2021). In addition to the specific method chosen to process the data, the selected software package can be a substantial source of variability. This topic was more tackled in fMRI as compared to EEG studies (Bowring, Maumet, and Nichols 2019; Glatard et al. 2015; Gronenschild et al. 2012). Recently, (Kabbara et al. 2022) examined the degree of consistency between EEG software toolboxes used to preprocess evoked-related potentials. Other sources of variability in EEG source connectivity analysis are related to the inverse solution parameters (regularization parameter for example (Grech et al. 2008)), head models (Cho et al. 2015; Brodbeck et al. 2011; Wolters et al. 2006), and channels locations (Shirazi and Huang 2019). The definition of network nodes (voxel-wise networks, anatomical or functional atlases) and the corresponding spatial resolution are also critical factors resulting in significant discrepancies in results (Yao et al. 2015; de Reus and van den Heuvel 2013; Stanley et al. 2013; Fornito, Zalesky, and Bullmore 2010; Hayasaka and Laurienti 2010; Zalesky et al. 2010; J. Wang et al. 2009), in addition to the approach used to extract a single time series representative of an ROI (mean, principal component analysis...) (Zhou et al. 2009). Related to the functional connectivity computation, some sub-parameters are to be cautiously chosen such as the epoch length (Fraschini et al. 2016; Wilson et al. 2015), and the number of trials (Marquetand et al. 2019; Bastos and Schoffelen 2015)... Finally, thresholding connectivity matrices (absolute vs proportional thresholds (van den Heuvel et al. 2017)) and whether to binarize them or not (Bassett and Bullmore 2017) are also debatable topics.

4.5. Possible solutions

The amount of analytical variability and its substantial impact on the results is a serious challenge for the neuroimaging community. To address this issue, several practices could be adopted. First, detailed documentation of the analysis is mandatory. However, with the emergent complexity of neuroimaging workflows, a detailed description of all analysis steps becomes exhausting, and even sometimes unachievable. In this case, the code itself becomes

the most accurate documentation of the performed analysis (Niso, Botvinik-Nezer, et al. 2022). As a consequence, sharing underlying data, codes, and methods should become the norm to promote analysis transparency (Niso, Botvinik-Nezer, et al. 2022; Niso, Krol, et al. 2022; Pernet et al. 2020; Botvinik-Nezer et al. 2020; Poldrack et al. 2017; Wicherts et al. 2016; Bishop et al. 2015; Pernet and Poline 2015). Making the data and analysis available to the community fosters research replicability, and enables 1) running alternative analyses on the same data, and 2) validating the codes that were used (Botvinik-Nezer et al. 2020). To address the issue of p-hacking, pre-registration could be adopted to prevent the misuse of analytical variability and exploitation of the researcher's degrees of freedom by setting analysis details prior to the study and prohibiting data-dependent choices. Although data and code sharing and pre-registration would not alleviate all the aspects of the problem of analytical variability, it would at least make the effect of variability transparent and quantified (Botvinik-Nezer et al. 2020). Another way to address the issue of analytical variability is to run many alternative analysis pipelines (and report them eventually) on the same data set (Botvinik-Nezer et al. 2020). This is becoming steadily more feasible with the increased automation of neuroimaging workflows. Such validation procedures could be, ideally, done by several teams. In this line, “multiverse analyses” have been proposed in other disciplines to increase analytic transparency (Steegen et al. 2016; Hall et al. 2022; Patel, Burford, and Ioannidis 2015; Simonsohn, Simmons, and Nelson 2019). This approach consists of running the whole (or a large) set of possible analytical combinations of choices and reporting the corresponding results. The advantages of a multiverse analysis are a presentation of the robustness or fragility of results across different analytical choices and an identification of critical choices highly affecting the outcomes. Finally, raising awareness about the topic of analytical variability and its substantial effects on reproducibility and sound neuroimaging research and practices is of the utmost importance. This can be promoted and disseminated through workshops, training (Bishop et al. 2015), and ongoing open discussions about possible solutions.

Code availability

The codes that support the results of this study are available at <https://github.com/sahar-allouch/var-EEG-FC>. We used Matlab (Matlab 2018), Brainstorm toolbox (Tadel et al. 2011), Fieldtrip toolbox ((Oostenveld et al. 2011); <http://fieldtriptoolbox.org>), OpenMEEG (Gramfort et al. 2010) implemented in fieldtrip, Automagic toolbox (Pedroni, Bahreini, and Langer 2019)

for EEG pre-processing, R (R Core Team 2020) for statistical analysis, and Seaborn (Waskom 2021) and Plotly (Plotly Technologies Inc 2015) for visualization.

Data availability

The data that support the findings of this study are available upon request from the author [V. P.].

Acknowledgments

The authors would like to acknowledge the Lebanese National Council for Scientific Research (CNRS-L), the Agence Universitaire de la Francophonie (AUF), and the Lebanese University for granting Ms. Allouch a doctoral scholarship. This work was also supported by the Labex Cominlabs project PKSTIM and by the Institute of Clinical Neuroscience of Rennes (Projects EEGCog and EENET3). The authors would also like to thank Campus France, Programme Hubert Curien CEDRE (PROJET N° 42257YA), and the Lebanese Association for Scientific Research (LASER) for their support.

Competing Interests

The authors declare that they have no competing interests.

References

- Allouch, Sahar, Aya Kabbara, Joan Duprez, Mohamad Khalil, Julien Modolo, and Mahmoud Hassan. 2022. “Effect of Channel Density, Inverse Solutions and Connectivity Measures on EEG Resting-State Networks: A Simulation Study.” *bioRxiv*. <https://doi.org/10.1101/2022.06.01.494301>.
- Allouch, Sahar, Maxime Yochum, Aya Kabbara, Joan Duprez, Mohamad Khalil, Fabrice Wendling, Mahmoud Hassan, and Julien Modolo. 2022. “Mean-Field Modeling of Brain-Scale Dynamics for the Evaluation of EEG Source-Space Networks.” *Brain Topography* 35 (1): 54–65.
- Anzolin, Alessandra, Paolo Presti, Frederik Van De Steen, Laura Astolfi, Stefan Haufe, and Daniele Marinazzo. 2019. “Quantifying the Effect of Demixing Approaches on Directed Connectivity Estimated Between Reconstructed EEG Sources.” *Brain Topography*. <https://doi.org/10.1007/s10548-019-00705-z>.
- Awan, Fahim Gohar, Omer Saleem, and Asima Kiran. 2019. “Recent Trends and Advances in Solving the Inverse Problem for EEG Source Localization.” *Inverse Problems in Science & Engineering* 27 (11): 1521–36.

- Baillet, Sylvain, John C. Mosher, and Richard M. Leahy. 2001. “Electromagnetic Brain Mapping.” *IEEE Signal Processing Magazine*, no. November: 14–30.
- Barton, K. 2009. “MuMIn: Multi-Model Inference.” *Http://r-Forge. R-Project. Org/projects/mumin/*. <https://ci.nii.ac.jp/naid/20001420752/>.
- Bassett, Danielle S., and Edward T. Bullmore. 2017. “Small-World Brain Networks Revisited.” *The Neuroscientist: A Review Journal Bringing Neurobiology, Neurology and Psychiatry* 23 (5): 499–516.
- Bastos, André M., and Jan-Mathijs Schoffelen. 2015. “A Tutorial Review of Functional Connectivity Analysis Methods and Their Interpretational Pitfalls.” *Frontiers in Systems Neuroscience* 9: 175.
- Bishop, Cantrell, Johnson, Kapur, and Macleod. 2015. “Reproducibility and Reliability of Biomedical Research: Improving Research Practise.” *The Academy of Medical*.
- Botvinik-Nezer, Rotem, Felix Holzmeister, Colin F. Camerer, Anna Dreber, Juergen Huber, Magnus Johannesson, Michael Kirchler, et al. 2020. “Variability in the Analysis of a Single Neuroimaging Dataset by Many Teams.” *Nature* 582 (7810): 84–88.
- Bowring, Alexander, Camille Maumet, and Thomas E. Nichols. 2019. “Exploring the Impact of Analysis Software on Task fMRI Results.” *Human Brain Mapping* 40 (11): 3362–84.
- Bradley, Allison, Jun Yao, Jules Dewald, and Claus Peter Richter. 2016. “Evaluation of Electroencephalography Source Localization Algorithms with Multiple Cortical Sources.” *PloS One* 11 (1): 1–14.
- Brodbeck, Verena, Laurent Spinelli, Agustina M. Lascano, Michael Wissmeier, Maria-Isabel Vargas, Serge Vulliemoz, Claudio Pollo, Karl Schaller, Christoph M. Michel, and Margitta Seeck. 2011. “Electroencephalographic Source Imaging: A Prospective Study of 152 Operated Epileptic Patients.” *Brain: A Journal of Neurology* 134 (Pt 10): 2887–97.
- Brookes, Matthew J., Joanne R. Hale, Johanna M. Zumer, Claire M. Stevenson, Susan T. Francis, Gareth R. Barnes, Julia P. Owen, Peter G. Morris, and Srikantan S. Nagarajan. 2011. “NeuroImage Measuring Functional Connectivity Using MEG : Methodology and Comparison with fcMRI.” *NeuroImage* 56 (3): 1082–1104.
- Brookes, Woolrich, and Barnes. 2012. “Measuring Functional Connectivity in MEG: A Multivariate Approach Insensitive to Linear Source Leakage.” *NeuroImage* 63 (2): 910–20.
- Cao, Jun, Yifan Zhao, Xiaocai Shan, Hua-Liang Wei, Yuzhu Guo, Liangyu Chen, John Ahmet Erkoyuncu, and Ptolemaios Georgios Sarigiannis. 2022. “Brain Functional and Effective Connectivity Based on Electroencephalography Recordings: A Review.” *Human Brain Mapping* 43 (2): 860–79.
- Carp, Joshua. 2012. “On the Plurality of (methodological) Worlds: Estimating the Analytic Flexibility of FMRI Experiments.” *Frontiers in Neuroscience* 6 (October): 149.
- Cho, Jae Hyun, Johannes Vorwerk, Carsten H. Wolters, and Thomas R. Knösche. 2015. “Influence of the Head Model on EEG and MEG Source Connectivity Analyses.” *NeuroImage* 110: 60–77.
- Clayson, Peter E., Scott A. Baldwin, Harold A. Rocha, and Michael J. Larson. 2021. “The Data-Processing Multiverse of Event-Related Potentials (ERPs): A Roadmap for the Optimization and Standardization of ERP Processing and Reduction Pipelines.” *NeuroImage* 245 (December): 118712.
- Colclough, G. L., M. J. Brookes, S. M. Smith, and M. W. Woolrich. 2015. “A Symmetric Multivariate Leakage Correction for MEG Connectomes.” *NeuroImage* 117 (August): 439–48.
- Colclough, G. L., M. W. Woolrich, P. K. Tewarie, M. J. Brookes, A. J. Quinn, and S. M. Smith. 2016. “How Reliable Are MEG Resting-State Connectivity Metrics?” *NeuroImage* 138: 284–93.

- Delamillieure, Pascal, Gaëlle Doucet, Bernard Mazoyer, Marie-Renée Turbelin, Nicolas Delcroix, Emmanuel Mellet, Laure Zago, et al. 2010. "The Resting State Questionnaire: An Introspective Questionnaire for Evaluation of Inner Experience during the Conscious Resting State." *Brain Research Bulletin* 81 (6): 565–73.
- Desikan, Rahul S., Florent Ségonne, Bruce Fischl, Brian T. Quinn, Bradford C. Dickerson, Deborah Blacker, Randy L. Buckner, et al. 2006. "An Automated Labeling System for Subdividing the Human Cerebral Cortex on MRI Scans into Gyral Based Regions of Interest." *NeuroImage* 31: 968–80.
- Finn, Emily S., Xilin Shen, Dustin Scheinost, Monica D. Rosenberg, Jessica Huang, Marvin M. Chun, Xenophon Papademetris, and R. Todd Constable. 2015. "Functional Connectome Fingerprinting: Identifying Individuals Using Patterns of Brain Connectivity." *Nature Neuroscience* 18 (11): 1664–71.
- Fornito, Alex, Andrew Zalesky, and Edward T. Bullmore. 2010. "Network Scaling Effects in Graph Analytic Studies of Human Resting-State fMRI Data." *Frontiers in Systems Neuroscience* 4: 1–16.
- Fraschini, Matteo, Matteo Demuru, Alessandra Crobe, Francesco Marroso, Cornelis J. Stam, and Arjan Hillebrand. 2016. "The Effect of Epoch Length on Estimated EEG Functional Connectivity and Brain Network Organisation." *Journal of Neural Engineering* 13 (3): 1–10.
- Fraschini, Matteo, Sara Maria Pani, Luca Didaci, and Gian Luca Marcialis. 2019. "Robustness of Functional Connectivity Metrics for EEG-Based Personal Identification over Task-Induced Intra-Class and Inter-Class Variations." *Pattern Recognition Letters* 125 (July): 49–54.
- Friston, Karl J. 2011. "Functional and Effective Connectivity: A Review." *Brain Connectivity* 1 (1): 13–36.
- Fuchs, Manfred, Michael Wagner, Thomas Köhler, and Hans Aloys Wischmann. 1999. "Linear and Nonlinear Current Density Reconstructions." *Journal of Clinical Neurophysiology: Official Publication of the American Electroencephalographic Society* 16 (3): 267–95.
- Glatard, Tristan, Lindsay B. Lewis, Rafael Ferreira da Silva, Reza Adalat, Natacha Beck, Claude Lepage, Pierre Rioux, et al. 2015. "Reproducibility of Neuroimaging Analyses across Operating Systems." *Frontiers in Neuroinformatics* 9 (April): 12.
- Gramfort, Alexandre, Théodore Papadopoulou, Emmanuel Olivi, and Maureen Clerc. 2010. "OpenMEEG: Opensource Software for Quasistatic Bioelectromagnetics." *Biomedical Engineering Online* 9 (45). <https://doi.org/10.1186/1475-925X-8-1>.
- Grech, Roberta, Tracey Cassar, Joseph Muscat, Kenneth P. Camilleri, Simon G. Fabri, Michalis Zervakis, Petros Xanthopoulos, Vangelis Sakkalis, and Bart Vanrumste. 2008. "Review on Solving the Inverse Problem in EEG Source Analysis." *Journal of Neuroengineering and Rehabilitation* 5 (25). <https://doi.org/10.1186/1743-0003-5-25>.
- Gronenschild, Ed H. B. M., Petra Habets, Heidi I. L. Jacobs, Ron Mengelers, Nico Rozendaal, Jim van Os, and Machteld Marcelis. 2012. "The Effects of FreeSurfer Version, Workstation Type, and Macintosh Operating System Version on Anatomical Volume and Cortical Thickness Measurements." *PloS One* 7 (6): e38234.
- Grova, C., J. Daunizeau, J. M. Lina, C. G. Bénar, H. Benali, and J. Gotman. 2006. "Evaluation of EEG Localization Methods Using Realistic Simulations of Interictal Spikes." *NeuroImage* 29: 734–53.
- Halder, Tamesh, Siddharth Talwar, Amit Kumar Jaiswal, and Arpan Banerjee. 2019. "Quantitative Evaluation in Estimating Sources Underlying Brain Oscillations Using Current Source Density Methods and Beamformer Approaches." *eNeuro* 6 (4): 1–14.

- Hall, Brian D., Yang Liu, Yvonne Jansen, Pierre Dragicevic, Fanny Chevalier, and Matthew Kay. 2022. “A Survey of Tasks and Visualizations in Multiverse Analysis Reports.” *Computer Graphics Forum: Journal of the European Association for Computer Graphics* 41 (1): 402–26.
- Hämäläinen, M. S., and R. J. Ilmoniemi. 1994. “Interpreting Magnetic Fields of the Brain: Minimum Norm Estimates.” *Medical & Biological Engineering & Computing* 32: 35–42.
- Hassan, M., P. Benquet, A. Biraben, C. Berrou, O. Dufor, and F. Wendling. 2015. “Dynamic Reorganization of Functional Brain Networks during Picture Naming.” *Cortex; a Journal Devoted to the Study of the Nervous System and Behavior* 73: 276–88.
- Hassan, M., O. Dufor, I. Merlet, C. Berrou, and F. Wendling. 2014. “EEG Source Connectivity Analysis: From Dense Array Recordings to Brain Networks.” *PloS One* 9 (8): e105041.
- Hassan, M., I. Merlet, A. Mheich, A. Kabbara, A. Biraben, A. Nica, and F. Wendling. 2017. “Identification of Interictal Epileptic Networks from Dense-EEG.” *Brain Topography* 30 (1): 60–76.
- Hassan, M., and F. Wendling. 2018. “Electroencephalography Source Connectivity: Aiming for High Resolution of Brain Networks in Time and Space.” *IEEE Signal Processing Magazine* 35 (3): 81–96.
- Hayasaka, Satoru, and Paul J. Laurienti. 2010. “Comparison of Characteristics between Region-and Voxel-Based Network Analyses in Resting-State fMRI Data.” *NeuroImage* 50: 499–508.
- He, Bin, Abbas Sohrabpour, Emery Brown, and Zhongming Liu. 2018. “Electrophysiological Source Imaging: A Noninvasive Window to Brain Dynamics.” *Annual Review of Biomedical Engineering* 20 (June): 171–96.
- Hedrich, T., G. Pellegrino, E. Kobayashi, J. M. Lina, and C. Grova. 2017. “Comparison of the Spatial Resolution of Source Imaging Techniques in High-Density EEG and MEG.” *NeuroImage* 157 (August): 531–44.
- Heuvel, Martijn P. van den, Siemon C. de Lange, Andrew Zalesky, Caio Seguin, B. T. Thomas Yeo, and Ruben Schmidt. 2017. “Proportional Thresholding in Resting-State fMRI Functional Connectivity Networks and Consequences for Patient-Control Connectome Studies: Issues and Recommendations.” *NeuroImage* 152 (May): 437–49.
- Hipp, Joerg F., David J. Hawellek, Maurizio Corbetta, Markus Siegel, and Andreas K. Engel. 2012. “Large-Scale Cortical Correlation Structure of Spontaneous Oscillatory Activity.” *Nature Neuroscience* 15 (6): 884–90.
- Hothorn, Torsten, Frank Bretz, and Peter Westfall. 2008. “Simultaneous Inference in General Parametric Models.” *Biometrical Journal. Biometrische Zeitschrift* 50 (3): 346–63.
- Kabbara, A., W. El Falou, M. Khalil, F. Wendling, and M. Hassan. 2017. “The Dynamic Functional Core Network of the Human Brain at Rest.” *Scientific Reports* 7 (1): 2936.
- Kabbara, Aya, Nina Forde, Camille Maumet, and Mahmoud Hassan. 2022. “Successful Reproduction of a Large EEG Study across Software Packages.” *bioRxiv*. <https://doi.org/10.1101/2022.08.03.502683>.
- Lachaux, Jean-Philippe, Eugenio Rodriguez, Michel Le Van Quyen, Antoine Lutz, Jacques Martinerie, and Francisco J. Varela. 2000. “Studying Single-Trials of Phase Synchronous Activity in the Brain.” *International Journal of Bifurcation and Chaos in Applied Sciences and Engineering* 10 (10): 2429–39.
- Lantz, Goran, R. Grave de Peralta, L. Spinelli, M. Seeck, and C. M. Michel. 2003. “Epileptic Source Localization with High Density EEG: How Many Electrodes Are Needed?” *Clinical Neurophysiology: Official Journal of the International Federation of Clinical Neurophysiology* 114 (1): 63–69.

- Lin, Fa Hsuan, Thomas Witzel, Seppo P. Ahlfors, Steven M. Stufflebeam, John W. Belliveau, and Matti S. Hämäläinen. 2006. “Assessing and Improving the Spatial Accuracy in MEG Source Localization by Depth-Weighted Minimum-Norm Estimates.” *NeuroImage* 31: 160–71.
- Mahjoory, Keyvan, Vadim V. Nikulin, Loïc Botrel, Klaus Linkenkaer-Hansen, Marco M. Fato, and Stefan Haufe. 2017. “Consistency of EEG Source Localization and Connectivity Estimates.” *NeuroImage* 152 (May): 590–601.
- Marquetand, Justus, Silvia Vannoni, Margherita Carboni, Yiwen Li Hegner, Christina Stier, Christoph Braun, and Niels K. Focke. 2019. “Reliability of Magnetoencephalography and High-Density Electroencephalography Resting-State Functional Connectivity Metrics.” *Brain Connectivity* 9 (7): 539–53.
- Matlab. 2018. “9.5.0.944444 (R2018b).” Natick, Massachusetts: The MathWorks Inc.
- Mehrkanon, Saeid, Michael Breakspear, Juliane Britz, and Tjeerd W. Boonstra. 2014. “Intrinsic Coupling Modes in Source-Reconstructed Electroencephalography.” *Brain Connectivity* 4 (10): 812–25.
- Michel, Christoph M., and Denis Brunet. 2019. “EEG Source Imaging: A Practical Review of the Analysis Steps.” *Frontiers in Neurology* 10 (April): 325.
- Michel, Christoph M., Micah M. Murray, Göran Lantz, Sara Gonzalez, Laurent Spinelli, and Rolando Grave de Peralta. 2004. “EEG Source Imaging.” *Clinical Neurophysiology: Official Journal of the International Federation of Clinical Neurophysiology* 115 (10): 2195–2222.
- Niso, Guiomar, Rotem Botvinik-Nezer, Stefan Appelhoff, Alejandro De La Vega, Oscar Esteban, Josep A. Etzel, Karolina Finc, et al. 2022. “Open and Reproducible Neuroimaging: From Study Inception to Publication.” <https://doi.org/10.31219/osf.io/pu5vb>.
- Niso, Guiomar, Laurens R. Krol, Etienne Combrisson, A. Sophie Dubarry, Madison A. Elliott, Clément François, Yseult Héjja-Brichard, et al. 2022. “Good Scientific Practice in EEG and MEG Research: Progress and Perspectives.” *NeuroImage* 257 (August): 119056.
- Oostenveld, Robert, Pascal Fries, Eric Maris, and Jan Mathijs Schoffelen. 2011. “FieldTrip: Open Source Software for Advanced Analysis of MEG, EEG, and Invasive Electrophysiological Data.” *Computational Intelligence and Neuroscience* 2011. <https://doi.org/10.1155/2011/156869>.
- Pascual-Marqui, Roberto D. 2007. “Discrete, 3D Distributed, Linear Imaging Methods of Electric Neuronal Activity. Part 1: Exact, Zero Error Localization.” <http://arxiv.org/abs/0710.3341>.
- Patel, Chirag J., Belinda Burford, and John P. A. Ioannidis. 2015. “Assessment of Vibration of Effects due to Model Specification Can Demonstrate the Instability of Observational Associations.” *Journal of Clinical Epidemiology* 68 (9): 1046–58.
- Pedroni, Andreas, Amirreza Bahreini, and Nicolas Langer. 2019. “Automagic: Standardized Preprocessing of Big EEG Data.” *NeuroImage* 200 (October): 460–73.
- Pereda, Ernesto, Rodrigo Quian Quiroga, and Joydeep Bhattacharya. 2005. “Nonlinear Multivariate Analysis of Neurophysiological Signals.” *Progress in Neurobiology* 77: 1–37.
- Pernet, Cyril, Marta I. Garrido, Alexandre Gramfort, Natasha Maurits, Christoph M. Michel, Elizabeth Pang, Riitta Salmelin, Jan Mathijs Schoffelen, Pedro A. Valdes-Sosa, and Aina Puce. 2020. “Issues and Recommendations from the OHBM COBIDAS MEEG Committee for Reproducible EEG and MEG Research.” *Nature Neuroscience* 23 (12): 1473–83.
- Pernet, Cyril, and Jean-Baptiste Poline. 2015. “Improving Functional Magnetic Resonance Imaging Reproducibility.” *GigaScience* 4 (March): 15.
- Plotly Technologies Inc. 2015. “Collaborative Data Science.” *Montreal: Plotly Technologies Inc Montral*. <https://plot.ly>.

- Poldrack, Russell A., Chris I. Baker, Joke Durnez, Krzysztof J. Gorgolewski, Paul M. Matthews, Marcus R. Munafò, Thomas E. Nichols, Jean-Baptiste Poline, Edward Vul, and Tal Yarkoni. 2017. “Scanning the Horizon: Towards Transparent and Reproducible Neuroimaging Research.” *Nature Reviews Neuroscience* 18 (2): 115–26.
- R Core Team. 2020. *R: A Language and Environment for Statistical Computing*. Vienna, Austria: R Foundation for Statistical Computing. <https://www.R-project.org/>.
- Reus, Marcel A. de, and Martijn P. van den Heuvel. 2013. “The Parcellation-Based Connectome: Limitations and Extensions.” *NeuroImage* 80 (October): 397–404.
- Robbins, Kay A., Jonathan Touryan, Tim Mullen, Christian Kothe, and Nima Bigdely-Shamlo. 2020. “How Sensitive Are EEG Results to Preprocessing Methods: A Benchmarking Study.” *IEEE Transactions on Neural Systems and Rehabilitation Engineering: A Publication of the IEEE Engineering in Medicine and Biology Society* 28 (5): 1081–90.
- Shirazi, Seyed Yahya, and Helen J. Huang. 2019. “More Reliable EEG Electrode Digitizing Methods Can Reduce Source Estimation Uncertainty, but Current Methods Already Accurately Identify Brodmann Areas.” *Frontiers in Neuroscience* 13 (November): 1159.
- Silberzahn, R., E. L. Uhlmann, D. P. Martin, P. Anselmi, F. Aust, E. Awtrey, Š. Bahník, et al. 2018. “Many Analysts, One Data Set: Making Transparent How Variations in Analytic Choices Affect Results.” *Advances in Methods and Practices in Psychological Science* 1 (3): 337–56.
- Simmons, Joseph P., Leif D. Nelson, and Uri Simonsohn. 2011. “False-Positive Psychology: Undisclosed Flexibility in Data Collection and Analysis Allows Presenting Anything as Significant.” *Psychological Science* 22 (11): 1359–66.
- Simonsohn, Uri, Joseph P. Simmons, and Leif D. Nelson. 2019. “Specification Curve: Descriptive and Inferential Statistics on All Reasonable Specifications.” [Https://papers.ssrn.com/sol3/Papers.html](https://papers.ssrn.com/sol3/Papers.html). <https://doi.org/10.2139/ssrn.2694998>.
- Sohrabpour, Abbas, Yunfeng Lu, Pongkiat Kankirawatana, Jeffrey Blount, Hyunmi Kim, and Bin He. 2015. “Effect of EEG Electrode Number on Epileptic Source Localization in Pediatric Patients.” *Clinical Neurophysiology: Official Journal of the International Federation of Clinical Neurophysiology* 126: 472–80.
- Song, J., C. Davey, C. Poulsen, P. Luu, S. Turovets, E. Anderson, K. Li, and D. Tucker. 2015. “EEG Source Localization: Sensor Density and Head Surface Coverage.” *Journal of Neuroscience Methods* 256: 9–21.
- Šoškić, Andela, Suzy J. Styles, Emily S. Kappenman, and Vanja Kovac. 2022. “Garden of Forking Paths in ERP Research – Effects of Varying Pre-Processing and Analysis Steps in an N400 Experiment.” <https://doi.org/10.31234/osf.io/8rjhj>.
- Srinivasan, Ramesh, Don M. Tucker, and Michael Murias. 1998. “Estimating the Spatial Nyquist of the Human EEG.” *Behavior Research Methods, Instruments, & Computers: A Journal of the Psychonomic Society, Inc* 30 (1): 8–19.
- Stam, Cornelis J., Guido Nolte, and Andreas Daffertshofer. 2007. “Phase Lag Index: Assessment of Functional Connectivity from Multi Channel EEG and MEG with Diminished Bias from Common Sources.” *Human Brain Mapping* 28: 1178–93.
- Stanley, Matthew L., Malaak N. Moussa, Brielle M. Paolini, Robert G. Lyday, Jonathan H. Burdette, and Paul J. Laurienti. 2013. “Defining Nodes in Complex Brain Networks.” *Frontiers in Computational Neuroscience* 7 (November): 169.
- Steegen, Sara, Francis Tuerlinckx, Andrew Gelman, and Wolf Vanpaemel. 2016. “Increasing Transparency Through a Multiverse Analysis.” *Perspectives on Psychological Science: A Journal of the Association for Psychological Science* 11 (5): 702–12.

- Tadel, Franois, Sylvain Baillet, John C. Mosher, Dimitrios Pantazis, and Richard M. Leahy. 2011. “Brainstorm: A User-Friendly Application for MEG/EEG Analysis.” *Computational Intelligence and Neuroscience* 2011. <https://doi.org/10.1155/2011/879716>.
- Tait, Luke, Aysegül Özkan, Maciej J. Szul, and Jiaxiang Zhang. 2021. “A Systematic Evaluation of Source Reconstruction of Resting MEG of the Human Brain with a New High-Resolution Atlas: Performance, Precision, and Parcellation.” *Human Brain Mapping* 42 (14): 4685–4707.
- Van Veen, B. D., W. van Drongelen, M. Yuchtman, and A. Suzuki. 1997. “Localization of Brain Electrical Activity via Linearly Constrained Minimum Variance Spatial Filtering.” *IEEE Transactions on Bio-Medical Engineering* 44 (9): 867–80.
- Vinck, Martin, Robert Oostenveld, Marijn Van Wingerden, Franscesco Battaglia, and Cyriel M. A. Pennartz. 2011. “An Improved Index of Phase-Synchronization for Electrophysiological Data in the Presence of Volume-Conduction, Noise and Sample-Size Bias.” *NeuroImage* 55 (4): 1548–65.
- Wang, Huifang E., Christian G. Bénar, Pascale P. Quilichini, Karl J. Friston, Viktor K. Jirsa, and Christophe Bernard. 2014. “A Systematic Framework for Functional Connectivity Measures.” *Frontiers in Neuroscience* 8. <https://doi.org/10.3389/fnins.2014.00405>.
- Wang, Jinhui, Liang Wang, Yufeng Zang, Hong Yang, Hehan Tang, Qiyong Gong, Zhang Chen, Chaozhe Zhu, and Yong He. 2009. “Parcellation-Dependent Small-World Brain Functional Networks: A Resting-State Fmri Study.” *Human Brain Mapping* 30: 1511–23.
- Waskom, Michael. 2021. “Seaborn: Statistical Data Visualization.” *Journal of Open Source Software* 6 (60): 3021.
- Wendling, Fabrice, Karim Ansari-Asl, Fabrice Bartolomei, and Lotfi Senhadji. 2009. “From EEG Signals to Brain Connectivity: A Model-Based Evaluation of Interdependence Measures.” *Journal of Neuroscience Methods* 183: 9–18.
- Wicherts, Jelte M., Coosje L. S. Veldkamp, Hilde E. M. Augusteijn, Marjan Bakker, Robbie C. M. van Aert, and Marcel A. L. M. van Assen. 2016. “Degrees of Freedom in Planning, Running, Analyzing, and Reporting Psychological Studies: A Checklist to Avoid P-Hacking.” *Frontiers in Psychology* 7 (November): 1832.
- Wilson, Rebecca S., Stephen D. Mayhew, David T. Rollings, Aimee Goldstone, Izabela Przezdzik, Theodoros N. Arvanitis, and Andrew P. Bagshaw. 2015. “Influence of Epoch Length on Measurement of Dynamic Functional Connectivity in Wakefulness and Behavioural Validation in Sleep.” *NeuroImage* 112 (May): 169–79.
- Wolters, C. H., A. Anwander, X. Tricoche, D. Weinstein, M. A. Koch, and R. S. MacLeod. 2006. “Influence of Tissue Conductivity Anisotropy on EEG/MEG Field and Return Current Computation in a Realistic Head Model: A Simulation and Visualization Study Using High-Resolution Finite Element Modeling.” *NeuroImage* 30 (3): 813–26.
- Yao, Zhijun, Bin Hu, Yuanwei Xie, Philip Moore, and Jiaxiang Zheng. 2015. “A Review of Structural and Functional Brain Networks: Small World and Atlas.” *Brain Informatics* 2 (1): 45–52.
- Zalesky, Andrew, Alex Fornito, Ian H. Harding, Luca Cocchi, Murat Yücel, Christos Pantelis, and Edward T. Bullmore. 2010. “Whole-Brain Anatomical Networks: Does the Choice of Nodes Matter?” *NeuroImage* 50: 970–83.
- Zhou, Zhenyu, Mingzhou Ding, Yonghong Chen, Paul Wright, Zuhong Lu, and Yijun Liu. 2009. “Detecting Directional Influence in fMRI Connectivity Analysis Using PCA Based Granger Causality.” *Brain Research* 1289 (September): 22–29.

Supplementary Materials

Effect of analytical variability in estimating EEG-based functional connectivity

Sahar Allouch^{1,2}, Aya Kabbara^{3,4}, Joan Duprez¹, Véronique Paban⁵, Mohamad Khalil^{2,6}, Julien Modolo¹, Mahmoud Hassan^{3,7}

¹ Univ Rennes, INSERM, LTSI - UMR 1099, F-35000 Rennes, France

² Azm Center for Research in Biotechnology and Its Applications, EDST, Tripoli, Lebanon

³ MINDig, F-35000 Rennes, France

⁴ LASER - Lebanese Association for Scientific Research, Tripoli, Lebanon

⁵ CRSI research center, Faculty of Engineering, Lebanese University, Beirut, Lebanon

⁶ Aix Marseille University, CNRS, LNSC, Marseille, France

⁷ School of Science and Engineering, Reykjavík University, Reykjavík, Iceland

Corresponding author: saharallouch@gmail.com

1. Materials and Methods

1.1. EEG pre-processing

EEG data were pre-processed using Automagic, a MATLAB-based toolbox. Pre-processing configuration is presented hereafter (all parameters definition can be found at <https://github.com/methlabUZH/automagic/wiki/Configurations>):

Residual Bad Channel Detection

- **High Variance Criterion (HVC)** = 20
- **Cut-off** = 80
- **Rejection Ratio** = $1/(512 \text{ Hz} * 10\text{sec})$
- **Minimum Variance Criterion (MVC)** = 1
- **High Pass Filter:** cut-off frequency = 45 Hz.
- **Low Pass Filter:** cutoff frequency = 0.1 Hz.
- The filter order will be estimated according to `eeg_filtnew()` of EEGLAB by default.
- **EOG regression** is checked (EOG channels = [65 66]).
- **ICLabel** is checked (with temporary high pass filter (cut-off = 2 Hz)).
- **Interpolation:** spherical
- Exclude ICLabel components
- **Probability thresholds for muscle artifacts:** [0.8 1]
- **Probability thresholds for eye artifacts:** [0.8 1]
- **Probability thresholds for heart artifacts:** [0.8 1]
- **Probability thresholds for line artifacts:** [0.8 1]
- **Probability thresholds for channel artifacts:** [0.8 1]
- **High Pass Filter:** cut-off = 0.1 Hz; (`pop_eegfiltnew()`).
- **Low Pass Filter:** cut-off = 45 Hz; (`pop_eegfiltnew()`).
- **Quality Rating:**
 - **Overall Threshold (mV):** [20 25 30 35 40]
 - **Time Threshold SD (mV):** [10 20 30 40 50]
 - **Channel Threshold SD (mV):** [10 20 30 40 50]
- **Downsampling Rate:** 1

2. Results

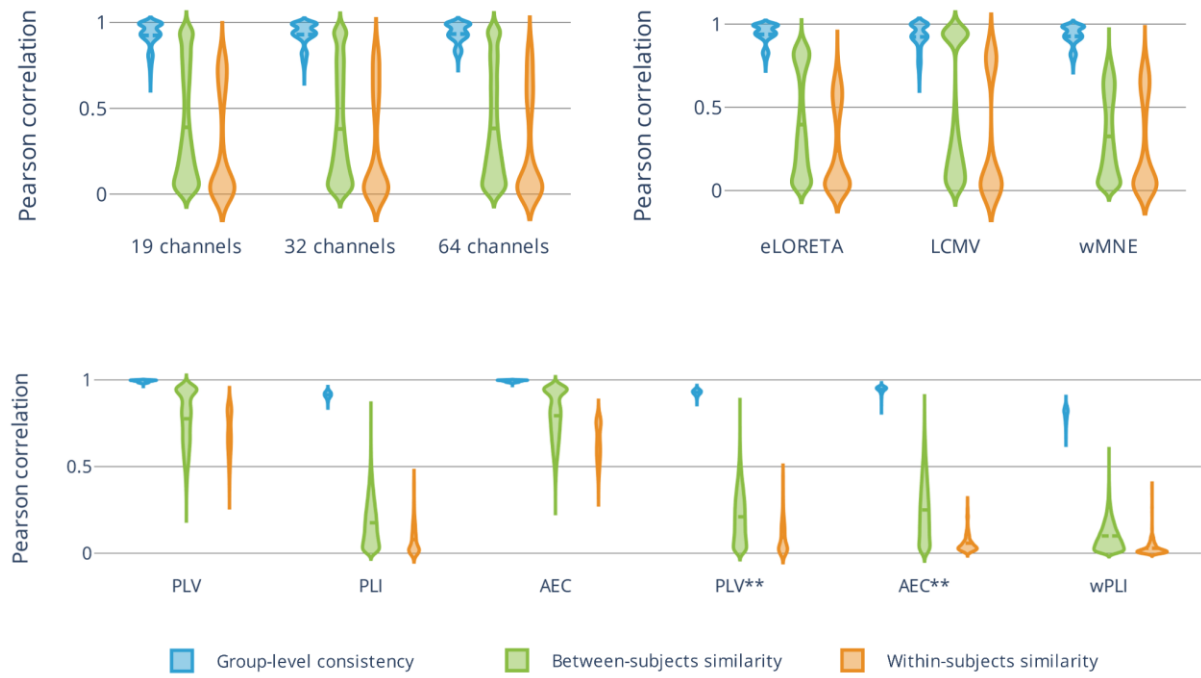


Fig. S1. Violin plots of the group-level consistency, between-, and within-subjects variability with respect to A) different electrode configurations, B) source reconstruction algorithms, and C) functional connectivity measures. Results correspond to the theta ([4-8]Hz) frequency band. *eLORETA* - exact low-resolution electromagnetic tomography. *LCMV* - linearly constrained minimum norm beamforming. *wMNE* - weighted minimum norm estimate. *PLV* - phase-locking value. *PLI* - phase-lag index. *AEC* - amplitude envelope correlation. *wPLI* - weighted phase-lag index. Asterisks (**) - source leakage correction.

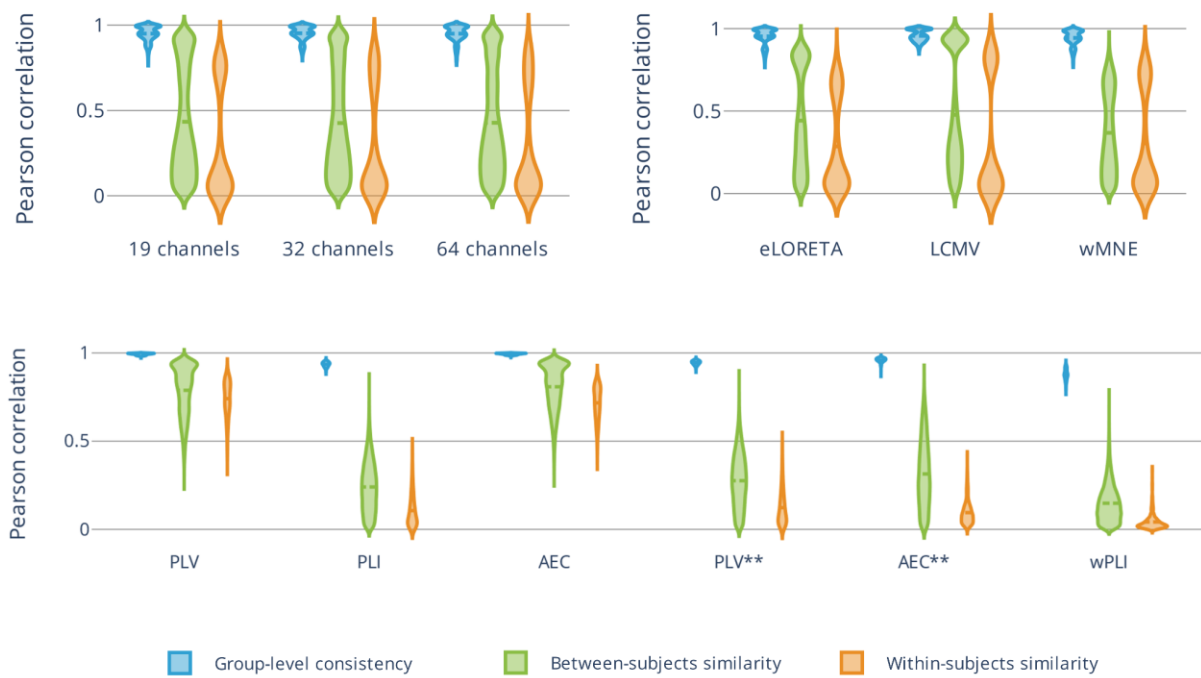


Fig. S2. Violin plots of the group-level consistency, between-, and within-subjects variability with respect to A) different electrode configurations, B) source reconstruction algorithms, and C) functional connectivity measures. Results correspond to the beta ([13-30]Hz) frequency band. *eLORETA* - exact low-resolution electromagnetic tomography. *LCMV* - linearly constrained minimum norm beamforming. *wMNE* - weighted minimum norm estimate. *PLV* - phase-locking value. *PLI* - phase-lag index. *AEC* - amplitude envelope correlation. *wPLI* - weighted phase-lag index. Asterisks (**) - source leakage correction.

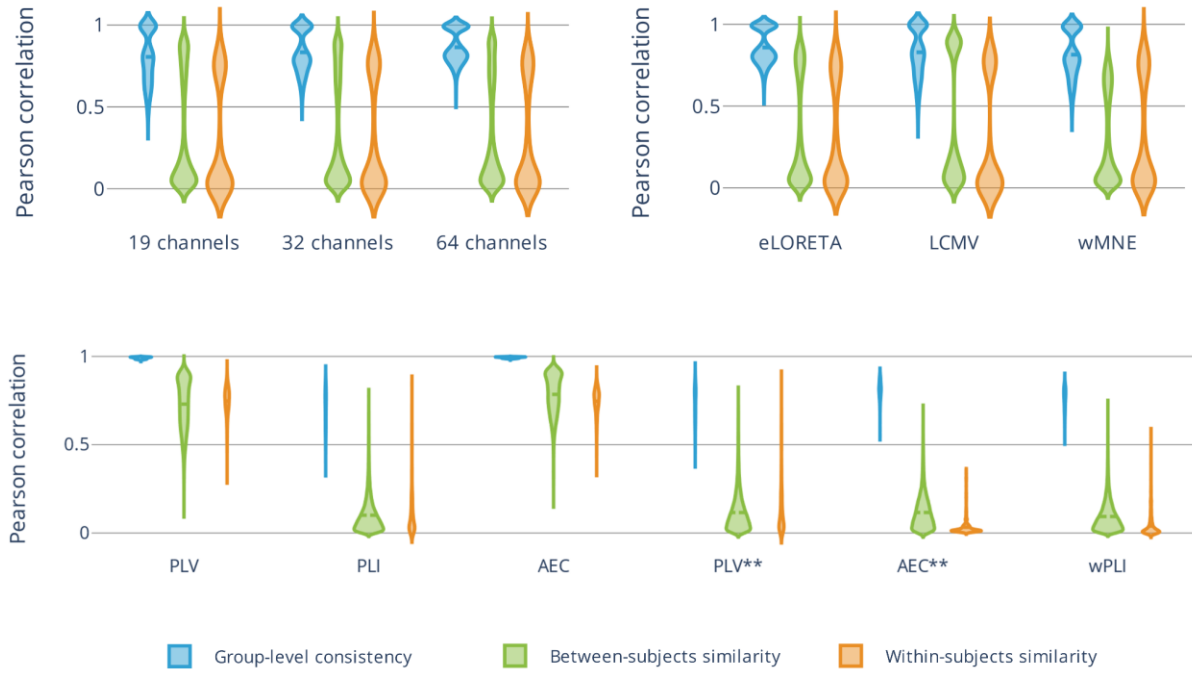


Fig. S3. Violin plots of the group-level consistency, between-, and within-subjects variability with respect to A) different electrode configurations, B) source reconstruction algorithms, and C) functional connectivity measures. Results correspond to the gamma ([30-45] Hz) frequency band. *eLORETA* - exact low-resolution electromagnetic tomography. *LCMV* - linearly constrained minimum norm beamforming. *wMNE* - weighted minimum norm estimate. *PLV* - phase-locking value. *PLI* - phase-lag index. *AEC* - amplitude envelope correlation. *wPLI* - weighted phase-lag index. Asterisks (**) - source leakage correction.

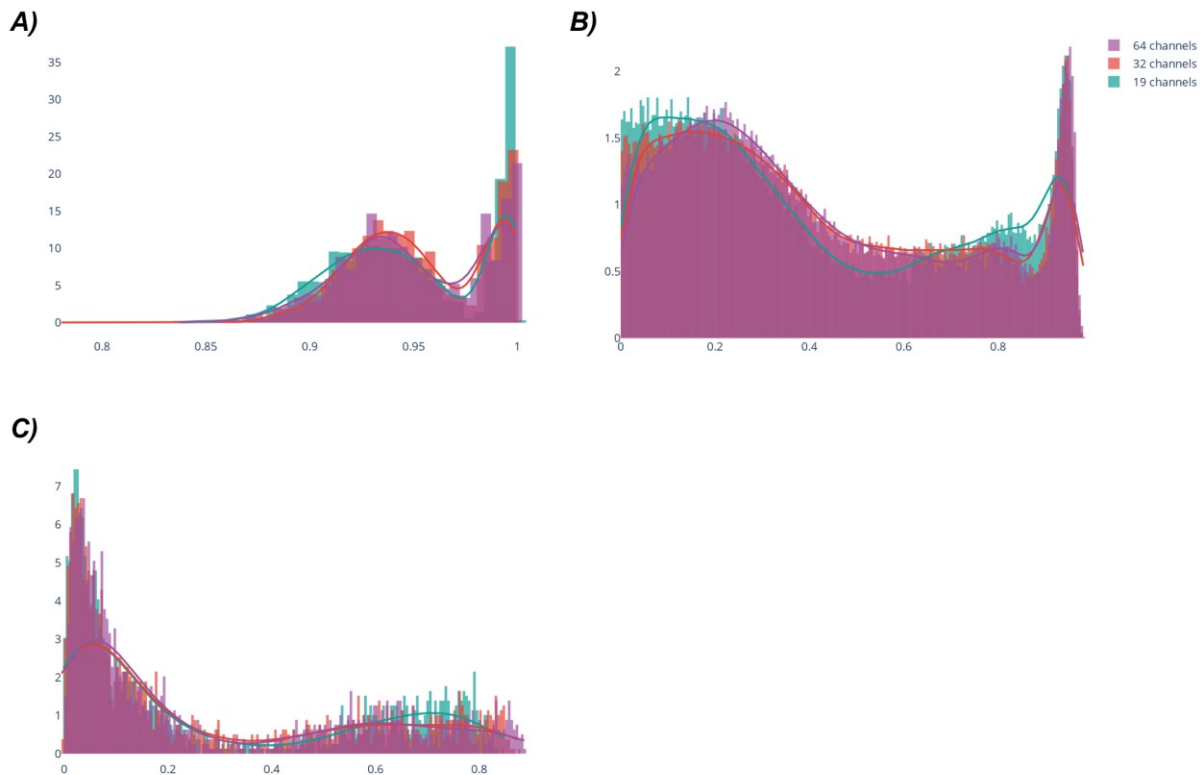
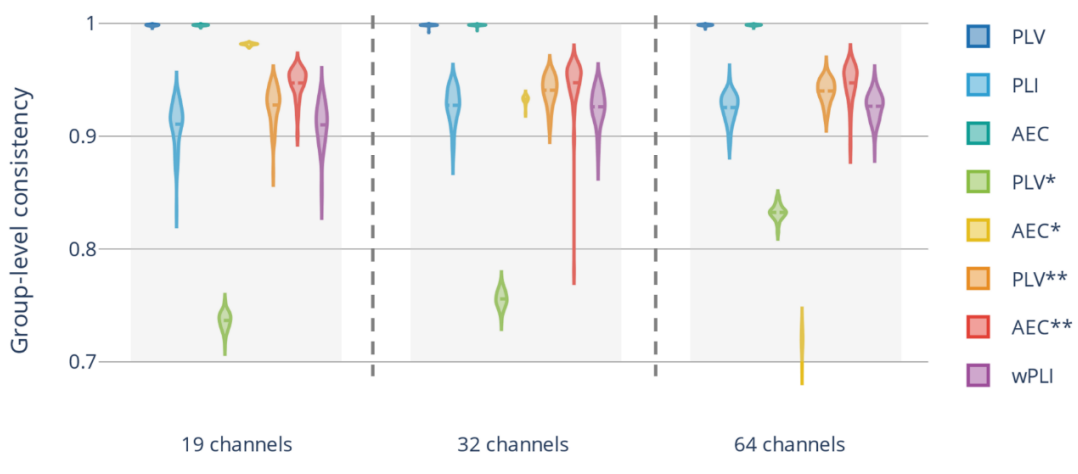


Fig. S4. Distributions of A) group-level consistency, B) between-, and C) within-subjects variability for different channel configurations (19, 32, and 64 electrodes). Significant differences obtained with statistical tests can be explained by the differences in the distribution plotted above (A-B).

eLORETA



LCMV



wMNE

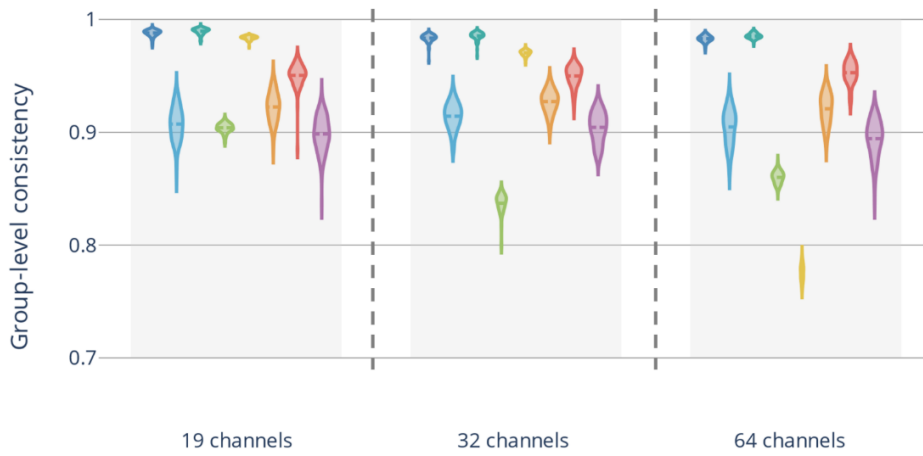
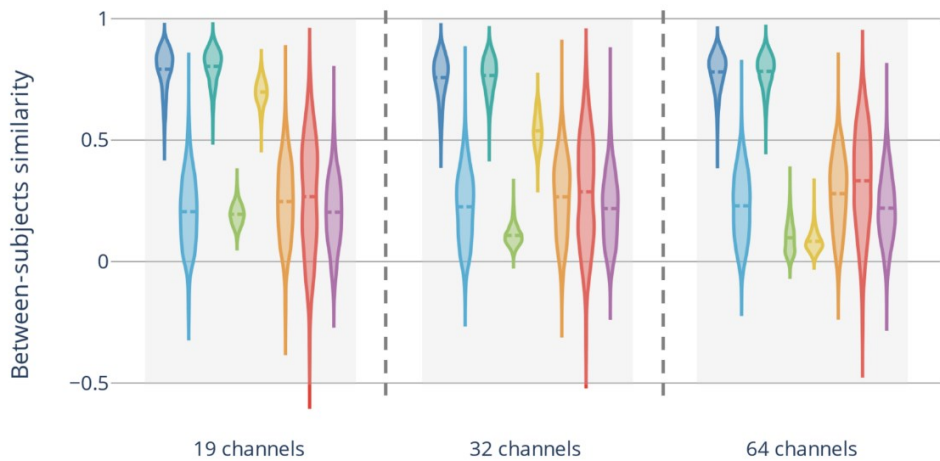


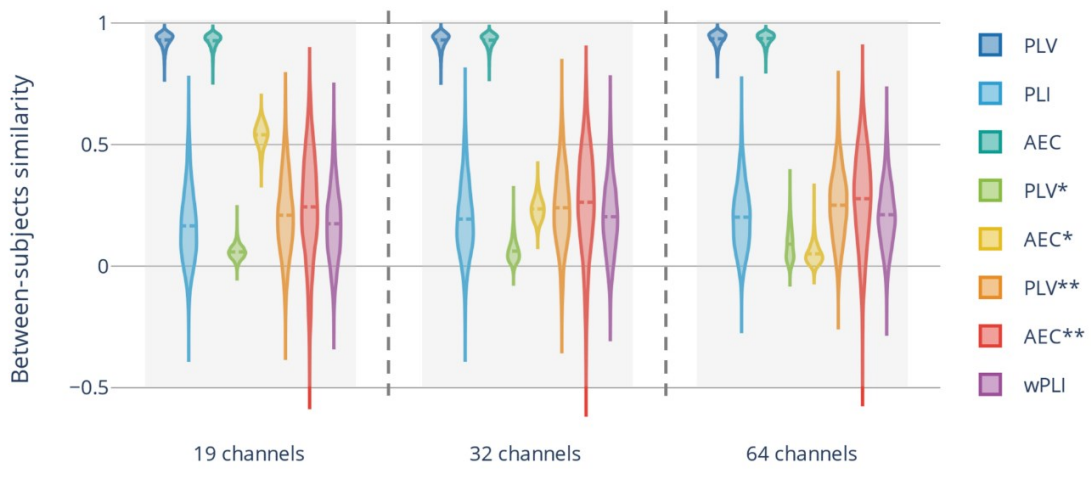
Fig. S5. Group-level consistency. The dataset was divided into two halves 100 times. For each condition (number of electrodes x inverse solution algorithm x connectivity measure), the Pearson correlation was computed between averaged connectivity matrices inferred from separate halves of the dataset. *eLORETA* - exact low-resolution electromagnetic tomography. *LCMV* - linearly constrained minimum norm beamforming. *wMNE* - weighted minimum norm estimate. *PLV* - phase-locking value. *PLI* -

phase-lag index. AEC - amplitude envelope correlation. wPLI - weighted phase-lag index. Asterisks: (*) - source leakage correction using the symmetric multivariate orthogonalization approach. (**) - source leakage correction using pairwise orthogonalization approach.

eLORETA



LCMV



wMNE

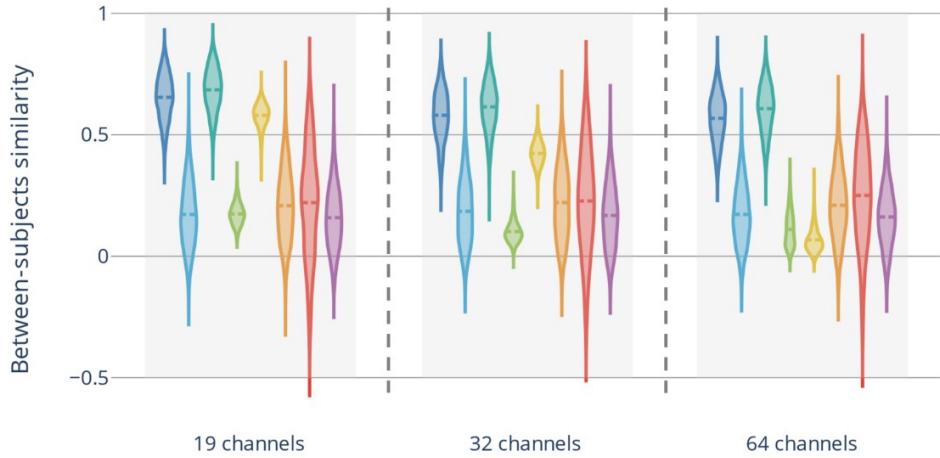


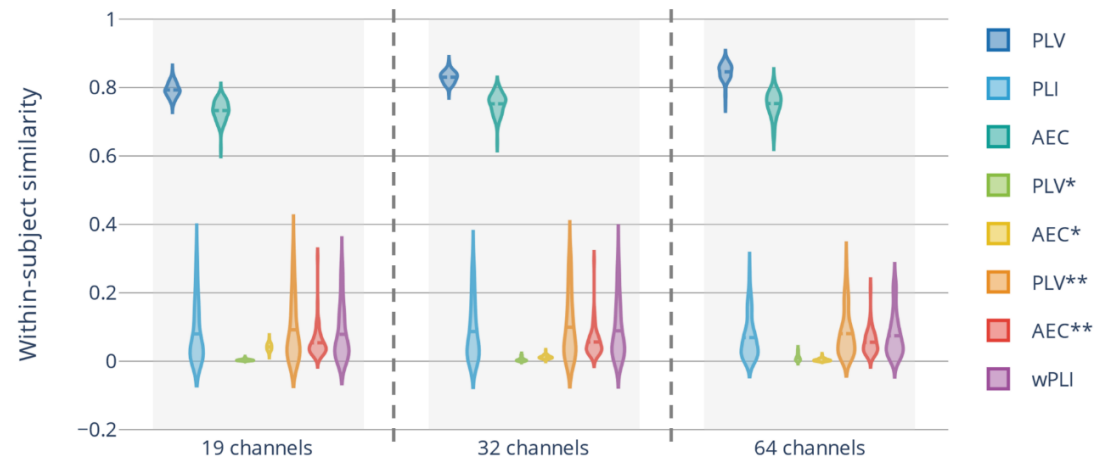
Fig. S6. Between-subjects similarity. Pearson correlation was computed between all subjects for each condition (number of electrodes x inverse solution algorithm x connectivity measure). *eLORETA* - exact

low-resolution electromagnetic tomography. LCMV - linearly constrained minimum norm beamforming. wMNE - weighted minimum norm estimate. PLV - phase-locking value. PLI - phase-lag index. AEC - amplitude envelope correlation. wPLI - weighted phase-lag index. Asterisks: () - source leakage correction using the symmetric multivariate orthogonalization approach. (**) - source leakage correction using pairwise orthogonalization approach.*

eLORETA



LCMV



wMNE

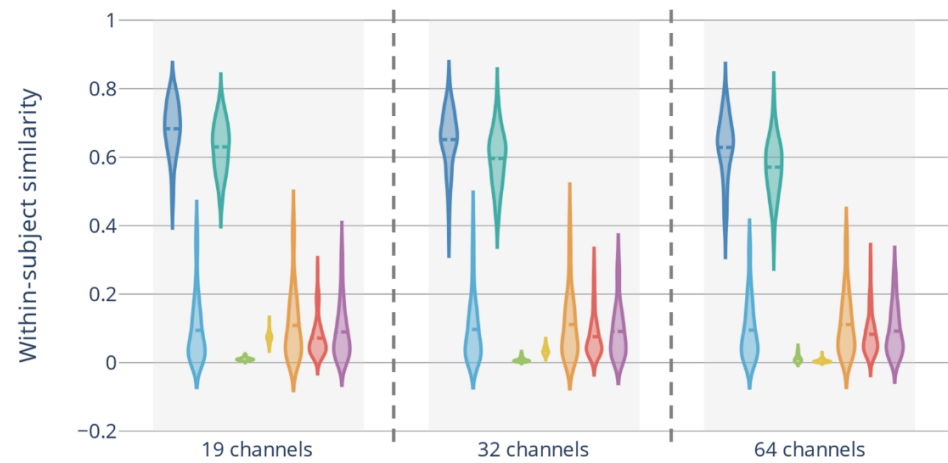


Fig. S7. Within-subject similarity. For each condition (number of electrodes x inverse solution algorithm x connectivity measure), and for each subject, Pearson correlation was computed between connectivity matrices inferred from different epochs. All correlation values for a single subject were averaged to obtain a single value representing the degree of within-subject similarity/consistency. *eLORETA* - exact low-resolution electromagnetic tomography. *LCMV* - linearly constrained minimum norm beamforming. *wMNE* - weighted minimum norm estimate. *PLV* - phase-locking value. *PLI* -

phase-lag index. AEC - amplitude envelope correlation. wPLI - weighted phase-lag index. Asterisks: () - source leakage correction using the symmetric multivariate orthogonalization approach. (**) - source leakage correction using pairwise orthogonalization approach.*

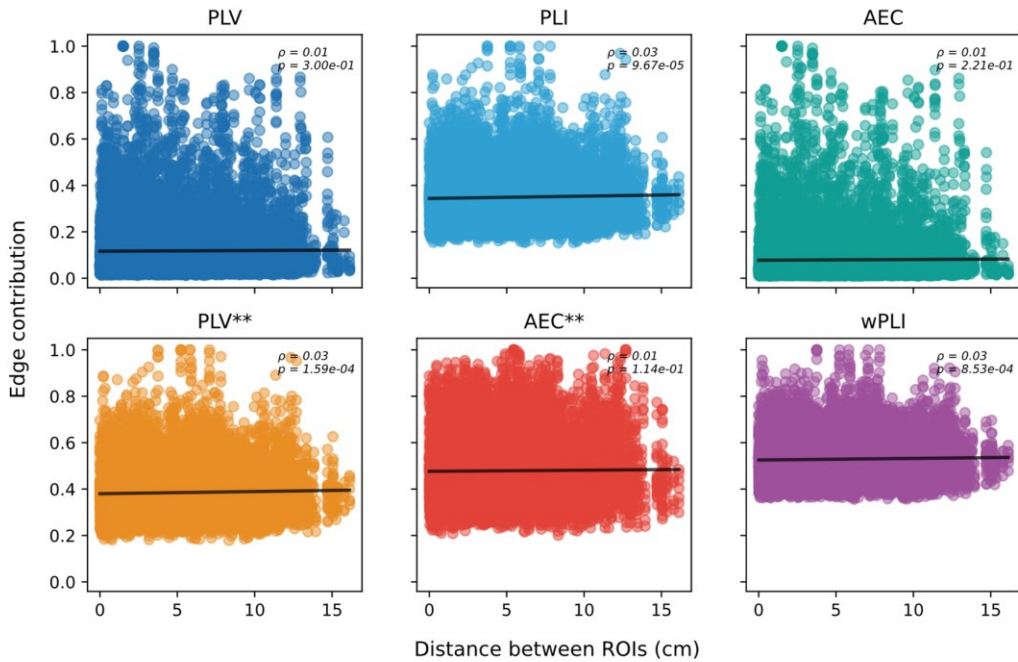


Fig. S8. Correlation between the edge contribution and the distance separating distinct ROIs for each connectivity measure (inverse solution algorithm = eLROETA, and number of electrodes = 64; similar result is obtained with different sensor density and source reconstruction algorithms). *PLV* - phase-locking value. *PLI* - phase-lag index. *AEC* - amplitude envelope correlation. *wPLI* - weighted phase-lag index. Asterisk (***) - source leakage correction.

4 DISCUSSION

As mentioned in the Introduction Chapter of this thesis, the issue of analytical variability, a natural consequence of the innumerable steps, parameters, and decisions often made arbitrarily within an analysis workflow; has two aspects. The first is when the researcher exploits all possible degrees of freedom to obtain satisfactory/expected significant results (p-hacking). In contrast, the second is the substantial amount of variability in studies' outcomes even with no intentional misconduct. To summarize, the issue is that the same data set could be analyzed, intentionally or unintentionally, in many different ways with the consequence that results could come out differently (Wicherts et al., 2016). Importantly, this makes research results harder to reproduce.

In neuroimaging research, the high dimensionality of the data and the complexity of analysis workflows are thought to be major drives of the analytical variability issue. In this thesis, we focused on investigating the impact of analytical variability in the context of EEG-based brain connectivity analysis. We mainly studied the effect of the choice of EEG electrode density, inverse solution algorithm, and functional connectivity measures on the discrepancy in studies' outcomes. The main results of this thesis can be summarized as follows:

1. EEG source connectivity analysis is largely affected by analytical variability. Practically, the analytical choices to be made are innumerable: for instance, restricting our possible choices to only 5 electrode montages, 3 inverse solutions, and 4 connectivity measures to test, already results in 60 different combinations. This is without mentioning all the parameters that have to be tuned within each method. Such high variability in the analysis causes substantial variability in research outcomes.

2. Electrophysiological computational models are of utmost importance in the context of investigating variability in analysis approaches and/or optimizing analytical pipelines since they are the only possible reasonable solution to provide ground truth. It is indeed very difficult, with the current technology, to obtain simultaneous acquisitions of thousands of scalp- and source-level recordings in humans. Knowledge of such ground truth offers the possibility to perform an accurate evaluation of tested methods and parameters, which is typically unachievable in experimental EEG data.
3. EEG simulations of epileptiform activity and resting-state networks show significant variability in reconstructed cortical networks due to the number of EEG electrodes, inverse solution, connectivity measure, as well as inverse solution/connectivity measure combination. This has a direct impact in terms of discussing the replicability of the associated results.
4. Our simulation results demonstrate that the spatial resolution of the sensor array dramatically affects the accuracy of network estimation: increasing spatial resolution significantly improves the accuracy of reconstructed networks. From our results, we recommend using at least 64 channels to accurately estimate EEG-based cortical networks.
5. The effect of analytical variability in the EEG source connectivity pipeline is also demonstrated in resting-state EEG in healthy controls. Group-level consistency, inter-, and intra-subjects similarity are substantially affected by the choice of the number of electrodes, source reconstruction algorithm, and functional connectivity measure.

4.1 Simulations vs empirical data

In this thesis, we adopted two approaches to test the effect of different analytical choices: simulation-based and empirical data-based studies. While ‘real’ data studies seem to predominate the neuroimaging field, simulation studies are highly relevant within the context of the present work. Using empirical data poses a serious challenge, since a direct comparison of source imaging and connectivity analysis is not obvious in the absence of a ‘ground truth’. Therefore, alternative approaches are usually adopted. For instance, we used group-level repeatability, inter-, and intra-subject similarities to assess the variability of the results induced by different analytical choices. The main advantage of a simulation-based study is the availability of a ground truth that enables an objective evaluation of different analyses. Moreover, having such a reference from simulated data offers the possibility to not only characterize the variability of the results caused by different analytical choices, as in our work;

but also, to optimize the analysis pipeline by searching for the ‘best’ (if any) method or attempting to understand when each method succeeds or fails. On the other hand, in experimental data, searching for a ‘best’ method is not obvious. Depending on the question of interest, one would adopt a ‘pragmatic’ approach to choose the optimal method in the context of the study. For instance, it is possible to compare the different methods based on their performance in patients/healthy controls classification, disease prediction contexts, etc... In this case, the performance of a method is a measure of its efficiency in answering a specific question in a specific context, but no inference can be drawn regarding the correspondence between the networks computed and the actual networks at the cortical level. As aforementioned, it is difficult, with the current technology, to obtain simultaneous acquisitions of thousands of scalp- and source-level recordings in humans.

4.2 Further aspects of analytical variability

There exist numerous factors that were not addressed in this work and that are thought to produce substantial variability in reported results. For instance, in (Šoškić et al., 2022), preprocessing and data cleaning steps such as high-pass filter cut-off, artifact removal method, baseline duration, reference, measurement latency, locations, and amplitude measure (peak vs. mean) were all shown to affect the outcomes in ERP analysis. Similar conclusions were obtained in (Clayson et al., 2021), following a multiverse analysis assessing the impact of key preprocessing steps. In addition to the specific method chosen to process the data, the selected software package can be a substantial source of variability. This topic was more tackled in fMRI as compared to EEG studies, where different analysis softwares (Bowring et al., 2019; Glatard et al., 2015), software versions (Gronenschild et al., 2012), and operating systems (Glatard et al., 2015; Gronenschild et al., 2012) have been compared. Recently, an EEG-based study revealed that considerable variability in results is observed when using different software tools to preprocess EEG signals (Aya Kabbara, Forde, et al., 2022). Other sources of variability in EEG source connectivity analysis are related to the inverse solution parameter (regularization parameter for example (Grech et al., 2008)), head models (simplified vs realistic head models, individual vs template MRI, tissue types, tissue conductivity) (Brodbeck et al., 2011; Cho et al., 2015; Wolters et al., 2006), and channels locations (template vs digitizing methods (ultrasound, structured-light 3D scan, infrared 3D scan, motion capture probe, and motion capture)) (Shirazi & Huang, 2019). The definition of network nodes (voxel-wise networks, anatomical or functional atlases) and the corresponding spatial resolution are also critical factors resulting in significant discrepancies in results (de Reus & van den Heuvel,

2013; Fornito et al., 2010; Hayasaka & Laurienti, 2010; Stanley et al., 2013; J. Wang et al., 2009; Yao et al., 2015; Zalesky et al., 2010), in addition to the approach used to extract a single time series representative of an ROI (mean, principal component analysis...) (Zhou et al., 2009). Related to the functional connectivity computation, some sub-parameters are to be cautiously chosen such as the epoch length (Fraschini et al., 2016; Wilson et al., 2015), and the number of trials (Bastos & Schoffelen, 2015; Marquetand et al., 2019)... Finally, thresholding connectivity matrices (absolute *vs* proportional thresholds (van den Heuvel et al., 2017)) and whether to binarize them or not (Bassett & Bullmore, 2017) are also debatable topics.

4.3 So, what now?... Possible solutions

The amount of analytical variability and its substantial impact on the results is a serious challenge for the neuroimaging community. Most strategies that have been proposed to address the issue of analytical variability in research are neither novel nor unknown (Bishop et al., 2015). Nevertheless, they are insufficiently implemented and embedded in daily scientific practices. First, detailed documentation of the analysis is mandatory. However, with the emergent complexity of neuroimaging workflows, a detailed description of all analysis steps becomes exhausting, and even sometimes unachievable. In this case, the code itself becomes the most accurate documentation of the performed analysis (Niso, Botvinik-Nezer, et al., 2022). As a consequence, sharing underlying data, codes, and methods should become the norm to promote analysis transparency (Bishop et al., 2015; Botvinik-Nezer et al., 2020; Niso, Botvinik-Nezer, et al., 2022; Niso, Krol, et al., 2022; Pernet et al., 2020; Pernet & Poline, 2015; Poldrack et al., 2017; Wicherts et al., 2016). Despite the increased interest in open science that marked recent years, this is unfortunately not a common practice yet. To overcome this, shifting toward open science practices should be an effort promoted both by individuals and organizations. Individual researchers must be convinced of the interest of open science, and willing to share their data and analysis pipelines. In the meantime, journals and funding agencies can promote analysis transparency by mandating data, methods, and codes to be openly shared (Bishop et al., 2015). Making the data and analysis available to the community fosters research replicability, and enables 1) running alternative analyses on the same data, and 2) validating the codes that were used on the other hand (Botvinik-Nezer et al., 2020). An additional measure that could be adopted is pre-registration, which specifically addresses the issue of p-hacking: this prevents the misuse of analytical variability and exploitation of the researcher's degrees of freedom by setting analysis details before the study and prohibiting data-dependent choices. Although data and code sharing and pre-registration would not

alleviate all the aspects of the problem of analytical variability, it would at least make the effect of variability transparent and quantified (Botvinik-Nezer et al., 2020). Another way to address the issue of analytical variability is to run many alternative analysis pipelines (and report them eventually) on the same dataset (Botvinik-Nezer et al., 2020). This is becoming increasingly feasible with the increased automation of neuroimaging workflows. Such validation procedures could be, ideally, done by several teams. In this line, “multiverse analyses” have been proposed in other disciplines to increase analytic transparency (Hall et al., 2022; Patel et al., 2015; Simonsohn et al., 2019; Steegen et al., 2016). This approach consists of running the whole (or a large) set of possible analytical combinations of choices and reporting the corresponding results. The advantages of a multiverse analysis are a presentation of the robustness or fragility of results across different analytical choices and an identification of critical choices highly affecting the outcomes. Finally, raising awareness about the topic of analytical variability and its substantial effects on reproducibility and sound neuroimaging research and practices is of the utmost importance. This can be promoted and disseminated through workshops, training (Bishop et al., 2015), and ongoing open discussions about possible solutions.

5 CONCLUSION

5.1 Summary

Reproducibility in scientific fields in general, and neuroimaging research in particular, is subject to an ongoing healthy debate. The self-correcting aspect of science cannot take place unless preceded by a self-criticism process. Such a process, we believe, has already begun in the neuroimaging community, with the rise of the reproducibility question. In this context, the issue of analytical variability in complex workflows has gained increased interest as a potential source of poor reproducibility. In line with this emergent topic, we studied in this thesis the effect of analytical variability in the context of the EEG source connectivity pipeline. We focused on the effect of sensor density, inverse solution algorithm, and connectivity measure, using both simulations and actual EEG data.

Overall, our results illustrated that the EEG source connectivity analysis is largely affected by the issue of analytical variability and that different analysis choices produce substantial variability in research outcomes.

5.2 Future work

In the following, we provide different possible directions to extend this work. In this thesis, we assessed the variability of the results at the level of connectivity matrices. Our incentive was to reduce further data manipulation and analytical choices as a first step. However, an extension of this work could be more goal-directed, such as assessing the effect of analytical variability in terms of the performance in classifying patients *vs* healthy subjects, biomarking, fingerprint performance, consistency of networks' topological characteristics...

Moreover, it would be especially interesting to reproduce this analysis on a large dataset with 256 channels. As the reader might have noticed, in the first two simulation studies, we indeed assessed the effect of electrode densities between 19 and 256 channels; however, in the third study, we were limited by a maximum of 64 available channels.

Among the numerous factors that could induce substantial variability (see Further aspects of analytical variability), we believe that the effect of the number of ROIs is key. Therefore, an extension of the present studies could be an evaluation of the impact of the source-space spatial resolution, both in simulations and experimental data

6 DATA AND CODE AVAILABILITY

Study I: Mean-Field Modeling of Brain-Scale Dynamics for the Evaluation of EEG Source-Space Networks

Data: <https://doi.org/10.5281/zenodo.6603054>

Code: <https://github.com/sahar-allouch/comp-epi>

Study II: Effect of channel density, inverse solutions, and connectivity measures on EEG resting-state networks reconstruction: a simulation study

Data: <https://doi.org/10.5281/zenodo.6597385>

Code: <https://github.com/sahar-allouch/var-RSNs>

Study III: Effect of analytical variability in estimating EEG-based functional connectivity

Code: <https://github.com/sahar-allouch/var-EEG-FC>

7 REFERENCES

- Alavash, M., Doebler, P., Holling, H., Thiel, C. M., & Gießing, C. (2015). Is functional integration of resting state brain networks an unspecific biomarker for working memory performance? *NeuroImage*, 108, 182–193. <https://doi.org/10.1016/j.neuroimage.2014.12.046>
- Allen, E. A., Damaraju, E., Eichele, T., Wu, L., & Calhoun, V. D. (2018). EEG Signatures of Dynamic Functional Network Connectivity States. *Brain Topography*, 31(1), 101–116. <https://doi.org/10.1007/s10548-017-0546-2>
- Allen, Elena A., Damaraju, E., Plis, S. M., Erhardt, E. B., Eichele, T., & Calhoun, V. D. (2014). Tracking Whole-Brain Connectivity Dynamics in the Resting State. *Cerebral Cortex*, 24, 663–676. <https://doi.org/10.1093/cercor/bhs352>
- Allouch, S., Yochum, M., Kabbara, A., Duprez, J., Khalil, M., Wendling, F., Hassan, M., & Modolo, J. (2022). Mean-Field Modeling of Brain-Scale Dynamics for the Evaluation of EEG Source-Space Networks. *Brain Topography*, 35(1), 54–65. <https://doi.org/10.1007/s10548-021-00859-9>
- Anzolin, A., Presti, P., Van De Steen, F., Astolfi, L., Haufe, S., & Marinazzo, D. (2019). Quantifying the Effect of Demixing Approaches on Directed Connectivity Estimated Between Reconstructed EEG Sources. *Brain Topography*. <https://doi.org/10.1007/s10548-019-00705-z>
- Avena-Koenigsberger, A., Misic, B., & Sporns, O. (2018). Communication dynamics in complex brain networks. *Nature Reviews Neuroscience*, 19, 17–33. <https://doi.org/10.1038/nrn.2017.149>
- Awan, F. G., Saleem, O., & Kiran, A. (2019). Recent trends and advances in solving the inverse problem for EEG source localization. *Inverse Problems in Science & Engineering*, 27(11), 1521–1536. <https://doi.org/10.1080/17415977.2018.1490279>
- Baillet, S., Mosher, J. C., & Leahy, R. M. (2001). Electromagnetic Brain Mapping. *IEEE Signal Processing Magazine, November*, 14–30.
- Baker. (2016). 1,500 scientists lift the lid on reproducibility. *Nature*, 533(7604), 452–454. <https://doi.org/10.1038/533452a>
- Baker, A. P., Brookes, M. J., Rezek, I. A., Smith, S. M., Behrens, T., Probert Smith, P. J., & Woolrich, M. (2014). Fast transient networks in spontaneous human brain activity. *eLife*, 3, e01867. <https://doi.org/10.7554/eLife.01867>
- Barton, K. (2009). MuMIn: multi-model inference. *Http://R-Forge.r-Project.Org/Projects/Mumin/*. <https://ci.nii.ac.jp/naid/20001420752/>

- Bassett, D. S., & Bullmore, E. T. (2017). Small-World Brain Networks Revisited. *The Neuroscientist: A Review Journal Bringing Neurobiology, Neurology and Psychiatry*, 23(5), 499–516. <https://doi.org/10.1177/1073858416667720>
- Bassett, D. S., & Sporns, O. (2017). Network neuroscience. *Nature Neuroscience*, 20(3), 353–364. <https://doi.org/10.1038/nn.4502>
- Bassett, D. S., Wymbs, N. F., Porter, M. A., Mucha, P. J., Carlson, J. M., & Grafton, S. T. (2011). Dynamic reconfiguration of human brain networks during learning. *Proceedings of the National Academy of Sciences of the United States of America*, 108(18), 7641–7646. <https://doi.org/10.1073/pnas.1018985108>
- Bastos, A. M., & Schoffelen, J.-M. (2015). A Tutorial Review of Functional Connectivity Analysis Methods and Their Interpretational Pitfalls. *Frontiers in Systems Neuroscience*, 9, 175. <https://doi.org/10.3389/fnsys.2015.00175>
- Bates, D., Mächler, M., Bolker, B. M., & Walker, S. C. (2015). Fitting linear mixed-effects models using lme4. *Journal of Statistical Software*, 67(1). <https://doi.org/10.18637/jss.v067.i01>
- Begley, C. G., & Ellis, L. M. (2012). Raise standards for preclinical cancer research. *Nature*, 483(7391), 531–533. <https://doi.org/10.1038/483531a>
- Bensaid, S., Modolo, J., Merlet, I., Wendling, F., & Benquet, P. (2019). COALIA: A Computational Model of Human EEG for Consciousness Research. *Frontiers in Systems Neuroscience*, 13, 1–18. <https://doi.org/10.3389/fnsys.2019.00059>
- Bishop, Cantrell, Johnson, Kapur, & Macleod. (2015). Reproducibility and reliability of biomedical research: improving research practise. *The Academy of Medical.*
- Boekel, W., Wagenmakers, E.-J., Belay, L., Verhagen, J., Brown, S., & Forstmann, B. U. (2015). A purely confirmatory replication study of structural brain-behavior correlations. *Cortex; a Journal Devoted to the Study of the Nervous System and Behavior*, 66, 115–133. <https://doi.org/10.1016/j.cortex.2014.11.019>
- Bola, M., & Sabel, B. A. (2015). Dynamic reorganization of brain functional networks during cognition. *NeuroImage*, 114, 398–413. <https://doi.org/10.1016/j.neuroimage.2015.03.057>
- Botvinik-Nezer, R., Holzmeister, F., Camerer, C. F., Dreber, A., Huber, J., Johannesson, M., Kirchler, M., Iwanir, R., Mumford, J. A., Adcock, R. A., Avesani, P., Baczkowski, B. M., Bajracharya, A., Bakst, L., Ball, S., Barilari, M., Bault, N., Beaton, D., Beitner, J., ... Schonberg, T. (2020). Variability in the analysis of a single neuroimaging dataset by many teams. *Nature*, 582(7810), 84–88. <https://doi.org/10.1038/s41586-020-2314-9>
- Bowring, A., Maumet, C., & Nichols, T. E. (2019). Exploring the impact of analysis software on task fMRI results. *Human Brain Mapping*, 40(11), 3362–3384. <https://doi.org/10.1002/hbm.24603>
- Bradley, A., Yao, J., Dewald, J., & Richter, C. P. (2016). Evaluation of electroencephalography source localization algorithms with multiple cortical sources. *PloS One*, 11(1), 1–14. <https://doi.org/10.1371/journal.pone.0147266>
- Braude, S. E. (1979). *ESP and psychokinesis. A philosophical examination*. Temple University Press.
- Braun, U., Schäfer, A., Walter, H., Erk, S., Romanczuk-Seiferth, N., Haddad, L., Schweiger, J. I., Grimm, O., Heinz, A., Tost, H., Meyer-Lindenberg, A., & Bassett, D. S. (2015). Dynamic reconfiguration of frontal brain networks during executive cognition in humans. *Proceedings of the National Academy of Sciences of the United States of America*, 112(37), 11678–11683. <https://doi.org/10.1073/pnas.1422487112>
- Brodbeck, V., Spinelli, L., Lascano, A. M., Wissmeier, M., Vargas, M.-I., Vulliemoz, S., Pollo, C., Schaller, K., Michel, C. M., & Seeck, M. (2011). Electroencephalographic source imaging: a prospective study of 152 operated epileptic patients. *Brain: A Journal of Neurology*, 134(Pt 10), 2887–2897. <https://doi.org/10.1093/brain/awr243>

- Brookes, M. J., Liddle, E. B., Hale, J. R., Woolrich, M. W., Luckhoo, H., Liddle, P. F., & Morris, P. G. (2012). Task induced modulation of neural oscillations in electrophysiological brain networks. *NeuroImage*, 63(4), 1918–1930. <https://doi.org/10.1016/j.neuroimage.2012.08.012>
- Brookes, Matthew J., Hale, J. R., Zumer, J. M., Stevenson, C. M., Francis, S. T., Barnes, G. R., Owen, J. P., Morris, P. G., & Nagarajan, S. S. (2011). NeuroImage Measuring functional connectivity using MEG : Methodology and comparison with fcMRI. *NeuroImage*, 56(3), 1082–1104. <https://doi.org/10.1016/j.neuroimage.2011.02.054>
- Brookes, Woolrich, & Barnes. (2012). Measuring functional connectivity in MEG: a multivariate approach insensitive to linear source leakage. *NeuroImage*, 63(2), 910–920. <https://doi.org/10.1016/j.neuroimage.2012.03.048>
- Bullmore, E., & Sporns, O. (2009). Complex brain networks: graph theoretical analysis of structural and functional systems. *Nature Reviews Neuroscience*, 10(3), 186–198. <https://doi.org/10.1038/nrn2575>
- Button, K. S., Ioannidis, J. P. A., Mokrysz, C., Nosek, B. A., Flint, J., Robinson, E. S. J., & Munafò, M. R. (2013). Power failure: why small sample size undermines the reliability of neuroscience. *Nature Reviews Neuroscience*, 14(5), 365–376. <https://doi.org/10.1038/nrn3475>
- Calhoun, V. D., & Adali, T. (2012). Multisubject independent component analysis of fMRI: a decade of intrinsic networks, default mode, and neurodiagnostic discovery. *IEEE Reviews in Biomedical Engineering*, 5, 60–73. <https://doi.org/10.1109/RBME.2012.2211076>
- Camerer, C. F., Dreber, A., Forsell, E., Ho, T.-H., Huber, J., Johannesson, M., Kirchler, M., Almenberg, J., Altmejd, A., Chan, T., Heikensten, E., Holzmeister, F., Imai, T., Isaksson, S., Nave, G., Pfeiffer, T., Razen, M., & Wu, H. (2016). Evaluating replicability of laboratory experiments in economics. *Science*, 351(6280), 1433–1436. <https://doi.org/10.1126/science.aaf0918>
- Camerer, C. F., Dreber, A., Holzmeister, F., Ho, T.-H., Huber, J., Johannesson, M., Kirchler, M., Nave, G., Nosek, B. A., Pfeiffer, T., Altmejd, A., Buttrick, N., Chan, T., Chen, Y., Forsell, E., Gampa, A., Heikensten, E., Hummer, L., Imai, T., ... Wu, H. (2018). Evaluating the replicability of social science experiments in Nature and Science between 2010 and 2015. *Nature Human Behaviour*, 2(9), 637–644. <https://doi.org/10.1038/s41562-018-0399-z>
- Cao, J., Zhao, Y., Shan, X., Wei, H.-L., Guo, Y., Chen, L., Erkoyuncu, J. A., & Sarrigiannis, P. G. (2022). Brain functional and effective connectivity based on electroencephalography recordings: A review. *Human Brain Mapping*, 43(2), 860–879. <https://doi.org/10.1002/hbm.25683>
- Carp, J. (2012). On the plurality of (methodological) worlds: estimating the analytic flexibility of FMRI experiments. *Frontiers in Neuroscience*, 6, 149. <https://doi.org/10.3389/fnins.2012.00149>
- Cheswick, B., Burch, H., & Branigan, S. (2000). Mapping and visualizing the internet. *Proceedings of the USENIX ... Annual Technical Conference. USENIX Technical Conference*. <https://www.usenix.org/conference/2000-usenix-annual-technical-conference/mapping-and-visualizing-internet>
- Cho, J. H., Vorwerk, J., Wolters, C. H., & Knösche, T. R. (2015). Influence of the head model on EEG and MEG source connectivity analyses. *NeuroImage*, 110, 60–77. <https://doi.org/10.1016/j.neuroimage.2015.01.043>
- Clark, T. D., Raby, G. D., Roche, D. G., Binning, S. A., Speers-Roesch, B., Jutfelt, F., & Sundin, J. (2020). Ocean acidification does not impair the behaviour of coral reef fishes. *Nature*, 577(7790), 370–375. <https://doi.org/10.1038/s41586-019-1903-y>
- Clayson, P. E., Baldwin, S. A., Rocha, H. A., & Larson, M. J. (2021). The data-processing multiverse of event-related potentials (ERPs): A roadmap for the optimization and standardization of ERP processing and reduction pipelines. *NeuroImage*, 245, 118712. <https://doi.org/10.1016/j.neuroimage.2021.118712>

- Colclough, G. L., Brookes, M. J., Smith, S. M., & Woolrich, M. W. (2015). A symmetric multivariate leakage correction for MEG connectomes. *NeuroImage*, 117, 439–448. <https://doi.org/10.1016/j.neuroimage.2015.03.071>
- Colclough, G. L., Woolrich, M. W., Tewarie, P. K., Brookes, M. J., Quinn, A. J., & Smith, S. M. (2016). How reliable are MEG resting-state connectivity metrics? *NeuroImage*, 138, 284–293. <https://doi.org/10.1016/j.neuroimage.2016.05.070>
- Damaraju, E., Allen, E. A., Belger, A., Ford, J. M., McEwen, S., Mathalon, D. H., Mueller, B. A., Pearlson, G. D., Potkin, S. G., Preda, A., Turner, J. A., Vaidya, J. G., van Erp, T. G., & Calhoun, V. D. (2014). Dynamic functional connectivity analysis reveals transient states of dysconnectivity in schizophrenia. *NeuroImage. Clinical*, 5, 298–308. <https://doi.org/10.1016/j.nicl.2014.07.003>
- Damoiseaux, J. S., Rombouts, S. A. R. B., Barkhof, F., Scheltens, P., Stam, C. J., Smith, S. M., & Beckmann, C. F. (2006). Consistent resting-state networks across healthy subjects. *Proceedings of the National Academy of Sciences of the United States of America*, 103(37), 13848–13853. <https://doi.org/10.1073/pnas.0601417103>
- de Pasquale, F., Corbetta, M., Betti, V., & Della Penna, S. (2018). Cortical cores in network dynamics. *NeuroImage*, 180(Pt B), 370–382. <https://doi.org/10.1016/j.neuroimage.2017.09.063>
- de Pasquale, F., Della Penna, S., Snyder, A. Z., Marzetti, L., Pizzella, V., Romani, G. L., & Corbetta, M. (2012). A cortical core for dynamic integration of functional networks in the resting human brain. *Neuron*, 74(4), 753–764. <https://doi.org/10.1016/j.neuron.2012.03.031>
- De Pasquale, F., Della Penna, S., Sporns, O., Romani, G. L., & Corbetta, M. (2016). A dynamic core network and global efficiency in the resting human brain. *Cerebral Cortex*, 26(10), 4015–4033. <https://academic.oup.com/cercor/article-abstract/26/10/4015/2196593>
- de Reus, M. A., & van den Heuvel, M. P. (2013). The parcellation-based connectome: limitations and extensions. *NeuroImage*, 80, 397–404. <https://doi.org/10.1016/j.neuroimage.2013.03.053>
- Desikan, R. S., Ségonne, F., Fischl, B., Quinn, B. T., Dickerson, B. C., Blacker, D., Buckner, R. L., Dale, A. M., Maguire, R. P., Hyman, B. T., Albert, M. S., & Killiany, R. J. (2006). An automated labeling system for subdividing the human cerebral cortex on MRI scans into gyral based regions of interest. *NeuroImage*, 31, 968–980. <https://doi.org/10.1016/j.neuroimage.2006.01.021>
- Destrieux, C., Fischl, B., Dale, A., & Halgren, E. (2010). Automatic parcellation of human cortical gyri and sulci using standard anatomical nomenclature. *NeuroImage*, 53(1), 1–15. <https://doi.org/10.1016/j.neuroimage.2010.06.010>
- Dinga, R., Schmaal, L., Penninx, B. W. J. H., van Tol, M. J., Veltman, D. J., van Velzen, L., Mennes, M., van der Wee, N. J. A., & Marquand, A. F. (2019). Evaluating the evidence for biotypes of depression: Methodological replication and extension of Drysdale et al. (2017). *NeuroImage. Clinical*, 22, 101796. <https://doi.org/10.1016/j.nicl.2019.101796>
- Elton, A., & Gao, W. (2015). Task-related modulation of functional connectivity variability and its behavioral correlations. *Human Brain Mapping*, 36(8), 3260–3272. <https://doi.org/10.1002/hbm.22847>
- Errington, T. M., Mathur, M., Soderberg, C. K., Denis, A., Perfito, N., Iorns, E., & Nosek, B. A. (2021). Investigating the replicability of preclinical cancer biology. *eLife*, 10. <https://doi.org/10.7554/eLife.71601>
- Fidler, F., & Wilcox, J. (2021). Reproducibility of Scientific Results. In E. N. Zalta (Ed.), *The Stanford Encyclopedia of Philosophy* (Summer 2021). Metaphysics Research Lab, Stanford University. <https://plato.stanford.edu/archives/sum2021/entries/scientific-reproducibility/>
- Finn, E. S., Shen, X., Scheinost, D., Rosenberg, M. D., Huang, J., Chun, M. M., Papademetris, X., & Constable, R. T. (2015). Functional connectome fingerprinting: identifying individuals using

- patterns of brain connectivity. *Nature Neuroscience*, 18(11), 1664–1671. <https://doi.org/10.1038/nn.4135>
- Fong, A. H. C., Yoo, K., Rosenberg, M. D., Zhang, S., Li, C.-S. R., Scheinost, D., Constable, R. T., & Chun, M. M. (2019). Dynamic functional connectivity during task performance and rest predicts individual differences in attention across studies. *NeuroImage*, 188, 14–25. <https://doi.org/10.1016/j.neuroimage.2018.11.057>
- Fornito, A., Zalesky, A., & Bullmore, E. T. (2010). Network scaling effects in graph analytic studies of human resting-state fMRI data. *Frontiers in Systems Neuroscience*, 4, 1–16. <https://doi.org/10.3389/fnsys.2010.00022>
- Fornito, A., Zalesky, A., & Bullmore, E. T. (2016). *Fundamentals of Brain Network Analysis*. Academic Press.
- Fox, J., & Weisberg, S. (2019). *An R Companion to Applied Regression (Third)*. Sage. <https://doi.org/10.1177/0049124105277200>
- Fox, M. D., & Raichle, M. E. (2007). Spontaneous fluctuations in brain activity observed with functional magnetic resonance imaging. *Nature Reviews Neuroscience*, 8(9), 700–711. <https://doi.org/10.1038/nrn2201>
- Fraschini, M., Demuru, M., Crobe, A., Marrosu, F., Stam, C. J., & Hillebrand, A. (2016). The effect of epoch length on estimated EEG functional connectivity and brain network organisation. *Journal of Neural Engineering*, 13(3), 1–10. <https://doi.org/10.1088/1741-2560/13/3/036015>
- Fraschini, M., Hillebrand, A., Demuru, M., Didaci, L., & Marcialis, G. L. (2015). An EEG-Based Biometric System Using Eigenvector Centrality in Resting State Brain Networks. *666 IEEE SIGNAL PROCESSING LETTERS*, 22(6), 666–670.
- Friston, K. J. (2011). Functional and Effective Connectivity: A Review. *Brain Connectivity*, 1(1), 13–36. <https://doi.org/10.1089/brain.2011.0008>
- Fuchs, M., Wagner, M., Köhler, T., & Wischmann, H. A. (1999). Linear and nonlinear current density reconstructions. *Journal of Clinical Neurophysiology: Official Publication of the American Electroencephalographic Society*, 16(3), 267–295. <https://doi.org/10.1097/00004691-199905000-00006>
- Ganapathiraju, M. K., Thahir, M., Handen, A., Sarkar, S. N., Sweet, R. A., Nimgaonkar, V. L., Loscher, C. E., Bauer, E. M., & Chaparala, S. (2016). Schizophrenia interactome with 504 novel protein–protein interactions. *Npj Schizophrenia*, 2(1), 1–10. <https://doi.org/10.1038/npj schz.2016.12>
- Geller, J., Thye, M., & Mirman, D. (2019). Estimating effects of graded white matter damage and binary tract disconnection on post-stroke language impairment. *NeuroImage*, 189, 248–257. <https://doi.org/10.1016/j.neuroimage.2019.01.020>
- Genon, S., Wensing, T., Reid, A., Hoffstaedter, F., Caspers, S., Grefkes, C., Nickl-Jockschat, T., & Eickhoff, S. B. (2017). Searching for behavior relating to grey matter volume in a-priori defined right dorsal premotor regions: Lessons learned. *NeuroImage*, 157, 144–156. <https://doi.org/10.1016/j.neuroimage.2017.05.053>
- Glatard, T., Lewis, L. B., Ferreira da Silva, R., Adalat, R., Beck, N., Lepage, C., Rioux, P., Rousseau, M.-E., Sherif, T., Deelman, E., Khalili-Mahani, N., & Evans, A. C. (2015). Reproducibility of neuroimaging analyses across operating systems. *Frontiers in Neuroinformatics*, 9, 12. <https://doi.org/10.3389/fninf.2015.00012>
- González, G. F., Molen, M. J. W. V. der, G.Zaric, Bonte, M., Tijms, J., Blomert, L., Stam, C. J., & Molen, M. W. V. der. (2016). Graph analysis of EEG resting state functional networks in dyslexic readers. *Clinical Neurophysiology Journal*, 127, 3165–3175. <https://doi.org/10.1016/j.clinph.2016.06.023>

- Goodman, S. N., Fanelli, D., & Ioannidis, J. P. A. (2016). What does research reproducibility mean? *Science Translational Medicine*, 8(341), 341ps12. <https://doi.org/10.1126/scitranslmed.aaf5027>
- Gould, J., & Kolb, W. L. (1964). *A dictionary of the social sciences*. New York : Free Press.
- Gramfort, A., Papadopoulou, T., Olivi, E., & Clerc, M. (2010). OpenMEEG: opensource software for quasistatic bioelectromagnetics. *Biomedical Engineering Online*, 9(45). <https://doi.org/10.1186/1475-925X-8-1>
- Gratton, C., Koller, J. M., Shannon, W., Greene, D. J., Maiti, B., Snyder, A. Z., Petersen, S. E., Perlmutter, J. S., & Campbell, M. C. (2018). Emergent Functional Network Effects in Parkinson Disease. *Cerebral Cortex*, 29(6), 2509–2523. <https://doi.org/10.1093/cercor/bhy121>
- Grave de Peralta Menendez, R., Gonzalez Andino, S., Lantz, G., Michel, C. M., & Landis, T. (2001). Noninvasive localization of electromagnetic epileptic activity. I. Method descriptions and simulations. *Brain Topography*, 14(2), 131–137. <https://doi.org/10.1023/a:1012944913650>
- Grech, R., Cassar, T., Muscat, J., Camilleri, K. P., Fabri, S. G., Zervakis, M., Xanthopoulos, P., Sakkalis, V., & Vanrumste, B. (2008). Review on solving the inverse problem in EEG source analysis. *Journal of Neuroengineering and Rehabilitation*, 5(25). <https://doi.org/10.1186/1743-0003-5-25>
- Greicius, M. D., Krasnow, B., Reiss, A. L., & Menon, V. (2003). Functional connectivity in the resting brain: a network analysis of the default mode hypothesis. *Proceedings of the National Academy of Sciences of the United States of America*, 100(1), 253–258. <https://doi.org/10.1073/pnas.0135058100>
- Gronenschild, E. H. B. M., Habets, P., Jacobs, H. I. L., Mengelers, R., Rozendaal, N., van Os, J., & Marcelis, M. (2012). The effects of FreeSurfer version, workstation type, and Macintosh operating system version on anatomical volume and cortical thickness measurements. *PloS One*, 7(6), e38234. <https://doi.org/10.1371/journal.pone.0038234>
- Grova, C., Daunizeau, J., Lina, J. M., Bénar, C. G., Benali, H., & Gotman, J. (2006). Evaluation of EEG localization methods using realistic simulations of interictal spikes. *NeuroImage*, 29, 734–753. <https://doi.org/10.1016/j.neuroimage.2005.08.053>
- Halder, T., Talwar, S., Jaiswal, A. K., & Banerjee, A. (2019). Quantitative evaluation in estimating sources underlying brain oscillations using current source density methods and beamformer approaches. *ENeuro*, 6(4), 1–14. <https://doi.org/10.1523/ENEURO.0170-19.2019>
- Hall, B. D., Liu, Y., Jansen, Y., Dragicevic, P., Chevalier, F., & Kay, M. (2022). A survey of tasks and visualizations in multiverse analysis reports. *Computer Graphics Forum: Journal of the European Association for Computer Graphics*, 41(1), 402–426. <https://doi.org/10.1111/cgf.14443>
- Hämäläinen, M. S., & Ilmoniemi, R. J. (1994). Interpreting magnetic fields of the brain: minimum norm estimates. *Medical & Biological Engineering & Computing*, 32, 35–42.
- Hassan, M., Benquet, P., Biraben, A., Berrou, C., Dufor, O., & Wendling, F. (2015). Dynamic reorganization of functional brain networks during picture naming. *Cortex; a Journal Devoted to the Study of the Nervous System and Behavior*, 73, 276–288. <https://doi.org/10.1016/j.cortex.2015.08.019>
- Hassan, M., Chaton, L., Benquet, P., Delval, A., Leroy, C., Plomhause, L., Moonen, A. J. H., Duits, A. A., Leentjens, A. F. G., van Kranen-Mastenbroek, V., Defebvre, L., Derambure, P., Wendling, F., & Dujardin, K. (2017). Functional connectivity disruptions correlate with cognitive phenotypes in Parkinson's disease. *NeuroImage Clinical*, 14, 591–601. <https://doi.org/10.1016/j.nicl.2017.03.002>

- Hassan, M., Dufor, O., Merlet, I., Berrou, C., & Wendling, F. (2014). EEG source connectivity analysis: from dense array recordings to brain networks. *PloS One*, 9(8), e105041. <https://doi.org/10.1371/journal.pone.0105041>
- Hassan, M., Merlet, I., Mheich, A., Kabbara, A., Biraben, A., Nica, A., & Wendling, F. (2017). Identification of Interictal Epileptic Networks from Dense-EEG. *Brain Topography*, 30(1), 60–76. <https://doi.org/10.1007/s10548-016-0517-z>
- Hassan, M., & Wendling, F. (2018). Electroencephalography Source Connectivity: Aiming for High Resolution of Brain Networks in Time and Space. *IEEE Signal Processing Magazine*, 35(3), 81–96. <https://doi.org/10.1109/MSP.2017.2777518>
- Hayasaka, S., & Laurienti, P. J. (2010). Comparison of characteristics between region-and voxel-based network analyses in resting-state fMRI data. *NeuroImage*, 50, 499–508. <https://doi.org/10.1016/j.neuroimage.2009.12.051>
- He, B., Sohrabpour, A., Brown, E., & Liu, Z. (2018). Electrophysiological Source Imaging: A Noninvasive Window to Brain Dynamics. *Annual Review of Biomedical Engineering*, 20, 171–196. <https://doi.org/10.1146/annurev-bioeng-062117-120853>
- Hedrich, T., Pellegrino, G., Kobayashi, E., Lina, J. M., & Grova, C. (2017). Comparison of the spatial resolution of source imaging techniques in high-density EEG and MEG. *NeuroImage*, 157, 531–544. <https://doi.org/10.1016/j.neuroimage.2017.06.022>
- Hipp, J. F., Hawellek, D. J., Corbetta, M., Siegel, M., & Engel, A. K. (2012). Large-scale cortical correlation structure of spontaneous oscillatory activity. *Nature Neuroscience*, 15(6), 884–890. <https://doi.org/10.1038/nn.3101>
- Hothorn, T., Bretz, F., & Westfall, P. (2008). Simultaneous inference in general parametric models. *Biometrical Journal. Biometrische Zeitschrift*, 50(3), 346–363. <https://doi.org/10.1002/bimj.200810425>
- Hunter. (2007). Matplotlib: A 2D Graphics Environment. *Computing in Science & Engineering*, 9, 90–95. <https://doi.org/10.1109/MCSE.2007.55>
- Ioannidis, J. P. A. (2005). Why most published research findings are false. *PLoS Medicine*, 2(8), e124. <https://doi.org/10.1371/journal.pmed.0020124>
- Iwasaki, M., Pestana, E., Burgess, R. C., Lüders, H. O., Shamoto, H., & Nakasato, N. (2005). Detection of epileptiform activity by human interpreters: blinded comparison between electroencephalography and magnetoencephalography. *Epilepsia*, 46(1), 59–68. <https://doi.org/10.1111/j.0013-9580.2005.21104.x>
- Jiao, Z., Wang, H., Cai, M., Cao, Y., Zou, L., & Wang, S. (2020). Rich club characteristics of dynamic brain functional networks in resting state. *Multimedia Tools and Applications*, 79(21), 15075–15093. <https://doi.org/10.1007/s11042-018-6424-4>
- Jimenez, A. M., Riedel, P., Lee, J., Reavis, E. A., & Green, M. F. (2019). Linking resting-state networks and social cognition in schizophrenia and bipolar disorder. *Human Brain Mapping*, 40(16), 4703–4715. <https://doi.org/10.1002/hbm.24731>
- Jockwitz, C., Caspers, S., Lux, S., Eickhoff, S. B., Jütten, K., Lenzen, S., Moebus, S., Pundt, N., Reid, A., Hoffstaedter, F., Jöckel, K.-H., Erbel, R., Cichon, S., Nöthen, M. M., Shah, N. J., Zilles, K., & Amunts, K. (2017). Influence of age and cognitive performance on resting-state brain networks of older adults in a population-based cohort. *Cortex; a Journal Devoted to the Study of the Nervous System and Behavior*, 89, 28–44. <https://doi.org/10.1016/j.cortex.2017.01.008>
- Kabbara, A., Eid, H., El Falou, W., Khalil, M., Wendling, F., & Hassan, M. (2018). Reduced integration and improved segregation of functional brain networks in Alzheimer's disease. *Journal of Neural Engineering*, 15(2), 026023. <https://doi.org/10.1088/1741-2552/aaaa76>

- Kabbara, A., El Falou, W., Khalil, M., Wendling, F., & Hassan, M. (2017). The dynamic functional core network of the human brain at rest. *Scientific Reports*, 7(1), 2936. <https://doi.org/10.1038/s41598-017-03420-6>
- Kabbara, A., Paban, V., & Hassan, M. (2021). The dynamic modular fingerprints of the human brain at rest. *NeuroImage*, 227, 117674. <https://doi.org/10.1016/j.neuroimage.2020.117674>
- Kabbara, Aya, Forde, N., Maumet, C., & Hassan, M. (2022). Successful reproduction of a large EEG study across software packages. In *bioRxiv* (p. 2022.08.03.502683). <https://doi.org/10.1101/2022.08.03.502683>
- Kabbara, Aya, Robert, G., Khalil, M., Verin, M., Benquet, P., & Hassan, M. (2022). An electroencephalography connectome predictive model of major depressive disorder severity. *Scientific Reports*, 12(1), 6816. <https://doi.org/10.1038/s41598-022-10949-8>
- Keller, J. B., Hedden, T., Thompson, T. W., Anteraper, S. A., Gabrieli, J. D. E., & Whitfield-Gabrieli, S. (2015). Resting-state anticorrelations between medial and lateral prefrontal cortex: association with working memory, aging, and individual differences. *Cortex; a Journal Devoted to the Study of the Nervous System and Behavior*, 64, 271–280. <https://doi.org/10.1016/j.cortex.2014.12.001>
- Kerr, N. L. (1998). HARKing: hypothesizing after the results are known. *Personality and Social Psychology Review: An Official Journal of the Society for Personality and Social Psychology, Inc*, 2(3), 196–217. https://doi.org/10.1207/s15327957pspr0203_4
- Kharabian Masouleh, S., Eickhoff, S. B., Hoffstaedter, F., Genon, S., & Alzheimer's Disease Neuroimaging Initiative. (2019). Empirical examination of the replicability of associations between brain structure and psychological variables. *ELife*, 8. <https://doi.org/10.7554/eLife.43464>
- Kitzbichler, M. G., Henson, R. N. A., Smith, M. L., Nathan, P. J., & Bullmore, E. T. (2011). Cognitive effort drives workspace configuration of human brain functional networks. *The Journal of Neuroscience: The Official Journal of the Society for Neuroscience*, 31(22), 8259–8270. <https://doi.org/10.1523/JNEUROSCI.0440-11.2011>
- Krienen, F. M., Yeo, B. T. T., & Buckner, R. L. (2014). Reconfigurable task-dependent functional coupling modes cluster around a core functional architecture. *Philosophical Transactions of the Royal Society of London. Series B, Biological Sciences*, 369(1653). <https://doi.org/10.1098/rstb.2013.0526>
- Lachaux, J.-P., Rodriguez, E., Le Van Quyen, M., Lutz, A., Martinerie, J., & Varela, F. J. (2000). Studying Single-Trials of Phase Synchronous Activity in the Brain. *International Journal of Bifurcation and Chaos in Applied Sciences and Engineering*, 10(10), 2429–2439. <https://doi.org/10.1142/s0218127400001560>
- Lantz, G., Grave de Peralta Menendez, R., Gonzalez Andino, S., & Michel, C. M. (2001). Noninvasive localization of electromagnetic epileptic activity. II. Demonstration of sublobar accuracy in patients with simultaneous surface and depth recordings. *Brain Topography*, 14(2), 139–147. <https://doi.org/10.1023/a:1012996930489>
- Lantz, Goran, Grave de Peralta, R., Spinelli, L., Seeck, M., & Michel, C. M. (2003). Epileptic source localization with high density EEG: How many electrodes are needed? *Clinical Neurophysiology: Official Journal of the International Federation of Clinical Neurophysiology*, 114(1), 63–69. [https://doi.org/10.1016/S1388-2457\(02\)00337-1](https://doi.org/10.1016/S1388-2457(02)00337-1)
- Laureys, Peigneux, & Goldman. (2002). Brain imaging. *Biological Psychiatry*, 155–166.
- Lin, F. H., Witzel, T., Ahlfors, S. P., Stufflebeam, S. M., Belliveau, J. W., & Hämäläinen, M. S. (2006). Assessing and improving the spatial accuracy in MEG source localization by depth-weighted minimum-norm estimates. *NeuroImage*, 31, 160–171. <https://doi.org/10.1016/j.neuroimage.2005.11.054>

- Luckhoo, H., Hale, J. R., Stokes, M. G., Nobre, A. C., Morris, P. G., Brookes, M. J., & Woolrich, M. W. (2012). Inferring task-related networks using independent component analysis in magnetoencephalography. *NeuroImage*, 62(1), 530–541. <https://doi.org/10.1016/j.neuroimage.2012.04.046>
- Mahjoory, K., Nikulin, V. V., Botrel, L., Linkenkaer-Hansen, K., Fato, M. M., & Haufe, S. (2017). Consistency of EEG source localization and connectivity estimates. *NeuroImage*, 152, 590–601. <https://doi.org/10.1016/j.neuroimage.2017.02.076>
- Marquetand, J., Vannoni, S., Carboni, M., Li Hegner, Y., Stier, C., Braun, C., & Focke, N. K. (2019). Reliability of Magnetoencephalography and High-Density Electroencephalography Resting-State Functional Connectivity Metrics. *Brain Connectivity*, 9(7), 539–553. <https://doi.org/10.1089/brain.2019.0662>
- Matamalas, J. T., Arenas, A., & Gómez, S. (2018). Effective approach to epidemic containment using link equations in complex networks. *Science Advances*, 4(12), eaau4212. <https://doi.org/10.1126/sciadv.aau4212>
- Matlab. (2018). *9.5.0.944444 (R2018b)*. The MathWorks Inc.
- McNerney, J., Fath, B. D., & Silverberg, G. (2013). Network structure of inter-industry flows. *Physica A: Statistical Mechanics and Its Applications*, 392(24), 6427–6441. <https://doi.org/10.1016/j.physa.2013.07.063>
- Mehrkanon, S., Breakspear, M., Britz, J., & Boonstra, T. W. (2014). Intrinsic Coupling Modes in Source-Reconstructed Electroencephalography. *Brain Connectivity*, 4(10), 812–825. <https://doi.org/10.1089/brain.2014.0280>
- Mheich, A., Wendling, F., & Hassan, M. (2020). Brain network similarity: Methods and applications. *Network Neuroscience*, 4(3), 507–527. https://doi.org/10.1162/netn_a_00133
- Michel, C. M., & Brunet, D. (2019). EEG Source Imaging: A Practical Review of the Analysis Steps. *Frontiers in Neurology*, 10, 325. <https://doi.org/10.3389/fneur.2019.00325>
- Michel, C. M., Murray, M. M., Lantz, G., Gonzalez, S., Spinelli, L., & Grave de Peralta, R. (2004). EEG source imaging. *Clinical Neurophysiology: Official Journal of the International Federation of Clinical Neurophysiology*, 115(10), 2195–2222. <https://doi.org/10.1016/j.clinph.2004.06.001>
- Müller, V. I., Cieslik, E. C., Serbanescu, I., Laird, A. R., Fox, P. T., & Eickhoff, S. B. (2017). Altered Brain Activity in Unipolar Depression Revisited: Meta-analyses of Neuroimaging Studies. *JAMA Psychiatry*, 74(1), 47–55. <https://doi.org/10.1001/jamapsychiatry.2016.2783>
- Munafò, M. R., Chambers, C. D., Collins, A. M., Fortunato, L., & Macleod, M. R. (2020). Research Culture and Reproducibility. *Trends in Cognitive Sciences*, 24(2), 91–93. <https://doi.org/10.1016/j.tics.2019.12.002>
- Munafò, M. R., Nosek, B. A., Bishop, D. V. M., Button, K. S., Chambers, C. D., du Sert, N. P., Simonsohn, U., Wagenmakers, E.-J., Ware, J. J., & Ioannidis, J. P. A. (2017). A manifesto for reproducible science. *Nature Human Behaviour*, 1, 0021. <https://doi.org/10.1038/s41562-016-0021>
- Natl. Acad. Sci. Eng. Med. (2019). *Reproducibility and Replicability in Science*. DC: Natl. Acad. Press.
- Nave, K., Hannon, E., & Snyder, J. S. (2022). Replication and extension of Nozaradan, Peretz, Missal and Mouraux (2011). In <https://osf.io/rpvde/>. Open Science Framework. <https://doi.org/10.17605/OSF.IO/RPVDE>
- Nieuwland, M. S., Politzer-Ahles, S., Heyselaar, E., Segaert, K., Darley, E., Kazanina, N., Von Grebmer Zu Wolfsturn, S., Bartolozzi, F., Kogan, V., Ito, A., Mézière, D., Barr, D. J., Rousselet, G. A., Ferguson, H. J., Busch-Moreno, S., Fu, X., Tuomainen, J., Kulakova, E., Husband, E. M., ... Huettig, F. (2018). Large-scale replication study reveals a limit on probabilistic prediction in language comprehension. *eLife*, 7. <https://doi.org/10.7554/eLife.33468>

- Niso, G., Botvinik-Nezer, R., Appelhoff, S., De La Vega, A., Esteban, O., Etzel, J. A., Finc, K., Ganz, M., Gau, R., Halchenko, Y. O., & al., E. (2022). *Open and reproducible neuroimaging: from study inception to publication*. <https://doi.org/10.31219/osf.io/pu5vb>
- Niso, G., Krol, L. R., Combrisson, E., Dubarry, A. S., Elliott, M. A., François, C., Héjja-Brichard, Y., Herbst, S. K., Jerbi, K., Kovic, V., Lehongre, K., Luck, S. J., Mercier, M., Mosher, J. C., Pavlov, Y. G., Puce, A., Schettino, A., Schön, D., Sinnott-Armstrong, W., ... Chaumon, M. (2022). Good scientific practice in EEG and MEG research: Progress and perspectives. *NeuroImage*, 257, 119056. <https://doi.org/10.1016/j.neuroimage.2022.119056>
- Nørgaard, M., Ganz, M., Svarer, C., Frokjaer, V. G., Greve, D. N., Strother, S. C., & Knudsen, G. M. (2020). Different preprocessing strategies lead to different conclusions: A [11C]DASB-PET reproducibility study. *Journal of Cerebral Blood Flow and Metabolism: Official Journal of the International Society of Cerebral Blood Flow and Metabolism*, 40(9), 1902–1911. <https://doi.org/10.1177/0271678X19880450>
- Nosek, B. A., Alter, G., Banks, G. C., Borsboom, D., Bowman, S. D., Breckler, S. J., Buck, S., Chambers, C. D., Chin, G., Christensen, G., Contestabile, M., Dafoe, A., Eich, E., Freese, J., Glennerster, R., Goroff, D., Green, D. P., Hesse, B., Humphreys, M., ... Yarkoni, T. (2015). Promoting an open research culture. *Science*, 348(6242), 1422–1425. <https://doi.org/10.1126/science.aab2374>
- Nosek, Brian A., Hardwicke, T. E., Moshontz, H., Allard, A., Corker, K. S., Dreber, A., Fidler, F., Hilgard, J., Kline Struhl, M., Nijtten, M. B., Rohrer, J. M., Romero, F., Scheel, A. M., Scherer, L. D., Schönbrodt, F. D., & Vazire, S. (2022). Replicability, Robustness, and Reproducibility in Psychological Science. *Annual Review of Psychology*, 73, 719–748. <https://doi.org/10.1146/annurev-psych-020821-114157>
- Nuzzo. (2014). Statistical errors: P values, the 'gold standard' of statistical validity, are not as reliable as many scientists assume. *Nature*. <https://go.gale.com/ps/i.do?id=GALE%7CA362064378&sid=googleScholar&v=2.1&it=r&lin=kaccess=abs&issn=00280836&p=HRCA&sw=w>
- O'Neill, G. C., Tewarie, P. K., Colclough, G. L., Gascoyne, L. E., Hunt, B. A. E., Morris, P. G., Woolrich, M. W., & Brookes, M. J. (2017). Measurement of dynamic task related functional networks using MEG. *NeuroImage*, 146, 667–678. <https://doi.org/10.1016/j.neuroimage.2016.08.061>
- Oostenveld, R., Fries, P., Maris, E., & Schoffelen, J. M. (2011). FieldTrip: Open source software for advanced analysis of MEG, EEG, and invasive electrophysiological data. *Computational Intelligence and Neuroscience*, 2011. <https://doi.org/10.1155/2011/156869>
- Open Science Collaboration. (2015). Estimating the reproducibility of psychological science. *Science*, 349(6251), aac4716. <https://doi.org/10.1126/science.aac4716>
- Palva, J. M., Wang, S. H., Palva, S., Zhigalov, A., Monto, S., Brookes, M. J., Schoffelen, J.-M., & Jerbi, K. (2018). Ghost interactions in MEG/EEG source space: A note of caution on inter-areal coupling measures. *NeuroImage*, 173, 632–643. <https://doi.org/10.1016/j.neuroimage.2018.02.032>
- Palva, S., & Palva, J. M. (2012). Discovering oscillatory interaction networks with M/EEG: challenges and breakthroughs. *Trends in Cognitive Sciences*, 16(4), 219–230. <https://doi.org/10.1016/j.tics.2012.02.004>
- Park, H. J., & Friston, K. (2013). Structural and functional brain networks: From connections to cognition. *Science*, 342(6158). <https://doi.org/10.1126/science.1238411>
- Pascual-Marqui, R. D. (2007). *Discrete, 3D distributed, linear imaging methods of electric neuronal activity. Part 1: exact, zero error localization*. <http://arxiv.org/abs/0710.3341>

- Patel, C. J., Burford, B., & Ioannidis, J. P. A. (2015). Assessment of vibration of effects due to model specification can demonstrate the instability of observational associations. *Journal of Clinical Epidemiology*, 68(9), 1046–1058. <https://doi.org/10.1016/j.jclinepi.2015.05.029>
- Pavlov, Y. G., Adamian, N., Appelhoff, S., Arvaneh, M., Benwell, C. S. Y., Beste, C., Bland, A. R., Bradford, D. E., Bublitzky, F., Busch, N. A., Clayson, P. E., Cruse, D., Czeszumski, A., Dreber, A., Dumas, G., Ehinger, B., Ganis, G., He, X., Hinojosa, J. A., ... Mushtaq, F. (2021). #EEGManyLabs: Investigating the replicability of influential EEG experiments. *Cortex; a Journal Devoted to the Study of the Nervous System and Behavior*, 144, 213–229. <https://doi.org/10.1016/j.cortex.2021.03.013>
- Pedroni, A., Bahreini, A., & Langer, N. (2019). Automagic: Standardized preprocessing of big EEG data. *NeuroImage*, 200, 460–473. <https://doi.org/10.1016/j.neuroimage.2019.06.046>
- Pereda, E., Quiroga, R. Q., & Bhattacharya, J. (2005). Nonlinear multivariate analysis of neurophysiological signals. *Progress in Neurobiology*, 77, 1–37. <https://doi.org/10.1016/j.pneurobio.2005.10.003>
- Pernet, C., Garrido, M. I., Gramfort, A., Maurits, N., Michel, C. M., Pang, E., Salmelin, R., Schoffelen, J. M., Valdes-Sosa, P. A., & Puce, A. (2020). Issues and recommendations from the OHBM COBIDAS MEEG committee for reproducible EEG and MEG research. *Nature Neuroscience*, 23(12), 1473–1483. <https://doi.org/10.1038/s41593-020-00709-0>
- Pernet, C., & Poline, J.-B. (2015). Improving functional magnetic resonance imaging reproducibility. *GigaScience*, 4, 15. <https://doi.org/10.1186/s13742-015-0055-8>
- Perrin, S. (2014). Preclinical research: Make mouse studies work. *Nature*, 507(7493), 423–425. <https://doi.org/10.1038/507423a>
- Poldrack, R. A., Baker, C. I., Durne, J., Gorgolewski, K. J., Matthews, P. M., Munafò, M. R., Nichols, T. E., Poline, J.-B., Vul, E., & Yarkoni, T. (2017). Scanning the horizon: towards transparent and reproducible neuroimaging research. *Nature Reviews Neuroscience*, 18(2), 115–126. <https://doi.org/10.1038/nrn.2016.167>
- Poldrack, R. A., Whitaker, K., & Kennedy, D. (2020). Introduction to the special issue on reproducibility in neuroimaging. *NeuroImage*, 218, 116357. <https://doi.org/10.1016/j.neuroimage.2019.116357>
- Ponten, S. C., Douw, L., Bartolomei, F., Reijneveld, J. C., & Stam, C. J. (2009). Indications for network regularization during absence seizures : Weighted and unweighted graph theoretical analyses. *Experimental Neurology*, 217, 197–204. <https://doi.org/10.1016/j.expneurol.2009.02.001>
- Prinz, F., Schlange, T., & Asadullah, K. (2011). Believe it or not: how much can we rely on published data on potential drug targets? *Nature Reviews Drug Discovery*, 10(9), 712–712. <https://doi.org/10.1038/nrd3439-c1>
- R Core Team. (2020). *R: A Language and Environment for Statistical Computing*. R Foundation for Statistical Computing. <https://www.R-project.org/>
- Radner, H. (1996). *In and About the World: Philosophical Studies of Science and Technology*. NY: SUNY Press.
- Raichle, M. E., MacLeod, A. M., Snyder, A. Z., Powers, W. J., Gusnard, D. A., & Shulman, G. L. (2001). A default mode of brain function. *Proceedings of the National Academy of Sciences of the United States of America*, 98(2), 676–682. <https://doi.org/10.1073/pnas.98.2.676>
- Raichle, M. E., & Snyder, A. Z. (2007). A default mode of brain function: A brief history of an evolving idea. *NeuroImage*, 37(4), 1083–1090. <https://doi.org/10.1016/j.neuroimage.2007.02.041>
- Ritchie, S. (2020). *Science Fiction: Exposing Fraud, Bias, Negligence and Hype in Science*. The Bodley Head.

- Robbins, K. A., Tournay, J., Mullen, T., Kothe, C., & Bigdely-Shamlo, N. (2020). How Sensitive Are EEG Results to Preprocessing Methods: A Benchmarking Study. *IEEE Transactions on Neural Systems and Rehabilitation Engineering: A Publication of the IEEE Engineering in Medicine and Biology Society*, 28(5), 1081–1090. <https://doi.org/10.1109/TNSRE.2020.2980223>
- Rosenthal, R. (1979). The file drawer problem and tolerance for null results. *Psychological Bulletin*, 86(3), 638–641. <https://doi.org/10.1037/0033-2909.86.3.638>
- Schilling, K. G., Rheault, F., Petit, L., Hansen, C. B., Nath, V., Yeh, F.-C., Girard, G., Barakovic, M., Rafael-Patino, J., Yu, T., Fischl-Gomez, E., Pizzolato, M., Ocampo-Pineda, M., Schiavi, S., Canales-Rodríguez, E. J., Daducci, A., Granziera, C., Innocenti, G., Thiran, J.-P., ... Descoteaux, M. (2021). Tractography dissection variability: What happens when 42 groups dissect 14 white matter bundles on the same dataset? *NeuroImage*, 243, 118502. <https://doi.org/10.1016/j.neuroimage.2021.118502>
- Schmidt, S. (2009). Shall we Really do it Again? The Powerful Concept of Replication is Neglected in the Social Sciences. *Review of General Psychology: Journal of Division 1, of the American Psychological Association*, 13(2), 90–100. <https://doi.org/10.1037/a0015108>
- Schoffelen, J.-M., & Gross, J. (2009). Source Connectivity Analysis With MEG and EEG. *Human Brain Mapping*, 30, 1857–1865. <https://doi.org/10.1002/hbm.20745>
- Shapin, S., & Schaffer, S. (1985). *Leviathan and the air-pump. Hobbes, Boyle, and the experimental life.* NJ: Princeton University Press.
- Sheline, Y. I., & Raichle, M. E. (2013). Resting state functional connectivity in preclinical Alzheimer's disease. *Biological Psychiatry*, 74(5), 340–347. <https://doi.org/10.1016/j.biopsych.2012.11.028>
- Shen, X., Cox, S. R., Adams, M. J., Howard, D. M., Lawrie, S. M., Ritchie, S. J., Bastin, M. E., Deary, I. J., McIntosh, A. M., & Whalley, H. C. (2018). Resting-State Connectivity and Its Association With Cognitive Performance, Educational Attainment, and Household Income in the UK Biobank. *Biological Psychiatry: Cognitive Neuroscience and Neuroimaging*, 3(10), 878–886. <https://doi.org/10.1016/j.bpsc.2018.06.007>
- Shine, J. M., Bissett, P. G., Bell, P. T., Koyejo, O., Balsters, J. H., Gorgolewski, K. J., Moodie, C. A., & Poldrack, R. A. (2016). The Dynamics of Functional Brain Networks: Integrated Network States during Cognitive Task Performance. *Neuron*, 92(2), 544–554. <https://doi.org/10.1016/j.neuron.2016.09.018>
- Shirazi, S. Y., & Huang, H. J. (2019). More Reliable EEG Electrode Digitizing Methods Can Reduce Source Estimation Uncertainty, but Current Methods Already Accurately Identify Brodmann Areas. *Frontiers in Neuroscience*, 13, 1159. <https://doi.org/10.3389/fnins.2019.01159>
- Shirer, W. R., Ryali, S., Rykhlevskaia, E., Menon, V., & Greicius, M. D. (2012). Decoding Subject-Driven Cognitive States with Whole-Brain Connectivity Patterns. *Cerebral Cortex*, 22(1), 158–165. <https://doi.org/10.1093/cercor/bhr099>
- Silberzahn, R., Uhlmann, E. L., Martin, D. P., Anselmi, P., Aust, F., Awtrey, E., Bahník, Š., Bai, F., Bannard, C., Bonnier, E., Carlsson, R., Cheung, F., Christensen, G., Clay, R., Craig, M. A., Dalla Rosa, A., Dam, L., Evans, M. H., Flores Cervantes, I., ... Nosek, B. A. (2018). Many Analysts, One Data Set: Making Transparent How Variations in Analytic Choices Affect Results. *Advances in Methods and Practices in Psychological Science*, 1(3), 337–356. <https://doi.org/10.1177/2515245917747646>
- Simmons, J. P., Nelson, L. D., & Simonsohn, U. (2011). False-positive psychology: undisclosed flexibility in data collection and analysis allows presenting anything as significant. *Psychological Science*, 22(11), 1359–1366. <https://doi.org/10.1177/0956797611417632>
- Simonsohn, U., Nelson, L. D., & Simmons, J. P. (2014). P-curve: a key to the file-drawer. *Journal of Experimental Psychology: General*, 143(2), 534–547. <https://doi.org/10.1037/a0033242>

- Simonsohn, U., Simmons, J. P., & Nelson, L. D. (2019). Specification Curve: Descriptive and Inferential Statistics on All Reasonable Specifications. In <https://papers.ssrn.com/sol3/papers>. <https://doi.org/10.2139/ssrn.2694998>
- Singh, K. D. (2012). NeuroImage Which “neural activity” do you mean? fMRI, MEG, oscillations and neurotransmitters. *NeuroImage*, 62, 1121–1130. <https://doi.org/10.1016/j.neuroimage.2012.01.028>
- Sohrabi, A., Lu, Y., Kankirawatana, P., Blount, J., Kim, H., & He, B. (2015). Effect of EEG electrode number on epileptic source localization in pediatric patients. *Clinical Neurophysiology: Official Journal of the International Federation of Clinical Neurophysiology*, 126, 472–480. <https://doi.org/10.1016/j.clinph.2014.05.038>
- Song, J., Davey, C., Poulsen, C., Luu, P., Turovets, S., Anderson, E., Li, K., & Tucker, D. (2015). EEG source localization: Sensor density and head surface coverage. *Journal of Neuroscience Methods*, 256, 9–21. <https://doi.org/10.1016/j.jneumeth.2015.08.015>
- Šoškić, A., Styles, S. J., Kappenman, E. S., & Kovac, V. (2022). *Garden of forking paths in ERP research – effects of varying pre-processing and analysis steps in an N400 experiment*. <https://doi.org/10.31234/osf.io/8rjh>
- Soto, C. J. (2019). How Replicable Are Links Between Personality Traits and Consequential Life Outcomes? The Life Outcomes of Personality Replication Project. *Psychological Science*, 30(5), 711–727. <https://doi.org/10.1177/0956797619831612>
- Sporns, O. (2014). *Networks of the Brain*. The MIT press.
- Sporns, O., Chialvo, D. R., Kaiser, M., & Hilgetag, C. C. (2004). Organization, development and function of complex brain networks. *Trends in Cognitive Sciences*, 8(9), 418–425. <https://doi.org/10.1016/j.tics.2004.07.008>
- Srinivasan, R., Tucker, D. M., & Murias, M. (1998). Estimating the spatial Nyquist of the human EEG. *Behavior Research Methods, Instruments, & Computers: A Journal of the Psychonomic Society, Inc*, 30(1), 8–19. <https://doi.org/10.3758/BF03209412>
- Stam, C. J., Nolte, G., & Daffertshofer, A. (2007). Phase lag index: Assessment of functional connectivity from multi channel EEG and MEG with diminished bias from common sources. *Human Brain Mapping*, 28, 1178–1193. <https://doi.org/10.1002/hbm.20346>
- Stanley, M. L., Moussa, M. N., Paolini, B. M., Lyday, R. G., Burdette, J. H., & Laurienti, P. J. (2013). Defining nodes in complex brain networks. *Frontiers in Computational Neuroscience*, 7, 169. <https://doi.org/10.3389/fncom.2013.00169>
- Steegen, S., Tuerlinckx, F., Gelman, A., & Vanpaemel, W. (2016). Increasing Transparency Through a Multiverse Analysis. *Perspectives on Psychological Science: A Journal of the Association for Psychological Science*, 11(5), 702–712. <https://doi.org/10.1177/1745691616658637>
- Sterling, T. D. (1959). Publication Decisions and their Possible Effects on Inferences Drawn from Tests of Significance—or Vice Versa. *Journal of the American Statistical Association*, 54(285), 30–34. <https://doi.org/10.1080/01621459.1959.10501497>
- Steward, O., Popovich, P. G., Dietrich, W. D., & Kleitman, N. (2012). Replication and reproducibility in spinal cord injury research. *Experimental Neurology*, 233(2), 597–605. <https://doi.org/10.1016/j.expneurol.2011.06.017>
- Tadel, F., Baillet, S., Mosher, J. C., Pantazis, D., & Leahy, R. M. (2011). Brainstorm: A user-friendly application for MEG/EEG analysis. *Computational Intelligence and Neuroscience*, 2011. <https://doi.org/10.1155/2011/879716>
- Tait, L., Özkan, A., Szul, M. J., & Zhang, J. (2021). A systematic evaluation of source reconstruction of resting MEG of the human brain with a new high-resolution atlas: Performance, precision, and parcellation. *Human Brain Mapping*, 42(14), 4685–4707. <https://doi.org/10.1002/hbm.25578>

- Uhlhaas, P. J., & Singer, W. (2006). Neural Synchrony in Brain Disorders : Relevance for Cognitive Dysfunctions and Pathophysiology. *Neuron*, 52, 155–168. <https://doi.org/10.1016/j.neuron.2006.09.020>
- Urigüen, J. A., & Garcia-Zapirain, B. (2015). EEG artifact removal - State-of-the-art and guidelines. *Journal of Neural Engineering*, 12, 1–23. <https://doi.org/10.1088/1741-2560/12/3/031001>
- van den Heuvel, M., Mandl, R., & Pol, H. H. (2008). Normalized cut group clustering of resting-state fMRI data. *PloS One*, 3(4). <https://doi.org/10.1371/journal.pone.0002001>
- van den Heuvel, M. P., de Lange, S. C., Zalesky, A., Seguin, C., Yeo, B. T. T., & Schmidt, R. (2017). Proportional thresholding in resting-state fMRI functional connectivity networks and consequences for patient-control connectome studies: Issues and recommendations. *NeuroImage*, 152, 437–449. <https://doi.org/10.1016/j.neuroimage.2017.02.005>
- Van Essen, D. C., Smith, S. M., Barch, D. M., Behrens, T. E. J., Yacoub, E., Ugurbil, K., & WU-Minn HCP Consortium. (2013). The WU-Minn Human Connectome Project: an overview. *NeuroImage*, 80, 62–79. <https://doi.org/10.1016/j.neuroimage.2013.05.041>
- Van Veen, B. D., van Drongelen, W., Yuchtman, M., & Suzuki, A. (1997). Localization of brain electrical activity via linearly constrained minimum variance spatial filtering. *IEEE Transactions on Bio-Medical Engineering*, 44(9), 867–880. <https://doi.org/10.1109/10.623056>
- Vecchio, F., Miraglia, F., Marra, C., Quaranta, D., Vita, M., Bramanti, P., & Rossini, P. M. (2014). Human brain networks in cognitive decline: a graph theoretical analysis of cortical connectivity from EEG data. *Journal of Alzheimer's Disease: JAD*, 41(1), 113–127. <https://doi.org/10.3233/JAD-132087>
- Vinck, M., Oostenveld, R., Van Wingerden, M., Battaglia, F., & Pennartz, C. M. A. (2011). An improved index of phase-synchronization for electrophysiological data in the presence of volume-conduction, noise and sample-size bias. *NeuroImage*, 55(4), 1548–1565. <https://doi.org/10.1016/j.neuroimage.2011.01.055>
- Vourkas, M., Karakonstantaki, E., Simos, P. G., Tsirka, V., Antonakakis, M., Vamvoukas, M., Stam, C., & Dimitriadis, S. (2014). Simple and difficult mathematics in children : A minimum spanning tree EEG network analysis. *Neuroscience Letters*. <https://doi.org/10.1016/j.neulet.2014.05.048>
- Wa, C. (1983). *IFCN recommendations for the practice of clinical neurophysiology* Amsterdam. New York, NY: Elsevier.
- Wang, H. E., Bénar, C. G., Quilichini, P. P., Friston, K. J., Jirsa, V. K., & Bernard, C. (2014). A systematic framework for functional connectivity measures. *Frontiers in Neuroscience*, 8. <https://doi.org/10.3389/fnins.2014.00405>
- Wang, J., Wang, L., Zang, Y., Yang, H., Tang, H., Gong, Q., Chen, Z., Zhu, C., & He, Y. (2009). Parcellation-dependent small-world brain functional networks: A resting-state fmri study. *Human Brain Mapping*, 30, 1511–1523. <https://doi.org/10.1002/hbm.20623>
- Waskom, M. (2021). seaborn: statistical data visualization. *Journal of Open Source Software*, 6(60), 3021. <https://doi.org/10.21105/joss.03021>
- Wendling, F., Ansari-Asl, K., Bartolomei, F., & Senhadji, L. (2009). From EEG signals to brain connectivity: A model-based evaluation of interdependence measures. *Journal of Neuroscience Methods*, 183, 9–18. <https://doi.org/10.1016/j.jneumeth.2009.04.021>
- Whiteford, K. L., Baltzell, L. S., Cooper, J. K., Irsik, V. C., Irvine, A., Mesik, J., Nolan, T., Oakes, B., Reed, A., Schrlau, A. E., & Others. (2019). *Association of musical training with auditory and speech neural coding and perception*. osf.io. <https://osf.io/pxwbu/download>
- Wicherts, J. M., Borsboom, D., Kats, J., & Molenaar, D. (2006). The poor availability of psychological research data for reanalysis. *The American Psychologist*, 61(7), 726–728. <https://doi.org/10.1037/0003-066X.61.7.726>

- Wicherts, J. M., Veldkamp, C. L. S., Augusteijn, H. E. M., Bakker, M., van Aert, R. C. M., & van Assen, M. A. L. M. (2016). Degrees of Freedom in Planning, Running, Analyzing, and Reporting Psychological Studies: A Checklist to Avoid p-Hacking. *Frontiers in Psychology*, 7, 1832. <https://doi.org/10.3389/fpsyg.2016.01832>
- Wilson, R. S., Mayhew, S. D., Rollings, D. T., Goldstone, A., Przezdzik, I., Arvanitis, T. N., & Bagshaw, A. P. (2015). Influence of epoch length on measurement of dynamic functional connectivity in wakefulness and behavioural validation in sleep. *NeuroImage*, 112, 169–179. <https://doi.org/10.1016/j.neuroimage.2015.02.061>
- Wolters, C. H., Anwander, A., Tricoche, X., Weinstein, D., Koch, M. A., & MacLeod, R. S. (2006). Influence of tissue conductivity anisotropy on EEG/MEG field and return current computation in a realistic head model: A simulation and visualization study using high-resolution finite element modeling. *NeuroImage*, 30(3), 813–826. <https://doi.org/10.1016/j.neuroimage.2005.10.014>
- Yao, Z., Hu, B., Xie, Y., Moore, P., & Zheng, J. (2015). A review of structural and functional brain networks: small world and atlas. *Brain Informatics*, 2(1), 45–52. <https://doi.org/10.1007/s40708-015-0009-z>
- Yassine, S., Gschwandtner, U., Auffret, M., Achard, S., Verin, M., Fuhr, P., & Hassan, M. (2022). Functional brain dysconnectivity in Parkinson's disease: A 5-year longitudinal study. *Movement Disorders: Official Journal of the Movement Disorder Society*. <https://doi.org/10.1002/mds.29026>
- Yeo, B. T. T., Krienen, F. M., Sepulcre, J., Sabuncu, M. R., Lashkari, D., Hollinshead, M., Roffman, J. L., Smoller, J. W., Zöllei, L., Polimeni, J. R., Fischl, B., Liu, H., & Buckner, R. L. (2011). The organization of the human cerebral cortex estimated by intrinsic functional connectivity. *Journal of Neurophysiology*, 106(3), 1125–1165. <https://doi.org/10.1152/jn.00338.2011>
- Zalesky, A., Fornito, A., Harding, I. H., Cocchi, L., Yücel, M., Pantelis, C., & Bullmore, E. T. (2010). Whole-brain anatomical networks: Does the choice of nodes matter? *NeuroImage*, 50, 970–983. <https://doi.org/10.1016/j.neuroimage.2009.12.027>
- Zhou, Z., Ding, M., Chen, Y., Wright, P., Lu, Z., & Liu, Y. (2009). Detecting directional influence in fMRI connectivity analysis using PCA based Granger causality. *Brain Research*, 1289, 22–29. <https://doi.org/10.1016/j.brainres.2009.06.096>

Titre : La variabilité analytique dans l'estimation des réseaux cérébraux fonctionnels à partir de l'électroencéphalographie

Mots clés : EEG connectivité de sources, problème inverse, connectivité fonctionnelle, nombre des électrodes, variabilité analytique

Résumé : Au cours des deux dernières décennies, l'étude des réseaux cérébraux fonctionnels a suscité un intérêt croissant. Dans ce contexte, l'approche de dite de la « connectivité de sources EEG » a émergé. D'un point de vue méthodologique, l'analyse « connectivité de sources EEG » se caractérise par une chaîne d'analyse souvent complexe : lorsqu'il/elle mène son étude, le/la chercheur(se) est confronté(e) à un grand nombre de choix souvent faits de manière arbitraire. Ces nombreux choix sont susceptibles d'être problématiques et de produire une variabilité substantielle dans les résultats, avec un impact potentiel sur la reproductibilité dans la recherche sur la méthode de connectivité des sources EEG. Cette thèse étudie spécifiquement la question de la variabilité analytique dans la chaîne d'analyse de la connectivité de sources EEG et

ses effets sur la cohérence des résultats. Nous nous sommes principalement concentrés sur la variabilité des résultats induite par trois facteurs clé de la chaîne d'analyse : 1) le nombre d'électrodes EEG, 2) les algorithmes de résolution du problème inverse, et 3) les méthodes de connectivité fonctionnelle. Nos résultats confirment que l'analyse de connectivité des sources est largement affectée par la question de la variabilité analytique. Les données EEG simulées relatifs à l'activité épileptiforme et aux réseaux resting-state montrent une variabilité significative au niveau des réseaux corticaux reconstruits en fonction du nombre d'électrodes EEG, de la solution inverse, de la méthode de connectivité. L'EEG à l'état de repos chez des contrôles sains montre un effet des facteurs mentionnés ci-dessus sur la cohérence au niveau du groupe ainsi que sur la variabilité inter et intra-sujets.

Title: Analytical variability in electroencephalography-based functional brain networks estimation

Keywords: EEG source connectivity, inverse problem, functional connectivity, number of electrodes, analytical variability

Abstract: Over the past two decades, there has been an increased interest in studying functional brain networks. In this context, the “EEG source connectivity” approach has emerged. From a methodological point of view, the EEG source connectivity is characterized by a complex workflow: in the course of running a study, the researcher is indeed faced with a large number of choices often made arbitrarily. Those numerous choices to be made have the potential to be problematic and produce substantial variability in results, ultimately hindering replicability in EEG source connectivity research. This dissertation calls into question the analytical variability in the EEG source connectivity pipeline and its effect

on the consistency of the outcomes. Mainly, we focused on the results’ variability induced by three factors along the analysis pipeline: 1) number of EEG electrodes, 2) inverse solution algorithms, and 3) functional connectivity metrics. Our findings confirm that the EEG source connectivity analysis is largely affected by the analytical variability. EEG simulations of epileptiform and resting-state activity show significant variability in reconstructed cortical networks due to the number of EEG electrodes, inverse solution, connectivity measure. Resting-state EEG in healthy controls shows an effect of the aforementioned factors on the group consistency, as well as the intra- and inter-subject variability.